Role of BDNF in cardiac remodeling and dysfunction in rats after myocardial infarction

Heow Won Lee

Thesis submitted to the Faculty of Graduate and Postdoctoral Studies in partial fulfillment of the requirements for the doctoral degree in Cellular and Molecular Medicine

Department of Cellular and Molecular Medicine

Faculty of Medicine

University of Ottawa

Contributions

Manuscripts published:

Lee HW, Ahmad M, Wang HW, Leenen FH (2017). Effects of exercise training on brain-derived neurotrophic factor in skeletal muscle and heart of rats post myocardial infarction. *Exp Physiol* **102**, 314–328.

Lee HW, Ahmad M, Weldrick JJ, Wang HW, Burgon PG, Leenen FH (2018). Effects of exercise training and TrkB blockade on cardiac function and BDNF-TrkB signaling post myocardial infarction in rats. *Am J Physiol Heart Circ Physiol* **315**, H1821–H1834.

Manuscript submitted:

Lee HW, Ahmad M, Wang HW, Leenen FH (2019). Effects of exercise on BDNF-TrkB signaling in the paraventricular nucleus and rostral ventrolateral medulla in rats post myocardial infarction. *Neuropeptides* (submitted).

Contribution by the author of the thesis:

1. Designed studies (Chapters 3, 4)
2. Performed citrate synthase activity assay (Chapter 2), real time PCR (Chapters 2, 3), Western blotting (Chapters 2, 3, 4), plasma BDNF assay (Chapter 3), and analyzed all the data
3. Performed rat exercise training (Chapters 2, 3, 4) and drug treatment (Chapters 3, 4), PVN and RVLM punches (Chapter 4)
4. Analyzed echocardiographic (Chapters 2, 3, 4) and hemodynamic (Chapters 2) measurements
5. Drafted and revised manuscripts, prepared figures, performed statistical analyses (Chapters 2, 3, 4)

Contribution of co-authors:

- Ahmad M
  - Performed MI surgery, echocardiography and hemodynamic measurements (Chapters 2, 3, 4)
  - Hemodynamic analysis (Chapters 3, 4)
- Wang HW
  - Designed primer sequences for gene expression analysis (Chapter 2, Table 2-1)
  - Performed Western Blotting for soleus muscle proteins and data analysis (Chapter 2, Figure 2-2A)
  - Performed Western Blotting for the PVN and RVLM and data analysis (Chapter 4, Experiment 2: high dose ANA-12 study)
- Weldrick JJ
  - Performed Western Blotting for AMPK protein measurement (Chapter 3, Figure 3-6A)
- Burgon PG
  - Critically reviewed Chapter 3
- Leenen FH
  - Designed studies (Chapters 2, 3, 4)
  - Revised manuscripts (Chapters 2, 3, 4)
  - Supervised the thesis

Funding:

- Canadian Institutes of Health Research Operating Grant FRN: MOP-136923
- University of Ottawa Endowed Graduate Award in Cardiac Research at the Heart Institute, supported by the University of Ottawa's Faculty of Medicine Endowed Funds in Cardiac Research and the University of Ottawa Heart Institute Foundation

Thesis Advisory Committee Members:

- Leo Renaud
- Patrick Burgon
- Balwant Tuana

Abstract

Myocardial infarction (MI) induced heart failure (HF) is a leading cause of morbidity and mortality over the world. Regular exercise improves quality of life and decreases hospitalization and mortality of patients with HF. In animals, exercise post MI attenuates progressive cardiac remodeling and cardiac dysfunction, and decreases neuronal activity in the paraventricular nucleus (PVN) and rostral ventrolateral medulla (RVLM), which are key brain nuclei contributing to sympathetic hyperactivity post MI. The peripheral and central molecular mechanisms underlying these beneficial effects of exercise are not well understood. We studied one possible mechanism, brain-derived neurotrophic factor (BDNF), an exercise-induced factor, which via binding to its receptor tropomyosin-related kinase B (TrkB) may contribute to improvement of cardiac function post MI. In the brain, the ratio between two isoforms of the TrkB receptor, full-length and truncated forms (TrkB.FL/TrkB.T1) determines the extent of intracellular responses to mature BDNF (mBDNF; an active form of BDNF) and a decrease in this ratio may reflect down-regulation of BDNF-TrkB.FL signaling. Ca^{2+}/calmodulin-dependent kinase II (CaMKII) and protein kinase B (Akt) are intracellular factors of BDNF-TrkB signaling in hippocampal/cortical neurons. Activation of cardiac BDNF-TrkB signaling may increase cardiomyocyte survival and myocardial contractility. In hypertensive rats, the role of BDNF-TrkB signaling in the PVN and RVLM appears opposite with activation of this axis in the PVN increasing, but in the RVLM decreasing sympathetic nerve activity (SNA). However, activation of CaMKII and Akt in the PVN and RVLM both mediate increase in SNA. The specific role of BDNF-TrkB signaling in the PVN and RVLM of rats with HF post MI has not yet been studied. We hypothesized that exercise training

post MI enhances BDNF-TrkB signaling pathways in the left ventricle (LV) and RVLM, but inhibits in the PVN, and thereby preserves cardiac structure and function post MI. We evaluated changes in BDNF-TrkB axis and intracellular factors CaMKII and Akt in the non-infarct area of the LV, PVN and RVLM in sedentary and exercising rats with MI. The impact of systemic blockade of BDNF-TrkB signaling was assessed with ANA-12, a selective non-competitive antagonist of TrkB receptors. In the infarct area of the LV, mBDNF protein decreased and TrkB.T1 protein increased. In the non-infarct area, mBDNF tended to be decreased without change in TrkB.T1 expression. The activities of CaMKII and Akt were decreased in the non-infarct area of the LV. In the PVN and RVLM, the TrkB.FL/TrkB.T1 ratio was decreased but without changes in mBDNF and downstream factors except for decrease in Akt activity in the RVLM. Exercise training improved ejection fraction (EF), cardiac index and LV end-diastolic pressure, but only the exercise-induced improvement of EF was blocked by ANA-12. In the non-infarct area of the LV, exercise prevented decreases in mBDNF, CaMKII and Akt, and these effects were prevented by ANA-12. In the PVN, exercise increased mBDNF and decreased Akt activity, whereas in the RVLM, exercise had no effect on mBDNF but decreased CaMKII activity. The exercise-induced increase mBDNF in the PVN and decrease in p-CaMKIIβ expression in the RVLM were prevented by ANA-12. Our findings suggest that down-regulation of BDNF-TrkB signaling post MI is prominent in the LV with decreases in mBDNF protein in the infarct area and intracellular factors CaMKII and Akt in the non-infarct area. Increases in mBDNF, CaMKII and Akt in the LV by exercise may contribute to improvement of EF. In the PVN and RVLM, despite a decrease in the ratio of TrkB.FL/TrkB.T1 in both brain nuclei, only Akt activity decreased in the RVLM post MI.

Exercise-induced decreases in activities of CaMKII in the RVLM and Akt in the PVN may both contribute to reduction in sympathetic hyperactivity post MI.

Authorization

Chapter 1

No authorizations are required. All the figures are adapted or newly generated based on the contents of the Chapter 1. References are indicated in the Figure legends if needed.

Chapter 2

Permission for the reproduction, as part of a thesis dissertation, of Lee HW et al. *Experimental Physiology* **102**, 314–328, © 2017 is provided by the authors and Wiley-Blackwell.

Chapter 3

The reproduction of the whole published article by author of the published work by the American Physiological Society is permitted to reuse as part of a thesis dissertation without charge and without requesting. Lee HW et al. *American Journal of Physiology Heart and Circulation* **315**, H1821–H1834, © 2018

Table of Contents

List of Tables

List of Figures

Chapter 1

Chapter 2

Chapter 3

Chapter 4

7. Appendix I

List of Abbreviations

Acc1	Acetyl-CoA carboxylase 1
Acc2	Acetyl-CoA carboxylase 2
ACE	Angiotensin converting enzyme
AMPA	α-amino-3-hydroxy-5-methyl-4-isoxazolepropionic acid
AMPK	AMP-activated protein kinase
ANA-12	Selective TrkB blocker; *N*-(2-{[(hexahydro-2-oxo-1H-azepin-3-yl)amino]carbonyl}phenyl)-benzo[b]thiophene-2-carboxamide
Ang I	Angiotensin I
Ang II	Angiotensin II
ANOVA	Analysis of variance
ANCOVA	Analysis of covariance
Akt	Protein kinase B
AR	Adrenergic receptor
ARK	Adrenergic receptor kinase
ATP	Adenosine triphosphate
AT_1R	Angiotensin II type 1 receptor
AVP	Arginine vasopressin
Bax	Bcl-2-associated X protein
BBB	Blood-brain barrier
BCA	Bicinchoninic acid
BDNF	Brain-derived neurotrophic factor
BP	Blood pressure
CaMKII	Ca^{2+}/calmodulin-dependent protein kinase II
CNS	Central nervous system
Cpt1a	Carnitine palmitoyltransferase 1a
Cpt1b	Carnitine palmitoyltransferase 1b
CREB	cAMP-response element binding protein
CRH	Corticotrophin-releasing hormone
CSAR	Cardiac sympathetic afferent reflex
CSNA	Cardiac sympathetic nerve activity
CVLM	Caudal ventrolateral medulla
CVOs	Circumventricular organs
DBHB	D-β-hydroxybutyrate
DNA	Deoxyribonucleic acid
DG	Dentate gyrus of the hippocampus
dmNTS	dorsal medial nucleus tractus solitarius
dP/dt_{max}	Maximal rate of pressure change
dP/dt_{min}	Minimal rate of pressure change

DMV	Dorsal motor nucleus of the vagus
ESV	End-systolic volume
EDV	End-diastolic volume
EF	Ejection fraction
ELISA	Enzyme-linked immunosorbent assay
ENaCs	Epithelial sodium channels
EO	Endogenous ouabain
ERK	Extracellular signal-regulated kinase
ExT-MI	Exercising MI
ExT-MI-Veh	Exercising MI treated with vehicle
ExT-MI-ANA-12	Exercising MI treated with ANA-12
FADD	Fas-associated death domains
FAT/Cd36	Fatty acid translocase
FNDC5	Fibronectin type III domain-containing protein 5
GABA	Gamma-aminobutyric acid
GAD67	Glutamic acid decarboxylase 67
GLT1	Glutamate transporter 1
Glut1	Glucose transporter type 1
Glut4	Glucose transporter type 4
GAPDH	Glyceraldehyde-3-phosphate dehydrogenase
GPCR	G-protein coupled receptor
GRK	G protein-coupled receptor kinase
HDAC	Histone deacetylase
HF	Heart failure
HR	Heart rate
ICAM	Intracellular adhesion molecule
icv	Intracerebroventricular
IL	Interleukin
IL-1R	Interleukin-1 receptor
IL-10R	Interleukin-10 receptor
IL-1RA	Interleukin-1 receptor antagonist
IL-1R1	Interleukin-1 receptor type I
IML	Intermediolateral nucleus
IP_3	Inositol-1,4,5-trisphosphate
JNK	c-Jun N-terminal kinase
K252a	Selective inhibitor of the tyrosine protein kinase activity of the trk family of neurotrophin receptors
LAD	Left anterior descending
LV	Left ventricle
LVEDP	Left ventricular end-diastolic pressure
LVPSP	Left ventricular peak systolic pressure
MAPK	Mitogen-activated protein kinase

mBDNF	Mature BDNF
MCT2	Monocarboxylate transporter 2
MI	Myocardial infarction
miRNA	MicroRNA
MnPO	Median preoptic nucleus
MR	Mineralocorticoid receptor
NA	Nucleus ambiguus
NADPH	Nicotinamide adenine dinucleotide phosphate
NE	Norepinephrine
NF-κB	Nuclear factor kappa B
NMDA(R)	N-methyl-D-aspartate (receptor)
NTS	Nucleus tractus solitarius
$p75^{NTR}$	Pan-neurotrophin receptor p75
$p\text{-}AMPK\alpha^{Thr172}$	Phosphorylated AMPK threonine residue targeting 172
$p\text{-}Akt^{Thr308}$	Phosphorylated Akt threonine residue targeting 308
$p\text{-}Akt^{Ser473}$	Phosphorylated Akt serine residue targeting 473
$p\text{-}CaMKII^{Thr286}$	Phosphorylated CaMKII threonine residue targeting 286
PGC-1α	Peroxisome proliferator-activated receptor γ coactivator-1α
PGK1	Phosphoglycerate kinase 1
PI3K	Phosphatidylinositol 3-kinase
PKC	Protein kinase C
PLB	phospholamban
PLC	Phospholipase C
PRR	(pro)renin receptor
PVN	Paraventricular nucleus of the hypothalamus
RAAS	Renin-angiotensin-adosterone system
RAS	Renin-angiotensin system
ROS	Reactive oxygen species
RSNA	Renal sympathetic nerve activity
RV	Right ventricle
RVLM	Rostral ventrolateral medulla
OAA	Oxaloacetate
OVLT	Organum vasculosum of the lamina terminalis
Sed-MI	Sedentary MI
Sed-MI-Veh	Sedentary MI treated with vehicle
Sed-MI-ANA-12	Sedentary MI treated with ANA-12
SFO	Subfornical organ
SIRT1	Sirtuin 1
SNA	Sympathetic nerve activity
SNS	Sympathetic nervous system
SON	Supraoptic nucleus

STAT3	Signal transducer and activator of transcription 3
SV	Stroke volume
TBST	Tris-buffered saline with Tween-20
Tbp	TATA box-binding protein
TGF-β1	Transforming growth factor β1
TLR4	Toll-like receptor 4
TNF	Tumor necrosis factor
TNFR1	TNF receptor 1
TRADD	TNFR1-associated death domain
TrkB	Tropomyosin-related kinase B
TrkB.FL	Full-length form of TrkB
TrkB.T1	Truncated form of TrkB
TUNEL	Terminal deoxynucleotidyl transferase dUTP nick end labeling
UCP2	Uncoupling protein 2
VCAM	Vascular cell adhesion molecule
V1aR	Vasopressin type 1a receptor
VO_2 max	Maximum rate of oxygen consumption during exercise
Y515	Tyrosine residue targeting 515
Y816	Tyrosine residue targeting 816

Acknowledgements

It is with gratitude that I thank my supervisor Dr. Frans Leenen, for his consistent guidance throughout my research project. Dr. Leenen's extensive efforts and valuable advice for performing experiments, preparing manuscripts and thesis writing enabled me to complete the required work and achieve my goals. I was inspired by his passionate attitude to research and was able to gain valuable experience and knowledge. I appreciate the involvement of my thesis advisory committee members Dr. Leo Renaud, Dr. Patrick Burgon and Dr. Balwant Tuana and thank them for their helpful advice and comments.

I would like to thank the Brain and Heart research group research associates Dr. Monir Ahmad and Dr. Hong-Wei Wang for their technical support and crucial guidance to me for performing experiments. Many thanks to past lab technicians Roselyn White and Cassandra Roeske for training me in several experimental skills. I would like to thank Cathy Proctor, research assistant, who has always treated me warmly and assisted with many administrative tasks. I would like to express my gratitude to my lab mates and best friends, Jiao Lu and Fatimah Najjar. I consider myself very lucky to have been a member in the same lab with them. They were always very professional and lend a helping hand inside and outside of the lab.

My deep gratitude also goes to my family. My father Hee-Kwon Lee has been guiding and encouraging me to keep on the right track. I thank him for believing in me and providing tremendous support over the duration of my Ph.D. study. I would like to thank my mother Soon-Ae Lee and my sister Heow-Jin Lee for their endless love and encouragement during this tough journey.

Being a Ph.D. student and conducting research have not been easy for me, and I have encountered many challenges, but this journey has led me to become more mature and responsible. I am truly grateful for this experience.

Chapter 1

General Introduction

1.0. Overview

Heart failure (HF) has a high prevalence around the world (Roger, 2013). Despite treatments such as angiotensin converting enzyme (ACE) inhibitors, angiotensin II (Ang II) type 1 receptor (AT_1R) blockers, β-blockers and mineralocortocoid receptor (MR) antagonists (McMurray et al., 2012), prognosis still remains poor (Yeung et al., 2012). Better understanding of the pathophysiology may lead to new therapeutic targets and possibly better outcomes. After cardiac injury by e.g. a myocardial infarction (MI), depressed cardiac function leads to activation of central angiotensinergic pathways, followed by activation of peripheral systems such as the sympathetic nervous system (SNS) and the circulating renin-angiotensin-aldosterone system (RAAS) (Leenen, 2007). Persistent activation of the SNS and RAAS contributes to progressive cardiac dysfunction and remodeling (Triposkiadis et al., 2009).

Exercise is a non-pharmacological approach to improve prognosis of HF. Regular exercise by patients with HF decreases resting muscle sympathetic nerve activity (SNA) and plasma norepinephrine (NE) levels (Roveda et al., 2003; Passino et al., 2006), reduces hospitalization (15% vs. 22%, exercise vs. control) (Davies et al., 2010) and improves quality of life (35% vs. control) (Belardinelli et al., 2012). In animal studies, early initiation of exercise training post MI decreases sympathetic hyperactivity (Zheng et al., 2012b), attenuates adverse cardiac remodeling and preserves cardiac function (Cai et al., 2016; Xu et al., 2008a; Xu et al., 2008b). The molecular mechanisms underlying these beneficial effects of exercise are not well understood. One possible mechanism is regulation of brain-derived neurotrophic factor (BDNF)-tropomyosin-related kinase B (TrkB) signaling in the heart, as well as the paraventricular nucleus (PVN) of the

hypothalamus and rostral ventrolateral medulla (RVLM) of the brainstem, which are key brain nuclei that contribute to sympathetic hyperactivity post MI (Kumagai et al., 2012; Shenton and Pyner, 2016). BDNF is a member of the neurotrophin family, along with nerve growth factor and neurotrophins 3 to 7, and it is well established that exercise increases hippocampal, skeletal muscle and circulating BDNF (Griffin et al., 2009; Matthews et al., 2009; Walsh and Tschakovsky, 2018). Overall, brain and cardiac BDNF-TrkB signaling may play a cardioprotective role post MI (Leenen and Tuana, 2012; Okada et al., 2012), because brain specific deletion of BDNF gene or cardiac specific deletion of TrkB gene further increased cardiac fibrosis and decreased ejection fraction (EF) post MI (Okada et al., 2012).

The following sections include an overview of central nervous system (CNS) afferent and efferent pathways contributing to HF post MI, characteristics of BDNF and TrkB, as well as the regulation and role of BDNF-TrkB signaling pathways. Moreover, regulation of BDNF-TrkB signaling pathways post MI, effects of exercise training post MI and regulation of BDNF-TrkB signaling in response to exercise will be discussed.

1.1. CNS afferent and efferent pathways contributing to HF post MI

1.1.1. Peripheral afferent mechanisms to the CNS

Several afferent mechanisms contribute to activation of CNS pathways post MI (Fig 1-1). First, the cardiac sympathetic afferent reflex (CSAR) is activated. CSAR is a sympathoexcitatory reflex originating in the heart (Wang et al., 2014). Cardiac sympathetic afferent nerve endings are located in the superficial epicardial layers of ventricles (Chen et al., 2015; Minisi and Thames, 1991) and transmit mechanosensitve and chemosensitive information to neurons in the nucleus tractus solitarius (NTS) (Wang

et al., 2005; Wang et al., 2006b). Afferent signals from cardiac receptors may activate neurons in the NTS, the signals are forwarded to the PVN (Ren et al., 2017; Zhong et al., 2008), and then project to the RVLM (Li et al., 2013; Zhou et al., 2010) to control sympathetic outflow (Zhong et al., 2008). After MI, CSAR is enhanced by activation of cardiac mechanoreceptors due to an increase in LV pressure and dimensions, and of cardiac chemoreceptors by increases in various substances such as bradykinin, adenosine and reactive oxygen species (ROS) released from the injured myocardium (Chen et al., 2015; Wang et al., 2017).

Second, arterial baroreflex responds to decrease in blood pressure (BP) post MI. The arterial baroreflex is a homeostatic mechanism which acutely regulates BP by sensing mechanical stretch of arterial baroreceptors (Zhang et al., 2015), located in the aortic arch and carotid sinus, then conveys this information to the dorsal medial NTS (dmNTS) via the glossopharyngeal nerve (carotid sinus baroreceptors) and vagus nerve (aortic arch baroreceptors) (Kougias et al., 2010; Tu et al., 2018). The NTS modulates excitability of parasympathetic preganglionic neurons which project to the dorsal motor nucleus of the vagus (DMV) and nucleus ambiguus (NA), and sympathetic neuronal groups which project to the caudal ventrolateral medulla (CVLM), which in turn, projects to the RVLM, and thereby regulating sympathetic outflow (Guyenet, 2006; Michelini and Stern, 2009). After MI, decreases in cardiac contractility and cardiac output lower BP, and therefore arterial baroreceptors are less stretched (Zhang et al., 2015).

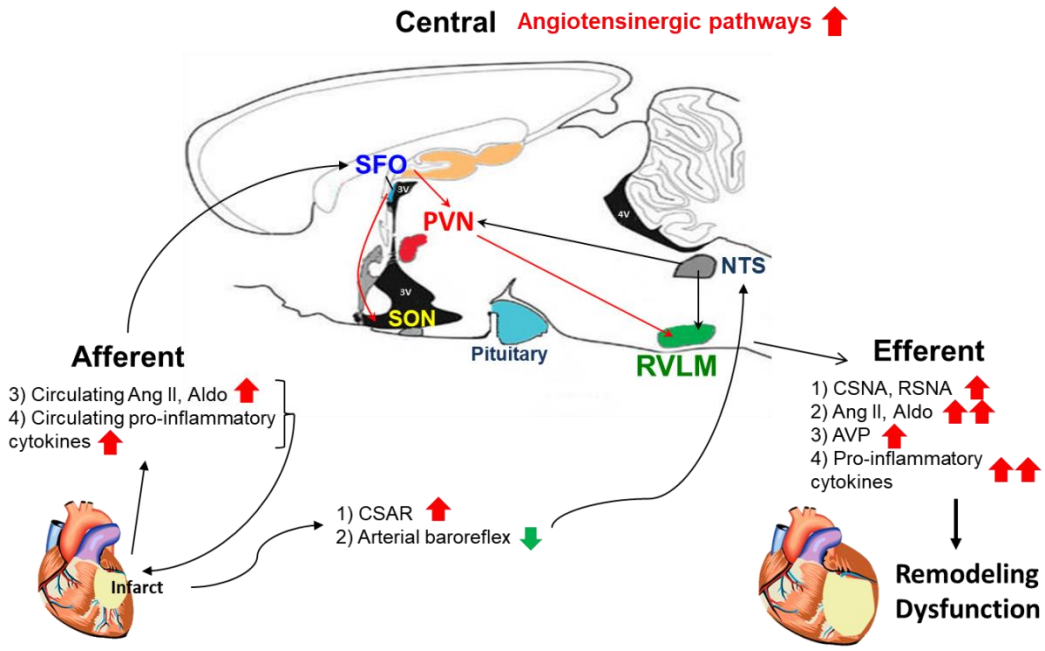

Figure 1-1. Afferent, central and efferent mechanisms contributing heart failure post MI
After myocardial infarction (MI), 1) activation of the cardiac sympathetic afferent reflex (CSAR) and 2) decrease in arterial baroreflex convey information to the nucleus tractus solitarius (NTS), forwarded directly to the paraventricular nucleus (PVN) and indirectly to the rostral ventrolateral medulla (RVLM) via caudal VLM. Increases in 3) angiotensin II (Ang II), aldosterone (Aldo) and 4) pro-inflammatory cytokines directly affect the heart, and thereby increases myocardial fibrosis and apoptosis, and activate central angiotensinergic pathways (indicated as the red arrows in the brain) from the subfornical organ (SFO) to PVN, supraoptic nucleus (SON) and RVLM. Activation of angiotensinergic pathways result in long-term activation of cardiac and renal sympathetic nerve activity (CSNA/RSNA), further increases in circulating Ang II and Aldo, increase in arginine vasopressin (AVP) and further increase in pro-inflammatory cytokines, leading to progressive cardiac remodeling and dysfunction. Adapted from Leenen (*Circ Res*, 2007) and Leenen et al. (2017).

Third, circulating Ang II and aldosterone increase rapidly post MI due to a decrease in BP and an increase in sympathetic activity (Leenen et al., 1999; Wang et al., 2004). They may bind to AT_1R and MR expressed in circumventricular organs (CVO), which are located outside the blood-brain barrier (BBB), such as the subfornical organ (SFO), then activate neurons in the SFO, followed by activation of neurons in the PVN and RVLM (Cato and Toney, 2005; Li et al., 2003; Xue et al., 2012).

Fourth, circulating pro-inflammatory cytokines increase post MI. After MI, inflammatory signaling such as danger-associated molecular patterns [e.g. Adenosine triphosphate (ATP), mitochondrial deoxyribonucleic acid (DNA)] and ROS released from necrotic cardiomyocytes in the infarct area, and the damaged extracellular matrix, activate pathogen recognition receptors (e.g. toll-like receptors), and thereby activate cardiac fibroblasts (de Haan et al., 2013; Frangogiannis, 2014; Ong et al., 2018). Activated cardiac fibroblasts release pro-inflammatory cytokines such as tumor necrosis factor (TNF)-α, interleukin (IL)-1β and IL-6 (Gullestad et al., 2012; Shinde and Frangogiannis, 2014), and increase chemokine synthesis (Frangogiannis, 2012). Chemokines interact with intracellular adhesion molecule (ICAM)-1, ICAM-2 and vascular cell adhesion molecule (VCAM)-1 on vascular endothelial cells, and thereby increases permeability to circulating neutrophils (Frangogiannis, 2012). Monocytes are released from the spleen to the circulation in response to increase in circulating Ang II (Leuschner et al., 2010; Swirski et al., 2009) and pro-inflammatory cytokines (Epstein et al., 2017), and circulating neutrophils and monocytes infiltrate to injured myocardium (Halade et al., 2018; Sager et al., 2017). Infiltrated neutrophils and monocytes (which become macrophages in cardiac tissue) further produce TNF-α and IL-1β (Dutta and

Nahrendorf, 2015) which are released to circulation from the cardiac tissue (Mann, 2002). Circulating pro-inflammatory cytokines bind to receptors [e.g. TNF receptor 1 (TNFR1), IL-1 receptor (IL-1R)] expressed in the SFO and activate neurons in the SFO (Wei et al., 2017; Wei et al., 2013), which in turn activate neurons in the PVN and RVLM (Dworak et al., 2014; Wu et al., 2012).

Activation of CSAR post MI inhibits barosensitive neurons and excites chemosensitive neurons in the NTS (Gao et al., 2005a; Wang et al., 2006b; Wang et al., 2008), resulting in sympathetic hyperactivity. Increases in circulating Ang II, aldosterone and pro-inflammatory cytokines increase local production of Ang II and pro-inflammatory cytokines in the SFO (Wei et al., 2017; Yu et al., 2018), contributing to activation of angiotensinergic pathways to the PVN (Wei et al., 2017; Zhu et al., 2004; Zhu et al., 2002) and RVLM (Huang et al., 2010), and thereby enhances SNA as well as further increases circulating Ang II and pro-inflammatory cytokines (Guggilam et al., 2008; Kang et al., 2006; Kang et al., 2008). Central and efferent pathways will be further discussed in the next two sections.

1.1.2. Central angiotensinergic pathways

In the CNS, glutamate and gamma-aminobutyric acid (GABA) are the two major neurotransmitters which regulate neural control of cardiovascular homeostasis (Leenen, 2014). An action potential releases glutamate or GABA to the synaptic cleft, which bind to their ligand-gated ionotropic receptors, leading to rapid opening of ion channels (milliseconds) and ion influx into the cell (Gabor and Leenen, 2012; Greengard, 2001). Glutamate binding to α-amino-3-hydroxy-5-methyl-4-isoxazolepropionic acid (AMPA) receptors triggers Na^+ influx, thereby depolarizing the neuron. In contrast, GABA

binding to $GABA_A$ receptors allows Cl^- influx, resulting in hyperpolarization of the neuron and inhibits membrane potentials. Glutamate and GABA can also activate slow transmission (seconds to minutes) by increasing second messengers and protein kinases to regulate the quantity released from presynaptic neurons and/or regulate their effectiveness by modulating sensitivity and quantity of receptors on the postsynaptic neurons (Gabor and Leenen, 2012; Greengard, 2001).

Central angiotensinergic pathways are slow-acting CNS pathways (seconds to minutes) which initiate sympathoexcitatory, neurohormonal and pressor responses to e.g. circulating/local Ang II (Leenen et al., 2017). Angiotensinergic neurons, a series of neurons that use Ang II as a neurotransmitter, project from the SFO directly to the supraoptic nucleus (SON), and directly to PVN neurons or indirectly through the median preoptic nucleus (MnPO) (Ferguson, 2009; Gabor and Leenen, 2012). PVN neurons project to the RVLM or directly to the intermediolateral nucleus (IML) of the spinal cord (Cato and Toney, 2005; Pyner and Coote, 2000). All components of the renin-angiotensin system (RAS) including angiotensinogen, renin, ACE and AT_1R are detectable in neurons and astrocytes in all these brain nuclei (Nakagawa and Sigmund, 2017). Although angiotensinogen is synthetized in astrocytes and constitutively released into the extracellular space, it is elusive whether local Ang II is produced by the classical RAS components because active renin is undetectable in the brain (Sigmund et al., 2017). On the other hand, prorenin, a precursor of renin, is synthetized in neurons (Buller and Feng, 2016) and its binding receptor, (pro)renin receptor (PRR), is highly expressed in neurons, but not found in astrocytes (Xu et al., 2016). Prorenin binding to PRRs may activate mitogen-activated protein kinase (MAPK) signaling pathway (Shan et al., 2008) to

produce Ang II (Li et al., 2012; Li et al., 2014; Nguyen et al., 2002). In neurons, prorenin binding to PRRs (intracellular or on the neuronal membrane) may contribute to conversion of angiotensinogen, secreted from astrocytes or neurons, to angiotensin I (Ang I) and ACE converts Ang I to Ang II (Sigmund et al., 2017; Xu et al., 2016). Ang II-containing neuronal cell bodies and axonal terminals are present in the SFO, MnPO, SON, PVN and RVLM, and AT_1Rs are expressed on both pre- and post-synaptic terminals (Leenen et al., 2017; Lind et al., 1985). AT_1Rs are also expressed in astrocytes and microglia in the SFO (Yu et al., 2018), PVN (Biancardi et al., 2015; Stern et al., 2016) and RVLM (Isegawa et al., 2014). Altogether, RAS components in neurons and glia and their interactions are required for local synthesis of Ang II (de Kloet et al., 2015), and Ang II binding to AT_1R in neurons and glia activates downstream signaling pathways, and thereby increases neuronal activity (Fig 1-2). In neurons, an action potential triggers release of Ang II from nerve terminal to synaptic cleft and Ang II binding to AT_1R activates slow G-protein signaling (Leenen, 2014), that increases nicotinamide adenine dinucleotide phosphate (NADPH) oxidase and ROS (Wang et al., 2006a; Zimmerman et al., 2002). Ang II-AT_1R signaling mediated elevation in ROS increases voltage-gated calcium current (Zimmerman et al., 2005) and inhibits voltage-gated potassium current (Sun et al., 2005), and thereby increases firing activity in neurons (Cato and Toney, 2005). Ang II-AT_1R signaling in astrocytes and microglia appears to increase NADPH oxidase and ROS similarly as in neurons. Ang II-AT_1R signaling in astrocytes in the PVN decreases inhibition of glutamate transporter 1 (GLT1) activity, preventing re-uptake of glutamate and leading to increase in extracellular glutamate levels.

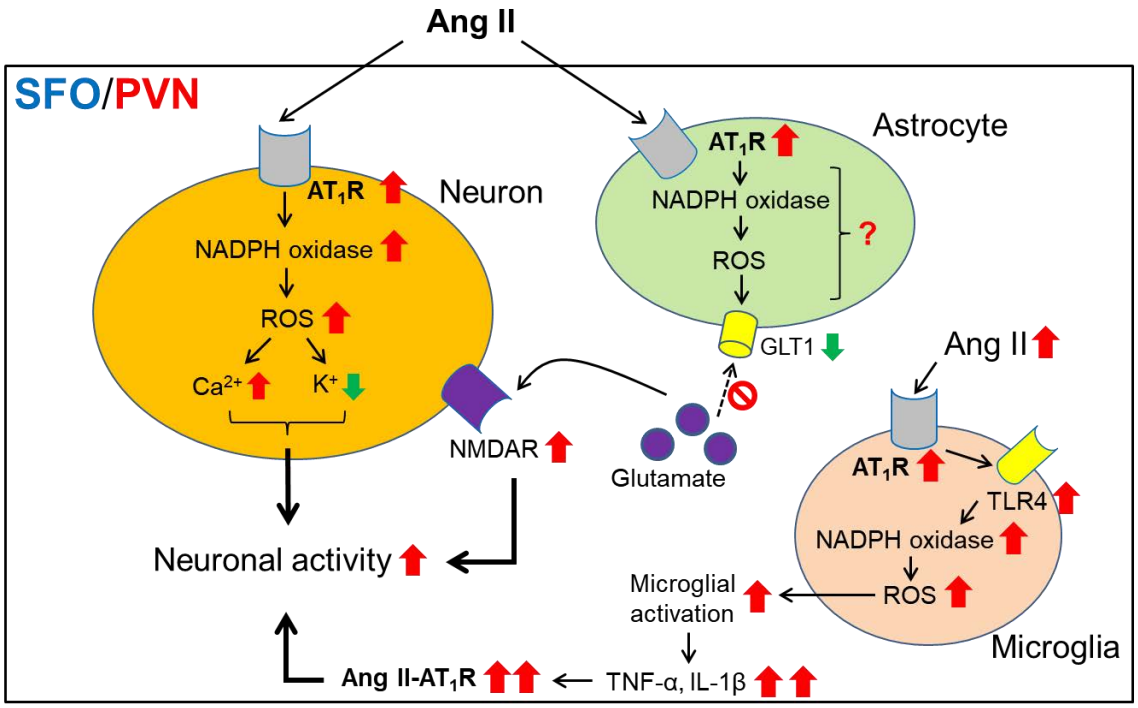

Figure 1-2. Classical and new pathways contributing to Ang II-AT_1R signaling mediated increase in neuronal activity in the SFO and PVN

Angiotensin II (Ang II) activates Ang II type 1 receptor (AT_1R) in neurons and increases nicotinamide adenine dinucleotide phosphate (NADPH) oxidase and reactive oxygen species (ROS). ROS increases Ca^{2+} and decreases K^+, leading to increase in neuronal activity. Ang II also binds to AT_1R in astrocyte and decreases activity of glutamate transporter 1 (GLT1), and thereby preventing re-uptake of glutamate. Glutamate binds to N-methyl-D-aspartate receptor (NMDAR) in neurons and increases neuronal activity. In microglia, Ang II-AT_1R signaling interacts with toll-like receptor 4 (TLR4) and increases microglial activation, followed by local production of pro-inflammatory cytokines [e.g. tumor necrosis factor (TNF)-α, interleukin (IL)-1β], which in turn further enhances Ang II-AT_1R signaling. SFO, subfornical organ; PVN, paraventricular nucleus

Increased glutamate activates N-methyl-D-aspartate (NMDA) receptors expressed in surrounding neurons, and thereby increases presympathetic neuronal activity (Stern et al., 2016). Ang II-AT_1R signaling activates microglia by activation of toll-like receptor 4 (TLR4), and increases production of ROS in the PVN (Biancardi et al., 2015), and TNF-α and IL-1β in the SFO and PVN (Yu et al., 2018).

In normal physiological conditions, sympathoexcitatory glutamatergic neurons are tonically inhibited by GABA (Leenen, 2014; Sousa-Pinto et al., 2014). Microinjection of an AT_1R blocker into the SFO, PVN or RVLM in normal rats does not affect SNA and baseline BP (Du et al., 2013; Llewellyn et al., 2014; Sheriff et al., 2006; Su et al., 2017), indicating that angiotensinergic pathways are not active under normal physiological conditions. After MI, increases in circulating Ang II, pro-inflammatory cytokines (e.g. TNF-α, IL-1β) and aldosterone activate AT_1R, TNFR1 and IL-1R, as well as MR in the SFO (Leenen et al., 2017; Yu et al., 2018), and thereby increase neuronal activity in the SFO (Simpson and Ferguson, 2017; Wei et al., 2017; Zubcevic et al., 2017). An increase in Ang II release from the SFO activates neurons projecting to glutamatergic interneurons and inhibits GABAergic interneurons in the PVN (Leenen, 2014; Sousa-Pinto et al., 2014). Prolonged activation of Ang II-AT_1R signaling in the SFO increases local synthesis of aldosterone in magnocellular neurons in the PVN and SON (Huang et al., 2010). Locally produced aldosterone binds to MR and activates epithelial sodium channels (ENaCs)-endogenous ouabain (EO) pathway (Huang and Leenen, 2005). EO inhibits Na^+, K^+-ATPase activity (Kent et al., 2004) and thereby lowers membrane potential and increases intracellular Ca^{2+}, leading to increase firing rate (Huang and Leenen, 2009; Leenen, 2010), and may activate Na^+-pump associated protein kinase

signaling (e.g. Src) (de Lores Arnaiz, 2007) that increases ACE and AT_1R expression, and subunits of NADPH oxidase (Huang et al., 2011; Tan et al., 2004). Ang II binding to AT_1R in microglia activates TLR4 expression, and increases NAPDH oxidase, ROS and nuclear factor kappa B (NF-κB), and thereby increases production of pro-inflammatory cytokines (Biancardi et al., 2017; Labandeira-Garcia et al., 2017). Pro-inflammatory cytokines bind to their receptors (e.g. TNFR1, IL-1R) in neurons and may induce formation of a signaling complex with associated proteins such as TNF-receptor-associated factors (Li et al., 2005), which phosphorylates $p47^{phox}$, a subunit of NADPH oxidase, and thereby activates NADPH oxidase/ROS/NF-κB pathway, leading to further increases in ACE and AT_1R expression (Kang et al., 2008; Wei et al., 2015). PVN neurons projecting to RVLM neurons are also activated post MI (Xu et al., 2012), and similar increases in expression of ACE, AT_1R, MR, and subunits of NADPH oxidase (Gao et al., 2004; Huang et al., 2014a; Kar et al., 2010) as well as pro-inflammatory cytokines (Guggilam et al., 2011) are observed in the RVLM post MI. There are no studies reporting the effects of microinjection of an AT_1R blocker or specific knockdown of AT_1R in the RVLM of MI rats. However, intracerebroventricular (icv) infusion of an AT_1R blocker in rats normalized the Ang II-induced increases in renal sympathetic nerve activity (RSNA), AT_1R mRNA and protein expression, subunits of NADPH oxidase and superoxide in the RVLM (Gao et al., 2005b), suggesting that activation of Ang II-AT_1R signaling, followed by increases in NADPH oxidase and ROS in the RVLM contribute to enhance sympathetic activity (Koba, 2018). Furthermore, aldosterone can be synthetized in the RVLM and activates MR and downstream mechanisms similar to the PVN, and thereby increases AT_1R (Oshima et al., 2013). Collectively, increases in local production

of aldosterone and pro-inflammatory cytokines enhance activity of angiotensinergic pathways, resulting in prolonged sympathetic hyperactivity (Leenen et al., 2017; Xu and Li, 2015) (Fig 1-3).

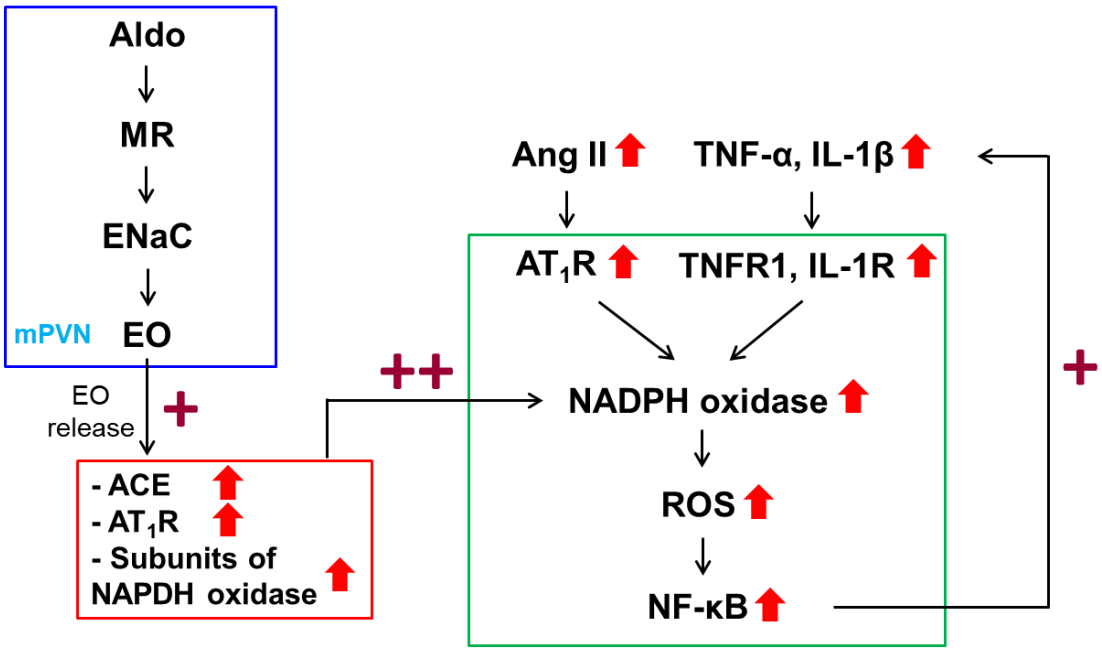

Figure 1-3. Activation of angiotensinergic pathways by aldosterone and pro-inflammatory cytokines in the PVN

Locally produced aldosterone (Aldo) activates mineralocorticoid (MR)-epithelial sodium channels (ENaCs)-endogenous ouabain (EO) pathway in magnocellular paraventricular nucleus (mPVN), and thereby increases expression of angiotensin converting enzyme (ACE), angiotensin II type 1 receptor (AT_1R) and subunits of nicotinamide adenine dinucleotide phosphate (NADPH) oxidase. Locally produced pro-inflammatory cytokines such as tumor necrosis factor (TNF)-α, interleukin (IL)-1β bind to their receptors (e.g. TNFR1, IL-1R) and activates NADPH oxidase/ROS/NF-κB pathway, which is also the downstream pathway of Ang II-AT_1R signaling. Activation of this pathway further increases ACE and pro-inflammatory cytokines and ultimately contributes to sympathetic hyperactivity. ROS, reactive oxygen speices; NF-κB, nuclear factor kappa B

1.1.3. CNS efferent mechanisms contributing to HF

Persistent activation of central angiotensinergic pathways post MI leads to long-term activation of efferent sympathetic outflow to the heart and kidneys and increases circulating and cardiac RAS, circulating arginine vasopressin (AVP) and pro-inflammatory cytokines. Acute activation of efferent cardiac sympathetic outflow post MI has positive chronotropic and inotropic effects (Gordan et al., 2015; Triposkiadis et al., 2009), but also may cause cardiac arrhythmias by e.g. enhancing the dispersion of repolarization in ischemic area (Kolettis, 2018; Leenen, 1999). A chronic increase in cardiac sympathetic nerve activity (CSNA) enhances NE spillover in the heart (Ramchandra et al., 2018) and downregulates NE transporter (Kreusser et al., 2017), leading to excessive NE release in the heart. Increased efferent sympathetic outflow to the adrenal medulla also stimulates epinephrine release from chromaffin cells, leading to spillover to the circulation (Mahata et al., 2016). Chronic sympathetic hyperactivation results in cardiomyocyte apoptosis, hypertrophy of remaining myocytes and interstitial fibrosis, and thereby contribute to progressive cardiac dysfunction (Huang and Leenen, 2009; Leenen, 1999). High level of NE release in the heart increases NADPH oxidase activity and ROS (Li et al., 2015; Sorescu and Griendling, 2002) in cardiomyocytes, followed by increase in caspase-3 activity, thus enhancing cardiomyocyte apoptosis (Baker, 2014; Fu et al., 2004) and loss of cardiomyocytes. Moreover, long-term increase in NE activates β-adrenergic receptor (AR) kinase 1 [βARK1, also known as G protein-coupled receptor kinase 2 (GRK2)] in cardiomyocytes, leading to β_1-AR desensitization (Lymperopoulos et al., 2013). This leads to less phosphorylation of substrates which regulate intracellular Ca^{2+} concentration, such as cardiac troponin I, L-type Ca^{2+} channels

and phospholamban (PLB) (de Lucia et al., 2018; Lymperopoulos et al., 2013), and thereby reduces the magnitude of the calcium transient in cardiac contraction and relaxation, leading to decrease in myocardial contractility (Bernstein et al., 2011; Hartupee and Mann, 2017; Madamanchi, 2007).

Activation of RSNA increases renal sodium retention and renin release from juxtaglomerular cells, leading to further elevation of circulating Ang II and aldosterone (Ramchandra and Barrett, 2015). Circulating Ang II binds and activates AT_1R on cardiac fibroblast, increases transforming growth factor β1 (TGF-β1), and thereby increases collagen synthesis and causes fibrosis, leading to increase stiffness of the myocardium (Ferrario, 2016). Ang II acting on AT_1R on cardiomyocytes increases pro-apoptotic factors such as Bcl-2-associated X protein (Bax) and decreases anti-apoptotic factor Bcl-2, as well as increases caspase-3 activity (Diep et al., 2002; Yang et al., 2014a), thus contributing to cardiomyocyte apoptosis (Goldenberg et al., 2001; Wang et al., 2013). Circulating aldosterone can bind to MR on cardiac fibroblasts, and activation of MR increases pro-fibrotic molecules such as TGF-β1 and connective tissue growth factor, and thereby increases collagen synthesis (Bunda et al., 2007; Cannavo et al., 2018). Aldosterone binding to MR on cardiomyocytes increases NADPH oxidase/ROS/NF-κB pathway, resulting in increases transcription of pro-inflammatory cytokines genes (Brown, 2013). MR activation in cardiomyocytes also enhances Ang II-AT_1R signaling by activation of GRK 2 and GRK5 (Cannavo et al., 2016), and thereby increases NADPH oxidase (Johar et al., 2006; Stas et al., 2007) and ROS (Cannavo et al., 2016).

After MI, vasopressinergic magnocellular neurons in the PVN and SON are also activated, and release AVP through the posterior pituitary gland to the circulation

(Ohbuchi et al., 2015). Circulating AVP acts on vasopressin type 1a receptors (V1aRs) on vascular smooth muscle cells resulting in vasoconstriction, and binds to vasopressin type 2 receptors located in renal collecting ducts, leading to decrease water excretion and fluid retention, which in turn, may lead to hyponatremia (Vinod et al., 2017; Wasilewski et al., 2016). Circulating AVP also binds to V1aR on cardiomyocytes and activates G-protein signaling pathway, followed by phospholipase C (PLC)-protein kinase C (PKC) signaling, increasing immediate early genes (e.g. c-fos, c-myc) and transcription factors (e.g. GATA-4), which contribute to cardiac hypertrophy (Sharma et al., 2007; Wasilewski et al., 2016). AVP binding to V1aR on fibroblasts enhances DNA synthesis, resulting in fibroblast proliferation and increase in collagen synthesis (Szczepanska-Sadowska et al., 2018), promoting cardiac fibrosis.

TNF-α binding to TNFR1 on cardiomyocytes increases apoptotic factors such as Fas- and TNFR1-associated death domains (FADD and TRADD), leading to cardiomyocyte apoptosis (Hedayat et al., 2010). TNF-α increases ROS and NF-κB (Higuchi et al., 2002; Roberge et al., 2014), and sustained activation of NF-κB contributes to cardiomyocyte hypertrophy and fibrosis, as well as further increases in TNF-α, IL-1β and IL-6 (Hamid et al., 2009; Hamid et al., 2010). TNFR1 knockout mice showed less increase in end-systolic and diastolic volume, and less decrease in EF post MI (Hamid et al., 2009), indicating that TNF-α decreases cardiac function post MI via TNFR1. Similarly, high levels of circulating IL-1β induce cardiomyocyte apoptosis and fibrosis (Frangogiannis, 2015; Ono et al., 1998). Altogether, long-term activation of several CNS efferent mechanisms contributes to progressive cardiac remodeling and cardiac dysfunction post MI.

1.2. BDNF, TrkB and BDNF-TrkB signaling pathways

1.2.1. General characteristics of BDNF and TrkB

The rat BDNF gene comprises of eight 5' untranslated exons and one protein coding 3' exon that encodes the proBDNF protein (Aid et al., 2007). 24 different mRNA transcripts can be generated by alternative splicing, but each of them is translated into the identical BDNF protein (Cunha et al., 2010; Greenberg et al., 2009). BDNF mRNA is translated onto a precursor protein (pre-proBDNF) in the endoplasmic reticulum (Greenberg et al., 2009). After cleavage of the signal peptide, a 32 kDa proBDNF is transported to the Golgi, and proBDNF can be converted into a 14 kDa mature BDNF (mBDNF) intracellularly in the trans-Golgi by endoproteases such as furin, or in the immature secretory granules by proconvertases (Greenberg et al., 2009; Mowla et al., 1999). ProBDNF also can be released and cleaved by extracellular proteases including plasmin (Pang et al., 2004) and matrix metalloproteinases (Ethell and Ethell, 2007; Lee et al., 2001). ProBDNF binds to pan-neurotrophin receptor p75 ($p75^{NTR}$) co-expressing with sortilin (Teng et al., 2005), and activates Rac-GTPase, an adaptor protein of $p75^{NTR}$, followed by phosphorylation of c-Jun N-terminal kinase (JNK) and activation of caspase-3 (Koshimizu et al., 2010), resulting in apoptosis of neurons (Hashimoto, 2012; Lu et al., 2005). ProBDNF-$p75^{NTR}$ signaling decreases dendrite branching and its spine density, and thereby decreases synaptic transmission and plasticity (Yang et al., 2014b). In contrast, mBDNF binds to two isoforms of TrkB receptors with similar affinity (Park and Poo, 2012), which are generated by alternative splicing at the transcription level: full-length and truncated forms (Klein et al., 1991; Middlemas et al., 1991). The full-length form of TrkB (TrkB.FL) and truncated forms of TrkB (TrkB.T1 and TrkB.T2 in rats)

have identical extracellular and transmembrane domains and the first 12 amino acids of the intracellular domain, but truncated forms lack intracellular tyrosine kinase domain (Middlemas et al., 1991). TrkB.T1 and TrkB.T2 have 23 and 21 amino acids in the intracellular domain, respectively (Baxter et al., 1997). Physiology and role of mBDNF-TrkB.FL and mBDNF-TrkB.T1 signaling and downstream pathways are further described in section *1.2.4.*

1.2.2. Distribution of BDNF and TrkB in the brain and periphery

In the rat adult brain, BDNF and TrkB mRNA and protein are widely expressed in the hippocampus, hypothalamus and brainstem (Castrén and Kojima, 2017) including SFO, PVN, NTS and RVLM (An et al., 2015; Becker et al., 2016; Chan et al., 2010; Schaich et al., 2018; Schaich et al., 2016). BDNF and TrkB are expressed in neurons and glia (Ferrini and De Koninck, 2013). TrkB.FL and TrkB.T1 are expressed in neurons and microglia (Spencer-Segal et al., 2011), whereas TrkB.T1 is the only form expressed in astrocytes (Aroeira et al., 2015; Saba et al., 2018). The ratio between TrkB.FL and TrkB.T1 shows regional differences in some brain areas (e.g. hippocampus and prefrontal cortex) (Azogu et al., 2018), but there is lack of information on the ratio in brain nuclei associated with cardiovascular regulation. Since TrkB.T1 can compete with TrkB.FL for the binding of mBDNF and mBDNF-TrkB.T1 signaling has a distinctive role in glia (Nagappan and Lu, 2005), regional specific ratio between TrkB.FL and TrkB.T1 may result in different responses on binding of mBDNF. This will be further discussed in section *1.2.4.1*.

In the periphery, BDNF is present in blood either bound to platelets or circulating freely in plasma (Walsh and Tschakovsky, 2018). In rats, BDNF levels are prominent in

endothelial cells of the endocardium in the heart and aorta (Prigent-Tessier et al., 2013) and cardiomyocytes (Okada et al., 2012). BDNF is also expressed in all types of muscle fibers [type I, slow oxidative (e.g. soleus muscle); type II, fast glycolytic (e.g. quadriceps)] and satellite cells in skeletal muscle (Cuppini et al., 2007; Matthews et al., 2009; Mousavi and Jasmin, 2006; Sakuma and Yamaguchi, 2011; Wrann et al., 2013). In general, TrkB.FL mRNA and protein are not detectable in the adult heart and skeletal muscle, although some studies reported their presence at very low levels, but TrkB.T1 is clearly expressed in the heart and skeletal muscles (Fulgenzi et al., 2015; Hurtado et al., 2017; Otani et al., 2017). BDNF-TrkB signaling in the heart will be further discussed in section *1.2.4.3*.

1.2.3. Regulation of BDNF expression and secretion

In the brain, BDNF is regulated by several stimuli. Membrane depolarization triggers BDNF expression and secretion, and increase in neuronal activity by e.g. Ang II or pro-inflammatory cytokines, enhances expression of BDNF (Nagappan and Lu, 2005; Park and Poo, 2012), so-called activity-dependent regulation of BDNF. In cultured hippocampal/cortical neurons, membrane depolarization induced by high K^+ or Ca^{2+} activates cAMP-response element binding protein (CREB), a transcription factor which regulates BDNF gene transcription, and thereby increases BDNF mRNA and protein expression (Kingsbury et al., 2003; Tao et al., 1998). In hypothalamic neurons, an increase in glutamate activates NMDA receptors, and thereby increases BDNF mRNA (Marmigère et al., 2001; Tapia-Arancibia et al., 2004). In contrast, GABA decreases glutamate-induced BDNF mRNA (Marmigère et al., 2003) and a $GABA_A$ receptor antagonist increases BDNF mRNA expression.

The effects of Ang II on regulation of BDNF have been studied in the PVN and RVLM. Subcutaneous infusion of Ang II at low dose (150 ng/kg/min) did not alter BDNF mRNA expression in the RVLM (not reported in the PVN), whereas high dose Ang II (500 ng/kg/min) increased BDNF mRNA in the RVLM, but not in the PVN (Wang et al., 2015). Intracisternal infusion or bilateral microinjection of Ang II into the RVLM activates NADPH oxidase, increases ROS and phosphorylates CREB, and thereby increases BDNF mRNA and protein expression (Chan et al., 2010). Ang II-induced increase in BDNF mRNA appears to be brain nucleus specific.

There are no *in vivo* studies on the effects of pro-inflammatory cytokines on BDNF expression in brain nuclei associated with cardiovascular regulation. Pro-inflammatory cytokines decrease BDNF mRNA and protein in the rat hippocampus (Calabrese et al., 2014; Guan and Fang, 2006; Lapchak et al., 1993), and a recent study showed a negative correlation between TNF-α and BDNF mRNA in the hippocampus of patients with schizophrenia (Zhang et al., 2018).

Exercise increases BDNF mRNA and protein expression in the hippocampus/cortex (Azimi et al., 2018; Uysal et al., 2015; Wrann et al., 2013) and skeletal muscle (Cuppini et al., 2007; Matthews et al., 2009; Zhan et al., 2018), as well as circulating BDNF (Jiménez-Maldonado et al., 2014; Walsh and Tschakovsky, 2018). Skeletal muscle contraction and an elevation in efferent nerve activity increases BDNF mRNA and protein in skeletal muscle (Hurtado et al., 2017; Matthews et al., 2009). Regulation of brain and circulating BDNF by exercise will be further discussed in section *1.4.2.*

1.2.4. Role of BDNF-TrkB signaling

1.2.4.1. General

mBDNF-TrkB.FL and mBDNF-TrkB.T1 signaling have been studied in hippocampal/cortical neuronal and astrocytes cultures, and play distinctive roles in neurons and astrocytes (Fig 1-4). In neurons, mBDNF binds to TrkB.FL and leads to dimerization and autophosphorylation of tyrosine residue targeting 515 (Y515), activates Ras-MAPK/extracellular signal-regulated kinase (ERK) and phosphatidylinositol 3-kinase (PI3K)-protein kinase B (Akt) pathways, and thereby increases neuronal survival (Kowiański et al., 2018; Park and Poo, 2012). mBDNF binding to TrkB.FL also phosphorylates tyrosine residue targeting 816 (Y816) and activates PLCγ-Ca^{2+}/calmodulin-dependent protein kinase II (CaMKII) pathway, thus enhancing synaptic plasticity (Cunha et al., 2010). It is unclear which factors determine phosphorylation of one or both tyrosine sites, followed by activation of specific intracellular downstream signaling pathways. mBDNF also can bind to TrkB.T1, which is co-expressed with TrkB.FL in the same neurons. mBDNF binding to TrkB.T1 in neurons inhibits mBDNF-induced phosphorylation of TrkB.FL by forming heterodimers with TrkB.FL, and thereby inhibits downstream signaling pathways of mBDNF-TrkB.FL (Carim-Todd et al., 2009; Haapasalo et al., 2001).

mBDNF has the same affinity for the two isoforms of TrkB (Nagappan and Lu, 2005; Park and Poo, 2012), and changes in their ratio may therefore affect the intracellular responses to mBDNF (Vidaurre et al., 2013; Wong et al., 2011). A decrease in the TrkB.FL/TrkB.T1 ratio in the hippocampus and cortex has been suggested as a marker for schizophrenia and stroke (Vidaurre et al., 2013; Wong et al., 2011).

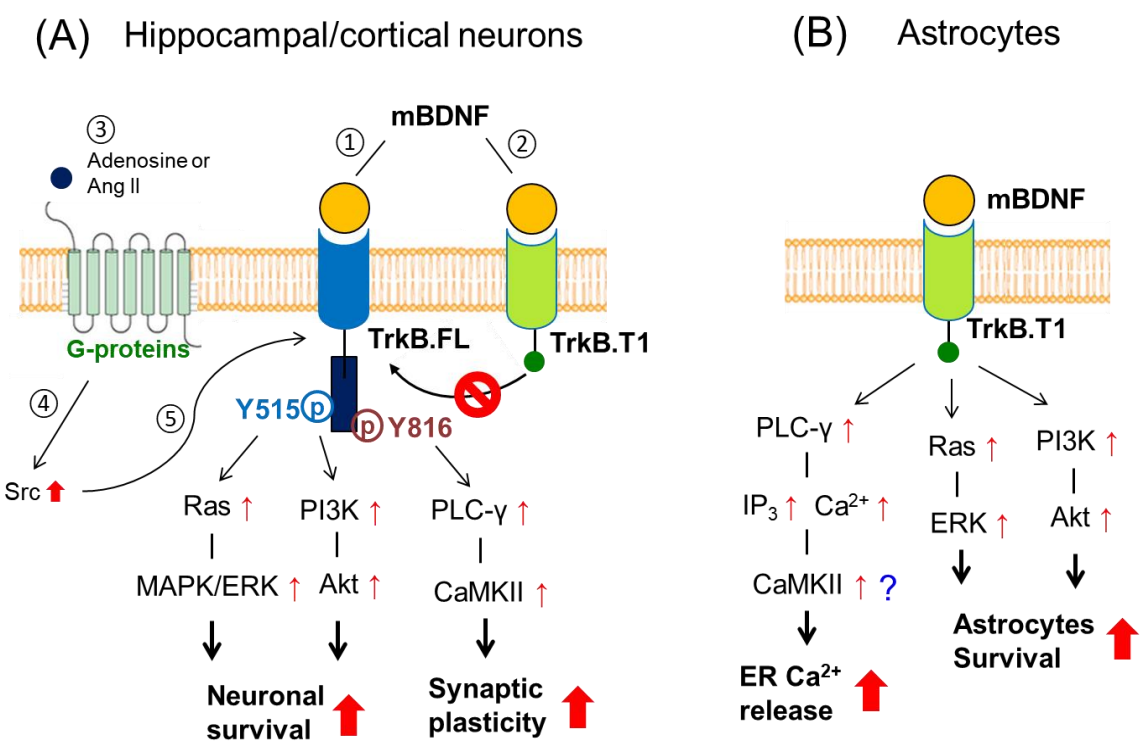
(A) Hippocampal/cortical neurons
(B) Astrocytes
mBDNF
Adenosine or Ang II
G-proteins
TrkB.FL
TrkB.T1
Y515(p)
(p)Y816
Src
Ras ↑
PI3K ↑
PLC-γ ↑
MAPK/ERK ↑
Akt ↑
CaMKII ↑
Neuronal survival
Synaptic plasticity
IP3 ↑ Ca2+ ↑
CaMKII ↑ ?
ER Ca2+ release
ERK ↑
Astrocytes Survival

Figure 1-4. Intracellular pathways of classical mBDNF-TrkB signaling and TrkB transactivation in hippocampal/cortical neurons and astrocytes

(A) Hippocampal/cortical neurons

Classical mature brain-derived neurotrophic factor (mBDNF)-TrkB (tropomyosin-related kinase B) signaling: ① mBDNF can bind to TrkB full-length form (TrkB.FL) or truncated form (TrkB.T1) with the same affinity. mBDNF binding to TrkB.FL phosphorylates the tyrosine residue targeting 515 (Y515) and activates Ras-mitogen-activated protein kinase (MAPK)/ extracellular signal-regulated kinase (ERK) and phosphatidylinositol 3-kinase (PI3K)-protein kinase B (Akt) pathways, leading to increase neuronal survival. Phosphorylation (p-) of the tyrosine residue targeting 816 (Y816) activates phospholipase Cγ (PLCγ)-Ca^{2+}/calmodulin-dependent protein kinase II (CaMKII) pathway, and thereby enhances synaptic plasticity. Determinants of phosphorylation sites and the extent of phosphorylation of each tyrosine residue remain unclear. ② mBDNF binding to TrkB.T1 inhibits phosphorylation of TrkB.FL, leading to down-regulation of intracellular signaling pathways.

TrkB transactivation: TrkB can be activated without mBDNF binding by activation of G-protein coupled receptors (GPCRs). ③ Ligands such as adenosine and angiotensin II (Ang II) binds to their receptors (e.g. adenosine 2a and angiotensin II type 2 receptors) and ④ phosphorylate Src kinase, and thereby ⑤ activates TrkB.FL, followed by intracellular signaling pathways.

(B) Astrocytes

In astrocytes, mBDNF binding to TrkB.T1 activates inositol-1,4,5-triphosphate (IP_3) and Ca^{2+} release from intracellular stores, and thereby increases Ca^{2+} release from endoplasmic reticulum (ER). mBDNF binding to TrkB.T1 also activates ERK and Akt, and thereby enhances astrocyte survival.

In the dorsolateral prefrontal cortex of patients with schizophrenia (postmortem), TrkB.FL mRNA and protein were decreased but TrkB.T1 mRNA and protein were increased, thus the TrkB.FL/TrkB.T1 ratio was lower than healthy controls (Wong et al., 2011). In this study, TrkB.FL mRNA was positively correlated, whereas TrkB.T1 mRNA was negatively correlated with glutamic acid decarboxylase 67 (GAD67), a key enzyme associated with the synthesis of GABA. Low level of GAD67 in the dorsolateral prefrontal cortex is a marker for schizophrenia in humans (Straub et al., 2007). In rats after focal cerebral ischemia induced by cerebral artery occlusion, TrkB.T1 levels in neurons in the cortex, but not in astrocytes, were increased in the ischemic area (evaluated by immunohistochemistry) (Vidaurre et al., 2013). In cultured hippocampal neurons, excitotoxicity induced by high dose of glutamate treatment caused a decrease in the TrkB.FL/TrkB.T1 ratio (Gomes et al., 2012). In cortical neuronal culture, activation of NMDA receptors decreased the TrkB.FL/TrkB.T1 ratio (Vidaurre et al., 2013). Collectively, reduction in the TrkB.FL/TrkB.T1 ratio in neurons indicates down-regulation of mBDNF-TrkB.FL signaling, leading to decrease in synaptic plasticity and neuronal survival. On the other hand, TrkB.FL can be activated without BDNF binding, so called TrkB transactivation. Ligands such as adenosine and Ang II bind to their G-protein coupled receptors [GPCRs (e.g. adenosine 2a receptors and angiotensin II type 2 receptors)], activating Src kinase, which in turn phosphorylates TrkB.FL and intracellular signaling pathways (Boulle et al., 2012; Diniz et al., 2018; Wiese et al., 2007).

mBDNF binding to TrkB.T1 in astrocytes directly activates intracellular signaling pathways independent of TrkB.FL. In mature astrocytes, mBDNF-TrkB.T1 increases inositol-1,4,5-trisphosphate (IP_3)-mediated Ca^{2+} release from intracellular stores (e.g.

endoplasmic reticulum) and increases systolic Ca^{2+} transients (Rose et al., 2003). TrkB.T1 receptors in astrocytes isolated from rat hippocampus sequester BDNF when extracellular BDNF is abundant, store active BDNF in transport vesicles, and release BDNF to extracellular space by exocytosis (Alderson et al., 2000; Fenner, 2012). Recently, it has been reported that in astrocytes cultures, BDNF increases astrocytes viability and decreases terminal deoxynucleotidyl transferase dUTP nick end labeling (TUNEL)-positive astrocytes, which were attenuated by either ERK or Akt inhibitors (Saba et al., 2018). This indicates that activation of mBDNF-TrkB.T1 axis in astrocytes increases intracellular ERK and Akt activities, and thereby enhances viability of astrocytes and prevents astrocytes death.

In the hypothalamus, BDNF plays an important role in regulating body weight and energy homeostasis. Deletion of the BDNF gene in the PVN increased body weight and fat mass in normal mice (An et al., 2015), whereas BDNF infusion into the PVN for 12 days decreased body weight and fat mass (Toriya et al., 2010). The BDNF-TrkB axis dependent regulation of energy homeostasis and body weight is mainly affected by circulating glucose, insulin and leptin levels (Wang et al., 2010). A reduction in these hormones reduces energy homeostasis and body weight, and decreases BDNF, but the downstream pathways and mechanisms have not yet been reported. Toriya et al. (2010) reported that decreases in body weight and fat mass induced by BDNF infusion into the PVN were counteracted by the co-infusion of a corticotrophin-releasing hormone (CRH) receptor antagonist, suggesting that BDNF-induced decrease in body weight and fat mass is mediated by CRH. BDNF-TrkB signaling in the hypothalamus and brainstem is also

associated with regulation of SNA and BP. This will be further discussed in the next section.

1.2.4.2. Role in specific brain nuclei for cardiovascular regulation

In the hypothalamus and brainstem, BDNF regulates SNA, BP and heart rate (HR), but its role appears brain nucleus specific (Fig 1-5). Icv infusion of *N*-(2-{[(hexahydro-2-oxo-1H-azepin-3-yl)amino]carbonyl}phenyl)-benzo[b]thiophene-2-carboxamide (ANA-12), a selective non-competitive antagonist of TrkB (Cazorla et al., 2011), alone did not affect baseline BP and RSNA, indicating that the overall effect of endogenous CNS BDNF-TrkB signaling in the brain is minimal in normal state (Becker et al., 2017). However, icv co-infusion of ANA-12 and Ang II attenuated the Ang II-induced increases in BP and RSNA (Becker et al., 2017). In the hypothalamus of normal rats, microinjection or chronic overexpression of BDNF in the PVN increased BP and HR, as well as tyrosine hydroxylase in the adrenal medulla (a marker for sympathetic activity), suggesting that BDNF contributes to sympathoexcitation (Erdos et al., 2015; Schaich et al., 2016). In contrast, microinjection of BDNF into the SFO decreased BP without affecting HR (Black et al., 2018).

In the brainstem, microinjection of BDNF into the RVLM in rats under anesthesia increased BP without change in HR (Wang and Zhou, 2002). In contrast, intracisternal infusion of BDNF in conscious rats did not alter BP, but attenuated Ang II-induced pressor response (Chan et al., 2010). Knockdown of BDNF gene or blockade of TrkB by K252a, which blocks tyrosine protein kinase activity of the Trk family receptors, in the RVLM increased NADPH oxidase and superoxide anion production, and thereby enhanced Ang II-induced increase in BP (Chan et al., 2010). This indicates that down-

regulation of BDNF-TrkB signaling in the RVLM potentiates the Ang II-induced pressor response. Microinjection of BDNF into the dmNTS decreased BP, HR and RSNA, whereas microinjection of ANA-12 increased these parameters and attenuated baroreflex sensitivity (Becker et al., 2016).

Determinants of these brain nuclei-specific responses of BDNF are largely unclear. Different experimental conditions (e.g. microinjection vs. chronic infusion) of BDNF may show different responses. The increase by exogenous BDNF may not reflect the effects of endogenous BDNF (Park and Poo, 2012). The TrkB.FL/TrkB.T1 ratio may differ in different brain nuclei and cause different responses since the two isoforms of TrkB have the same affinity to BDNF (Nagappan and Lu, 2005; Park and Poo, 2012), but they have their own signaling pathways and mBDNF binding to TrkB.T1 inhibits TrkB.FL downstream signaling pathways. Long-term overexpression of BDNF can actually down-regulate TrkB signaling through a negative feedback loop by depleting TrkB receptors, leading to desensitization to BDNF (Frank et al., 1996; Sommerfeld et al., 2000). Another possible factor could be heterogeneous properties of neurons in different brain nuclei (Black et al., 2018). McIsaac and Ferguson (2017) recently reported that PVN neurons show heterogenous responses to BDNF with 54% of neurons being depolarized, 23% of neurons hyperpolarized and rest of neurons not responding.

Downstream factors of BDNF-TrkB signaling, Akt and CaMKII are present in the PVN and RVLM (Gao et al., 2007b; Li et al., 2017; Sun et al., 2016), but it is unknown whether BDNF-TrkB signaling regulates Akt and CaMKII similar as in the hippocampus. In the PVN of spontaneously hypertensive rats, activation PI3K-Akt and PLCγ-CaMKII pathways contribute to increase in sympathetic activity and BP (Sun et al., 2016; Li et al.,

2017). Microinjection of Ang II into the PVN of normal rats increased lumber SNA and BP, and these increases were attenuated by co-infusion of PI3K (upstream factor of Akt) inhibitor (Buttler et al., 2016). Microinjection of Ang II into the RVLM activates PLC-CaMKII, and thereby increases sympathetic activity and BP (Gao et al., 2007b).

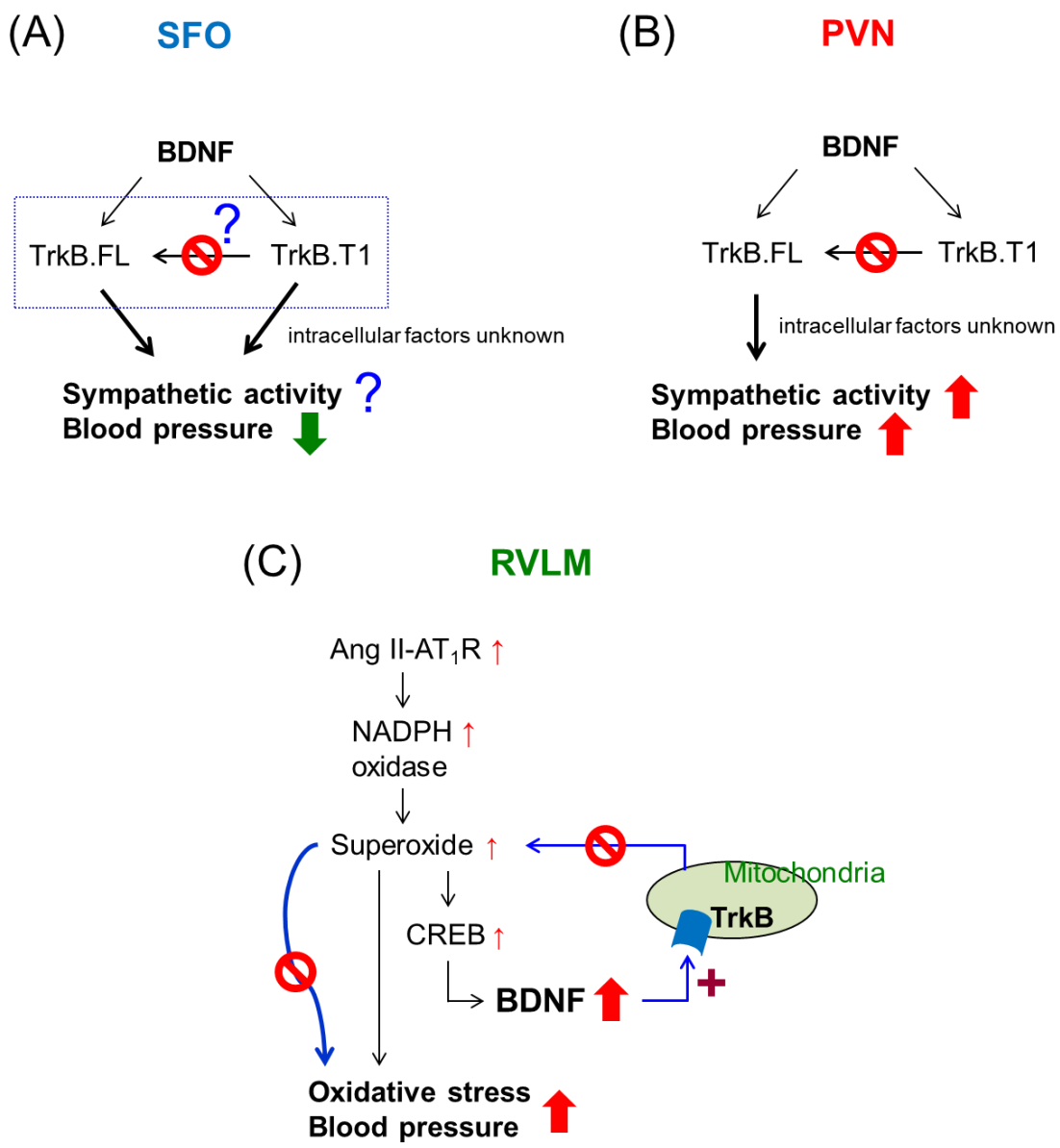
(A)
SFO
BDNF
?
TrkB.FL
TrkB.T1
intracellular factors unknown
Sympathetic activity
Blood pressure
?
(B)
PVN
BDNF
TrkB.FL
TrkB.T1
intracellular factors unknown
Sympathetic activity
Blood pressure
(C)
RVLM
Ang II-AT1R ↑
NADPH ↑
oxidase
Superoxide ↑
Mitochondria
TrkB
CREB ↑
BDNF
+
Oxidative stress
Blood pressure

Figure 1-5. Role of BDNF-TrkB signaling in the SFO, PVN and RVLM for sympathetic activity and blood pressure

(A) Subfornical Organ (SFO)

Microinjection of brain-derived neurotrophic factor (BDNF) into the SFO decreased blood pressure (Black et al., 2018), but it is unclear which isoform of tropomyosin-related kinase B (TrkB) (TrkB.FL, full-length form of TrkB; TrkB.T1; truncated form of TrkB) mediates this response.

(B) Paraventricular nucleus (PVN)

Microinjection of BDNF into the PVN phosphorylates TrkB (tyrosine sites not specified), and increases sympathetic activity and blood pressure (Schaich et al., 2016). The BDNF-induced increase in blood pressure is blocked by overexpression of TrkB.T1 (Schaich et al., 2018), indicating that the effect of BDNF on blood pressure is mediated by TrkB.FL.

(C) Rostral ventrolateral medulla (RVLM)

Activation of angiotensin II (Ang II)-Ang II type 1 receptor (AT_1R) increases NADPH oxidase, followed by superoxide and phosphorylation of cAMP-response element binding protein (CREB), a transcription factor that increases BDNF mRNA. BDNF binds to TrkB in mitochondria and increases mitochondrial uncoupling protein 2 (UCP2), which in turn, attenuates Ang II-induced oxidative stress and pressor response (Chan et al., 2010).

Questions marks in the panel (A) indicate unknown mechanisms.

1.2.4.3. Role in the heart

In vitro studies reported that BDNF increases cell survival and angiogenesis in normal cardiomyocytes or endothelial cells (Cai et al., 2006; Okada et al., 2012). BDNF (100 ng/mL) treatment of normal mouse cardiomyocytes resulted in an increase in phosphorylation of Akt and ERK (peak level at 5 and 15 min, respectively and returned to baseline by 30 min) with a concurrent increase in cell viability (Okada et al., 2012). Cardiac microvascular endothelial cells treated with BDNF showed an increase in migration of these cells, an initial phase of angiogenesis (Cai et al., 2006).

Two *in vivo* studies reported that BDNF-TrkB signaling in the heart is involved in cardiac contractility and relaxation (Feng et al., 2015; Fulgenzi et al., 2015). Feng et al. (2015) reported BDNF increased CaMKII, which leads to an increase in activity of L-type Ca^{2+} channels and Ca^{2+} release from the sarcoplasmic reticulum, and thereby enhances myocardial contractility and relaxation. Fulgenzi et al. (2015) reported that cardiomyocyte-specific deletion of BDNF (myosin 6-specific-cre; Myh6-cre) or TrkB.T1 (Myh6-cre/TrkB.T1^{loxP}) in mice (2–3 month old) caused cardiac dilation with reduced LV wall thickness and inhibition of BDNF-induced inotropic effects. BDNF treatment of isolated cardiomyocytes from wild-type mice increased Ca^{2+} transients, but not in cardiomyocytes isolated from cardiomyocytes-specific TrkB.T1 knockout mice. This indicates BDNF-induced increase in Ca^{2+} transient is mediated by TrkB.T1 (Fulgenzi et al., 2015).

1.3. Regulation of BDNF-TrkB signaling pathways post MI

1.3.1. Alterations in BDNF and TrkB expression post MI in the brain and heart

In mice at 2 weeks post MI, BDNF protein was increased (1.5-fold) in the forebrain (thalamus/hypothalamus) (Okada et al., 2012). In rats at 14 weeks post MI, BDNF mRNA was 2 to 2.5 fold increased in the dmNTS, without change in BDNF protein level, whereas TrkB mRNA and protein were decreased (Becker et al., 2016). Whether a change in the TrkB.FL/TrkB.T1 happens in the PVN and RVLM, and plays a significant role post MI has not yet been reported.

In the non-infact area of the LV of rats, BDNF and TrkB protein were increased at 1 h and 6 h post MI and returned to baseline level at 24 h (Hang et al., 2015). In the infarct area of mice heart, BDNF protein was increased at 1, 3 and 5 days, but normalized at 7 days post MI (Halade et al., 2013). Hong et al. (2014) showed that in rats, in the infarct and peri-infarct areas of the LV, BDNF protein in cardiomyocytes transiently increased at 1 day post MI, whereas BDNF protein in macrophages remained increased up to 7 days post MI (assessed by immunohistochemistry). In mice at 2 weeks post MI, BDNF protein was markedly decreased in the whole heart (Okada et al., 2012), whereas in rats at 6 weeks post MI, BDNF protein was higher in the whole heart than in Sham rats (Katare et al., 2009). Wang et al. (2018) reported that in rats, BDNF protein was decreased and TrkB protein was increased in the ischemic heart zone of the LV at 9 weeks post MI (Wang et al., 2018). Moreover, an increase in plasma BDNF level was found at 6 h and 2 weeks post MI in mice (Hang et al., 2015; Okada et al., 2012). In patients with HF, plasma BDNF levels were significantly lower than in healthy subjects (Takashio et al., 2015), and serum/plasma BDNF levels were negatively correlated with severity of HF

and adverse outcomes (Fukushima et al., 2015; Takashio et al., 2015). In the heart, changes in BDNF and TrkB appear therefore dependent on areas of the LV and different type of cardiac cells, as well as different time points. Acutely, mBDNF protein is increased in cardiomyocytes in the infarct and peri-infarct areas, but gradually decreased up to 1 week post MI, but mBDNF protein remains increased in macrophages. In the chronic phase, mBDNF protein is decreased in the infarct, but there is no information on changes in peri- and non-infarct areas.

1.3.2. Role of BDNF-TrkB signaling post MI in the brain and heart

In mice, brain specific deletion of BDNF gene resulted an increase in cardiac fibrosis by 40% and a further decrease in EF by 30–40% post MI (Okada et al., 2012), suggesting that brain BDNF plays a cardioprotective role. In mice, intramyocardial injection of recombinant BDNF (1 day prior to MI) increased anti-apoptotic factor Bcl-2 mRNA and protein expression, and attenuated increases in TUNEL-positive cells and caspase-3 activity in cardiomyocytes at 3 days post MI (Hang et al., 2015). BDNF also reduced infarct size by 40% and improved EF by 30% at 3 days post MI (Hang et al., 2015). In contrast in mice, deletion of cardiomyocyte specific TrkB (isoforms not specified) increased fibrosis and TUNEL-positive cardiomyocytes in the peri-infarct area of the LV at 2 weeks post MI, and further decreased EF by 20% (Okada et al., 2012). Altogether, activation of brain and cardiac BDNF-TrkB signaling may attenuate cardiomyocyte apoptosis in the heart, leading to attenuation of cardiac remodeling and dysfunction post MI.

1.4. Effects of exercise training post MI

1.4.1. Effects of exercise training post MI and contributing mechanisms

Exercise training attenuates sympathetic hyperactivity and progressive cardiac remodeling and dysfunction post MI in both patients and animals with HF. During exercise, contracting skeletal muscle synthetizes IL-6, the primary myokine (muscle-derived pro-inflammatory cytokine) (Gleeson et al., 2011; Pedersen and Fischer, 2007). Muscle-derived IL-6 is released to the circulation after cessation of exercise and triggers production of anti-inflammatory cytokines such as IL-10 in regulatory T cells and macrophages, and IL-1 receptor antagonist (IL-1RA) in monocytes and macrophages (Gleeson et al., 2011). IL-10 binds to cardiac IL-10 receptor (IL-10R) and activates signal transducer and activator of transcription 3 (STAT3), the transcription factor which suppress transcription of TNF-α and IL-1β (Krishnamurthy et al., 2009; Murray, 2005), and decreases in TNF-α and IL-1β ultimately reduce their secretion to the circulation (Nunes et al., 2013). IL-1RA binds to IL-1 receptor type I (IL-1R1) in cardiomyocytes, and thereby blocks IL-1α and IL-1β binding to this receptor, preventing activation of IL-1/IL-1R1 signaling pathways (Frangogiannis, 2015; Vecile et al., 2013).

In patients with HF, exercise reduced the elevated resting muscle SNA (Roveda et al., 2003) and plasma NE levels (Passino et al., 2006). In rats, exercise post MI attenuated the increase in RSNA and decreased circulating NE (Kleiber et al., 2008; Zheng et al., 2012b). The exercise-induced decrease in circulating pro-inflammatory cytokines will lead to less binding to their receptors in the SFO (Wei et al., 2017; Wei et al., 2015), which reduces local production of pro-inflammatory cytokines, and attenuation of Ang II-AT_1R signaling in the SFO (Simpson and Ferguson, 2018). Exercise post MI decreases

neuronal activity and AT_1R immunoreactivity in the SFO (Llewellyn et al., 2014), and this may lead to decrease in neuronal activity in the PVN and RVLM, and attenuate activation of central angiotensinergic pathways post MI.

Several mechanisms in the PVN and RVLM have been suggested to contribute to reduction in neuronal activity in the PVN and RVLM, and in sympathoexcitation by exercise training in rodents post MI. In the PVN and RVLM, exercise normalizes the increases in GRK5, a protein responsible for phosphorylation of AT_1R, and NF-κB, a transcription factor associated with the up-regulation of AT_1R (Haack et al., 2012), which in turn, decreases AT_1R expression (Haack et al., 2012; Zheng et al., 2012b; Zucker et al., 2014). It is still unclear how exercise reduces the increased GRK5 post MI. Exercise-induced normalization of AT_1R results in reduced NADPH oxidase activity (decrease in phosphorylation of subunits of NADPH oxidase) and increased superoxide dismutase (Gao et al., 2007a). These changes lead to normalization of the down-regulated neuronal nitric oxide synthase mRNA and protein levels (Zheng et al., 2005), and the enhanced glutamatergic and decreased GABAergic mechanisms post MI (Kleiber et al., 2008; Patel et al., 2013), and thereby decrease neuronal activity in the PVN (Shen et al., 2018; Zheng et al., 2012b) and RVLM (Ichige et al., 2016).

Exercise post MI also decreases circulating Ang II (Llewellyn et al., 2014; Wan et al., 2007) and aldosterone (Wan et al., 2007). The mechanisms responsible for these decreases are not clear, but it is possible that exercise-induced reduction in RSNA attenuates the activated systemic RAAS, and thereby reduces circulating Ang II and aldosterone (Waldman et al., 2017). Reductions in circulating Ang II and aldosterone attenuate their role in progressive cardiac remodeling and dysfunction by less activation

of their receptors in CVOs such as the SFO and the organum vasculosum of the lamina terminalis (OVLT) as discussed above, as well as in the heart. In the LV, exercise decreased ACE mRNA expression, ACE binding and AT_1R protein (Xu et al., 2008b), as well as collagen content (Nunes et al., 2013), and attenuated myocardial fibrosis. Furthermore, exercise post MI increased Bcl-2 protein, but decreased Bax and caspase-3 proteins in the LV (Lu et al., 2015), indicating that exercise decreases cardiomyocyte apoptosis. Exercise increases the decrease in β-AR density in the LV post MI by reduction in GRK2, which leads to β-AR desensitization, indicating that exercise improves the down-regulated β-AR signaling, and thereby enhances myocardial contractility (Leosco et al., 2007). Decrease in scar thinning (Puhl et al., 2015) and less accumulation of collagen content (Nunes et al., 2013; Xu et al., 2008b) may contribute to increase in ventricular compliance, and thereby improves diastolic function. Several studies reported that early initiation (1–2 weeks post MI) of exercise training attenuates the decrease in EF and the increase in LV end-diastolic pressure (LVEDP) post MI (Cai et al., 2016; Wang et al., 2018; Xu et al., 2008a; Xu et al., 2008b), indicating that exercise training improves both systolic and diastolic functions. In contrast, some studies started the first exercise session at 3–4 weeks post MI and did not observe improvements in these parameters (Kleiber et al., 2008; Patel et al., 2013; Zheng et al., 2012b).

In addition, Ang II and pro-inflammatory cytokines regulate BDNF, and exercise-induced activation of BDNF-TrkB signaling may contribute to the beneficial effects of exercise training post MI.

1.4.2. Effect of exercise training on BDNF-TrkB signaling pathways

Effect of exercise training on brain BDNF-TrkB signaling pathways has been reported mainly in the hippocampus of rodents. 5–7 days free wheel running or treadmill exercise in rats increased mBDNF and phosphorylated (p-)TrkB protein levels, as well as downstream signaling factors including p-Akt, p-ERK and p-CaMKII in the hippocampus (Ding et al., 2011; Fang et al., 2013). In rats, a 4-week treadmill exercise in rats increased BDNF protein without change in p-CaMKII (Dao et al., 2015), and in mice, 5 weeks free wheel running increased BDNF protein [assessed by enzyme-linked immunosorbent assay (ELISA)] and TrkB in astrocytes in the dentate gyrus (DG) of the hippocampus (evaluated by immunohistochemistry) (Fahimi et al., 2017). Activation of hippocampal BDNF-TrkB signaling pathways by exercise training contributes to learning and memory (Griffin et al., 2009; Vaynman et al., 2004). For example, exercise in mice increased BDNF protein and neurogenesis in the DG of the hippocampus (Choi et al., 2018). Injection of a specific immunoadhesin chimera of TrkB (TrkB-IgG) in the hippocampus, which mimics TrkB receptor and thereby blocks BDNF binding to the endogenous TrkB receptor, prevented the exercise-induced increase in BDNF mRNA (Vaynman et al., 2004). In mice lacking TrkB gene in the hippocampus, exercise did not increase neurogenesis (Li et al., 2008). In exercising rats, escape latency in the Morris water maze test, which indicates spatial learning, was shorter, and time spent in the target quadrant, which evaluates long-term memory, was longer than in sedentary rats (Uysal et al., 2015; Vaynman et al., 2004). These effects were absent in TrkB chimera treated rats (Vaynman et al., 2004). Collectively, exercise activates BDNF-TrkB signaling in the hippocampus and contributes to learning and memory by enhancement of neurogenesis.

Mechanisms through which exercise contributes to increase in hippocampal BDNF have not fully elucidated. Two exercise metabolites, a ketone body D-β-hydroxybutyrate (DBHB) and lactate, have been suggested as peripheral factors contributing to increase BDNF in the hippocampus (El Hayek et al., 2019; Sleiman et al., 2016). During exercise, blood glucose level is decreased due to increase in glucose demand of working skeletal muscle, and thereby ketone bodies are produced in the liver from fatty acids to serve as an energy source (Evans et al., 2017). Sleiman et al. (2016) reported that exercise increased plasma DBHB, leading to increase in DBHB in the hippocampus. The increase in DBHB inhibits histone deacetylase (HDAC), and thereby enhances acetylation of histone, which in turn increases transcription of BDNF gene in the hippocampus (Sleiman et al., 2016). El Hayek et al. (2019) reported that lactate, an end product of glycolysis (Rogatzki et al., 2015), is released into the blood during exercise and crosses the BBB. In the brain, lactate may be transported to the hippocampal neurons through monocarboxylate transporter 2 (MCT2), a proton-linked plasma membrane transporter, and thereby activates Sirtuin 1 (SIRT1), NAD^+-dependent deacetylase. SIRT1 increases peroxisome proliferator-activated receptor γ coactivator-1α (PGC-1α) protein, followed by fibronectin type III domain-containing protein 5 (FNDC5) protein, a glycosylated type I membrane protein, and thereby increases BDNF mRNA expression in the hippocampus (El Hayek et al., 2019). FNDC5 also can be produced in skeletal muscle by exercise and secreted into blood as irisin after proteolytic cleavage (Boström et al., 2012), and irisin appears to increase BDNF in the hippocampus (Wrann et al., 2013). However, molecular mechanisms how irisin increases BDNF in the hippocampus remain unknown.

Only one study reported the effect of exercise on BDNF in the PVN (Noble, 2014). In aged rats (1 year old), 5 days wheel running significantly increased BDNF immunoreactivity. However, 8 weeks wheel running or treadmill exercise did not affect BDNF and TrkB immunoreactivity (Noble, 2014). There are no studies on the effects of exercise on BDNF-TrkB signaling in the RVLM.

One bout of exercise in healthy humans increases circulating BDNF by 60%, and returned to baseline level after 15–60 min of exercise (Dinoff et al., 2017; Huang et al., 2014b; Knaepen et al., 2010; Szuhany et al., 2015). Regular chronic exercise (3 months to 1 year) increases resting circulating BDNF in healthy humans with the average of 38% (Dinoff et al., 2016; Huang et al., 2014b; Seifert et al., 2010). In normal rats, a 8-week period of moderate (60% of VO_2 max; the maximum rate of oxygen consumption during exercise) or high (80% of VO_2 max) intensities of treadmill exercise significantly increased plasma BDNF by 40% without differences in intensity of exercise (Jiménez-Maldonado et al., 2014). The brain is the major source of circulating BDNF at rest and during exercise, as measured by differences in plasma BDNF in arterial and jugular vein (jugular-arterial difference) (Seifert et al., 2010; Walsh and Tschakovsky, 2018). After 3 months of endurance exercise, jugular-arterial difference of plasma BDNF at rest was higher than control group (Seifert et al., 2010).

In skeletal muscle of rats, 5-day treadmill exercise increased BDNF mRNA and protein in the soleus muscle (Cuppini et al., 2007), but not in rats exercised for 10 days (Ogborn and Gardiner, 2010). Surprisingly, in rat soleus muscle, increases in BDNF mRNA and protein were observed at 7 and 14 days, after a single bout of treadmill exercise (Yu et al., 2017). An increase in BDNF in skeletal muscle after a single bout of

exercise activates AMP-activated protein kinase (AMPK), and thereby improves muscle energy metabolism by enhancing fat oxidation (Matthews et al., 2009), and more chronically after a single bout of exercise appears not only to enhance muscle energy metabolism, but also increases muscle regeneration by activation of satellite cells, which contributes to skeletal muscle growth (Yu et al., 2017). Zhang et al. (2019) reported that in soleus muscle of mice, BDNF mRNA and protein expression were decreased at 12 weeks post MI, but was normalized by exercise. Muscle-derived BDNF in response to a single bout of exercise does not appear to be released into the circulation and acts as autocrine/paracrine manner within skeletal muscle, because a significant elevation of serum BDNF was observed 2 h after an exercise and normalized at 24 h, but a significant increase in mBDNF protein in the skeletal muscle cells (assessed by immunohistochemistry) was only found at 24 h, but not at 3 h, after exercise (Matthews et al., 2009). However, it is unclear whether chronic exercise increases skeletal muscle BDNF and is released to circulation, and thereby contributes to increase in circulating BDNF at rest.

There are two studies reporting the effects of exercise on cardiac BDNF and TrkB. In normal rats, 7 days treadmill exercise did not change cardiac mBDNF protein, but exercise normalized the decrease in mBDNF in spontaneously hypertensive rats (Prigent-Tessier et al., 2013). In rats at 9 weeks post MI, BDNF protein was decreased and TrkB protein was increased in the ischemic heart zone of the LV, and 8 weeks treadmill exercise (the first exercise was initiated at 1 week post MI) normalized the decrease in BDNF protein without affecting the increase in TrkB protein (Wang et al., 2018). In this study, K252a prevented the exercise-induced improvement of EF, but it is unclear

whether this effect is TrkB specific because K252a can block other Trk family receptors (e.g. TrkA and TrkC) as well.

1.5. Rationale

1.5.1. Summary of BDNF-TrkB signaling in cardiovascular regulation

BDNF and TrkB are expressed in the heart (Okada et al., 2012). Treatment of cardiomyocytes of rodents with BDNF promotes cardiomyocyte survival and enhances cardiomyocyte contractility (Feng et al., 2015; Okada et al., 2012), whereas cardiac specific deletion of TrkB gene deteriorates cardiac dysfunction post MI (Okada et al., 2012). BDNF and TrkB are also expressed in the PVN and RVLM (An et al., 2015; Castren et al., 1995). Microinjection or chronic overexpression of BDNF in the PVN of normal rats increases sympathetic activity, BP and HR (Erdos et al., 2015; Schaich et al., 2016). Similarly, microinjection of BDNF into the RVLM increases arterial pressure measured by cannulation in the left femoral artery of normal rats under anesthesia (Wang and Zhou, 2002). In contrast, knockdown of BDNF gene in the RVLM potentiates Ang II-induced increase in BP, and BDNF infusion attenuates the Ang II-induced pressor response (Chan et al., 2010). These findings indicate that BDNF-TrkB signaling in the PVN and RVLM is associated with cardiovascular regulation, but its role may be different in different brain nuclei and experimental conditions.

Exercise training activates BDNF-TrkB signaling in the hippocampus (Fang et al., 2013; Wrann et al., 2013) which contributes to learning, memory and mood (Griffin et al., 2009; Vaynman et al., 2004). Exercise training increases circulating and skeletal muscle BDNF (Cuppini et al., 2007; Jiménez-Maldonado et al., 2014). Only one study reported

that in rats post MI, 8 weeks treadmill exercise normalized the decrease in mBDNF protein in the ischemic heart zone and serum BDNF (Wang et al., 2018).

1.5.2. Unknown questions

It has not yet been studied whether 1) MI alters BDNF-TrkB signaling in the viable area of the LV and 2) exercise training post MI increases BDNF in the viable area of the LV and skeletal muscle. If so, 3) whether exercise-induce increase in BDNF-TrkB signaling in the viable area of the LV attenuates cardiac dysfunction post MI. There are no reports on 4) effects of MI on BDNF-TrkB signaling in the PVN or RVLM and 5) whether exercise training post MI affects BDNF-TrkB signaling and intracellular factors in the PVN and RVLM.

1.6. Hypotheses

1.6.1. General hypothesis

Exercise training enhances BDNF-TrkB signaling pathways in the LV and RVLM, but inhibits in the PVN post MI, and thereby preserves cardiac function post MI.

1.6.2. Specific hypotheses

Chapter 2: Exercise training post MI increases FNDC5 and BDNF expression in parallel in skeletal muscle and in the LV, and the increase in cardiac BDNF correlates with the improvement of cardiac function by exercise.

Chapter 3: Exercise-induced increase in mBDNF and downstream effectors (Akt, CaMKII and AMPK) in the LV are prevented by a TrkB blocker, and thereby limits improvement of cardiac function by exercise.

Chapter 4: Exercise training post MI inhibits BDNF-TrkB signaling in the PVN and activates in the RVLM, and chronic treatment of a TrkB blocker limits these effects.

1.7. Objectives

To determine

1) Effects of MI and exercise training post MI on cardiac function, and BDNF-TrkB signaling in periphery (skeletal muscle and LV) and brain nuclei (PVN and RVLM)

2) Impact of systemic TrkB blockade on BDNF-TrkB signaling in the LV and brain nuclei, and on cardiac dysfunction post MI with or without exercise training.

1.8. Outline of each chapter

Chapter 2: Assessment of BDNF and TrkB mRNA and protein levels in the LV (non-, peri- and infarct areas) at 2 and 5 weeks post MI with or without exercise training

Chapter 3: Assessment of changes in BDNF-TrkB signaling in the non-infarct area of the LV at 5 weeks post MI and effect of exercise training with or without TrkB blockade

Chapter 4: Assessment of alterations in BDNF-TrkB signaling in the PVN and RVLM at 5 weeks post MI with or without TrkB blockade or exercise training

1.9. Future implication

Understanding the actions of BDNF-TrkB signaling in the heart, PVN and RVLM post MI and exercise post MI may provide new perspectives on brain-heart interactions to attenuate progressive cardiac dysfunction in patients with HF. This may lead to new therapeutic strategies including development of “gymno-mimetic” drugs for patients who cannot exercise.

Chapter 2

Effects of exercise training on brain-derived neurotrophic factor in skeletal muscle and heart of rats post myocardial infarction

Effects of exercise training on brain-derived neurotrophic factor in skeletal muscle and heart of rats post myocardial infarction

Heow Won Lee, Monir Ahmad, Hong-Wei Wang, Frans H.H. Leenen

Hypertension Unit, University of Ottawa Heart Institute, Ottawa, Ontario, Canada

Running Title: Cardiac brain-derived neurotrophic factor post myocardial infarction

First published: January 9, 2017, *Exp Physiol* **102**, 314–328

New Findings

- **What is the central question of this study?**

Exercise training increases brain-derived neurotrophic factor (BDNF) in the hippocampus, which depends on a myokine, fibronectin type III domain-containing protein 5 (FNDC5). Whether exercise training after myocardial infarction (MI) induces parallel increases in FNDC5 and BDNF expression in skeletal muscle and the heart has not yet been studied.

- **What is the main finding and its importance?**

Exercise training after myocardial infarction increases BDNF protein in skeletal muscle and the non-infarct area of the LV without changes in FNDC5 protein, suggesting that BDNF is not regulated by FNDC5 in skeletal muscle and heart. An increase in cardiac BDNF may contribute to the improvement of cardiac function by exercise training.

Abstract

Exercise training after myocardial infarction (MI) attenuates progressive left ventricular (LV) remodelling and dysfunction, but the peripheral stimuli induced by exercise that trigger these beneficial effects are still unclear. We investigated as possible mediators fibronectin type III domain-containing protein 5 (FNDC5) and brain-derived neurotrophic factor (BDNF) in the skeletal muscle and heart. Male Wistar rats underwent either sham surgery or ligation of left descending coronary artery, and surviving MI rats were allocated to either a sedentary (Sed-MI) or an exercise group (ExT-MI). Exercise training was done for 4 weeks on a motor-driven treadmill. At the end, LV function was evaluated, and *FNDC5* and *BDNF* mRNA and protein were assessed in soleus muscle, quadriceps and non-, peri- and infarct areas of the LV. At 5 weeks post MI, *FNDC5* mRNA was decreased in soleus muscle and all areas of the LV, but FNDC5 protein was increased in the soleus muscle and the infarct area. Mature BDNF (mBDNF) protein was decreased in the infarct area without change in mRNA. Exercise training attenuated the decrease in ejection fraction and the increase in LV end-diastolic pressure post MI. Exercise training had no effect on *FNDC5* mRNA and protein, but increased mBDNF protein in soleus muscle, quadriceps and the non-infarct area of the LV. The mBDNF protein in the non-infarct area correlated positively with ejection fraction and inversely with LV end-diastolic pressure. In conclusion, mBDNF is induced by exercise training in skeletal muscle and the non-infarct area of the LV, which may contribute to improvement of muscle dysfunction and cardiac function post MI.

Introduction

After myocardial infarction (MI), sympathetic hyperactivity, inflammatory responses, including increases in pro-inflammatory cytokines [e.g. tumour necrosis factor-α (TNF-α), interleukin-1β (IL-1β) and interleukin-1 (IL-6)] and activation of angiotensin II (Ang II)-type 1 receptor (AT_1R) signalling in the infarct, peri-infarct and non-infarct areas of the left ventricle (LV) (Nio *et al.* 1995; Ono *et al.* 1998), contribute to cardiomyocyte apoptosis, fibrosis and progressive LV remodelling and dysfunction (Sam *et al.* 2000; Sutton & Sharpe, 2000; Palojoki *et al.* 2001; Rafatian *et al.* 2014).

Exercise training improves quality of life and reduces the risk of hospital admissions in patients with heart failure (HF) by decreasing neurohormonal activity and improving cardiorespiratory fitness (Gielen *et al.* 2015). Early initiation of exercise training post MI in rodents down-regulates the expression of angiotensin-converting enzyme (ACE) and AT_1R protein (Xu *et al.* 2008*a,b*), and reduces *TNF-α*, *IL-1β* and *IL-6* mRNA in the LV (Puhl *et al.*, 2015). Exercise training post MI increases anti-apoptotic factor Bcl-2 protein, and decreases pro-apoptotic factors Bax and caspase-3 protein in the LV (Lu *et al.* 2015). Exercise attenuates the progressive cardiac remodelling and decrease in ejection fraction (EF) post MI (Xu *et al.* 2008*a,b*). The peripheral stimuli induced by exercise that trigger these beneficial effects of exercise training on the heart are still unclear.

In rats, brain-derived neurotrophic factor (BDNF) protein is transiently increased in cardiomyocytes in infarct and peri-infarct areas early post MI (Hong *et al.* 2014), and in the whole LV at 6 weeks post MI (Katare *et al.* 2009). Cardiac BDNF may play a cardioprotective role post MI by inhibiting apoptosis in ischemic myocardium. In mice, intramyocardial injection of recombinant BDNF (1 day before MI) increased *Bcl-2*

mRNA and protein expression, and attenuated increases in terminal deoxynucleotidyl transferase dUTP nick end labeling (TUNEL)-positive cells and caspase-3 activity in cardiomyocytes at 3 days post MI. This treatment with BDNF also reduced infarct size by 40% and improved EF by 30% at 3 days post MI (Hang *et al.* 2015). In contrast, deletion of cardiomyocyte-specific tropomyosin-related kinase B (TrkB), the binding receptor of BDNF, further increased fibrosis and TUNEL-positive cardiomyocytes in the peri-infarct area of the LV at 2 weeks post MI, and further decreased EF by 20% (Okada *et al.* 2012). These results suggest that activation of cardiac BDNF–TrkB signaling attenuates cardiomyocyte apoptosis and improves cardiac function post MI.

It is well established that exercise training increases BDNF expression in the hippocampus (Neeper *et al.* 1996; Fang *et al.* 2013; Wrann *et al.* 2013), which plays a beneficial role for learning and memory (Vaynman *et al.* 2004; Griffin *et al.* 2009). The increase in hippocampal BDNF after exercise training appears to be initiated by up-regulation of fibronectin type III domain-containing protein 5 (FNDC5) in the hippocampus, possibly by the myokine irisin released into the circulation from skeletal muscle FNDC5 (Wrann *et al.* 2013). In skeletal muscle, BDNF is released by contracting muscle cells and improves skeletal muscle metabolism by increasing fat oxidation (Matthews *et al.* 2009), but it is unknown whether this increase is FNDC5 dependent. *FNDC5* mRNA is also highly expressed in normal hearts (Wrann *et al.* 2013), but its function in adult hearts and its relationship with cardiac BDNF have not yet been investigated. Whether exercise training in animals with HF post MI affects FNDC5, BDNF and TrkB expression in skeletal muscle and the heart, and these changes contribute to attenuating progressive cardiac dysfunction is unknown. Skeletal muscle is

the principal contributor to exercise-induced physiological adaptations (Egan & Zierath, 2013), and FNDC5 in skeletal muscle might be the primary stimulus for exercise-induced changes in BDNF not only in the hippocampus, but also in skeletal muscle and the heart. We hypothesized that exercise training post MI increases in parallel FNDC5 and BDNF expression in skeletal mucle and the heart, and the increase in cardiac BDNF correlates with the improvement in cardiac function by exercise.

The aims of the study were therefore to determine the following: (i) the time course of changes in FNDC5, BDNF and TrkB in the heart at 2 and 5 weeks post MI; and (ii) the effects of exercise training on cardiac function and on *FNDC5*, *BDNF*, and *TrkB* mRNA and protein in skeletal muscle and the heart post MI. Exercise training was done for 4 weeks, which is commonly used for rats (Zheng *et al.* 2012*b*). In the LV, *FNDC5*, *BDNF* and *TrkB* expression was measured separately in non-infarct, peri-infarct and infarct areas because regional differences exist in gene expression between peri-infarct and remote non-infarct regions during LV remodelling post MI (Loennechen *et al.* 2001).

Methods

Ethical Approval

All experiments were approved by the University of Ottawa Animal Care Committee, and conform to the *Guide for the Care and Use of Laboratory Animals* published by the US National Institutes of Health (8th Edition, 2011).

Animals

Male Wistar rats weighing 200–250 g (Charles River, Montreal, QC, Canada) were allowed to acclimate for 5–7 days in a room maintained at a constant temperature and humidity. Rats were housed under a 12 h–12 h light–dark cycle with standard laboratory chow and tap water *ad libitum*.

For induction of MI, slow-release buprenorphine (1 mg kg^{-1}) (Chiron Compounding Pharmacy Inc., Guelph, ON, Canada) was injected s.c. 1–2 h before surgery, which provides adequate analgesia for 3 days. Anaesthesia was induced with a 2% mixture of isoflurane and oxygen in a transparent chamber. Anaesthetized rats were intubated with a 51 mm long and 1.7 mm diameter polyethylene tube and connected to a Harvard Rodent Respirator (Harvard Apparatus Co., Holliston, MA, USA) set to a frequency of 75 strokes min^{-1} of 2.0 ml volume. Thoracotomy was performed via the fourth intercostal space. The pericardium was opened and the left anterior descending (LAD) coronary artery permanently ligated 1–2 mm distal to its origin with a 6–0 silk suture on an atraumatic needle. The fourth and fifth ribs were closed by two separate 4.0 vicryl sutures. Lungs were inflated and air was removed from the thoracic cavity. Isoflurane was stopped and rats remained ventilated with 100% oxygen until waking up or breathing spontaneously. Sham-operated animals underwent a similar procedure except for ligation of LAD

coronary artery. Rats with a small MI (<20% of LV) and minimal or no LV dysfunction at the end of the study were excluded from further analyses.

Experimental groups

The experimental time line is outlined in Fig. 2-1. A total of 103 rats were used for this study. For the 5 week study, after LAD coronary artery ligation (n = 56), the 32 surviving MI rats were randomly divided into either a sedentary (Sed-MI) or an exercise group (ExT-MI). Among 17 Sed-MI rats, seven rats had a small MI. Fifteen rats were allocated to ExT-MI, but five rats refused to run and one rat had a small MI (<20% of LV). Rats refusing to run had similar cardiac dysfunction as the overall sedentary group. Therefore, 10 rats for the Sed-MI and nine rats for the ExT-MI group are included in the final analyses for this study. A sedentary sham-operated group (n = 7) served as control group.

To obtain some insights into the time course of cardiac changes post MI, sedentary rats were also studied at 2 weeks post sham or MI surgery. Twenty-seven rats underwent LAD coronary artery ligation and 16 rats survived, of which eight rats had small MI. Thus, eight rats were included in the MI group and seven rats in the Sham group.

Exercise training protocol and citrate synthase activity assay

An exercise programme was conducted for a period of 4 weeks (5 days week^{-1}), which is commonly used for rats, as described by Zheng *et al.* (2012*b*). The exercise was started 5–7 days after recovery from the chest surgery and every session was conducted after 12.00 h. For the first 3 days of the first week, rats were trained to exercise on a motor-driven treadmill (Columbus Instruments, Columbus, OH, USA) at low speed (10 m min^{-1}), gradient 0%, for a short duration (10–15 min day^{-1}) to familiarize the rats with running. On days 4–5 of the first week and second week of exercise, the speed, gradient and

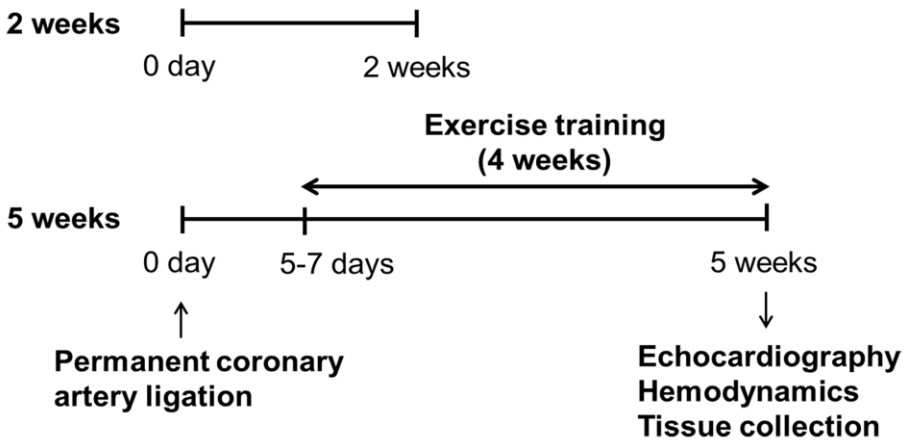

Figure 2-1. Experimental time line

The 2 and 5 weeks post myocardial infarction (MI) studies were done separately. For the 5 weeks post MI study, exercise training was initiated 5–7 days after permanent coronary artery ligation and continued for 4 weeks. Cardiac function was evaluated at 2 and 5 weeks post MI.

duration were gradually increased to 20 m min^{-1}, 5–10% and 60 min day^{-1}, respectively. In the third and fourth weeks, maximal levels were maintained constantly. This level of exercise is considered moderate for rats (Zheng *et al.* 2012*b*). The sedentary rats were handled daily and treated similar manner to the exercising rats except that the treadmill was not put in motion.

To test exercise efficiency, citrate synthase activity was measured spectrophotometrically from homogenates of soleus muscle. Total muscle protein content was determined by bicinchoninic acid (BCA) assay using bovine serum albumin standards (Thermo Scientific Inc., Rockford, IL, USA). The total reaction mixture was prepared according to the manufarcture's instruction (CS0720; Sigma-Aldrich, St Louis, MO, USA). Baseline absorbance was recorded and reactions were initiated by adding the 10 μl of 10 mM oxaloacetate (OAA), and the change in absorbance was monitored at a wavelength of 410 nm at 25°C at 30 s intervals for a period of 3 min. Citrate synthase activity was measured by calculating the difference in OAA reaction absorbance change to the baseline absorbance change.

Echocardiographic and hemodynamic measurements

Echocardiography was done under 2% isoflurane and oxygen anaesthesia 2–3 h after the last exercise session. A VisualSonic Vevo 770 system (VisualSonics, Toronto, ON, Canada) was used to analyze functional parameters of the heart. In M-mode recording, internal dimensions of the LV in systole and diastole were measured, and EF was calculated. Haemodynamic measurements were done under 2% isoflurane and oxygen anaesthesia in the morning the day after echocardiography. A Millar catheter was inserted into the LV via the right carotid artery. Two minutes later, this catheter was connected to

a Harvard Data Acquisition system, interfaced with a PC, using AcqKnowledge III software. The level of anaesthesia was gradually reduced to the point when rats just started responding to the toe pinch. At this point, LV peak systolic pressure (LVPSP), LV end-diastolic pressure (LVEDP) and $dP/dt_{max/min}$ (maximal/minimal rate of pressure change) were measured for 30–60 s.

Tissue collection

Trunk blood and tissues (hearts, quadriceps and soleus muscle) were collected the day after haemodynamic measurements, within 48 h of the last exercise session. After decapitation, trunk blood was collected into a prechilled 50 ml conical tube containing heparin. Blood was centrifuged at 1,935 *g* at 4°C for 30 min and plasma collected for BDNF assay. The hearts were immediately removed and placed in ice-cold saline. The right ventricle (RV) was separated from the LV. The LV was opened flat through a long cut on the septum and additional 2–3 small cuts on the apex. The LV was placed under a transparent sheet and its circumference and the MI borders were traced, and then snap-frozen in liquid nitrogen. To measure the infarct size, the LV demarcation on the transparent sheet was scanned and its digital image quantified using Image Pro 6.2. The infarct size is expressed as a percentage of the total LV area.

Both soleus muscle and quadriceps were selected since skeletal muscle adaptation to exercise differs by muscle fibre types (Egan & Zierath, 2013). Soleus muscle and quadriceps were snap-frozen in liquid nitrogen. All tissues and plasma samples were stored at –80 ºC until further analysis.

Isolation of RNA and real-time qPCR for FNDC5, BDNF, TrkB, AT_1R and TNF-α

The LV was separated into non-infarct (3–4 mm away from infarct area), peri-infarct (1–2 mm away from infarct area) and infarct areas (Rafatian *et al.* 2014). Total RNA was extracted from each area of the LV, soleus muscle and quadriceps with 1 ml QIAzol Lysis Reagent (Qiagen Inc., Mississauga, ON, Canada). After DNase I (Thermo Scientific Inc.) treatment, 5 μg of total RNAs were reverse transcribed into cDNA with oligo dT primers (Thermo Scientific Inc.) and Superscript II RNase H reverse transcriptase (Thermo Scientific Inc.) at 42°C for 60 min. The specific primers for phosphoglycerate kinase 1 (*PGK1*), *FNDC5*, *BDNF*, *TrkB*, AT_1R and *TNF-α* (Table 2-1) were designed based on the published Genbank sequences. Primers and PCR conditions for *PGK1* and AT_1R were the same as previously described (Wang *et al.* 2010; Chen *et al.* 2014). Real-time PCR was performed using LightCycler 480 SYBR Green I (Roche Diagnostics, Laval, QC, Canada). The PCR conditions were set as follows: an initial step at 95°C for 10 min, followed by 45 cycles of denaturation at 95°C for 10 s; annealing for 15 s at 57ºC for *BDNF* and *FNDC5*, 59ºC for *TrkB* and *TNF-α*; and extension at 72°C for 15 s.

The standard curve method was used to determine the mRNA levels of *FNDC5*, *BDNF*, *TrkB*, AT_1R and *TNF-α*, followed by normalization using the housekeeping gene *PGK1*. In order to generate the standard curves, the following PCR fragments were amplified: 316 bp PCR fragment corresponding to position 208–523 (*FNDC5*), 165 bp fragment at 1212–1372 position (*BDNF*), 197 bp fragment at 1502–1698 position (*TrkB*), and 113 bp fragment at 542–654 (*TNF-α*). The PCR products of various genes were purified and then subcloned into pCRII-TA vector (Invitrogen, Burlington, ON, Canada).

Table 2-1. Primer sequences used for gene expression analysis

Target gene		Primer sequence (5' − 3')	Amplicon length (bp)
PGK1	Forward	GCTGCAGAACTCAAATCTCT	268
	Reverse	TGTGTGCAGTCCCAAAAGCA	
FNDC5	Forward	CAGCAGAAGAAGGATGTGAG	316
	Reverse	GGCAGAAGAGAGCTATGACA	
BDNF	Forward	CGAGACCAAGTGTAATCCCATG	165
	Reverse	CAGGAAGTGTCTATCCTTATGAACC	
TrkB	Forward	CAAGACTCTGTGAACCTCACTG	197
	Reverse	TCCGTGTGATTGGTGACGTGTA	
AT_1R	Forward	GCACACTGGCAATGTAATGC	385
	Reverse	GTTGAACAGAACGTGACC	
TNF-α	Forward	GGCTGTACCTTATCTACTC	113
	Reverse	GCTGACTTTCTCCTGGTATG	

Plasmid containing target DNA fragment was verified by restriction endonuclease analysis and PCR analysis using specific primers. The concentrations of the plasmids were measured via NanoDrop spectrophotometry at 260 nm. An external standard curve for each gene was created using serial 10-fold dilutions (e.g. from 100 to 0.001 pg μl^{-1}) of plasmid in the same real-time PCR conditions. The mRNA expression level of each gene was represented as the ratio of target gene and *PGK1*. As the *PGK1* mRNA level was downregulated in the infarct area, mRNA expression for all areas of the LV is shown as the absolute value of each gene per total 5 μg of RNA initial input used to generate cDNA.

Western blotting

Immunoblotting was performed using 30–50 μg of total protein from each area of the LV, soleus muscle and quadriceps. Samples were homogenized in ice-cold modified RIPA buffer (50 mM Tris pH 8.0, 150 mM NaCl, 0.5% sodium deoxycholate, 1% NP-40, 1 mM EDTA pH 8.0, and 0.1% SDS) containing 1% protease inhibitor cocktail (Sigma-Aldrich). The homogenate was centrifuged at 10,000*g* for 30 min at 4°C, the supernatant was collected and the protein concentration measured using the BCA assay (Thermo Scientific Inc.). Proteins were separated by SDS-PAGE (12% gel for BDNF, 10% gel for FNDC5 and 8% gel for TrkB), and transferred onto 0.2 μm PVDF membranes (Bio-Rad, Mississauga, ON, Canada). After blocking for 1 h with 5% milk in Tris-buffered saline with Tween-20 (TBST) at room temperature, the membranes were probed with rabbit polyclonal anti-BDNF (1:1000, ANT-010; Alomone Labs, Jerusalem, Israel) or anti-FNDC5 (1:5000, ab174833; Abcam, Toronto, ON, Canada) or anti-TrkB (1:1,000, 07–225, Millipore, Toronto, ON, Canada) at 4°C overnight. Then the blots were incubated

with goat anti-rabbit IgG-HRP (1:5000, SC-2004, Santa Cruz Biotechnology, Dallas, TX, USA) for 1 h at room temperature. After washing, the blot was developed with Clarity Western ECL Substrate (Bio-Rad) and visualized with a ChemiDoc XRS+ imager (Bio-Rad). Band densities were quantified using Image Lab software (Bio-Rad). The membranes were reprobed with anti-Glyceraldehyde-3-phosphate dehydrogenase (GAPDH) (1:10,000, MAB374; Millipore) as a protein loading control. The expression of each protein was calculated as the ratio of its band density relative to the density of the GAPDH band in the same sample. Although GAPDH is a common housekeeping protein to control for protein loading, its level varies in certain diseased tissues (Ferguson *et al.* 2005) and we found that GAPDH was significantly downregulated in the infarct area of the LV. Therefore, for the LV, Ponceau S (P7170; Sigma-Aldrich) staining was used to assess equal loading, which is considered more reliable as a loading control than housekeeping protein levels in diseased tissues (Thacker *et al.* 2016), and the measured band density for each protein was used.

Plasma BDNF assay

Total BDNF in plasma was measured using a commercial enzyme-linked immunosorbent assay kit (CYT306; Millipore), which has a range of detection from 15 to 1000 pg ml^{-1}. All samples were measured in duplicate. One hundred microlitres of BDNF standards and plasma samples were added to a 96-well plate, and the plate was incubated overnight at 4°C. After washing the plate with the wash buffer, 100 μl of the diluted biotinylated mouse anti-BDNF monoclonal antibody (1:1000) was added to each well. The plate was incubated at room temperature for 2 h and 100 μl of the diluted streptavidin-HRP conjugate solution (1:1000) was added to each well, then incubated for 1 h. After

washing the plate, 100 µl of TMB/E substrate was added to each well. The reaction was stopped with stop solution and the absorbances of BDNF standards and samples were read at 450 nm. A standard curve was plotted as known concentration of BDNF standards on the *x*-axis and the corresponding absorbances on the *y*-axis, and BDNF concentrations in plasma samples were determined.

Statistical analyses

Comparisons between two groups were tested with Student's unpaired *t* test, and for three or more groups, by one-way analysis of variance (ANOVA) followed by Bonferroni *post hoc* test. To compare time course changes (2 and 5 weeks of Sham and Sed-MI groups), two-way ANOVA was done with Bonferroni *post hoc* test. Correlations analyses were performed by Pearson's correlation analysis. A value of $P < 0.05$ was considered statistically significant.

Results

Effect of exercise training on cardiac function

At 2 and 5 weeks post MI, body weight did not differ compared with Sham groups (Table 2-2). By two-way ANOVA, there were no interactions between the effect of MI and time points on cardiac function. All parameters were significantly different between Sham and MI groups. Both LV and RV weight were increased post MI (Table 2-2). Systolic and diastolic diameters were increased by 75–100 and 20–30%, respectively, and EF decreased by 27–34% (Table 2-2). The LVEDP was increased to 15.5 ± 4.2 mmHg at 2 weeks and 21.2 ± 10 mmHg at 5 weeks, and LVPSP and dP/dt_{max} and dP/dt_{min} were decreased, indicating marked cardiac dysfunction post MI.

In the ExT-MI group, MI size was somewhat less (not significant) compared with Sed-MI (Table 2-2). In the ExT-MI group, LV weight was increased a similar extent as Sed-MI, but RV weight was only modestly increased (Table 2-2). Left ventricular dimensions tended to be less increased, and EF was significantly less decreased compared with the Sed-MI group ($P < 0.05$). The increase in LVEDP was markedly attenuated in the ExT-MI group ($P < 0.01$ *versus* Sed-MI), but there was no significant effect of exercise on dP/dt_{max} and dP/dt_{min} (Table 2-2). These results indicate that exercise training attenuates cardiac dysfunction post MI.

Table 2-2. General characteristics and echocardiographic and haemodynamic measurements at 2 and 5 weeks post MI, and effect of exercise training at 5 weeks post MI

	Sham	Sed-MI	ExT-MI
Body weight (g)			
2 weeks	349 ± 18	364 ± 26	n.d.
5 weeks	490 ± 24	477 ± 41	460 ± 14
MI size (% of LV)			
2 weeks	—	28 ± 5	n.d.
5 weeks	—	30 ± 6	25 ± 4
LV weight [mg (100g BW)$^{-1}$]			
2 weeks	194 ± 11	205 ± 18**	n.d.
5 weeks	180 ± 13	203 ± 14**	204 ± 11**
RV weight [mg (100g BW)$^{-1}$]			
2 weeks	50 ± 4	60 ± 14**	n.d.
5 weeks	40 ± 5	69 ± 29**	52 ± 7
Echocardiographic parameters			
Systolic diameter (mm)			
2 weeks	3.6 ± 0.6	6.3 ± 0.8**	n.d.
5 weeks	3.5 ± 0.4	7.0 ± 0.9**	5.9 ± 1.3**
Diastolic diameter (mm)			
2 weeks	7.1 ± 0.6	9.1 ± 0.7**	n.d.
5 weeks	7.7 ± 0.6	10.0 ± 0.8**	9.4 ± 1.3*
Ejection fraction (%)			
2 weeks	77 ± 6	56 ± 8**	n.d.
5 weeks	84 ± 3	54 ± 8**	65 ± 7**††
Haemodynamic parameters			
LVPSP (mmHg)			
2 weeks	115 ± 9	107 ± 10**	n.d.
5 weeks	117 ± 9	109 ± 5**	109 ± 8**
LVEDP (mmHg)			
2 weeks	2.6 ± 1.3	15.5 ± 4.2**	n.d.
5 weeks	2.9 ± 1.2	21.2 ± 10**	9.9 ± 3.5††
dP/dt_{max} (mmHg s^{-1})			
2 weeks	7343 ± 393	5240 ± 572**	n.d.
5 weeks	6946 ± 590	5123 ± 890**	5809 ± 645*
dP/dt_{min} (mmHg s^{-1})			
2 weeks	6076 ± 555	4127 ± 675**	n.d.
5 weeks	5958 ± 829	3986 ± 837**	4530 ± 565**
Soleus muscle weight at 5 weeks [mg (100g BW)$^{-1}$]	50 ± 3	47 ± 5	49 ± 3
Citrate synthase activity at 5 weeks [nmol (mg protein)$^{-1}$ min^{-1})]	425 ± 44	445 ± 48	537 ± 49**††

Abbreviations: Sed-MI, sedentary MI; ExT-MI, exercise MI; BW, body weight; dP/dt_{max}, maximal first derivative of change in pressure over time; dP/dt_{min}, minimal first derivative of change in pressure over time; LV, left ventricle; LVEDP, left ventricular end-diastolic pressure; LVPSP, left ventricular peak systolic pressure; MI, myocardial infarction; n.d., not determined; and RV, right ventricle. Values are means ± SD. For 2 weeks, Sham, $n = 7$; and MI, $n = 8$. For 5 weeks, Sham, $n = 7$; Sed-MI, $n = 10$; and ExT-MI, $n = 9$. Two-way ANOVA was done for time course changes in Sham and MI. For LV weight, group, $F = 11.2$, $P < 0.01$; for RV weight, group, $F = 11.3$, $P < 0.01$; for systolic diameter, group, $F = 139.2$, $P < 0.001$; for diastolic diameter, group, $F = 80$, $P < 0.001$; for ejection fraction, group, $F = 115.2$, $P < 0.001$; for LVPSP, group, $F = 7.8$, $P < 0.01$; for LVEDP, group, $F = 61.8$, $P < 0.001$; for dP/dt_{max}, group, $F = 77.8$, $P < 0.001$; and for dP/dt_{min}, group, $F = 59.4$, $P < 0.001$. None of the group × time point interactions was significant. Time points were significant only for diastolic diameter ($F = 10.5$, $P < 0.01$). One-way ANOVA followed by Bonferroni *post hoc* test was done for the effect of exercise training at 5 weeks post MI. For LV weight, $F = 7.4$, $P < 0.01$; for RV weight, $F = 4.7$, $P < 0.05$; for systolic diameter, $F = 24.0$, $P < 0.001$; for diastolic diameter, $F = 9.8$, $P < 0.01$; for ejection fraction, $F = 36.1$, $P < 0.001$; for LVEDP, $F = 14.4$, $P < 0.001$; for dP/dt_{max}, $F = 10.9$, $P < 0.01$; and for dP/dt_{min}, $F = 12.5$, $P < 0.001$. *$P < 0.05$ and **$P < 0.01$ *versus* Sham. $^{\dagger\dagger}P < 0.01$ *versus* Sed-MI.

Effect of exercise training on FNDC5, BDNF and TrkB mRNA and protein expression in skeletal muscle

At 5 weeks post MI, in sedentary rats (Sed-MI) the soleus muscle weight did not differ compared with the Sham group (Table 2-2). The exercise training did not affect body weight or soleus muscle weight (Table 2-2). In the soleus muscle, citrate synthase activity, an indicator of cellular aerobic metabolism, was ~30% higher in ExT-MI compared with sedentary rats (Sham and Sed-MI; $P < 0.01$ *versus* Sham and $P < 0.05$ *versus* Sed-MI; Table 2-2).

At 5 weeks post MI, in the soleus muscle of sedentary rats, *FNDC5* mRNA expression was decreased ($P < 0.05$), whereas FNDC5 protein was increased eightfold compated with Sham ($P < 0.05$; Fig. 2-2*A*). *BDNF* mRNA and mature BDNF (mBDNF) protein, and *TrkB* mRNA and a truncated form of TrkB protein (TrkB.T1) were not affected (Fig. 2-2*A*). In the quadriceps, *FNDC5* and *BDNF* mRNA and protein were not different in MI rats compared with Sham (Fig. 2-2*B*). In contrast, *TrkB* mRNA was threefold higher in Sed-MI ($P < 0.05$ *versus* Sham), but TrkB.T1 protein was not changed (Fig. 2-2*B*).

In the soleus muscle, exercise training post MI did not affect the reduction in *FNDC5* mRNA and the increase in FNDC5 protein (Fig. 2-2*A*). *BDNF* mRNA was not altered by exercise, but mBDNF protein was significantly higher than in Sham group ($P < 0.05$; Fig. 2-2*A*). *TrkB* mRNA was not affected by exercise training, whereas TrkB.T1 protein was significantly increased compared with Sed-MI ($P < 0.05$; Fig. 2-2*A*). In the quadriceps, *FNDC5* mRNA and protein and *BDNF* mRNA were unchanged by exercise training, but mBDNF protein significantly increased by 60% compared to Sed-MI ($P < 0.05$; Fig. 2-2*B*). *TrkB* mRNA and TrkB.T1 protein were not affected by exercise training.

There were no correlations between *FNDC5* and *BDNF* mRNA and/or protein in the soleus muscle and quadriceps. These results indicate that after MI, FNDC5 protein increases in the soleus muscle, but not in the quadriceps, without changes in BDNF and TrkB protein. Exercise training significantly increases BDNF protein (but not mRNA) in both soleus muscle and quadriceps.

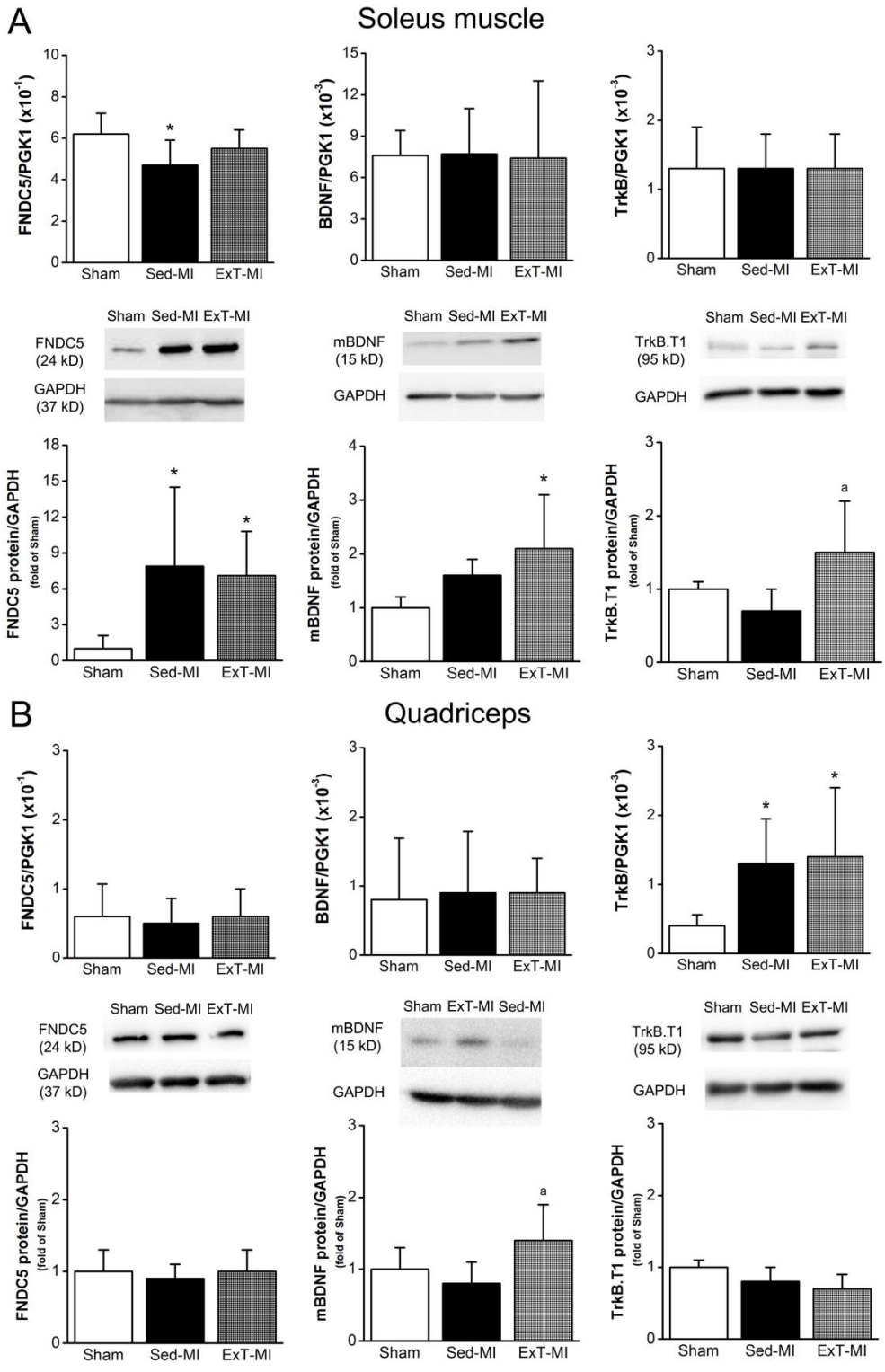
A
Soleus muscle
FNDC5/PGK1 (x10-1)
BDNF/PGK1 (x10-3)
TrkB/PGK1 (x10-3)
Sham Sed-MI ExT-MI
FNDC5 (24 kD)
GAPDH (37 kD)
mBDNF (15 kD)
GAPDH
TrkB.T1 (95 kD)
GAPDH
FNDC5 protein/GAPDH (fold of Sham)
mBDNF protein/GAPDH (fold of Sham)
TrkB.T1 protein/GAPDH (fold of Sham)
B
Quadriceps
Sham ExT-MI Sed-MI

Figure 2-2. *FNDC5*, *BDNF* and *TrkB* mRNA and protein expression in skeletal muscle at 5 weeks post MI with or without exercise training

Fibronectin type III domain containing 5 (*FNDC5*), brain derived-neurotrophic factor (*BDNF*) and tropomyosin-related kinase B receptor (*TrkB*) mRNA and protein in the soleus muscle (*A*) and quadriceps (*B*) of Sham and MI rats with (ExT-MI) or without exercise (Sed-MI). For soleus muscle and quadriceps mRNA, and mBDNF protein in quadriceps: Sham, $n = 7$; Sed-MI, $n = 10$; and ExT-MI, $n = 9$. For FNDC5 and TrkB.T1 (truncated form of TrkB) protein, $n = 6$ per group. Values are means ± SD. Statistical analysis was by one-way ANOVA followed by Bonferroni *post hoc* test. For soleus muscle: *FNDC5* mRNA, $F = 4.1$, $P < 0.05$; FNDC5 protein, $F = 2.9$, $P = 0.09$ (Sham *versus* allMI, Student's unpaired *t* test, $P < 0.05$); mature BDNF (mBDNF) protein, $F = 3.8$, $P < 0.05$; and TrkB.T1 protein, $F = 4.7$, $P < 0.05$. For quadriceps: *TrkB* mRNA, $F = 3.3$, $P = 0.06$ (Sham *versus* all MI, Student's unpaired *t* test, $P < 0.05$); and mBDNF protein, $F = 3.8$, $P < 0.05$. *$P < 0.05$ *versus* Sham. [a]$P < 0.05$ *versus* Sed-MI.

Effect of exercise training post MI on FNDC5, BDNF, TrkB, AT_1R and TNF-α mRNA and protein expression in the LV

At 2 weeks post MI, *FNDC5* mRNA tended to be lower in the peri-infarct area ($P = 0.06$) and significantly lower in the infarct area compared with Sham and other areas ($P < 0.01$; Table 2-3). At 5 weeks post MI, *FNDC5* mRNA in all areas of the LV was lower than Sham, the most in the infarct area (Table 2-3). In contrast, at 5 weeks post MI, FNDC5 protein was fourfold increased in the infarct area (Fig. 2-3*B*). For *BDNF* mRNA, no changes were observed at 2 and 5 weeks post MI (Table 2-3). At 5 weeks post MI, mBDNF protein in non- and peri-infarct areas was also not changed, but was significantly decreased in the infarct area (Fig. 2-4*B*). *TrkB* mRNA was increased twofold in the infarct area at both 2 and 5 weeks post MI ($P < 0.01$ *versus* Sham and other areas; Table 2-3), and at 5 weeks post MI, TrkB.T1 protein was also increased twofold in the infarct area ($P < 0.05$ *versus* Sham; Fig. 2-5*B*). At 2 and 5 weeks post MI, AT_1R mRNA was markedly increased in the infarct area ($P < 0.01$ *versus* Sham and other areas; Table 2-3). *TNF-α* mRNA was increased in the infarct area compared with the non-infarct area at 2 weeks post MI ($P < 0.01$; Table 2-3) and higher in the peri-infarct area compared with non-infarct and infarct areas at 5 weeks (Table 2-3).

Exercise training did not affect the decrease in *FNDC5* mRNA or the increase in FNDC5 protein in the infarct area (Fig. 2-3*A* and *B*). Exercise training significantly increased *BDNF* mRNA in the peri-infarct area ($P < 0.01$) and mBDNF protein in the non-infarct area ($P < 0.05$) compared with Sed-MI, but did not affect *BDNF* mRNA or protein in the infarct area (Fig 2-4*A* and *B*). Exercise training had no effect on *TrkB*

mRNA and protein (Fig. 2-5*A* and *B*), as well as *AT_1R* and *TNF-α* mRNA in all areas (Table 2-3).

These results indicate that the infarct area shows prominent changes after MI, including an increase in FNDC5 protein and TrkB.T1 protein, but decrease in mBDNF protein. Exercise training post MI does not affect these proteins in the infarct area, but significantly increases mBDNF protein in the non-infarct area.

The mBDNF protein in the non-infarct area was correlated positively with EF (r = 0.76, $P < 0.001$) and negatively with LVEDP (r = –0.55, $P < 0.05$; Fig. 2-6). FNDC5 protein did not correlate with BDNF mRNA or protein.

Plasma BDNF in the Sed-MI group was not different from the Sham group, but exercise training tended to increase plasma BDNF (F = 3.2, P = 0.06; Fig. 2-7).

Table 2-3. *FNDC5*, *BDNF*, *TrkB*, *AT$_1$R* and *TNF-α* mRNA expression in the LV at 2 and 5 weeks post MI, and effect of exercise training at 5 weeks post MI

	Sham	MI		
		Non-infarct	Peri-infarct	Infarct
FNDC5 mRNA per 5 μg RNA (x10^{-1})				
2 weeks	6.1 ± 0.8	5.6 ± 1.4	4.4 ± 1.2	1.9 ± 0.9**††
5 weeks	8.5 ± 1.6	5.4 ± 1.3**	3.6 ± 0.9**‡	1.8 ± 1.1**††
BDNF mRNA per 5 μg RNA (x10^{-2})				
2 weeks	16 ± 9.8	12 ± 9.3	18 ± 3.7	8.5 ± 3.5
5 weeks	10 ± 3.7	8.5 ± 3.3	9.3 ± 0.8	8.1 ± 3.3
TrkB mRNA per 5 μg RNA (x10^{-3})				
2 weeks	9.8 ± 2.4	6.5 ± 2.5	10 ± 4.3	23 ± 5.4**††
5 weeks	7.9 ± 2.1	6.2 ± 2.4	9.7 ± 4.2	16 ± 6.8**††
AT$_1$R mRNA per 5 μg RNA (x10^{-2})				
2 weeks	5.3 ± 1.3	3.4 ± 1.2	7.1 ± 3.2	27 ± 5.5**††
5 weeks	3.1 ± 0.5			
Sed-MI		3.3 ± 0.6	5.5 ± 1.3	20 ± 8.2**††
ExT-MI		3.8 ± 1.2	6.0 ± 0.9**	20 ± 5.8**
TNF-α mRNA per 5 μg RNA (x10^{-2})				
2 weeks	1.8 ± 0.7	1.4 ± 0.6	2.1 ± 0.3	2.3 ± 0.5‡‡
5 weeks	2.1 ± 0.1			
Sed-MI		1.7 ± 0.3	2.4 ± 0.6^{a}	1.6 ± 0.6
ExT-MI		1.9 ± 0.5	2.8 ± 0.6	1.9 ± 0.6

Abbreviations: Sed-MI, sedentary MI; ExT-MI, exercise MI; AT$_1$R, angiotensin II-type 1 receptor; BDNF, brain-derived neurotrophic factor; FNDC5, fibronectin type III domain-containing protein; TNF-*α*, tumour necrosis factor-*α*; and TrkB, tropomyosin-related kinase B. Values are means ± SD. For 2 weeks, Sham, $n = 7$; and MI, $n = 8$. For 5 weeks, Sham, $n = 7$; Sed-MI, $n = 10$; and ExT-MI, $n = 9$. Two-way ANOVA was done for time course changes in Sham and MI. For *FNDC5*, group, $F = 55.8$, $P < 0.001$; group × time points, $F = 4.6$, $P < 0.01$; for *BDNF*, group, $F = 3.2$, $P < 0.05$; time points, $F = 10.3$, $P < 0.01$; for *TrkB*, group, $F = 26.3$, $P < 0.001$; time points, $F = 4.7$, $P < 0.05$; for *AT$_1$R*, group, $F = 85.9$, $P < 0.001$; time points, $F = 7.0$, $P < 0.05$; for *TNF-α*, group, $F = 5.0$, $P < 0.01$; and group × time points, $F = 3.4$, $P < 0.05$. One-way ANOVA followed by Bonferroni *post hoc* test was done for the effect of exercise training at 5 weeks post MI in each area of the LV. For *AT$_1$R*, peri-infarct, $F = 15.5$, $P < 0.001$; and infarct, $F = 16.7$, $P < 0.001$. **$P < 0.01$ *versus* Sham. $^{\dagger}P < 0.05$ and $^{\dagger\dagger}P < 0.01$ *versus* other areas. $^{\ddagger}P < 0.05$ and $^{\ddagger\ddagger}P < 0.01$ *versus* non-infarct area.

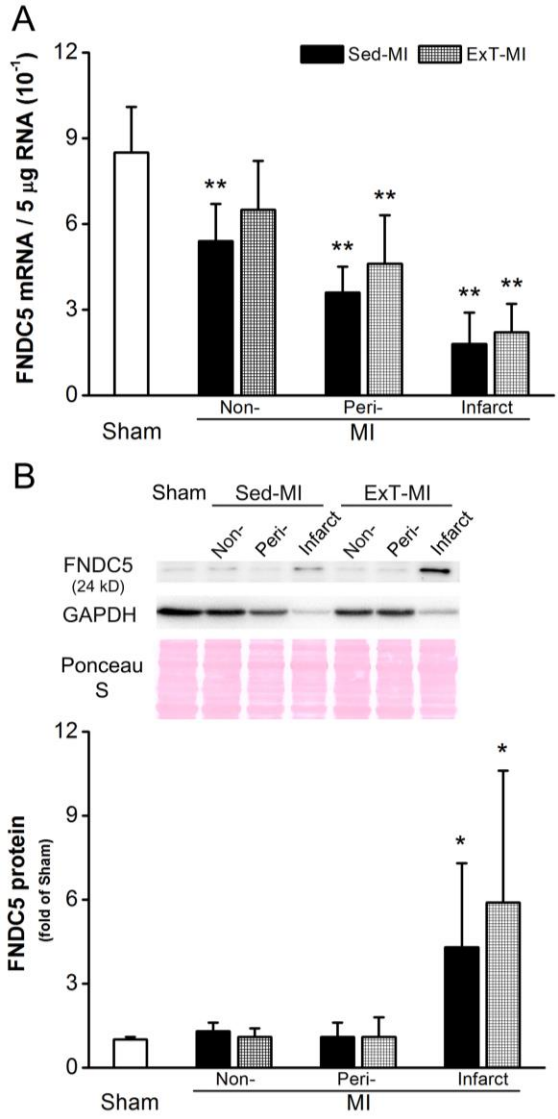

Figure 2-3. *FNDC5* mRNA and protein expression in the left ventricle (LV) at 5 weeks post MI with or without exercise

FNDC5 mRNA (*A*) and protein (*B*) in the LV of Sham and MI rats with (ExT-MI) or without exercise (Sed-MI). For mRNA; Sham, $n = 7$; Sed-MI, $n = 10$; and ExT-MI, $n = 9$. For protein, $n = 6$ per group. Values are means ± SD. Statistical analysis was by one-way ANOVA followed by Bonferroni *post hoc* test in each area. For *FNDC5* mRNA: non-infarct, $F = 7.4$, $P < 0.01$; peri-infarct, $F = 21.9$, $P < 0.001$; and infarct, $F = 61.8$, $P < 0.001$. For FNDC5 protein: infarct, $F = 3.0$, $P = 0.08$ (Sham *versus* all MI, Student's unpaired *t* test, $P < 0.05$). *$P < 0.05$ and **$P < 0.01$ *versus* Sham. Ponceau S staining is shown as the loading control.

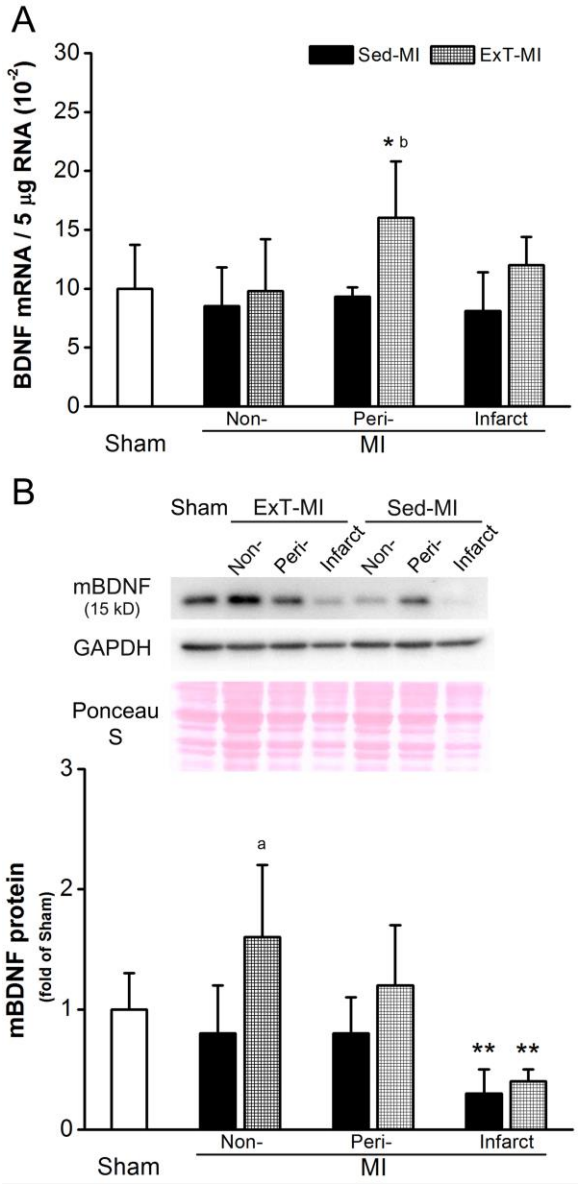

Figure 2-4. *BDNF* mRNA and protein expression in the LV at 5 weeks post MI with or without exercise *BDNF* mRNA (*A*) and mBDNF protein (*B*) in the LV of Sham and MI rats with (ExT-MI) or without exercise (Sed-MI). For mRNA and protein: Sham, $n = 7$; Sed-MI, $n = 10$; and ExT-MI, $n = 9$. Values are means ± SD. Statistical analysis was by one-way ANOVA followed by Bonferroni *post hoc* test in each area. For BDNF mRNA: peri-infarct, $F = 7.6$, $P < 0.01$. For mBDNF protein: non-infarct, $F = 5.8$, $P < 0.05$; and infarct, $F = 18.6$, $P < 0.001$. *$P < 0.05$ and **$P < 0.01$ *versus* Sham. [a]$P < 0.05$ and [b]$P < 0.01$ *versus* Sed-MI. Ponceau S staining is shown as the loading control.

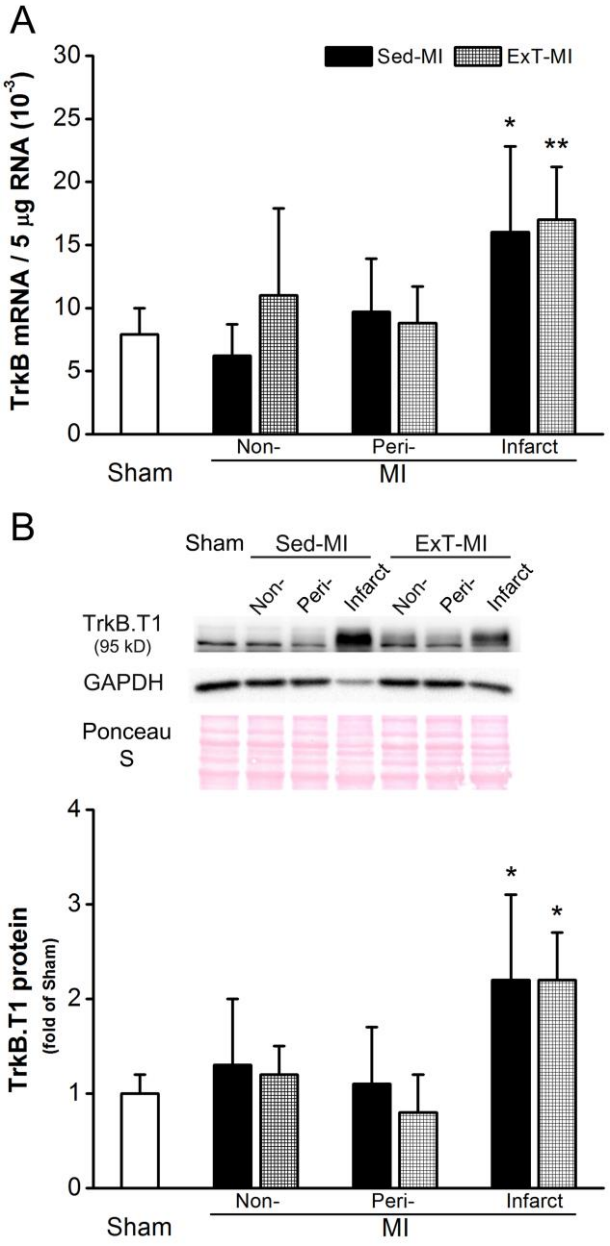

Figure 2-5. *TrkB* mRNA and protein expression in the LV at 5 weeks post MI with or without exercise

TrkB mRNA (*A*) and protein (*B*) in the LV of Sham and MI in rats with (ExT-MI) or without exercise (Sed-MI). For mRNA: Sham, $n = 7$; Sed-MI, $n = 10$; and ExT-MI, $n = 9$. For protein: $n = 6$ per group. Values are means ± SD. Statistical analysis was by one-way ANOVA followed by Bonferroni *post hoc* test in each area. For TrkB mRNA: infarct, $F = 6.8$, $P < 0.01$. For TrkB.T1 protein: infarct, $F = 5.2$, $P < 0.05$. $^{*}P < 0.05$ and $^{**}P < 0.01$ *versus* Sham. Ponceau S staining is shown as the loading control.

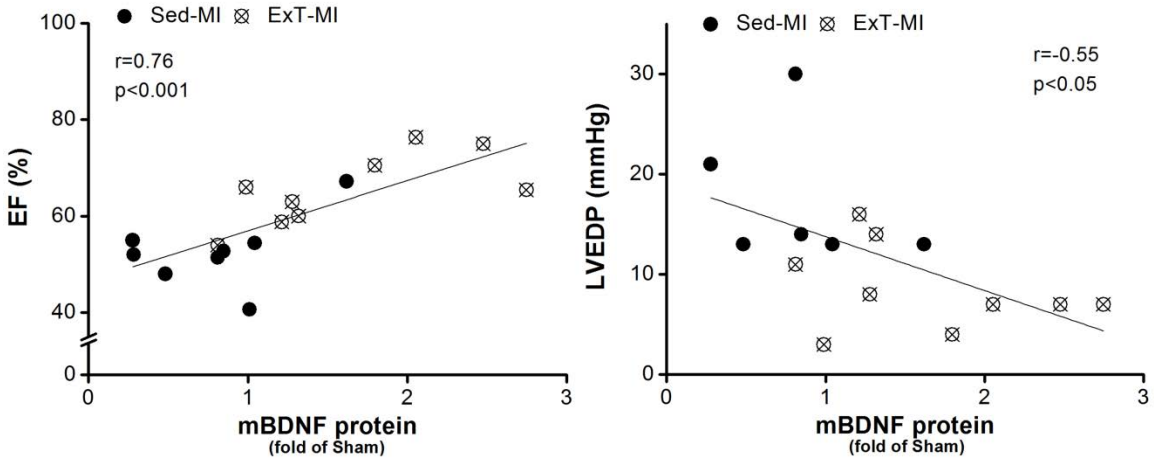

Figure 2-6. Correlations between mBDNF protein and cardiac function

Correlations between mBDNF protein in the non-infarct area of the left ventricle and ejection fraction (EF) or left ventricular end-diastolic pressure (LVEDP).

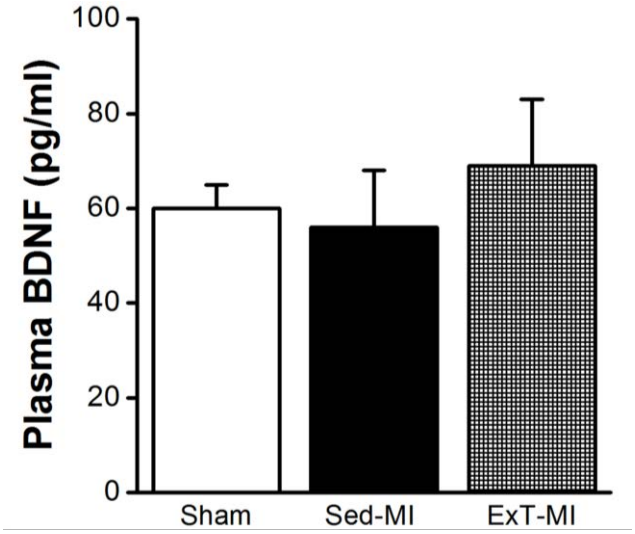

Figure 2-7. Plasma BDNF at 5 weeks post MI with or without exercise training
Plasma BDNF in Sham (n = 7) and MI rats with (ExT-MI, n = 9) or without exercise (Sed-MI, n = 10). Values are means ± SD. Statistical analysis by one-way ANOVA. F = 3.2, P = 0.06.

Discussion

The major findings of the present study are as follows. First, at 5 weeks post MI, FNDC5 protein is increased in the soleus muscle and the infarct area; mBDNF protein is decreased, whereas TrkB.T1 protein is increased in the infarct area. Second, exercise training does not change FNDC5 protein, but increases mBDNF protein in soleus muscle, quadriceps and the non-infarct area of the LV. Exercise training significantly attenuates the decrease in EF and the increase in LVEDP post MI. These improvements are correlated with the increase in mBDNF protein in the non-infarct area of the LV, suggesting that the increase in cardiac BDNF induced by exercise training might contribute to the improvement of cardiac function. The increase in cardiac BDNF after exercise post MI is prominent in the non-infarct area without a parallel increase in FNDC5 protein, indicating that FNDC5 does not regulate BDNF in the heart after MI and exercise training.

FNDC5, BDNF and TrkB in skeletal muscle

Expression levels of FNDC5 in skeletal muscle are regulated by peroxisome proliferator-activated receptor γ coactivator-1α (PGC-1α), a transcriptional coactivator which is a key modulator in energy metabolism, and increased by exercise training (Boström *et al.* 2012). Indeed, some studies reported 30–40% increases in FNDC5 expression in skeletal muscle by exercise training (Wrann *et al.* 2013; Norheim *et al.* 2014), but others showed no effect (Timmons *et al.* 2012; Pekkala *et al.* 2013; Knudsen *et al.* 2014). Determinants of these variable responses of FNDC5 expression to exercise training are not readily apparent.

In the present study, there were no changes in *FNDC5* mRNA and protein in the quadriceps at 5 weeks post MI. In contrast, Matsuo *et al.* (2015) reported that *FNDC5* mRNA and protein were decreased in the quadriceps at 7 weeks post MI in rats. This difference may reflect the worse severity of the HF in the study by Matsuo *et al.* (2015) study. On the contrary, in the soleus muscle, which is a more oxidative muscle, *FNDC5* mRNA was decreased, but FNDC5 protein was markedly increased. The dissociation of *FNDC5* mRNA and protein levels may be attributable to changes in skeletal muscle metabolism after MI, such as decreased oxidative capacity and mitochondrial enzyme activity (Garnier *et al.* 2003), which may inhibit normal turnover of FNDC5 protein (Vogel *et al.* 2011) and the higher protein then decreasing mRNA expression. In the present study, exercise did not affect the increased FNDC5 protein in the soleus muscle of MI rats and did not affect FNDC5 in the quadriceps.

BDNF and its binding receptor TrkB are highly expressed in skeletal muscle (Cuppini *et al.* 2007; Ogborn & Gardiner, 2010). TrkB.T1, a truncated form of TrkB lacking the tyrosine kinase domain, is mainly expressed in skeletal muscle rather than the full-length form (Sakuma & Yamaguchi, 2011). BDNF is produced by muscle cells in response to muscle contraction and acts in an autocrine/paracrine manner, but is not released into the circulation (Cuppini *et al.* 2007; Matthews *et al.* 2009). Muscle BDNF acts locally and increases fat oxidation mediated by AMP-activated protein kinase (AMPK; Matthews *et al.* 2009). In rats, treadmill exercise for 5 days increased *BDNF* mRNA in soleus muscle (Cuppini *et al.* 2007), but not for 10 days (Ogborn & Gardiner, 2010). Jimenez-Maldonado *et al.* (2015) reported higher *BDNF* mRNA but lower protein in soleus muscle after 8 weeks of high-intensity treadmill exercise, but after moderate-

intensity. These results suggest that moderate chronic exercise training increases *BDNF* mRNA only transiently, but high-intensity exercise increases it persistently.

Effects of HF on BDNF and TrkB levels in skeletal muscle have not yet been reported. In the present study, at 5 weeks post MI, *BDNF* mRNA and protein levels were not changed in both soleus muscle and quadriceps, whereas *TrkB* mRNA, but not the protein, was increased in the quadriceps. Further studies are needed to determine whether changes in BDNF and TrkB levels are dependent on the duration and/or severity of HF. Exercise training increased mBDNF protein in both soleus muscle and quadriceps. This increase in mBDNF protein in skeletal muscle might improve energy metabolism by increasing fat oxidation (Matthews *et al.* 2009). FNDC5 protein was not correlated with *BDNF* mRNA or protein, suggesting that FNDC5 might not regulate BDNF expression directly.

FNDC5, BDNF and TrkB in the heart

FNDC5 mRNA is highly expressed in hearts of adult mice (Wrann *et al.* 2013) or rats (present study), but its role in response to physiological/pathological stress, such as exercise and MI, has not yet been studied.

In the present study, *FNDC5* mRNA was decreased at both 2 and 5 weeks post MI, the most in the infarct area, whereas the FNDC5 protein level was markedly increased only in the infarct area, which is similar to the opposite changes in mRNA and protein in the soleus muscle. An increase in oxidative stress in the infarct area can inhibit proteasome activity, resulting in accumulation of misfolded proteins (Grune *et al.* 2004). To understand FNDC5 regulation and function post MI, further investigations could

assess which proteasomes contribute to proteolysis of FNDC5 protein (Erickson, 2013) or whether proteolytic cleavage of FNDC5 occurs in the heart.

Cardiac BDNF increases rapidly in response to ischemic injury and might play a protective role by inhibiting cardiomyocyte apoptosis (Okada *et al.* 2012; Hang *et al.* 2015) and improving angiogenesis (Cao *et al.* 2012; Hong *et al.* 2014). In the whole LV, mBDNF protein was increased 1 h and 6 h post MI in rats (Hang *et al.* 2015), and was decreased at 1 day to 2 weeks post MI in mice (Okada *et al.* 2012). Immunohistochemical staining showed that BDNF protein increased early post MI in cardiomyocytes and coexpressed with macrophages, which were infiltrated around endothelial cells in peri- and infarct areas (Hong *et al.* 2014). Halade *et al.* (2013) reported an increase in mBDNF protein in the infarct area on days 1, 3 and 5 and a return to the baseline level on day 7. In the more chronic phase post MI, a fourfold increase in total BDNF (measured by enzyme-linked immunosorbent assay) in the whole LV was reported at 6 weeks post MI (Katare *et al.* 2009). In the present study, *BDNF* mRNA was not changed in the LV at 5 weeks, whereas mBDNF protein was significantly decreased in the infarct area, suggesting that post-transcriptional mechanisms might be involved in the reduction in mBDNF. MicroRNAs (miRNAs) repress translation or regulate protein degradation at the post-transcriptional level. miRNA-1 and miRNA-210 are highly expressed in cardiomyocytes, target the *BDNF* gene (Lin *et al.* 2010; Ma *et al.* 2015*a*), and may contribute to the decrease in mBDNF protein in the infarct area. In contrast, *TrkB* mRNA was increased in the infarct area at 2 and 5 weeks post MI, and TrkB.T1 protein at 5 weeks post MI. Likewiase, in mice, TrkB protein was markedly increased at 2 weeks post MI (Okada *et al.* 2012). In adult hearts, TrkB.T1 protein is the dominant isoform of TrkB,

and specific knockout of TrkB.T1 in cardiomyocytes led to cardiomyopathy (Fulgenzi *et al.* 2015), suggesting that BDNF–TrkB.T1 signalling plays an important role in normal cardiac function. Altogether, these results suggest that FNDC5, BDNF and TrkB are differently regulated in different areas of the LV post MI. In the infarct area, FNDC5 protein increased, whereas mBDNF protein was decreased, but TrkB.T1 protein increased. FNDC5 protein was not correlated with *BDNF* mRNA or protein, suggesting that in the heart, FNDC5 does not activate BDNF, as reported in neurons (Wrann *et al.* 2013). Factors contributing to this differential regulation are unclear, and the possible functional implications require further study.

Exercise training post MI may decrease plasma Ang II and reduce pro-inflammatory cytokines and decrease cardiomyocyte apoptosis in the LV (Gomes-Santos *et al.* 2014; Lu *et al.* 2015; Puhl *et al.* 2015). Consistent with other studies (Xu *et al.* 2008*a,b*) exercise training markedly attenuated the decrease in EF and increase in LVEDP, indicating that exercise training improved cardiac function post MI. Exercise training significantly increased mBDNF protein in the non-infarct area, and mBDNF protein was positively correlated with EF and negatively correlated with LVEDP, suggesting that the exercise training-induced increase in BDNF might contribute to the improvement of cardiac function. This would be consistent with studies by Okada *et al.* (2012) and Hang *et al.* (2015) showing that deletion of cardiac TrkB increased fibrosis and further decreased EF, whereas intramyocardial or peripheral administration of BDNF normalized the decrease in EF and increase in fibrosis. Further studies can address this in rats by chronic blockade of TrkB receptors. Several mechanisms might contribute to the exercise-induced increase in cardiac mBDNF. Cardiac *FNDC5* mRNA and protein did

not change, and cardiac FNDC5 therefore probably did not contribute to the increase in cardiac mBDNF protein. Another possible regulator of cardiac BDNF may be pro- and anti-inflammatory cytokines, such as TNF-α and IL-1*β* (pro-) and IL-10 (anti-). Pro-inflammatory cytokines reduced *BDNF* mRNA and protein expression in rat brain (Lapchak *et al.* 1993; Guan & Fang, 2006). Given that exercise training attenuates the increase in TNF-α, IL-1*β* and IL-6 post MI (Puhl *et al.* 2015), and increases IL-10 (Kesherwani *et al.* 2015) in the LV, it is possible that the increase in mBDNF is mediated by a decrease in these pro-inflammatory cytokines and an increase in anti-inflammatory cytokines. Finally, as cardiac *BDNF* mRNA did not increase in parallel with protein, one cannot exclude the possibility that uptake from the circulation might play a role (Knaepen *et al.* 2010). The brain is a major source of circulating BDNF during exercise (Rasmussen *et al.* 2009; Seifert *et al.* 2010). Acute exercise increases circulating BDNF transiently, and an increase in resting plasma BDNF may occur after chronic exercise training (Knaepen *et al.* 2010, Seifert *et al.* 2010). In the present study, plasma BDNF concentrations still showed a modest (P = 0.06) increase ~48h after the last exercise session.

In conclusion, after MI, FNDC5 protein increases and mBDNF protein decreases in the infarct area of the LV. Exercise training increases mBDNF in skeletal muscle and the non-infarct area of the LV, without changes in mRNA level, suggesting that post-transcriptional mechanisms contribute to the increase in mBDNF induced by exercise training. The increases in mBDNF in the LV and skeletal muscle induced by exercise training are not associated with changes in FNDC5, indicating that FNDC5 does not contribute to the changes in mBDNF levels in the heart or skeletal muscle. Increasing

cardiac and skeletal muscle mBDNF–TrkB signalling may represent a good therapeutic target to attenuate development of HF and skeletal muscle dysfunction post MI.

Additional Information

Competing interests

None declared

Author Contributions

F.H.H.L. conceived and designed the study. H.W.L., M.A. and H.W.W. collected the data. H.W.L. drafted the manuscript. H.W.L., M.A., H.W.W. and F.H.H.L. analysed and interpreted the data and critically revised the draft for intellectual content. All authors approved the final version of the manuscript and agree to be accountable for all aspects of the work in ensuring that questions related to the accuracy or integrity of any part of the work are appropriately investigated and resolved. All persons designated as authors qualify for authorship, and all those who qualify for authorship are listed.

Funding

This study was supported by operating grant no. FRN: MOP-136923 from the Canadian Institutes of Health Research. F.H.H.L. holds the Pfizer Chair in Hypertension Research, an endowed chair supported by Pfizer Canada, University of Ottawa Heart Institute Foundation and Canadian Institutes of Health Research. H.W.L. was the recipient of a University of Ottawa Endowed Graduate Award in Cardiac Research at the Heart Institute, supported by the University of Ottawa's Faculty of Medicine Endowed Funds in Cardiac Research and the University of Ottawa Heart Institute Foundation.

Chapter 3

Effects of exercise training and TrkB blockade on cardiac function and BDNF-TrkB signaling postmyocardial infarction in rats

Effects of exercise training and TrkB blockade on cardiac function and BDNF-TrkB signaling postmyocardial infarction in rats

Heow Won Lee[1], Monir Ahmad[1], Jonathan J. Weldrick[2], Hong-Wei Wang[1], Patrick G. Burgon[2] and Frans H.H. Leenen[1]

[1]Brain and Heart Research Group, University of Ottawa Heart Institute, Ottawa, Ontario, Canada

[2]Department of Cellular and Molecular Medicine, Faculty of Medicine, University of Ottawa, Ottawa, Ontario, Canada

Running Title: Exercise and cardiac BDNF-TrkB signaling post-MI

First Published: October 12, 2018, *Am J Physiol Heart Circ Physiol* **315**, H1821–1834

ABSTRACT

Exercise training is beneficial for preserving cardiac function postmyocardial infarction (post-MI), but the underlying mechanisms are not well understood. We investigated one possible mechanism, brain-derived neurotrophic factor (BDNF)-tropomyosin-related kinase B (TrkB) signaling with the TrkB blocker ANA-12 (0.5 $mg \cdot kg^{-1} \cdot day^{-1}$). Male Wistar rats underwent sham surgery or ligation of the left descending coronary artery. The surviving MI rats were allocated to as follows: sedentary MI treated with vehicle, exercise-trained MI rats treated with vehicle, and exercise-trained MI rats treated with ANA-12. Exercise training was done 5 days/wk for 4 wk on a motor-driven treadmill. At the end, left ventricular (LV) function was evaluated by echocardiography and a Millar catheter. Mature BDNF and downstream effectors of BDNF-TrkB signaling, Ca^{2+}/calmodulin-dependent protein kinase II (CaMKII), Akt and AMP-activated protein kinase (AMPK), were assessed in the noninfarct area of the LV by Western blot analysis. Exercise training increased stroke volume and cardiac index and attenuated the decrease in ejection fraction (EF) and the increase in LV end-diastolic pressure post-MI. ANA-12 blocked the improvement of EF and attenuated the increases in stroke volume and cardiac index but did not affect LV end-diastolic pressure. Exercise training post-MI prevented decreases in mature BDNF, phosphorylated (p-)CaMKII, p-Akt and p-AMPKα expression. These effects were all blocked by ANA-12 except for p-AMPKα. In conclusion, the exercise-induced improvement of EF is mediated by the BDNF-TrkB axis and the downstream effectors CaMKII and Akt. BDNF-TrkB signaling appears to contribute to the improvement in systolic function by exercise training.

NEW & NOTEWORTHY

Exercise training improves ejection fraction and left ventricular end-diastolic pressure (LVEDP) and increases stroke volume and cardiac index in rats postmyocardial infarction (post-MI). The improvement of EF but not LVEDP is mediated by activation of the brain derived neurotrophic factor (BDNF)-tropomyosin-related kinase B (TrkB) axis and the downstream effectors Ca^{2+}/calmodulin-dependent protein kinase II (CaMKII) and Akt. This suggests that activation of BDNF-TrkB signaling and CaMKII and Akt is a promising target to attenuate progressive cardiac dysfunction post-MI.

Keywords: ANA-12; brain-derived neurotrophic factor-tropomyosin-related kinase B signaling; exercise training; heart failure; tropomyosin-related kinase B blockade

INTRODUCTION

Regular exercise in patients with heart failure (HF) improves quality of life and decreases hospitalization and mortality (Belardinelli et al., 2012; Gielen et al., 2015). In animal studies, early initiation of exercise training postmyocardial infarction (post-MI) mitigates adverse cardiac remodeling and preserves cardiac function (Lee et al., 2017; Puhl et al., 2015; Xu et al., 2008b). The molecular mechanisms underlying these beneficial effects of exercise training are not well understood. One possible mechanism is activation of brain-derived neurotrophic factor (BDNF)-tropomyosin-related kinase B (TrkB) signaling in the heart. In our previous study (Lee et al., 2017), we showed that exercise training post-MI increases protein expression of mature BDNF (mBDNF; the active form of BDNF) in the noninfarct area of the left ventricle (LV). The increase in mBDNF was positively correlated with the improvement of ejection fraction (EF) and LV end-diastolic pressure (LVEDP), suggesting that the exercise-induced increase in mBDNF in the noninfarct area of the LV may contribute to improved cardiac function post-MI. Such effects may be mediated by downstream signaling pathways of BDNF via its binding to TrkB receptors in the heart.

In cardiomyocytes of rodents, BDNF increases phosphorylation of Akt [phosphorylated (p-)Akt], promoting cardiomyocyte survival (Okada et al., 2012) and of Ca^{2+}/calmodulin-dependent protein kinase II (p-CaMKII), enhancing cardiomyocyte contractility and relaxation (Feng et al., 2015). In rat skeletal muscle, BDNF-TrkB signaling also increases phosphorylation of AMP-activated protein kinase (p-AMPK), enhancing fatty acid oxidation (Matthews et al., 2009). In the heart, activation of AMPK enhances both glucose and fatty acid metabolism (Bairwa et al., 2016; Kim and Dyck,

2015). The effects of BDNF on cardiac AMPK activity and factors associated with cardiac energy metabolism have not yet been studied.

Several studies evaluated in rodents changes in Akt, CaMKII, and AMPK in the LV post-MI. At 4–6 wk post-MI in rats, p-Akt-to-total Akt ratio in the non- and peri-infarct areas of the LV was not changed (Cai et al., 2016; Manchini et al., 2017). Exercise training increased p-Akt-to-total Akt ratio in the peri-infarct area of the LV (noninfarct area was not assessed), and attenuated the increase in TUNEL-positive cells and Bax-to-Bcl-2 ratio (Cai et al., 2016). This suggests that exercise-induced activation of Akt may attenuate cardiomyocyte apoptosis. On the other hand, in rats at 2 wk post-MI, both total CaMKII and p-CaMKII protein expression in the LV (area not specified) was decreased by 70% compared with the sham level, without a change in the p-CaMKII-to-total CaMKII ratio (Zhao et al., 2014). At 8 wk post-MI in rats, both CaMKII protein expression and CaMKII activity were reduced in the noninfarct area of the LV (Netticadan et al., 2000). In healthy exercised mice, an increase in p-CaMKII-to-total CaMKII ratio in the LV was observed with enhancement of fractional shortening compared with nonexercised mice (Burgos et al., 2017; Kemi et al, 2007). Treatment with a CaMKII inhibitor limited the exercise-induced increase in fractional shortening (Kaurstad et al., 2012), indicating that the exercise-induced increase in CaMKII activity contributes to an improvement of cardiac function. At 3–4 wk post-MI, p-AMPK expression was increased in the infarct and peri-infarct areas of the LV (Li et al., 2016) but was unchanged in the peri-infarct area (Wu et al., 2014) or in the whole LV (Chen et al., 2017). In mice with isoproterenol-induced cardiac hypertrophy, p-AMPK expression in the heart was similar to control mice, and exercise training increased p-AMPK

expression similarly (Ma et al., 2015b). The effects of exercise training on CaMKII and AMPK activities in the LV post-MI have not yet been reported. Collectively, activation of Akt, CaMKII, and AMPK in response to exercise training post-MI in the noninfarct area of the LV may attenuate progressive cardiac remodeling and dysfunction. Whether the exercise-induced improvement of cardiac function post-MI depends on BDNF-TrkB signaling and thereby activates Akt, CaMKII, and AMPK has not yet been assessed.

We hypothesized that chronic administration of a TrkB blocker will block BDNF-TrkB signaling and decrease the activities of downstream effectors Akt, CaMKII and AMPK in the non-infarct area of the LV, and thereby inhibit beneficial effects of exercise training. The selective non-competitive antagonist of TrkB receptors, (N-[2-[[(hexahydro-2-oxo-1H-azepin-3-yl) amino] carbonyl] phenyl]-benzothiophene-2-carboxamide) (ANA-12) is a small molecule that crosses the blood-brain barrier (Cazorla et al., 2011) and is a good tool to block BDNF-TrkB signaling (Arbat-Plana et al., 2017). We assessed in rats the effects of treatment with ANA-12 from 1 to 5 wk post-MI for exercise-induced changes in cardiac function and mBDNF, TrkB expression, and Akt, CaMKII and AMPK activities as well as expression of relevant metabolic genes encoding transporters and enzymes in the noninfarct area of the LV.

MATERIALS AND METHODS

Ethical approval and animals

All experiments were approved by the University of Ottawa Animal Care Committee and conformed with the National Institutes of Health *Guide for the Care and Use of Laboratory Animals* (8th ed., 2011). Male Wistar rats weighing 200–250g (Charles River, Montreal, QC, Canada) were acclimatized for 5–7 days in a room at a constant temperature and humidity with 12:12-h light-dark cycle and allowed free access to standard laboratory chow and tap water.

Experimental design and groups

The experimental timeline is outlined in Fig. 3-1. A total 69 rats were used for this experiment. Fifty-nine rats underwent permanent ligation of the left descending coronary artery (LAD), and ten rats underwent sham surgery. For the 33 surviving MI rats, EF was assessed at 2–4 days after the surgery by echocardiography. Three rats with high EF (>70%) were excluded from the study. Thirty MI rats were divided into the following three groups: sedentary MI with vehicle treatment (Sed-MI-Vehicle; n = 9), exercise-trained MI rats with vehicle treatment (ExT-MI-Vehicle, n = 11), and exercise-trained MI rats with ANA-12 treatment (ExT-MI-ANA-12, n = 10). To achieve similar baseline EF and body weight for the three MI groups, rats were arranged from high to low EF measured at 2–4 days after the MI surgery and then sequentially allocated to one of the three MI groups. Average body weight in each group was then calculated, and some of the rats switched among the groups to make the average baseline body weight similar in the three groups. At the end of the study, one rat in the ExT-MI-ANA-12 group died

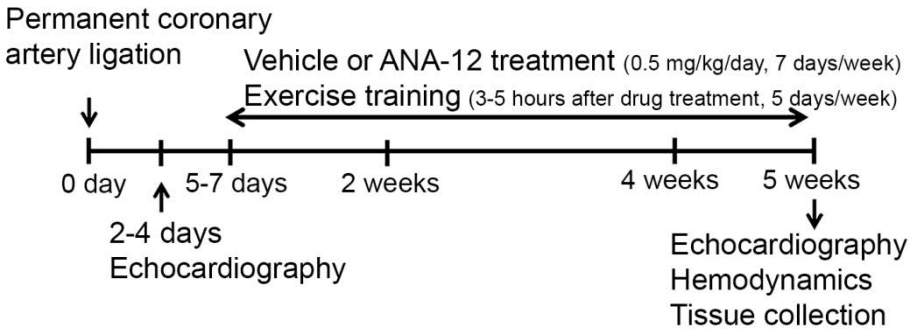

Figure 3-1. Experimental timeline

Exercise training was initiated 5–7 days after permanent ligation of the left descending coronary artery. Vehicle or ANA-12 treatment was initiated 1 day before the first exercise session and administered 3–5 h before each exercise bout. Exercise training was done for 5 days/wk and continued for 4 wk. Cardiac function was evaluated at 2–4 days and 5 wk postmyocardial infarction.

during echocardiography and four rats had small (defined a priori as MI size < 15% of the LV) or no MI. Therefore, eight Sed-MI-Vehicle, nine ExT-MI-Vehicle, and eight ExT-MI-ANA-12 rats were included in the final analyses. A sedentary sham-operated group (sham group; n = 10) was included as control group. To increase the statistical power for assessment of changes in cardiac function relative to MI size (Fig. 3-2, *A–F*), data for Sed-MI (n = 10) and ExT-MI (n = 9) from our previous study following the same protocol (Lee et al., 2017) were added.

MI surgery

Slow-release buprenorphine (1 mg/kg) (Chiron Compounding Pharmacy Inc., Guelph, ON, Canada) was subcutaneously injected 1–2 h before surgery, which provides adequate analgesia for 3 days. Rats were anesthetized by a 2% mixture of isoflurane and oxygen, and then intubated with a 2-in 16-gauge polyethylene tube and connected to a Harvard Rodent Respirator (Harvard Apparatus Co., Holliston, MA) set to a frequency of 75 strokes of 2.0 ml volume/min. Thoracotomy was performed via the fourth intercostal space, the pericardium was opened, and the LAD was permanently ligated 1–2 mm distal to its origin with a 6-0 silk suture on an atraumatic needle. The fourth and fifth ribs were closed by two separate 4.0 Vicryl sutures. Lungs were inflated, and air was removed from the thoracic cavity. Isoflurane was stopped, and rats remained ventilated with 100% oxygen until waking up or breathing spontaneously. Sham animals underwent a similar procedure except for ligation of the LAD.

Exercise training

Exercise training using a motor-driven treadmill (Columbus Instruments, Columbus, OH) was conducted for 4 wk (5 days/wk) as previously described (Lee et al., 2017). The first exercise session was initiated 5–7 days after recovery from the MI surgery. In the first week, rats were trained at 10 m/min, 0% gradient, and 10–15 min/day for the first 3 days. The speed, grade, and duration were gradually increased to 20 m/min, 5–10%, and 60 min/day, respectively, by the end of the second week and then maintained for 2 wk. None of the exercising rats refused to run. Sedentary rats were handled and treated in a similar manner to the exercise-trained rats without the motion of the treadmill.

ANA-12 preparation and oral administration

Starting 1 wk before MI surgery each morning, 1 g of peanut butter was provided to all rats to make them familiar to eat peanut butter for drug treatment. The dose of ANA-12 was based on previous studies showing that a single intraperitoneal injection of ANA-12 (0.5 mg/kg) decreased p-TrkB-to-TrkB ratio up to 25% at 4 h in the whole brain of mice (Cazorla et al., 2011), and oral administration of ANA-12 (0.5 $mg \cdot kg^{-1} \cdot day^{-1}$) for 28 days attenuated beneficial effects of calorie restriction on cognitive function in rats (Kishi et al., 2015). ANA-12 (0.5 mg/kg, S7745, Selleckchem, Houston, TX) was dissolved in 0.5% methyl celluose (M7140, Sigma-Aldrich, St Louis, MO) (Kishi et al., 2015; Vidal-Martínez et al., 2016), mixed with 1 g of peanut butter, and administered daily early in the morning. ANA-12 administration was initiated on the day before the first day of exercise and 3–5 h before each exercise session. For vehicle-treated groups including the sham group, peanut butter mixed with 0.5% methyl celluose was given without ANA-12.

Assessment of cardiac function

Echocardiography was performed blindly for drug treatment using a VisualSonic Vevo 770 imaging system (VisualSonics, Toronto, ON, Canada) 2–4 days after MI and at 5 wk post-MI, 2–3 h after the last exercise session under 2% mixture of isoflurane and oxygen anesthesia. In M-mode recordings, LV systolic and diastolic dimensions were measured, and end-systolic volume (ESV), end-diastolic volume (EDV), stroke volume (SV), cardiac index, and EF were calculated. Hemodynamic measurements were conducted under anesthesia as described above, 3–4 h after the last vehicle or ANA-12 treatment. A Millar catheter was inserted into the LV via the right carotid artery. The catheter was connected to a Harvard data-acquisition system interfaced with a PC using AcqKnowledge III software. The level of anesthesia was gradually decreased to the point when rats started responding to the toe pinch. At this point, LV peak systolic pressure, LVEDP, and maximal rate of pressure change (dP/dt_{max}) were measured for 30–60 s.

Tissue collection and measurement of infarct size

Trunk blood and hearts were collected 2–3 h after hemodynamic measurements, 5–7 h after the last vehicle or ANA-12 treatment, and within 36 h of the last exercise session. Rats were decapitated, and trunk blood was collected in a prechilled 50-ml conical tube containing 0.3 M EDTA. Blood was centrifuged at 3,000 rpm at 4°C for 30 min, and plasma was collected for the plasma BDNF assay. Hearts were immediately removed and washed in ice-cold saline. After removal of atria, the right ventricle (RV) and LV were separated. The LV was opened flat through a long cut on the septum and 2–3 small cuts on the apex. The whole LV, including the septum, was placed under a transparent sheet and its circumference and infarct borders were traced to measure infarct size. The whole

LV, including the septum, and RV were weighed separately and snap frozen in liquid nitrogen. To measure infarct size, the LV demarcation on the transparent sheet was scanned, and its digital image was quantified using Image Pro 6.2. Infarct size was expressed as a percentage of the total LV area. All tissues and plasma samples were kept at –80°C until further analyses.

Western blot analysis

For Western blot analysis, the remote noninfarct area of the LV (3–4 mm away from the infarct area) was homogenized in ice-cold lysis buffer [50 mM Tris (pH 8.0), 150 mM NaCl, 0.5% sodium deoxycholate, 1% Nonidet P-40, 0.1% SDS, and 5 mM EDTA (pH 8.0)] with phosphatase inhibitors (10 mM sodium fluoride and 2 mM sodium orthovanadate) and 1% protease inhibitor cocktail (Sigma-Aldrich). The supernatant was collected after centrifugal separation at 10,000 *g*, 4°C for 30 min. Protein concentration was determined by the bicinchoninic acid assay (Thermo Scientific, Rockford, IL). Proteins (15–30 μg) were separated by SDS-PAGE [12% gels for mBDNF; 10% gels for p-Akt (Thr^{308}), p-Akt (Ser^{473}), Akt (pan), p-CaMKII (Thr^{286}), CaMKII (pan), p-AMPKα (Thr^{172}) and AMPKα; and 8% gels for TrkB] and then transferred to 0.2-μm PVDF membranes (Bio-Rad, Mississauga, ON, Canada). One hour of blocking was done at room temperature with either 5% milk in Tris-buffered saline with 1% Tween 20 for mBDNF, Akt (pan), and TrkB or 5% BSA in Tris-buffered saline with 1% Tween 20 for p-Akt (Thr^{308}), p-Akt (Ser^{473}), p-CaMKII (Thr^{286}), CaMKII (pan), p-AMPKα (Thr^{172}), and AMPKα. Membranes were incubated at 4°C overnight with primary antibodies as follows: anti-BDNF (1:1,000, ANT-010, Alomone Laboratories, Jerusalem, Israel), anti-TrkB (1:1,000, 07-225; Millipore, Toronto, ON, Canada), p-CaMKII (Thr^{286}, 1:1,000, no.

12716, Cell Signaling Technology, Beverly, MA), CaMKII (pan, 1:1,000, no. 4436, Cell Signaling Technology), p-Akt (Thr^{308}, 1:1,000, no. 2965, Cell Signaling Technology), p-Akt (Ser^{473}, 1:2,000, no. 4060, Cell Signaling Technology), Akt (pan, 1:2,000, no. 4691, Cell Signaling Technology), p-AMPKα (Thr^{172}) (1:1,000, no. 2535, Cell Signaling Technology), and AMPKα (1:1,000, no. 2603, Cell Signaling Technology). After a wash, blots were incubated with goat anti-rabbit IgG-horseradish peroxidase (HRP; 1:5,000, HAF008, R&D Systems, Minneapolis, MN) for 1 h at room temperature. The blot was incubated with Luminata Forte Western HRP substrate (WBLUF0500, Millipore) and visualized with a ChemiDoc XRS + imager (Bio-Rad). Membranes were reprobed with anti-GAPDH (1:10,000, MAB374, Millipore) as a loading control. Band densities were quantified using Image Laboratory software (Bio-Rad). The density of each protein was normalized to its density of GAPDH and expressed as relative fold changes of the sham group. To determine activities of Akt, CaMKII, and AMPKα, the ratios between p-Akt (Thr^{308} and Ser^{473}) and Akt (pan), p-CaMKII (Thr^{286}) and CaMKII (pan), and p-AMPKα and total AMPKα (t-AMPKα) were calculated.

Plasma BDNF assay

The BDNF level in plasma was measured using a commercial ELISA kit (CYT306, Millipore) according to the manufacturer's instruction. All samples were measured in duplicate. BDNF (100 µl) standards and diluted plasma samples (1:2) were loaded to a microplate, precoated with mouse monoclonal antibodies generated against human BDNF, and incubated overnight at 4°C. The next day, the plate was washed four times with the wash buffer and 100 µl of diluted biotinylated mouse anti-BDNF (1:1,000) was added to each well. The plate was incubated at room temperature for 3 h. After the plate had been

washed, 100 µl of the diluted streptavidin-HRP conjugate solution (1:1,000) were added to each well, and samples were then incubated for 1 h. After the plate had been washed, 100 µl of TMB/E substrate were added to each well and incubated for 15 min. The reaction was stopped by the stop solution and the absorbances of BDNF standards and samples were obtained at 450 nm. The plasma BDNF concentration was determined from a standard curve generated with the known concentration of BDNF standards on the *x*-axis and the corresponding absorbances on the *y*-axis.

RNA isolation and real-time PCR for metabolic gene analysis

To determine whether exercise training post-MI affects cardiac glucose and fatty acid metabolism, mRNA expression of transporters and enzymes related to glucose and fatty acid metabolism was assessed in the noninfarct area of the LV. Noninfarct areas of the LV was homogenized with 1 ml QIAzol Lysis Reagent (Qiagen, Mississauga, ON, Canada), and total RNA was extracted. cDNA was synthetized from 5 µg of DNase I-treated total RNA by reverse transcription with oligo dT primers (Thermo Scientific) and Superscript II RNase H reverse transcriptase (Thermo Scientific) at 42°C for 60 min. The sequences of primers are shown in Table 3-1. Real-time PCR was performed using SYBR Green PCR Master Mix (no. 4364344, Applied Biosystems, Foster City, CA) in 384-well plates. The PCR conditions were as follows: an initial step at 95 °C for 10 min, 40 cycles of denaturation at 95 °C for 15 s, and annealing and extension at 60°C for 1 min, followed by a final dissociation cycle at 95°C for 15s, 60°C for 1 min, and 95°C for 15 s. All samples were measured in triplicate. The relative transcript quantity was calculated by the comparative threshold cycle (C_T) method (Schmittgen and Livak, 2008). Fold changes ($2^{-\Delta\Delta CT}$) in the expression level of each gene were calculated for each

experimental group using C_T values subtracted by the average of C_T value of internal reference gene, TATA-box binding protein (ΔC_T).

Statistical analyses

One-way ANOVA was done to compare all groups followed by a Bonferroni post hoc test. Two-way repeated measures ANOVA was done to assess changes in EF measured at 2–4 days and 5 wk post-MI. To compare cardiac function relative to MI size, linear regression and analysis of covariance were done. To enhance statistical power for this analysis, the Sed-MI and ExT-MI groups from our previous study (Lee et al., 2017) were combined with the Sed-MI-Vehicle and ExT-MI-Vehicle groups, respectively of the present study. $P \leq 0.05$ was considered statistically significant.

Table 3-1. Sequences of primers used for metabolic gene expression analysis

Gene	Primer sequence (5' − 3')
Glut1 (Slc2a1)	
Forward	5'-TGGCCAAGGACACACGAATACTGA-3'
Reverse	5'-TGGAAGAGACAGGAATGGGCGAAT-3'
Glut4 (Slc2a4)	
Forward	5'-AGTTGGAAAGAGAGCGTCCACTGT-3'
Reverse	5'-GCTGCAGCACCACTGCAATAATCA-3'
Pfk	
Forward	5'-TGGCACTGATATGACCATTGGT-3'
Reverse	5'-TGAGCGGTGGTGGTGATG-3'
FAT/Cd36	
Forward	5'-GCCTCCTTTCCACCTTTTGT-3'
Reverse	5'-GATTCAAACACAGCATAGATGGAC-3'
Cpt1a	
Forward	5'-CTCAGTGGGAGCGACTCTTCA-3'
Reverse	5'-GGCCTCTGTGGTACACGACAA-3'
Cpt1b	
Forward	5'-CAGCCATGCCACCAAGATC-3'
Reverse	5'-CTTGGGCAGTGATGTTTGGA-3'
Acc1	
Forward	5'-GCCATCCGGTTTGTTGTCA-3'
Reverse	5'-GGATACCTGCAGTTTGAGCCA-3'
Acc2	
Forward	5'-GAGGCACAGGTGAAGCAGGAG-3'
Reverse	5'-TCGGATAGTGGAACGCAGGTTG-3'
Tbp	
Forward	5'-ACCCTTCACCAATGACTCCTATG-3'
Reverse	5'-ATGATGACTGCAGCAAATCGC-3'

Glut1 and *Glut4*, glucose transporter type 1 and 4; *Pfk*, phosphofructokinase; *FAT/Cd36*, fatty acid translocase; *Cpt1a* and *Cpt1b*, carnitine palmitoyltransferase 1a and 1b; *Acc1* and *Acc2*, acetyl-CoA carboxylase 1 and 2; *Tbp*, TATA box-binding protein (housekeeping gene).

RESULTS

Effect of exercise training post-MI with or without ANA-12 on cardiac function

At 5 weeks post-MI, body weight was not different in the Sed-MI-Vehicle group compared with the sham group, but LV and RV weight were significantly increased (Table 3-2). Exercise training had no effect on body weight, MI size, and LV weight, but RV weight of the ExT-MI groups was not significantly different from the sham group, indicating that the increase in RV weight post-MI is attenuated by exercise training (Table 3-2). There was no obvious effect of ANA-12 in exercise-trained MI rats on body weight, MI size, and LV and RV weight (Table 3-2).

In the Sed-MI-Vehicle group, echocardiographic and hemodynamic parameters showed clear cardiac dysfunction at 5 wk post-MI. ESV and EDV were increased, and EF was decreased. LVEDP was increased, and LV peak systolic pressure and dP/dt_{max} were decreased (Table 3-3). In both ExT-MI groups, ESV was not different from the Sed-MI-Vehicle group, but EDV and SV were significantly higher compared with sham and Sed-MI-Vehicle groups (Table 3-3). The cardiac index was significantly higher in the ExT-MI-Vehicle group and tended to be higher in both ExT-MI-ANA-12 group (P = 0.1) compared with the sham group and significantly higher in both ExT-MI groups compared to Sed-MI-Vehicle rats (Table 3-3). In the Sed-MI-Vehicle group, EF at 5 wk post-MI had decreased 1% compared with EF at 2–4 days post MI, whereas in the ExT-MI-Vehicle group, EF at 5 wk post-MI increased by ~9% compared with EF at 2–4 days post-MI (Table 3-3). Both ΔEF (differences in EF between 5 wk post-MI and 2–4 days post-MI) and EF at 5 wk post-MI tended (P = 0.1 for both) to be increased by exercise training.

Table 3-2. General characteristics of rats at 5 wk post-MI with or without exercise training or ANA-12 treatment

		MI		
	Sham	Sed-Vehicle	ExT-Vehicle	ExT-ANA-12
Number of rats/group	10	8	9	8
Body weight, g				
Baseline	277 ± 5	290 ± 4	290 ± 6	288 ± 4
Final	505 ± 8	514 ± 9	490 ± 15	488 ± 9
Soleus muscle weight, mg/100g body wt	44 ± 1	45 ± 1	46 ± 1	47 ± 1
MI size, %		26 ± 2	27 ± 2	26 ± 2
Left ventricular weight, mg/100g body wt	180 ± 3	197 ± 3*	197 ± 5*	201 ± 5†
Right ventricular weight, mg/100g body wt	43 ± 1	60 ± 8*	51 ± 3	51 ± 2

Values are presented as means ± SE. MI, myocardial infarction; Sed, sedentary; ExT, exercise training. One-way ANOVA followed by a post hoc Bonferroni test was used. Baseline body weight, $F = 1.6$, not significant; final body weight, $F = 1.1$, not significant; soleus muscle weight, $F = 1.8$, not significant; MI size, $F = 0.07$, not significant; left ventricular weight, $F = 5.2$, $P < 0.01$; right ventricular weight, $F = 3.0$, $P < 0.05$. *$P < 0.05$ and †$P = 0.01$ vs. the sham group.

Table 3-3. Echocardiographic and hemodynamic measurements in rats at 5 wk post-MI with or without exercise training or ANA-12 treatment

		MI		
	Sham	Sed-Vehicle	ExT-Vehicle	ExT-ANA-12
Number of rats/group	10	8	9	8
Echocardiographic parameters				
End-systolic volume, µl/100g body wt	12 ± 1	38 ± 5[c]	44 ± 4[c]	49 ± 4[c]
End-diastolic volume, µl/100g body wt	61 ± 4	84 ± 7[a]	111 ± 5[c,d]	110 ± 6[c,d]
Stroke volume, µl/100g body wt	48 ± 3	46 ± 3	68 ± 3[c,f]	61 ± 3[a,d]
Heart rate, beats/min	406 ± 8	378 ± 13	379 ± 14	384 ± 10
Cardiac index, $ml \cdot min^{-1} \cdot kg^{-1}$	195 ± 10	174 ± 13	254 ± 9[b,f]	235 ± 12[e]
EF, % at 2–4 days post-MI	N/D	56 ± 2	53 ± 2	54 ± 2
EF, % at 5 weeks post-MI	80 ± 1	55 ± 2[c]	61 ± 2[c]	56 ± 2[c]
ΔEF, %	NA	–0.9 ± 2.9	8.6 ± 3.3	1.8 ± 2.6
Hemodynamic parameters				
Left ventricular peak systolic pressure, mmHg	120 ± 2	101 ± 5[b]	106 ± 3[a]	104 ± 3[a]
Left ventricular end diastolic pressure, mmHg	2.8 ± 0.2	14.0 ± 1.6[c]	12.7 ± 1.1[c]	12.1 ± 1.5[c]
dP/dt_{max}, mmHg/sec	7,581 ± 104	5,620 ± 387[c]	5,683 ± 149[c]	5,701 ± 232[c]
Heart rate, beats/min	376 ± 7	369 ± 7	351 ± 12	363 ± 10

Values are means ± SE. MI, myocardial infarction; Sed, sedentary; ExT, exercise training; EF, ejection fraction; ΔEF, differences between EF at 5 wk post-MI and 2–4 days post-MI; ND, not determined; NA, not applicable. One-way ANOVA followed by a Bonferroni post hoc test was done. For end-systolic volume, $F = 20.1$, $P < 0.001$; for end-diastolic volume, $F = 19.2$, $P < 0.001$; for stroke volume, $F = 11.8$, $P < 0.001$; for heart rate (calculated from M-mode), $F = 1.3$, not significant; for cardiac index, $F = 9.96$, $P < 0.001$; for EF at 2–4 days post-MI, $F = 0.47$, not significant; for EF at 5 wk post-MI, $F = 44.1$, $P < 0.001$; for ΔEF, $F = 2.46$, $P = 0.11$; for left ventricular peak systolic pressure, $F = 5.9$, $P < 0.001$; for left ventricular end-diastolic pressure, $F = 18.6$, $P < 0.001$; for dP/dt_{max}, $F = 17.0$, $P < 0.001$; for HR, $F = 1.2$, not significant. Two-way repeated-measures ANOVA was done for comparison of EF at 2–4 days versus EF at 5 wk. Group, $F = 0.4$, not significant; time points, $F = 2.97$, $P = 0.1$, time points x group, $F = 2.46$, $P = 0.11$. [a]$P < 0.05$, [b]$P < 0.01$, and [c]$P < 0.001$ vs. the sham group; [d]$P < 0.05$, [e]$P < 0.01$, and [f]$P < 0.001$ vs. the Sed-MI-Vehicle group.

Relative to MI size, including our previous data (Lee et al., 2017), EDV was significantly higher in the ExT-MI-Vehicle group and tended to be higher in the ExT-MI-ANA-12 group (P = 0.1) compared with the Sed-MI-Vehicle group (Fig 3-2*A*). EF, SV and cardiac index were all significantly higher in the ExT-MI-Vehicle group compared with the Sed-MI-Vehicle group (Fig 3-2, *B-D*). In contrast, in the ExT-MI-ANA-12 group, EF was not different from the Sed-MI-Vehicle group and was significantly lower compared to ExT-MI-Vehicle group (Fig 3-2*B*). Increases in SV and cardiac index were attenuated by ANA-12 and thereby became not different from either the Sed-MI-Vehicle or ExT-MI-Vehicle groups (Fig 3-2*C* and 3-2*D*). The increase in LVEDP was somewhat attenuated by exercise training with or without ANA-12 treatment (Table 3-3). Relative to MI size, including our previous data (Lee et al., 2017), LVEDP was significantly lower in the ExT-MI-Vehicle group ($P < 0.05$) and tended to be lower in the ExT-MI-ANA-12 group (P = 0.1) compared to the Sed-MI-Vehicle rats (Fig 3-2*E*). dP/dt_{max} was not affected by exercise training with or without ANA-12 treatment (Table 3-3 and Fig 3-2*F*). Collectively, exercise training post MI improved EDV, EF, SV, cardiac index, and LVEDP. ANA-12 treatment prevented the improvement of EF, and attenuated the increases in SV and cardiac index, but not of EDV and LVEDP.

Effect of exercise training post MI with or without ANA-12 on plasma BDNF

The plasma BDNF level tended to be lower in the Sed-MI-Vehicle group compared to Sham group (P = 0.088). Exercise training significantly increased plasma BDNF and ANA-12 did not block this effect of exercise (Fig 3-3*A*).

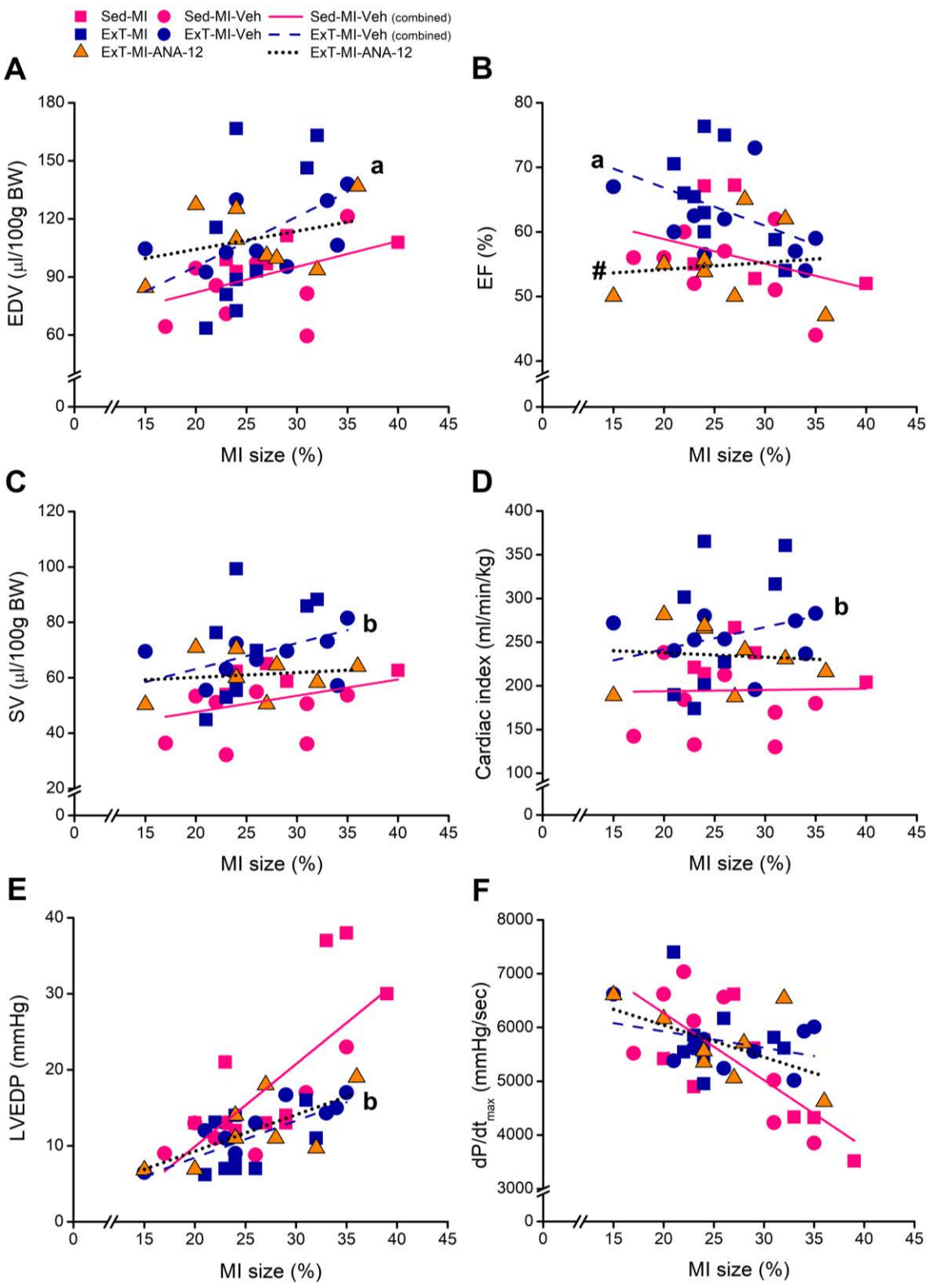
Sed-MI
ExT-MI
ExT-MI-ANA-12
Sed-MI-Veh
ExT-MI-Veh
Sed-MI-Veh (combined)
ExT-MI-Veh (combined)
ExT-MI-ANA-12
A
EDV (μl/100g BW)
MI size (%)
a
B
EF (%)
MI size (%)
a
#
C
SV (μl/100g BW)
MI size (%)
b
D
Cardiac index (ml/min/kg)
MI size (%)
b
E
LVEDP (mmHg)
MI size (%)
b
F
dP/dt max (mmHg/sec)
MI size (%)

Figure 3-2. Changes in end-diastolic volume (EDV), ejection fraction (EF), stroke volume (SV), cardiac index, left ventricle end-diastolic pressure (LVEDP), and maximal first derivative of change in pressure over time (dP/dt_{max}) relative to myocardial infarction (MI) size

Correlations between MI size versus EDV (*A*), EF (*B*), SV (*C*), cardiac index (*D*), LVEDP (*E*), and dP/dt_{max} (*F*) are shown. Group differences were analyzed by analysis of covariance followed by a Bonferroni post hoc test. For EDV, $F = 3.84$, $P < 0.05$; for EF, $F = 5.97$, $P < 0.05$; for SV, $F = 8.74$, $P < 0.01$; for cardiac index, $F = 6.29$, $P < 0.01$; for LVEDP, $F = 5.8$, $P < 0.01$; for dP/dt_{max}, $F = 0.78$, not significant. For all, data include the present study and our previous study [sedentary MI (Sed-MI) group ($n = 10$) and exercise-trained (ExT-MI) group ($n = 9$) (31)]. $^{a}P < 0.05$ and $^{b}P < 0.01$, sedentary MI rats treated with vehicle (Sed-MI-Veh group; solid line) vs. exercise-trained MI rats treated with vehicle (ExT-MI-Veh; dashed line); $\#P < 0.05$, ExT-MI-Veh vs. exercise-trained MI rats treated with ANA-12 (ExT-MI-ANA-12 group; dotted line). BW, body weight.

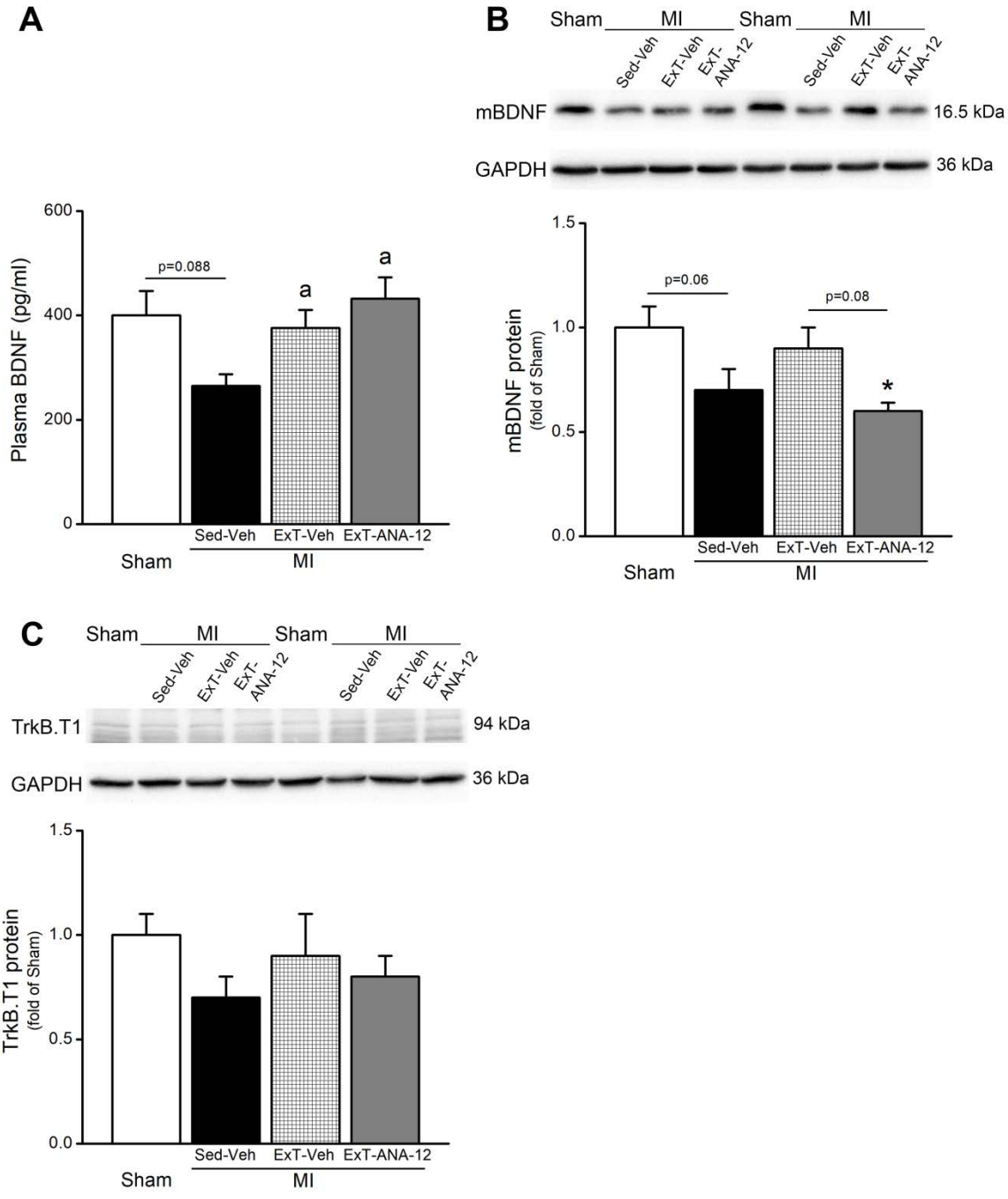
A
Plasma BDNF (pg/ml)
600
400
200
0
p=0.088
a
a
Sed-Veh
ExT-Veh
ExT-ANA-12
Sham
MI
B
Sham
MI
Sham
MI
Sed-Veh
ExT-Veh
ExT-ANA-12
mBDNF
16.5 kDa
GAPDH
36 kDa
mBDNF protein
(fold of Sham)
1.5
1.0
0.5
0.0
p=0.06
p=0.08
*
Sed-Veh
ExT-Veh
ExT-ANA-12
Sham
MI
C
Sham
MI
Sham
MI
Sed-Veh
ExT-Veh
ExT-ANA-12
TrkB.T1
94 kDa
GAPDH
36 kDa
TrkB.T1 protein
(fold of Sham)
1.5
1.0
0.5
0.0
Sed-Veh
ExT-Veh
ExT-ANA-12
Sham
MI

Figure 3-3. Plasma brain-derived neurotrophic factor (BDNF) and myocardial mature BDNF (mBDNF) and truncated form of tropomyosin-related kinase B (TrkB.T1) protein expression with representative Western blot images at 5 wk postmyocardial infarction (post-MI) with or without exercise training or ANA-12 treatment

Plasma BDNF (*A*), mBDNF protein (*B*), and TrkB.T1 (*C*) in the noninfarct area of the left ventricle of sham and MI rats with or without exercise training or ANA-12 treatment are shown. Values are means ± SE. Sham group, $n = 10$; sedentary MI with vehicle treatment (Sed-MI-Veh) group, $n = 8$; exercise training with MI and vehicle treatment (ExT-MI-Veh) group, $n = 9$; and exercise training with MI and ANA-12 treatment (ExT-MI-ANA-12) group, $n = 8$. All bands were normalized to GAPDH and are shown as fold values of the sham group. Statistical analysis was done by one-way ANOVA followed by a Bonferroni post hoc test. For plasma BDNF, $F = 3.7$, $P < 0.05$; for myocardial mBDNF protein, $F = 4.9$, $P < 0.01$; for TrkB.T1, $F = 0.69$, not significant. $^{*}P < 0.05$ vs. the sham group; $^{a}P < 0.05$ vs. the Sed-MI-Veh group.

Effect of exercise training post-MI with or without ANA-12 on mBDNF, the truncated form of TrkB as well as CaMKII and Akt expression

mBDNF protein in the noninfarct area of the LV tended to be lower in the Sed-MI-Vehicle group compared to the sham group (P = 0.06; Fig 3-3*B*). Exercise training increased mBDNF protein to the sham level, which was prevented by ANA-12 treatment (Fig 3-3*B*). The truncated form of TrkB (TrkB.T1) protein was not different among the groups (Fig 3-3*C*). The p-CaMKII protein level was significantly decreased in the Sed-MI-Vehicle group compared with sham, and exercise training attenuated the decrease in p-CaMKII protein, which was prevented by ANA-12 treatment (Fig 3-4, *A* and *B*). The p-CaMKII-to-CaMKII (pan) ratio, which indicates CaMKII activity, was lower in all MI groups compared with the sham group without differences between MI groups (Fig 3-4*D*). p-Akt (Thr^{308}) and p-Akt (Ser^{473}) protein expression and p-Akt (Thr^{308})-to-Akt (pan) and p-Akt (Ser^{473})-to-Akt (pan) ratios were significantly lower in Sed-MI-Vehicle rats than in sham rats, which were prevented by exercise training (Fig 3-5, *A*-*F*). ANA-12 treatment blocked the effect of exercise on p-Akt (Thr^{308}) and p-Akt (Ser^{473}) expression and p-Akt (Thr^{308})-to-Akt (pan) and p-Akt (Ser^{473})-to-Akt (pan) ratios (Fig 3-5, *A*-*F*). Altogether, exercise training post MI prevents decreases in mBDNF, p-CaMKII, p-Akt (Thr^{308}), and p-Akt (Ser^{473}) expression as well as activity of Akt in the noninfarct area of the LV, which were all blocked by ANA-12 treatment.

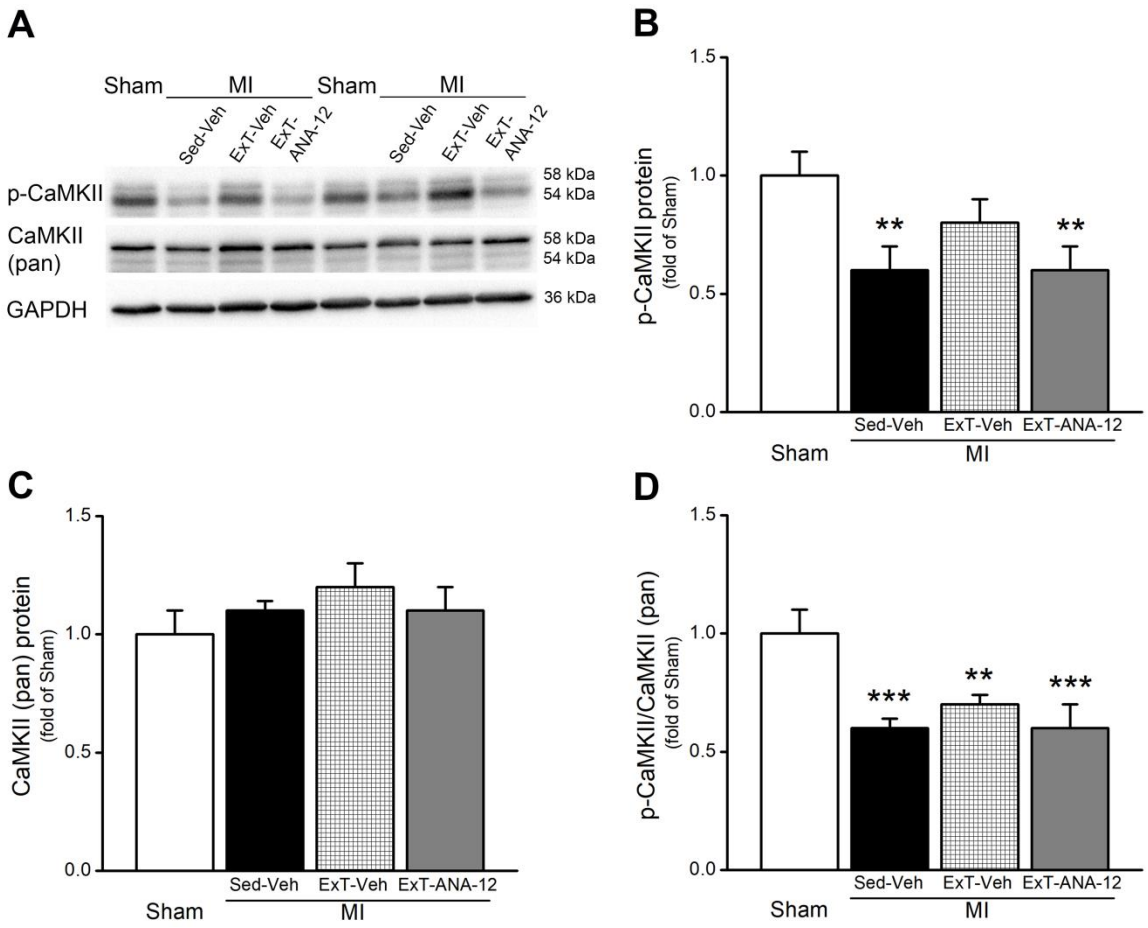

Figure 3-4. Total Ca^{2+}/calmodulin-dependent protein kinase II (CaMKII) (pan) and phosphorylated (p-)CaMKII protein expression with representative Western blot images and p-CaMKII-to-CaMKII (pan) ratio in the noninfarct area of the left ventricle (LV) of rats at 5 wk postmyocardial infarction (post-MI) with or without exercise training or ANA-12 treatment

Representative Western blot images of p-CaMKII and CaMKII (pan) with GAPDH as the loading control (*A*), p-CaMKII (*B*) and CaMKII (pan) (*C*) protein expression, and the p-CaMKII-to-CaMKII (pan) ratio in the LV of sham and MI rats with or without exercise training or ANA-12 treatment (*D*) are shown. Values are means ± SE. Sham group, $n = 10$; sedentary MI with vehicle treatment (Sed-MI-Veh) group, $n = 8$; exercise training with MI and vehicle treatment (ExT-MI-Veh) group, $n = 9$; and exercise training with MI and ANA-12 treatment (ExT-MI-ANA-12) group, $n = 8$. All bands were normalized to GAPDH and are shown as fold values of the sham group. Statistical analysis was done by one-way ANOVA followed by a Bonferroni post hoc test. For p-CaMKII, $F = 6.1$, $P < 0.01$; for CaMKII (pan), $F = 1.5$, not significant; for p-CaMKII/CaMKII (pan), $F = 12.9$, $P < 0.001$. $^{**}P < 0.01$, and $^{***}P < 0.001$ vs. the sham group.

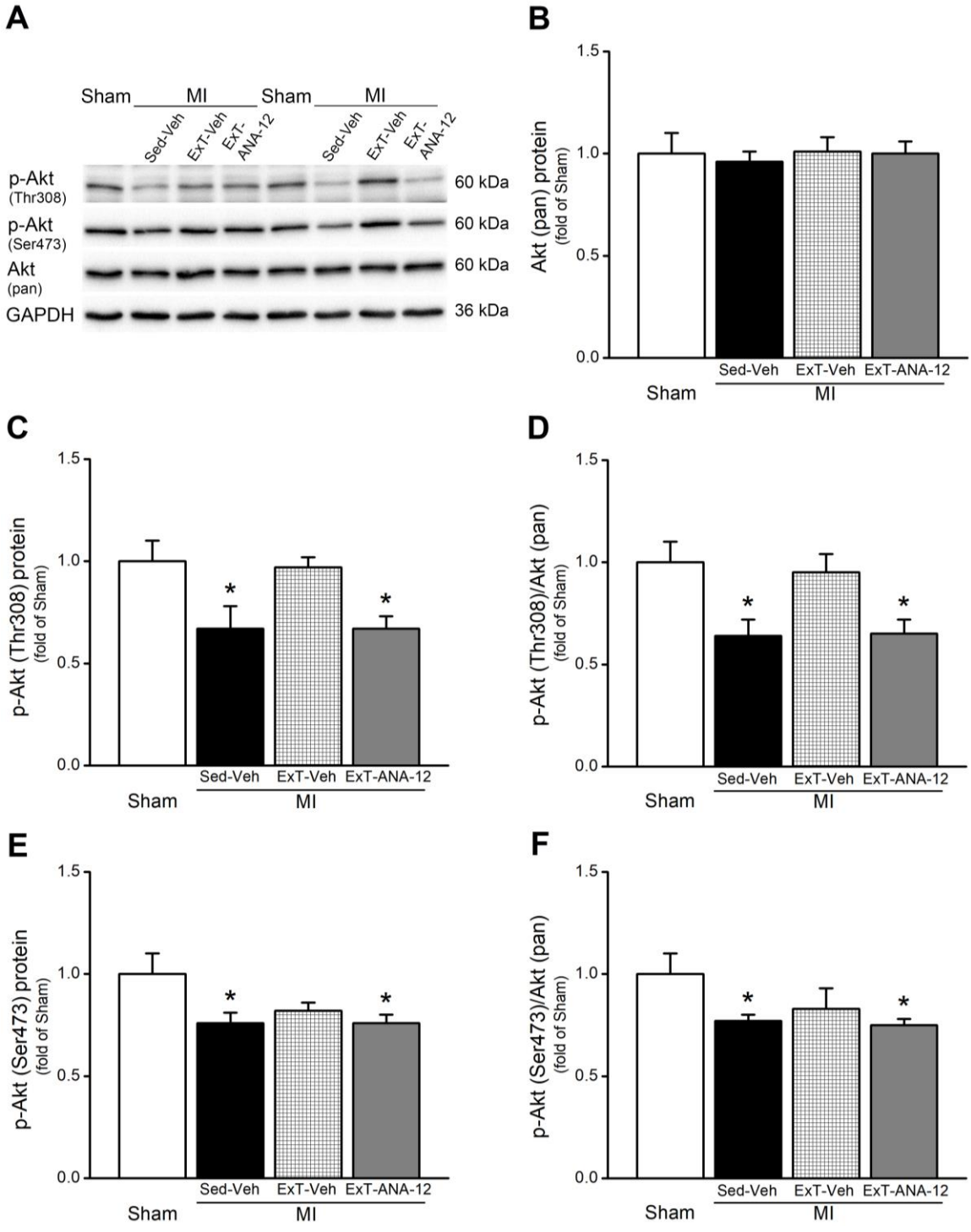
A
Sham
MI
Sham
MI
Sed-Veh
ExT-Veh
ExT-ANA-12
Sed-Veh
ExT-Veh
ExT-ANA-12
p-Akt (Thr308)
p-Akt (Ser473)
Akt (pan)
GAPDH
60 kDa
60 kDa
60 kDa
36 kDa
B
Akt (pan) protein (fold of Sham)
C
p-Akt (Thr308) protein (fold of Sham)
D
p-Akt (Thr308)/Akt (pan) (fold of Sham)
E
p-Akt (Ser473) protein (fold of Sham)
F
p-Akt (Ser473)/Akt (pan) (fold of Sham)
1.5
1.0
0.5
0.0
*
Sham
MI
Sed-Veh
ExT-Veh
ExT-ANA-12

Figure 3-5. Total Akt (pan), phosphorylated (p-)Akt (Thr^{308}) and p-Akt (Ser^{473}) protein expression with representative Western blot images, and p-Akt (Thr^{308})-to-Akt (pan) and p-Akt (Ser^{473})-to-Akt (pan) ratios in the noninfarct area of the left ventricle (LV) of rats at 5 wk postmyocardial infarction (post-MI) with or without exercise training or ANA-12 treatment

Representative Western blot images of p-Akt (Thr^{308}), p-Akt (Ser^{473}), Akt (pan), and GAPDH as the loading control (*A*); Akt (pan; *B*), p-Akt (Thr^{308}; *C*), p-Akt (Thr^{308})-to-Akt (pan) (*D*); p-Akt (Ser^{473}; *E*); and p-Akt (Ser^{473})-to-Akt (pan) (*F*) ratio in the LV of sham and MI rats with or without exercise training or ANA-12 treatment are shown. Values are means ± SE. Sham group, $n = 10$; sedentary MI with vehicle treatment (Sed-MI-Veh) group, $n = 8$; exercise training with MI and vehicle treatment (ExT-MI-Veh) group, $n = 9$; and exercise training with MI and ANA-12 treatment (ExT-MI-ANA-12) group, $n = 8$. All bands were normalized to GAPDH and shown as fold values of the sham group. Statistical analysis was done by one-way ANOVA followed by a Bonferroni post hoc test. For Akt (pan), $F = 0.08$, not significant; for p-Akt (Thr^{308}), $F = 4.9$, $P < 0.01$; for p-Akt (Thr^{308})/Akt (pan), $F = 4.9$, $P < 0.01$; for p-Akt (Ser^{473}), $F = 4.9$, $P < 0.01$; for p-Akt (Ser^{473})/Akt (pan), $F = 3.6$, $P < 0.05$. $^{*}P \leq 0.05$ vs. the sham group.

Effect of exercise training post-MI with or without ANA-12 on AMPK and metabolic gene expression

p-AMPKα protein in the noninfarct area of the LV was significantly lower in the Sed-MI-Vehicle group ($P = 0.05$), and the p-AMPKα-to-total-AMPKα ratio tended to be lower ($P = 0.11$) compared with the sham group (Fig 3-6, *A-D*). Exercise training prevented the decrease in p-AMPKα post-MI, but ANA-12 did not block this effect (Fig 3-6, *A-D*). mRNA expression of genes related to glucose metabolism, glucose transporter (Glut)4 and phosphofructokinase (Pfk), did not change, but Glut1 significantly increased in all MI groups (Table 3-4). mRNA expression of genes related to fatty acid metabolism, fatty acid translocase (FAT/Cd36), carnitine palmitoyl-CoA transferase (Cpt)1a and Cpt1b, and acetyl CoA carboxylase 1 (Acc1), was not different between sham and MI groups (Table 3-4). In contrast, mRNA expression of Acc2 decreased post-MI ($P < 0.01$), and exercise training prevented this decrease. Acc2 mRNA expression in the ExT-MI-ANA-12 group was not significantly different compared to other MI groups (Table 3-4).

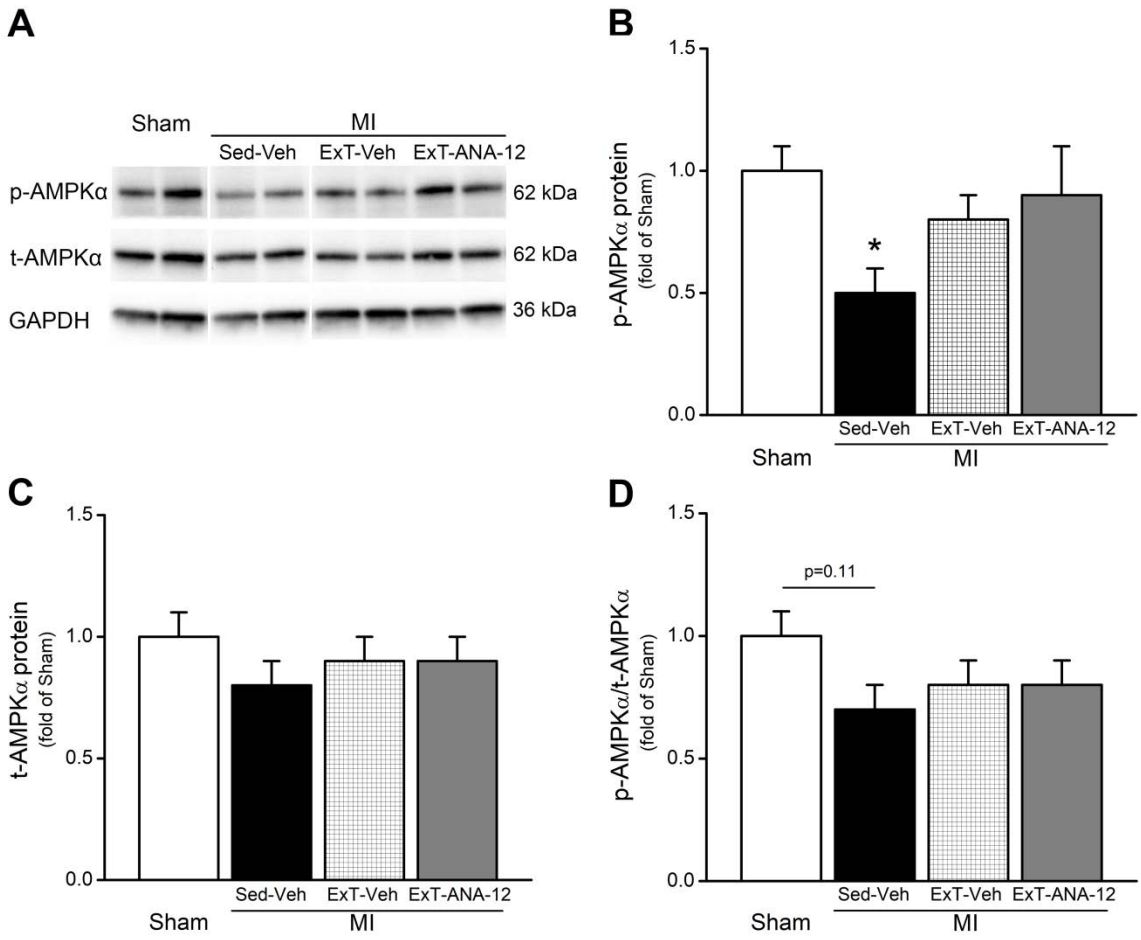

Figure 3-6. Total AMP-activated protein kinase (t-AMPKα) and phosphorylated (p-)AMPKα protein expression with representative Western blot images as well as the p-AMPKα-to-total AMPKα ratio in the noninfarct area of the left ventricle (LV) of rats at 5 wk postmyocardial infarction (post-MI) with or without exercise training or ANA-12 treatment

Representative Western blot images of p-AMPK_, total AMPK_, and GAPDH as the loading control (*A*), p-AMPKα (*B*) and total AMPKα (*C*) protein expression, and the p-AMPKα-to-t-AMPKα ratio of sham and MI rats with or without exercise training or ANA-12 treatment (*D*) are shown. Values are means ± SE; n = 8 per group. All bands were normalized to GAPDH and shown as fold values of the sham group. Statistical analysis was done by one-way ANOVA followed by a Bonferroni post hoc test. For p-AMPKα, F = 3.2, P = 0.05; for total AMPKα, F = 1.5, not significant; for p-AMPKα/total AMPKα, F = 2.4, P = 0.11. *P = 0.05 vs. the sham group. Sed-MI-Veh, sedentary MI with vehicle treatment group; ExT-MI-Veh, exercise training with MI and vehicle treatment group; ExT-MI-ANA-12, exercise training with MI and ANA-12 treatment group.

Table 3-4. Metabolic gene expression in the noninfarct area of the left ventricle of rats at 5 wk post-MI with or without exercise training or ANA-12 treatment

		MI		
	Sham	Sed-Vehicle	ExT-Vehicle	ExT-ANA-12
Number of rats/group	10	8	9	8
Glucose metabolism				
Glut1	1.0 ± 0.1	1.5 ± 0.1*	1.4 ± 0.1*	1.5 ± 0.1*
Glut4	1.0 ± 0.1	0.9 ± 0.1	1.0 ± 0.03	0.9 ± 0.1
Pfk	1.0 ± 0.04	0.9 ± 0.1	0.9 ± 0.03	0.9 ± 0.1
Fatty acid metabolism				
FAT/Cd36	1.0 ± 0.1	0.9 ± 0.1	0.9 ± 0.04	0.9 ± 0.1
Cpt1a	1.0 ± 0.1	1.0 ± 0.1	0.9 ± 0.1	0.8 ± 0.1
Cpt1b	1.0 ± 0.04	1.0 ± 0.1	1.1 ± 0.04	1.1 ± 0.1
Acc1	1.0 ± 0.1	1.1 ± 0.03	1.1 ± 0.1	1.1 ± 0.1
Acc2	1.0 ± 0.04	0.7 ± 0.04†	0.9 ± 0.03	0.8 ± 0.1

Values are expressed as means ± SE of mRNA expression (fold values of the sham group). MI, myocardial infarction; Sed, sedentary; ExT, exercise training; *Glut1* and *Glut4*, glucose transporter types 1 and 4; *Pfk*, phosphofructokinase; *FAT/Cd36*, fatty acid translocase; *Cpt1a* and *Cpt1b*, carnitine palmitoyltransferase 1a and 1b; *Acc1* and *Acc2*, acetyl-CoA carboxylase 1 and 2. One-way ANOVA followed by a Bonferroni post hoc test was done. For *Glut1*, $F = 4.6$, $P < 0.01$; for *Glut4*, $F = 1.1$, $P = 0.35$; for *Pfk*, $F = 1.3$, $P = 0.31$; for *FAT/Cd36*, $F = 1.3$, $P = 0.28$; for *Cpt1a*, $F = 1.2$, $P = 0.34$; for *Cpt1b*, $F = 0.2$, $P = 0.9$; for *Acc1*, $F = 0.27$, $P = 0.85$; for *Acc2*, $F = 5.2$, $P < 0.01$. *$P < 0.05$ and †$P < 0.01$ vs. the sham group.

DISCUSSION

The present study investigated the effect of exercise training on cardiac BDNF-TrkB signaling and its role in improving cardiac function in rats post-MI (Fig 3-7). The main findings of the study are that *1)* exercise training post-MI improves EF and LVEDP and increases SV and cardiac index, and ANA-12 treatment prevents the improvement of EF and attenuates the increases in SV and cardiac index but does not affect the decrease in LVEDP; *2)* at 5 wk post-MI, cardiac BDNF, p-CaMKII, p-Akt (Thr^{308}), and p-Akt (Ser^{473}) protein expression and CaMKII and Akt activities are decreased. These decreases are prevented by exercise training post-MI, and ANA-12 treatment attenuates these effects of exercise; and *3)* at 5 wk post-MI, p-AMPKα protein is decreased, exercise training prevents this decrease, and ANA-12 does not inhibit the effect of exercise training on p-AMPKα protein. These results suggest that the improvement of EF and part of increases in SV and cardiac index in response to exercise training post-MI is mediated by the BDNF-TrkB axis and downstream effectors CaMKII and Akt but not of AMPKα.

Effects of exercise training on cardiac function with or without ANA-12 treatment

Previous studies reported that early initiation of exercise training post-MI improves EF and LVEDP (Cai et al., 2016; Xu et al., 2008a; Xu et al., 2008b). Our findings are consistent with these previous reports, showing that relative to MI size, EF is higher and LVEDP is lower in the ExT-MI-Vehicle group compared with the Sed-MI-Vehicle group. Moreover, exercise training post-MI significantly increased cardiac index similarly as previously observed in healthy rats with treadmill (Jin et al., 2000) or swimming (Radovits et al., 2013) exercise training.

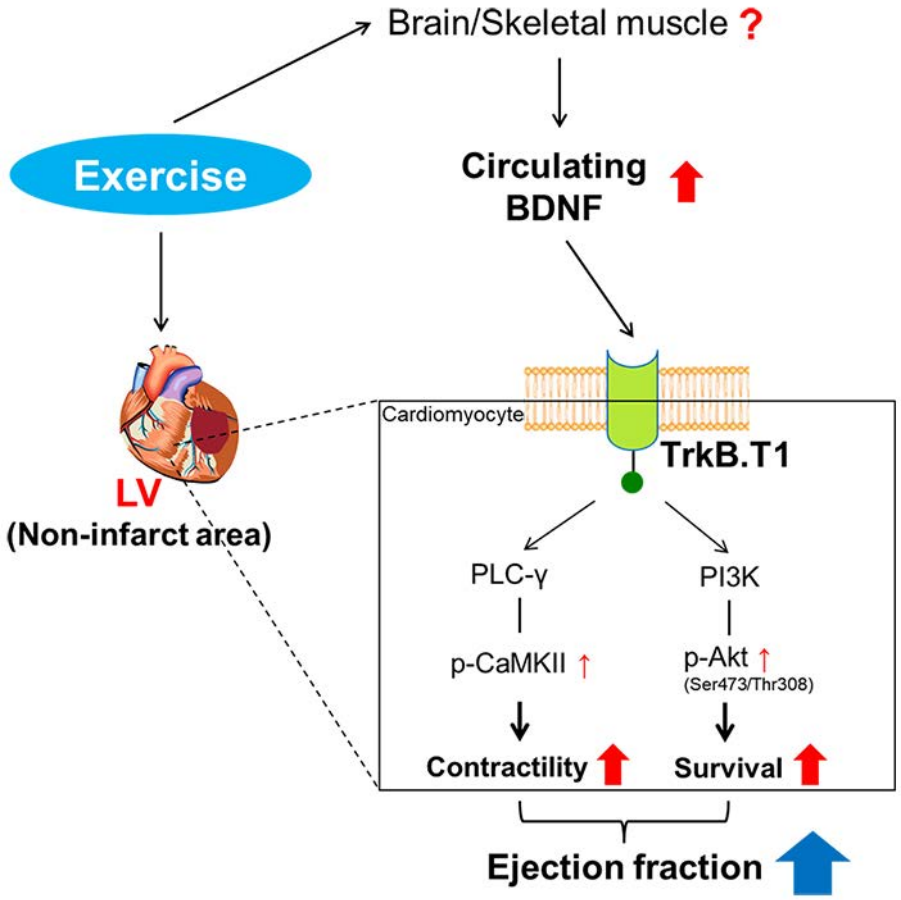

Figure 3-7. Proposed role of brain-derived neurotrophic factor (BDNF)-tropomyosin-related kinase B (TrkB) signaling and downstream factors in the left ventricle (LV) in response to exercise training postmyocardial infarction

Exercise training increases circulating BDNF, which may be released from the brain and/or skeletal muscle. Cardiomyocytes may sequester circulating BDNF via the truncated form of TrkB (TrkB.T1), thereby activating the downstream signaling pathways phospholipase Cγ (PLCγ)-Ca^{2+}/calmodulin-dependent protein kinase II (CaMKII), enhancing myocardial contractility and phosphatidylinositol 3-kinase (PI3K)-Akt, and increasing cardiomyocyte survival. These effects ultimately may contribute to the improvement of ejection fraction by exercise. p-Akt/CaMKII, phosphorylated Akt/CaMKII.

To our knowledge, there are no reports about the effect of exercise training post-MI on cardiac index of rodents. The increase in cardiac index by exercise training was due to an increase in EDV and SV but not in heart rate, consistent with a previous study in healthy rats (Jin et al., 2000). Exercise training post-MI may increase venous return to the heart by reduction in vascular resistances similarly as observed in healthy and diabetic rats (Freitas et al., 2015; Jin et al., 2000) and patients with HF (Hambrecht et al., 2000), as well as an increase in ventricular compliance by minimizing additional scar thinning (Puhl et al., 2015; Xu et al., 2008b) and collagen accumulation (Xu et al., 2008b). In the present study, the increase in resting LVEDP post-MI was attenuated by exercise training, which may reflect the larger LV volume and improved ventricular compliance (Radovits et al., 2013). Altogether, exercise training post-MI improved both systolic and diastolic functions.

A previous study (Allen et al., 2018), has shown that blockade of BDNF-TrkB signaling by ANA-12 abolished the beneficial effects of exercise training on cognitive function in diabetic rats, but there are no reports on the effects of ANA-12 on the exercise-induced improvement of cardiac function post-MI. In the present study, ANA-12 treatment prevented the increase in EF and attenuated the increases in SV and cardiac index, but did not affect the increase in EDV and the decrease in LVEDP. These findings suggest that increases in SV and cardiac index by exercise training are caused by improvement in both systolic and diastolic function. Activation of BDNF-TrkB signaling by exercise training appears to contribute to the component because of improvement of systolic function but not of diastolic function. ANA-12 is a small molecule which binds to extracellular domain of TrkB and induces conformational change of the receptor,

resulting in blockade of BDNF binding (Cazorla et al., 2011). ANA-12 binds the full length form of TrkB in the whole brain of normal mice, decreasing the p-TrkB-to-TrkB ratio (Cazorla et al., 2011). ANA-12 likely also binds to the full length form of TrkB receptors in brain areas associated with cardiovascular regulation such as paraventricular nucleus and rostral ventricular medulla, and thereby may prevent exercise-induced attenuation of sympathetic hyperactivity (Zheng et al., 2012b) and improvement of EF. In the heart, TrkB.T1, lacking the tyrosine kinase domain, is the dominant form of TrkB (Fulgenzi et al., 2015). Since the two isoforms of TrkB receptors have an identical extracellular domain (Middlemas et al., 1991), it is likely that ANA-12 also binds to cardiac TrkB.T1 and blocks cardiac BDNF-TrkB.T1 signaling. Previous studies have reported that constitutive cardiac BDNF-TrkB signaling is necessary for normal myocardial contractility (Feng et al., 2015), and that TrkB.T1 in the heart mediates the BDNF-dependent inotropic effect (Fulgenzi et al., 2015). Taken together, improvement of systolic function by exercise training post-MI might be mediated by cardiac BDNF-TrkB.T1 and/or central BDNF-TrkB signaling, and other mechanisms may contribute to the improvement of diastolic function.

Effects of exercise training on BDNF-TrkB axis in the LV post MI with or without ANA-12 treatment

Exercise training prevented the decrease in mBDNF protein in the noninfarct area of the LV, and ANA-12 treatment inhibited this effect. Mechanisms that contribute to an increase in cardiac BDNF in response to exercise training are not clear. Similar to skeletal muscle or myotubes (Hurtado et al., 2017; Matthews et al., 2009), enhanced cardiac muscle contraction or cardiac efferent nerve activity by exercise may increase

BDNF expression in the heart (Hurtado et al., 2017; Matthews et al., 2009). Since exercise training increases mBDNF protein, but not BDNF mRNA in the noninfarct area (Lee et al., 2017), it is also possible that circulating BDNF may sequester in the heart through cardiac TrkB.T1, leading to an increase in cardiac BDNF. Exercise training increases circulating BDNF in healthy rats (Jiménez-Maldonado et al., 2014). In the present study, exercise training prevented the decrease in plasma BDNF level post-MI and this response was not affected by ANA-12 treatment. Sequestration of BDNF by TrkB.T1 has been demonstrated in chick embryo cells and neuroblastoma cells and in astrocytes isolated from rat hippocampus (Alderson et al., 2000; Fenner, 2012). Our findings suggest that cardiomyocytes may increase cardiac BDNF by sequestering circulating BDNF through TrkB.T1 receptors, which can be blocked by ANA-12.

Changes in CaMKII in the LV post-MI and effects of exercise

CaMKII is a Ca^{2+}-regulated protein kinase which regulates Ca^{2+} homeostasis in the heart, and modulates cardiac contraction in normal conditions (Zhang, 2017; Zhang and Brown, 2004). CaMKII is one of the downstream effectors of the cardiac BDNF-TrkB axis (Feng et al., 2015). Feng et al. (2015) showed that BDNF in normal cardiomyocytes increases p-CaMKII protein expression and enhances cardiomyocytes fractional shortening, which was inhibited by a CaMKII inhibitor, suggesting that activation of cardiac BDNF-TrkB signaling, followed by increase in p-CaMKII contributes to enhancement of myocardial contractility. After MI induced by coronary artery ligation, p-CaMKII and CaMKII protein expression were decreased at 2 wk post-MI without a change in the p-CaMKII-to-CaMKII ratio (Zhao et al., 2014), and CaMKII protein expression and CaMKII activity were reduced in the noninfarct area of the LV at 8 wk post-MI (Netticadan et al., 2000).

We observed a decrease in p-CaMKII protein expression and the p-CaMKII-to-CaMKII (pan) ratio in the noninfarct area of the LV at 5 wk post-MI without significant change in CaMKII (pan) expression. Other models of HF, such as pressure overload-induced cardiac hypertrophy by transverse aortic constriction, showed large (two- to fourfold) increases in total CaMKII and p-CaMKII protein (Respress et al., 2012; Zhang et al., 2003), which may promote pathological hypertrophy and cardiac apoptosis (Backs et al., 2009; Ling et al., 2009; Zhang et al., 2003). The rat MI model and transverse aortic constriction model therefore show opposite changes in CaMKII activity. Stimulus-specific heterogeneity of cardiac hypertrophy (e.g. pressure vs. volume) results in different molecular adaptations in the heart (You et al., 2017).

Exercise-induced increase in p-CaMKII expression has been reported in the hearts of healthy exercised mice (Burgos et al., 2017; Kemi et al., 2007). Similarly, we observed that exercise training prevented the decrease in p-CaMKII in the noninfarct area of the LV. ANA-12 treatment prevented this effect of exercise, indicating that BDNF-TrkB signaling mediates the effect of exercise on p-CaMKII. Collectively, a reduction in p-CaMKII protein expression and CaMKII activity in the noninfarct area of the LV post-MI may be a consequence of decrease in cardiac BDNF-TrkB signaling post-MI and contribute to a decrease in myocardial contractility. Prevention of the decrease in p-CaMKII by exercise training may represent a favorable adaptive response in MI hearts.

Changes in Akt in the LV post-MI and effects of exercise

Akt is a serine/threonine protein kinase which increases cell survival, growth, and proliferation (Abeyrathna and Su, 2015; Chaanine and Hajjar, 2011). Akt has two phosphorylation sites: one is Thr^{308} and the other one is Ser^{473} (Abeyrathna and Su, 2015;

Chaanine and Hajjar, 2011). Although downstream pathways of each phosphorylation site and the extent of phosphorylation of Thr^{308} and Ser^{473} vary in different diseases, phosphorylation of both Thr^{308} and Ser^{473} is required for maximal activation of the kinase (Manning and Toker, 2017). BDNF-induced phosphorylation of both Thr^{308} and Ser^{473} of Akt was reported in cortical/hippocampal neurons (Johnson-Farley et al., 2006; Zheng et al., 2008), and phosphorylation of Ser^{473} of Akt in cardiomyocytes (Okada et al., 2012). Previous studies have shown that the p-Akt (Ser^{473})-to-total Akt ratio was not changed in the noninfarct area of the LV at 5 wk post-MI (Manchini et al., 2017) and p-Akt-to-total Akt ratio (phosphorylation site not specified) in the peri-infarct area at 6 wk post-MI (Cai et al., 2016). In contrast, the present study showed a significant reduction in both p-Akt (Thr^{308})-to-Akt (pan) and p-Akt (Ser^{473})-to-Akt (pan) ratios at 5 wk post-MI. These different changes may reflect different experimental conditions. Manchini et al. (2017) used female rats and their MI rats did not show a significant increase in LVEDP, although some other parameters showed significant cardiac dysfunction. Although Cai et al. (2016) did not show significant change in the p-Akt-to-total Akt ratio in the peri-infarct post-MI, phosphatidylinositol 3-kinase (an upstream factor of Akt) was significantly lower. Furthermore, the extent of downregulation of Akt activity may be region specific in the LV (noninfarct vs. peri-infarct).

The decreases in p-Akt (Thr^{308}) and p-Akt (Ser^{473}) protein expression and their ratios to Akt (pan) post-MI were prevented by exercise training, and ANA-12 treatment prevented these effects, indicating that BDNF-TrkB signaling mediates the effect of exercise on p-Akt protein expression and Akt activities. Cai et al. (2016) reported that the p-Akt-to-Akt ratio in the peri-infarct area was increased after exercise training,

accompanied by a decrease in TUNEL-positive cells and Bax-to-Bcl-2 ratio. Exercise training appears to downregulate proapoptotic factor (Bax) and upregulate antiapoptotic factor (Bcl-2), leading to increase in cardiomyocytes survival (Cai et al., 2016). BDNF-induced activation of Akt and an increase in cardiomyocyte viability were observed in doxorubicin-induced cardiac injury (Hang et al., 2017). Moreover, cardiac-specific overexpression of Akt improved myocardial contractility in healthy mice (Condorelli et al., 2002) and in mice with aortic constriction (Shiojima et al., 2012). Altogether, exercise-induced prevention of the decrease in Akt activities in the noninfarct area of the LV may promote cardiomyocyte survival and may lead to improvement of EF.

Changes in AMPK and metabolic gene expression in the LV post-MI and effects of exercise

AMPK is one of the key regulators of cardiac glucose/fatty acid metabolism (Bairwa et al., 2016). BDNF-TrkB signaling-dependent regulation of AMPK has been reported in rat skeletal muscle, in which BDNF phosphorylates AMPK and enhances fatty acid oxidation (Matthews et al., 2009).

At 3–4 weeks post MI induced by LAD ligation, AMPK activation was found increased in the infarct and peri-infarct areas of the LV (Li et al., 2016) but unchanged in the peri-infarct area (Wu et al., 2014) or in the whole LV (Chen et al., 2017). In the present study, p-AMPKα expression was measured in the noninfarct area of the LV post-MI and showed a decrease, suggesting that AMPK-dependent regulation of glucose/fatty acid metabolism might be impaired. Exercise training prevented the decrease in p-AMPKα, consistent with a previous study (Ma et al., 2015b) in mice with isoproterenol-induced cardiac hypertrophy, suggesting that AMPK-mediated cardiac energy

metabolism might be improved in the noninfarct area of the LV by exercise. The prevention of the decrease in p-AMPKα by exercise was not affected by TrkB blockade. This indicates that activation of AMPK-dependent pathways by exercise training post-MI does not appear to depend on BDNF-TrkB signaling.

In the heart, activation of AMPK increases translocation of GLUT4 to the plasma membrane and activates enzymes such as PFK, resulting in enhancement of glucose metabolism (Bairwa et al., 2016; Kim and Dyck, 2015). AMPK activation also promotes translocation of FAT/CD36 and phosphorylates and thereby inhibits ACC1/2 activity and increases fatty acid metabolism (Bairwa et al., 2016; Kim and Dyck, 2015). However, AMPK activation appears not to affect expression of these genes per se (Xing et al., 2003). After MI, expression of genes related to glucose/fatty acid metabolism shows time-dependent changes or no change (Amorim et al., 2010; Rosenblatt-Velin et al., 2001; Tao et al., 2015). Different types of exercise (e.g. swimming and running on a treadmill) and duration differently affect gene/protein expression related to glucose/fatty acid metabolism in healthy, MI, or hypertensive rodents (Lehnen et al., 2011; Tao et al., 2015). We found that 4 wk treadmill exercise training did not affect the increase in Glut1 but prevented the decrease in Acc2 mRNA post-MI. Cardiac-specific knockout of Acc2 in mice results in an increase in cardiac fatty acid oxidation (Kolwicz Jr et al., 2012). The prevention of the decrease in Acc2 mRNA by exercise may suggest a decrease in fatty acid oxidation, but this may be offset by the prevention of the decrease in p-AMPKα. Since AMPK-ACC axis independent pathways also can regulate cardiac fatty acid oxidation (Sung et al., 2015; Zordoky et al., 2014), further studies are clearly needed to

assess the actual effects of exercise training on cardiac energy metabolism in this MI model.

In conclusion, exercise training post-MI improves cardiac function including EF, SV, cardiac index and LVEDP. ANA-12 treatment prevents the improvement of EF and attenuates the increases in SV and cardiac index but does not affect the decrease in LVEDP. Exercise training prevents the decrease in mBDNF, p-CaMKII, p-Akt, and p-AMPKα in the noninfarct area of the LV post-MI. TrkB blockade inhibits exercise-induced changes in mBDNF, p-CaMKII, and p-Akt but not of p-AMPKα. These results indicate that the BDNF-TrkB axis and the downstream effectors CaMKII and Akt mediate the improvement of cardiac systolic function induced by exercise training post-MI. These findings suggest that activation of the BDNF-TrkB axis by exercise training is a promising target to preserve cardiac function post-MI.

ACKNOWLEDGMENTS

We would like to thank Drs. Kyoung-Han Kim and Riyoun Kim for providing the primers and interpreting the metabolic gene analysis.

GRANTS

This study was supported by operating grant # FRN: MOP-136923 from the Canadian Institutes of Health Research. Frans H.H. Leenen holds the Pfizer Chair in Hypertension Research, an endowed chair supported by Pfizer Canada, University of Ottawa Heart Institute Foundation, and Canadian Institutes of Health Research. Heow Won Lee was the recipient of a University of Ottawa Endowed Graduate Award in Cardiac Research at the Heart Institute, supported by the University of Ottawa's Faculty of Medicine Endowed Funds in Cardiac Research and the University of Ottawa Heart Institute Foundation.

DISCLOSURES

No conflicts of interest, financial or otherwise, are declared by the authors.

AUTHOR CONTRIBUTIONS

H.W.L. and F.H.H.L. conceived and designed research; H.W.L., M.A. and J.J.W. performed experiments; H.W.L. and M.A. analyzed data; H.W.L., M.A., H.W.W, P.G.B. and F.H.H.L. interpreted results of experiments; H.W.L. prepared figures; H.W.L. drafted manuscript; H.W.L. and F.H.H.L., edited and revised manuscript; H.W.L., M.A., J.J.W., H.W.W, P.G.B. and F.H.H.L. approved final version of manuscript.

Chapter 4

Effects of exercise on BDNF-TrkB signaling in the paraventricular nucleus and rostral ventrolateral medulla in rats post myocardial infarction

Effects of exercise on BDNF-TrkB signaling in the paraventricular nucleus and rostral ventrolateral medulla in rats post myocardial infarction

Heow Won Lee, Monir Ahmad, Hong-Wei Wang and Frans H.H. Leenen

Brain and Heart Research Group, University of Ottawa Heart Institute, Ottawa, Ontario, Canada

Running Title: Exercise and BDNF-TrkB signaling in the PVN and RVLM post MI

Submitted: *Neuropeptides*

Abstract

Brain-derived neurotrophic factor (BDNF)-tropomyosin-related kinase B (TrkB) signaling in the paraventricular of nucleus (PVN) and rostral ventrolateral medulla (RVLM) is associated with cardiovascular regulation. Exercise increases plasma BDNF and attenuates activation of central pathways in the PVN and RVLM post myocardial infarction (MI). The present study assessed whether MI alters BDNF-TrkB signaling and intracellular factors Ca^{2+}/calmodulin-dependent protein kinase II (CaMKII) and Akt in the PVN and RVLM of male Wistar rats with or without exercise training or treatment with the TrkB blocker ANA-12. A 4-week period of treadmill exercise training was performed in MI rats. A separate experiment was conducted with 2.5 mg/kg ANA-12 in sedentary MI rats. At 5 weeks post MI, in both the PVN and RVLM, the ratio of full-length TrkB (TrkB.FL) and truncated TrkB (TrkB.T1) was decreased. Only Akt activity was decreased in the RVLM. 0.5 mg/kg ANA-12 did not affect BDNF-TrkB signaling and cardiac function post MI, but 2.5 mg/kg ANA-12 further decreased EF. Exercise increased mBDNF and decreased Akt activity in the PVN, whereas in the RVLM, exercise did not affect mBDNF but lowered p-CaMKIIβ. ANA-12 prevented the exercise-induced increase in mBDNF in the PVN and decrease in p-CaMKIIβ in the RVLM. Collectively, the TrkB.FL/TrkB.T1 ratio was decreased in the PVN and RVLM, but downstream factors showed different patterns. BDNF-TrkB signaling mediates the exercise-induced increase in mBDNF in the PVN and decrease in p-CaMKIIβ in the RVLM. Whether reductions in Akt in the PVN and p-CaMKIIβ in the RVLM by exercise contribute to the decrease in sympathetic hyperactivity post MI will require further study.

Key words: Exercise training, Heart failure, PVN, RVLM, BDNF, ANA-12

Introduction

In animal models of HF post myocardial infarction (MI), activation of central pathways involving important cardiovascular regulatory nuclei, such as the paraventricular of nucleus (PVN) in the hypothalamus and rostral ventrolateral medulla (RVLM) in the brainstem, contributes to sympathetic hyperactivity (Kumagai et al., 2012; Shenton and Pyner, 2016) and progressive cardiac dysfunction (Huang et al., 2009; Huang et al., 2014). Exercise training post MI decreases neuronal activity in the PVN (Shen et al., 2018; Zheng et al., 2012b) and RVLM (Ichige et al., 2016), attenuates sympathetic hyperactivity post MI (Zheng et al., 2012b) and improves cardiac dysfunction (Cai et al. 2016; Lee et al., 2017). Underlying central molecular mechanisms are not yet fully understood.

It is well established that exercise increases circulating brain-derived neurotrophic factor (BDNF) (Máderová et al., 2019; Walsh and Tschakovsky, 2018) and the brain is the major source (Seifert et al., 2010; Rasmussen et al., 2009). BDNF-TrkB signaling has been studied in the hippocampus and cortex. In hippocampal/cortical neurons, mature BDNF (mBDNF; active form of BDNF) binds to either the full-length form of its binding receptor tropomyosin-related kinase B (TrkB.FL) or truncated form of TrkB (TrkB.T1) (Park and Poo, 2012). TrkB.FL and TrkB.T1 share identical first 12 amino acids in their intracellular domains, but only TrkB.FL contains tyrosine kinase in its intracellular domain where phosphorylation occurs (Boulle et al., 2012; Fenner, 2012; Klein et al., 1991). mBDNF binds to TrkB.FL and TrkB.T1 with similar affinity (Park and Poo, 2012), and mBDNF binding to TrkB.T1 inhibits mBDNF-TrkB.FL signaling in neurons (Fenner, 2012; Tapia-Arancibia et al., 2004). Changes in the ratio of TrkB.FL and TrkB.T1 may

therefore affect responses to mBDNF. In neurons, mBDNF binds to plasma membrane TrkB.FL, and phosphorylation of TrkB.FL (p-TrkB) targeting tyrosine residues (Y) 515 activates phosphatidylinositol 3-kinase (PI3K)-Akt pathway, and phosphorylation of Y816 activates phospholipase Cγ (PLCγ)-Ca^{2+}/calmodulin dependent protein kinase II (CaMKII) pathway (Greenberg et al., 2009; Park and Poo, 2012). In the hippocampus and cortex of rats, exercise increases BDNF protein and phosphorylation of TrkB, as well as increases activities of intracellular factors, Akt and CaMKII (Ding et al., 2011; Fang et al., 2013). Whether exercise training affects BDNF-TrkB signaling in the PVN and RVLM has not yet been assessed.

Recent studies showed that BDNF can contribute to regulation of sympathetic nerve activity (SNA), blood pressure (BP) and heart rate (HR) in the PVN (Erdos et al., 2015; Schaich et al., 2016) and RVLM (Chan et al., 2010; Wang and Zhou, 2002), but the role of BDNF appears different in the PVN and RVLM. In the PVN of normal rats, microinjection or chronic overexpression of BDNF increased sympathetic activity, BP and HR (Erdos et al., 2015; Schaich et al., 2016). In the brainstem, intracisternal infusion of BDNF did not change BP in conscious rats, but attenuated angiotensin II (Ang II)-induced increase in BP (Chan et al., 2010). Specific knockdown of Bdnf gene in the RVLM did not affect BP of conscious normal rats, but potentiated the Ang II-induced increase in BP (Chan et al., 2010). Moreover, microinjection of BDNF into the dorsal medial nucleus tractus solitarius (dmNTS) in the brainstem of normal rats decreased renal SNA (RSNA), BP and HR, whereas microinjection of *N*-(2-{[(hexahydro-2-oxo-1H-azepin-3-yl)amino]carbonyl}phenyl)-benzo[b]thiophene-2-carboxamide (ANA-12), a selective noncompetitive antagonist of TrkB receptors (Cazorla et al., 2011), increased

these factors and blunted baroreflex sensitivity, indicating that endogenous BDNF-TrkB signaling in the NTS contributes to BP and baroreflex regulation (Becker et al., 2016).

The role of brain BDNF post MI has been evaluated in rodents post MI. In mice at 2 weeks post MI, BDNF protein was increased in the forebrain (thalamus/hypothalamus) and brain specific deletion of the Bdnf gene further increased cardiac fibrosis and decreased ejection fraction (EF) (Okada et al., 2012). In rats at 14 weeks post MI, in the dmNTS, BDNF protein was not changed but TrkB protein was decreased (Becker et al., 2016). In response to microinjection of either BDNF or into the dmNTS, the extent of decreases and increases in RSNA, BP and HR were attenuated, as well as the blunting of baroreflex sensitivity by ANA-12 was reduced in MI rats, suggesting that BDNF-TrkB signaling in the NTS is decreased post MI (Becker et al., 2016). After MI, activation of the BDNF-TrkB signaling in the forebrain may therefore play a cardioprotective role (Leenen and Tuana, 2012; Okada et al., 2012), whereas decrease in BDNF-TrkB signaling in the NTS may contribute to sympathoexcitation and baroreflex desensitization (Becker et al., 2016). We reported that exercise training prevents the decrease in cardiac BDNF-TrkB signaling and improves EF post MI, and these effects are blocked by ANA-12 at the regular dose of 0.5 mg/kg (Lee et al., 2018). It is unknown whether BDNF-TrkB signaling is affected post MI in the PVN and RVLM and regulates intracellular factors, Akt and CaMKII similar as in the hippocampus/cortex, and whether exercise training post MI affects such changes.

The aim of the present study was therefore to determine 1) changes in BDNF and TrkB expression and activities of intracellular factors Akt and CaMKII in the PVN and RVLM in rats post MI, and 2) the effect of exercise and TrkB blockade on BDNF-TrkB

signaling post MI. We assessed mBDNF, TrkB.FL and TrkB.T1 protein including p-TrkB (Y515) and p-TrkB (Y816), and their downstream factors Akt and CaMKII activities in the PVN and RVLM.

Material and Method

Experimental animals and groups

All animal experiments followed the US National Institutes of Health *Guide for the Care and Use of Laboratory Animals* (8th ed., 2011) and were approved by the University of Ottawa Animal Care Committee. Male Wistar rats weighing 200–250g (Charles River, Montreal, Canada) were housed in a room at a constant temperature and humidity for 5–7 days under a 12:12-hr light-dark cycle and allowed standard laboratory chow and tap water *ad libitum*. Two experiments were conducted separately: regular dose ANA-12 (0.5 mg/kg) and high dose ANA-12 (2.5 mg/kg) studies.

Experiment 1: Effect of exercise or regular dose of ANA-12 post MI on BDNF-TrkB signaling in the PVN and RVLM

To assess effects of MI with or without exercise or ANA-12 on BDNF-TrkB signaling in the PVN and RVLM, 6 groups are included in the present study. Except for two ANA-12 treated groups (Sham-ANA-12 and Sed-MI-ANA-12), cardiac function data and cardiac BDNF-TrkB signaling were recently published (Lee et al., 2018). In the present study, brain samples of these rats were used for analyses of BDNF-TrkB signaling in the PVN and RVLM. 15 rats underwent sham surgery and 80 rats MI surgery. Sham operated rats were divided into two groups: Sham with vehicle (Sham-Veh, n=9) and Sham with ANA-12 (Sham-ANA-12, n=6). 47 surviving MI rats were divided into four groups: sedentary MI with vehicle (Sed-MI-Veh, n=12), sedentary MI with ANA-12 (Sed-MI-ANA-12, n=14), exercise MI with vehicle (ExT-MI-Veh, n=11) and exercise MI with ANA-12 (ExT-MI-ANA-12, n=10). At the end of the study, rats with small (MI size <20% of LV) or no MI were removed, and 1 rat in the ExT-MI-ANA-12 group died during

echocardiography. 9 Sed-MI-Veh, 9 Sed-MI-ANA-12, 8 ExT-MI-Veh and 7 ExT-MI-ANA-12 rats are included in the final analyses.

Experiment 2: Effect of high dose ANA-12 on cardiac function and BDNF-TrkB signaling in the PVN and RVLM

Since the 0.5 mg/kg dose ANA-12 did not affect cardiac dysfunction post MI, a high dose (2.5 mg/kg) of ANA-12 was used to assess whether ANA-12 dose-dependently deteriorates cardiac function post MI. 30 rats underwent MI surgery and 21 surviving MI rats were divided into two groups (9 MI-Veh and 12 MI-ANA-12). At the end of experiment, after excluding rats with a small MI, 6 MI-Veh and 8 MI-ANA-12 were used for analyses. 7 Sham rats were included as a control.

MI surgery

1–2 hours prior to surgery, slow release Buprenorphine (1 mg/kg; Chiron Compounding Pharmacy Inc., Guelph, ON, Canada) was subcutaneously injected which provides adequate analgesia for 3 days. MI surgery was performed as previously described (Lee et al., 2017). In brief, thoracotomy was performed under 2% mixture of isoflurane and oxygen anesthesia, pericardium was opened and the left descending coronary artery (LAD) was permanently ligated. Sham surgery was performed similarly without ligation of the LAD.

Exercise training

Exercise was initiated 5–7 days post MI and conducted for 4 weeks (5 days per week) using a motor-driven treadmill (Columbus Instruments, Columbus, OH, USA) as previously described (Lee et al., 2017). All rats in exercise groups run successfully.

Sedentary Sham and MI rats were treated similarly to the exercising rats without motion of the treadmill. Electrical stimulus was not used during exercise.

ANA-12 preparation and oral administration

ANA-12 (S7745; Selleckchem, Houston, TX, USA) stock was prepared by dissolving in 0.5% methyl celluose (M7140; Sigma-Aldrich, St Louis, MO, USA) and mixed with 1 g of peanut butter, and administered once per day (7 days per week) early in the morning. For vehicle-treated groups, 1 g of peanut butter mixed with 0.5% methyl celluose was provided without ANA-12. For the regular dose study, the dose of ANA-12 (0.5 mg/kg) was selected as discussed recently (Lee et al., 2018). ANA-12 administration was started one day before the first exercise, and 3–5 hours before each exercise session. For the high dose study, ANA-12 (2.5 mg/kg) or vehicle administration was initiated 4–5 days post MI and continued for 5 weeks.

Echocardiographic and hemodynamic measurements

Echocardiography was conducted under 2% mixture of isoflurane and oxygen anesthesia at 2–4 days after the MI surgery, and blindly for drug treatment at 5 weeks post MI using a VisualSonic Vevo 770 imaging system (VisualSonics, Toronto, ON, Canada). LV systolic and diastolic diameters were measured from M-mode images, and LV end-systolic volume (LVESV), LV end-diastolic volume (LVEDV) and EF were calculated. Hemodynamic measurements were conducted with a Millar catheter under the same anesthesia as described above. LV peak-systolic pressure (LVPSP), LV end-diastolic pressure (LVEDP) and maximal/minimal rate of pressure changes ($dP/dt_{max/min}$) were measured (Lee et al., 2017).

Tissue collection and measurement of infarct size

After decapitation, whole brains were collected and frozen in -20 to -30°C pre-chilled 2-Methylbutane (M32631, Sigma-Aldrich). The hearts were removed and washed in ice-cold 0.9% saline. Atria were removed and the whole ventricles were separated into the right ventricle (RV) and LV. The LV was opened flat and the circumference and the infarct borders of the LV were traced under a transparent sheet for measurement of the infarct size. The infarct size was calculated from the scanned digital image of the LV demarcation, and presented as a percentage of the infarct area of total LV area. All tissues were kept at -80°C until further analyses.

Micro-brain punches and protein preparation

A cryostat (CM3050S, Leica) was used for sectioning of the brain and 50 μm of sections were obtained from posterior of bregma 0.9 mm to 2.2 mm for the PVN of the hypothalamus, and posterior of bregma 11.80 mm to 13.80 mm for the RVLM of the brainstem according to the rat brain atlas of Paxinos and Watson (1998). PVN and RVLM were micro-punched separately using a tissue puncher with 1.0 mm of diameter (57397, Stoelting Co., Wood Dale, IL, USA) and homogenized in ice-cold CelLytic MT Cell Lysis Reagent (C3228, Sigma-Aldrich) contained with 0.25 mM sucrose, 0.5M EDTA, PhosSTOP (4906845001, Roche) and 1% protease inhibitor cocktail (P8340, Sigma-Aldrich). Supernatant was collected after centrifugal separation at 12,000g, 4°C for 20 min. Micro bicinchoninic acid (BCA) assay (23235, Thermo scientific Inc., Rockford, IL, USA) was performed to measure protein concentration.

Western blotting

15µg of protein was separated using 4–15% Criterion™ TGX™ Precast Midi Protein Gel (5671084, Bio-Rad, Mississauga, ON, Canada) and transferred to 0.2 µm PVDF membranes (Bio-Rad). After transfer, the membranes were cut into three pieces according to the molecular weight of the target proteins and blocked for 1h at room temperature either with 5% non-fat dry milk in Tris-buffered saline with 1% Tween-20 (TBST) for TrkB, mBDNF, or 5% bovine serum albumin (BSA) in TBST for phosphorylated (p-)Trk (Y785/Y816), p-Trk (Y490/Y515), p-CaMKII (Thr286), total (t-)CaMKII, p-Akt (Ser473) and t-Akt. The membranes were incubated separately at 4°C overnight with each primary antibody. All phosphorylated and total proteins were measured in separate blots. Membranes above 75 kDa were incubated with TrkB (1:5,000, 07-225; Millipore, Toronto, ON, Canada), p-Trk (Y490/515) (1:1,000, 4619; Cell Signaling Technology, Beverly, MA, USA) or p-Trk (Y785/Y816) (1:1000, 4618; Cell Signaling Technology) antibodies. Three separate blots were used for measurements of p-TrkB (Y515), p-TrkB (Y816) and TrkB (TrkB.FL, at 140 kDa; TrkB.T1 at 90 kDa). Membranes at 25 kDa–75 kDa were incubated with p-CaMKII (Thr286) (1:10,000, 12716; Cell Signaling Technology), CaMKII (pan) (1:5000, 4436; Cell Signaling Technology), p-Akt (Ser473) (1:10,000, 4060; Cell Signaling Technology) and Akt (pan) (1:10,000, 4691; Cell Signaling Technology). Membranes lower than 25 kDa were incubated with BDNF antibody (1:2,000, ab108319; Abcam). The specificity of BDNF bands was confirmed with BDNF peptide (ab182199; Abcam) according to the manufacturer's instruction (Fig 4-1). Next day, the membranes were washed with TBST three times for 10 min, then incubated with goat anti-rabbit IgG-HRP (1:5,000 or

1:10,000, 111-035-144; Jackson ImmunoResearch Laboratories, Inc., West Grove, PA, USA**)** for 1 h at room temperature. The blot was developed with either Immobilon Forte Western HRP substrate (WBLUF0500; Millipore) or Immobilon Classico HRP substrate (WBLUC0500; Millipore) Western HRP substrates and visualized with a ChemiDoc XRS + imager (Bio-Rad). The membranes at 25 kDa–75 kDa were stripped using stripping buffer (21059; Thermo scientific Inc.) and re-probed with anti-GAPDH (1:10,000, MAB374; Millipore) followed by anti-mouse (1:10,000, NXA931V; GE Healthcare; Chicago, IL, USA) as a loading control. Band densities were quantified using Image Lab software (Bio-Rad). The density of each protein band was normalized to the density of the GAPDH band, and shown as fold changes of the Sham-Veh group. Ratios of phosphorylated proteins to total proteins for TrkB, CaMKII and Akt were calculated to determine their activities.

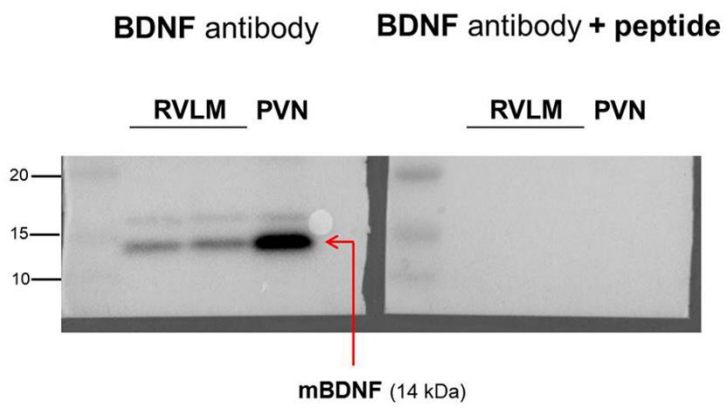

Figure 4-1. BDNF antibody specificity

Brain-derived neurotrophic factor (BDNF) antibody (ab108319, 1:2,000, Abcam) and BDNF peptide (ab182199, Abcam) were used to confirm specificity of BDNF bands. 15µg protein of the paraventricular nucleus (PVN) and rostral ventrolateral medulla (RVLM) were loaded. mBDNF, mature BDNF

Statistical analyses

For the regular dose study, cardiac function data was analyzed by two-way analysis of variance (ANOVA) followed by Bonferroni *post hoc* test to compare the effects of MI and drug among Sham and sedentary MI groups (Sham-Veh, Sham-ANA-12, Sed-MI-Veh and Sed-MI-ANA-12). For protein data analysis, two-way ANOVAs followed by Bonferroni *post hoc* test were done among Sham and sedentary MI groups, and in MI groups (Sed-MI-Veh, Sed-MI-ANA-12, ExT-MI-Veh and ExT-MI-ANA-12) to compare the effects of exercise and drug. For the high dose study, one-way ANOVAs were done for cardiac function and protein data analyses. For both studies, a student unpaired t-test was performed to compare MI size between MI-Veh and MI-ANA-12, and analysis of covariance (ANCOVA) to compare EF relative to MI size. $P \leq 0.05$ was considered statistically significant.

Results

Effect of MI with regular dose (0.5 mg/kg) or high dose (2.5 mg/kg) of ANA-12 on cardiac function

In Sham rats, 0.5 mg/kg of ANA-12 did not affect body weight, or echocardiographic and hemodynamic parameters (Table 4-1). In the Sed-MI-Veh group, increases in LVESV, LVEDV and LVEDP, and decreases in EF, LVPSP, dP/dt_{max} and dP/dt_{min}, indicate clear cardiac dysfunction at 5 weeks post MI (Table 4-1). Both regular and high dose ANA-12 had no obvious effects on echocardiographic and hemodynamic measurements of cardiac dysfunction in sedentary rats post MI (Table 4-1 and 4-2), except for EF relative to MI size in the high dose MI-ANA-12 group. By ANCOVA, EF in the MI-ANA-12 group was significantly lower than in the MI-Veh group ($F=8.6$, $P<0.05$; Fig 4-2), but not in the regular dose group. In conclusion, ANA-12, dose-related further decreases EF post MI in sedentary rats. We reported already that ANA-12 (0.5 mg/kg) prevents the exercise-induced improvement of EF (Lee et al., 2018).

Table 4-1. General characteristics, echocardiographic and hemodynamic measurements at 5 weeks post MI with or without regular dose ANA-12 (0.5 mg/kg)

	Sham		MI	
	Veh (n=9)	ANA-12 (n=6)	Sed-Veh (n=9)	Sed-ANA-12 (n=9)
Body weight (g)				
Baseline	277 ± 6	286 ± 3	292 ± 3	289 ± 5
Final	510 ± 7	478 ± 12	515 ± 16	503 ± 11
MI size (%)	N/A	N/A	28 ± 2	25 ± 1
Echocardiographic parameters				
LVESV (µl/100g BW)	12 ± 1	10 ± 2	39 ± 5**	38 ± 6**
LVEDV (µl/100g BW)	61 ± 4	61 ± 4	87 ± 7*	91 ± 11*
EF (%)	80 ± 1	84 ± 2	55 ± 2**	60 ± 2**
Hemodynamic parameters				
LVPSP (mmHg)	120 ± 2	127 ± 3	101 ± 5**	106 ± 2**
LVEDP (mmHg)	2.7 ± 0.3	2.5 ± 0.4	14.1 ± 1.4**	11.7 ± 0.9**
dP/dt_{max} (mmHg/sec)	7633 ± 102	8272 ± 230	5598 ± 345**	5881 ± 164**
dP/dt_{min} (mmHg/sec)	6526 ± 96	7087 ± 296	4454 ± 400**	4879 ± 202**
HR (bpm)	376 ± 8	368 ± 6	362 ± 6	370 ± 8

Values are means ± SE. Veh, vehicle; ANA-12, TrkB blocker; Sed, sedentary; MI, myocardial infarction; N/A, not applicable. BW, body weight; LVESV, left ventricle end-systolic volume; LVEDV, LV end-diastolic volume; EF; ejection fraction; LVPSP, LV peak-systolic pressure; LVEDP, LV end-diastolic pressure; $dP/dt_{max/min}$, maximal/minimal rate of pressure changes; HR, heart rate.

*P<0.01 and **P<0.001 vs. Sham groups.

Two-way analysis of variance (ANOVA) was done for MI and drug effects except for MI size. For MI size, student unpaired t-test was done.

For baseline body weight, MI, F=3.0, not significant; for final body weight, MI, F=1.4, not significant; for LVESV, MI, F=38.5, P<0.001; for LVEDV, MI, F=11.4, P<0.01; for EF, MI, F=181.6, P<0.001; for LVPSP, MI, F=30.7, P<0.001; LVEDP, MI, F=89.9, P<0.001; for dP/dt_{max}, F=73.7, P<0.001; for dP/dt_{min}, F=46.0, P<0.001; for HR, F=0.6, not significant

None of the drug effects and MI x drug interactions was significant.

Foot note: cardiac function of the Sham-Veh group and Sed-MI-Veh group with two more rats on the published data (Lee et al., 2018) are included in this table for comparison of cardiac function with ANA-12 treated groups.

Table 4-2. General characteristics, echocardiography and hemodynamic measurements at 5 weeks post MI with or without high dose ANA-12 (2.5 mg/kg)

	Sham-Veh (n=7)	MI-Veh (n=6)	MI-ANA-12 (n=8)
Body weight (g)			
Baseline	274 ± 8	278 ± 6	265 ± 5
Final	501 ± 18	494 ± 21	480 ± 13
MI size (%)	N/A	32 ± 1	32 ± 2
Echocardiographic parameters			
LVESV (μl/100g BW)	11 ± 1	49 ± 4**	53 ± 4**
LVEDV(μl/100g BW)	64 ± 3	120 ± 6**	115 ± 7**
EF (%)	84 ± 1	59 ± 2**	54 ± 2**
Hemodynamic parameters			
LVPSP (mmHg)	120 ± 3	103 ± 2*	103 ± 3*
LVEDP (mmHg)	4.2 ± 0.4	16.7 ± 2.0**	19.3 ± 2.4**
dP/dt_{max} (mmHg/sec)	7313 ± 82	5425 ± 138**	5298 ± 239**
dP/dt_{min} (mmHg/sec)	6343 ± 107	3920 ± 251**	4018 ± 288**
HR (bpm)	393 ± 4	367 ± 9	389 ± 12

Values are means ± SE. Veh, vehicle; ANA-12, TrkB blocker; MI, myocardial infarction; N/A, not applicable. BW, body weight; LVESV, left ventricle end-systolic volume; LVEDV, LV end-diastolic volume; EF; ejection fraction; LVPSP, LV peak-systolic pressure; LVEDP, LV end-diastolic pressure; $dP/dt_{max/min}$, maximal/minimal rate of pressure changes; HR, heart rate.

*P<0.01 and **P<0.001 vs. Sham-Veh.

One-way analysis of variance (ANOVA) was done except for MI size. For MI size, student unpaired t-test was done.

For baseline body weight, F=1.0, not significant; for final body weight, F=0.4, not significant; for LVESV, F=44.7, P<0.001; for LVEDV, F=24.9, P<0.001; for EF, F=115.4, P<0.001; for LVPSP, F=8.3, P<0.01; LVEDP, F=16.0, P<0.001; for dP/dt_{max}, F=34.6, P<0.001; for dP/dt_{min}, F=28.9, P<0.001; for HR, F=1.8, not significant.

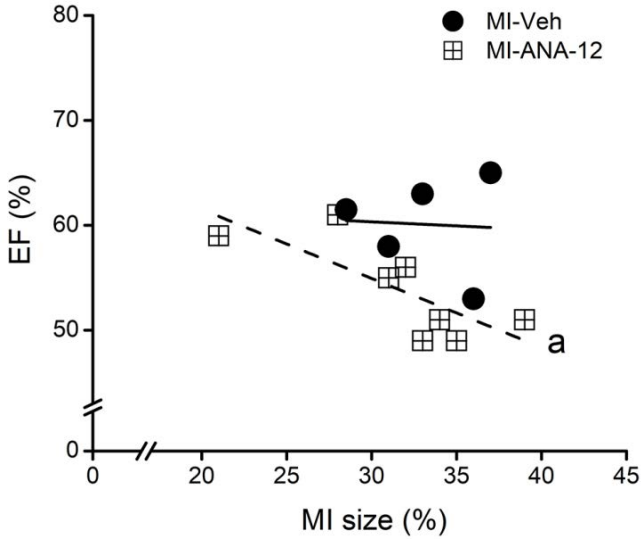

Figure 4-2. Correlation between MI size and EF in rats treated with vehicle or high dose ANA-12 post MI

By analysis of covariance, ejection fraction (EF) in the myocardial infarction (MI) rats treated with high dose ANA-12 (MI-ANA-12) is significantly lower than in MI rats with vehicle (MI-Veh; F=8.6, $P<0.05$). [a]$P<0.05$ vs. MI-Veh

Effect of ANA-12 on BDNF-TrkB signaling post MI with or without exercise

1. mBDNF and TrkB in the PVN

Representative blot images are presented in Fig 4-3A for mBDNF and in Fig 4-3B for p-TrkB, TrkB.FL and TrkB.T1. mBDNF protein was similar in Sham and Sed-MI rats, and not affected by ANA-12 (Fig 4-3C). Exercise training significantly increased mBDNF, and ANA-12 attenuated this increase (Fig 4-3C). TrkB.FL and TrkB.T1 expression were not different in Sham and Sed-MI rats, and ANA-12 had no effects on their expression (Table 4-3). TrkB.FL/TrkB.T1 ratio tended to be lower in Sham rats treated with ANA-12 (P=0.11; Fig 4-3D). In Sed-MI rats, the TrkB.FL/TrkB.T1 ratio was significantly lower compared to the Sham-Veh group without further effect of ANA-12 (Fig 4-3D). ExT-MI groups showed similar changes in TrkB.FL, TrkB.T1 and the TrkB.FL/TrkB.T1 ratio compared to the Sed-MI groups (Table 4-3 and Fig 4-3D).

In Sham rats, ANA-12 significantly increased p-TrkB (Y515)/TrkB.FL (Fig 4-3E). p-TrkB (Y515)/TrkB.FL was significantly increased post MI, but ANA-12 had no effect on this increase (Fig 4-3E). Exercise with vehicle or ANA-12 did not affect the increase in p-TrkB (Y515)/TrkB.FL post MI (Fig 4-3E). p-TrkB (Y816)/TrkB.FL was similar in Sham and Sed-MI rats, and was not altered by ANA-12 (Fig 4-3F). Two-way ANOVA showed a significant drug effect between Sed-MI and ExT-MI groups for p-TrkB (Y816)/TrkB.FL (F=4.4, P<0.05; Fig 4-3F) with lower p-TrkB (Y816)/TrkB.FL in the ExT-MI-ANA-12 group compared to the ExT-MI-Veh group (Fig 4-3F).

Table 4-3. TrkB.FL and TrkB.T1 expression in the PVN at 5 weeks post MI with or without exercise training or regular dose ANA-12

	Sham		MI			
	Veh (n=9)	ANA-12 (n=6)	Sed-Veh (n=7)	Sed-ANA-12 (n=9)	ExT-Veh (n=8)	ExT-ANA-12 (n=7)
	TrkB expression (fold of Sham-Veh, normalized to GAPDH)					
TrkB.FL	1.0 ± 0.04	0.88 ± 0.04	0.92 ± 0.04	0.88 ± 0.03	0.85 ± 0.03	0.87 ± 0.03
TrkB.T1	1.0 ± 0.03	0.96 ± 0.04	1.06 ± 0.03	1.00 ± 0.03	1.01 ± 0.04	0.97 ± 0.05

Values are means ± SE. Veh, vehicle; ANA-12, TrkB blocker; Sed-Veh, sedentary MI with Veh, Sed-ANA-12, sedentary MI with ANA-12; ExT-Veh, exercising MI with Veh; ExT-ANA-12, exercising MI with ANA-12. TrkB.FL, full-length form of tropomyosin-related kinase B; TrkB.T1, truncated form of TrkB; PVN, paraventricular nucleus.

Two-way analysis of variance (ANOVA) followed by Bonferroni
Effects of MI and drug (Sham groups vs. Sed-MI groups)
For TrkB.FL, MI, F=0.8, *P*=0.4; Drug, F=3.4, *P*=0.08; MI x Drug, F=1.1, *P*=0.3
For TrkB.T1, MI, F=2.2, *P*=0.2; Drug, F=2.0, *P*=0.2; MI x Drug, F=0.02, *P*=0.1

Effect of exercise and drug (within MI groups)
For TrkB.FL, ExT, F=1.4, *P*=0.2; Drug, F=0.01, *P*=0.9; ExT x Drug, F=0.7, *P*=0.4
For TrkB.T1, ExT, F=0.9, *P*=0.4; Drug, F=1.2, *P*=0.3; ExT x Drug, F=0.03, *P*=0.9

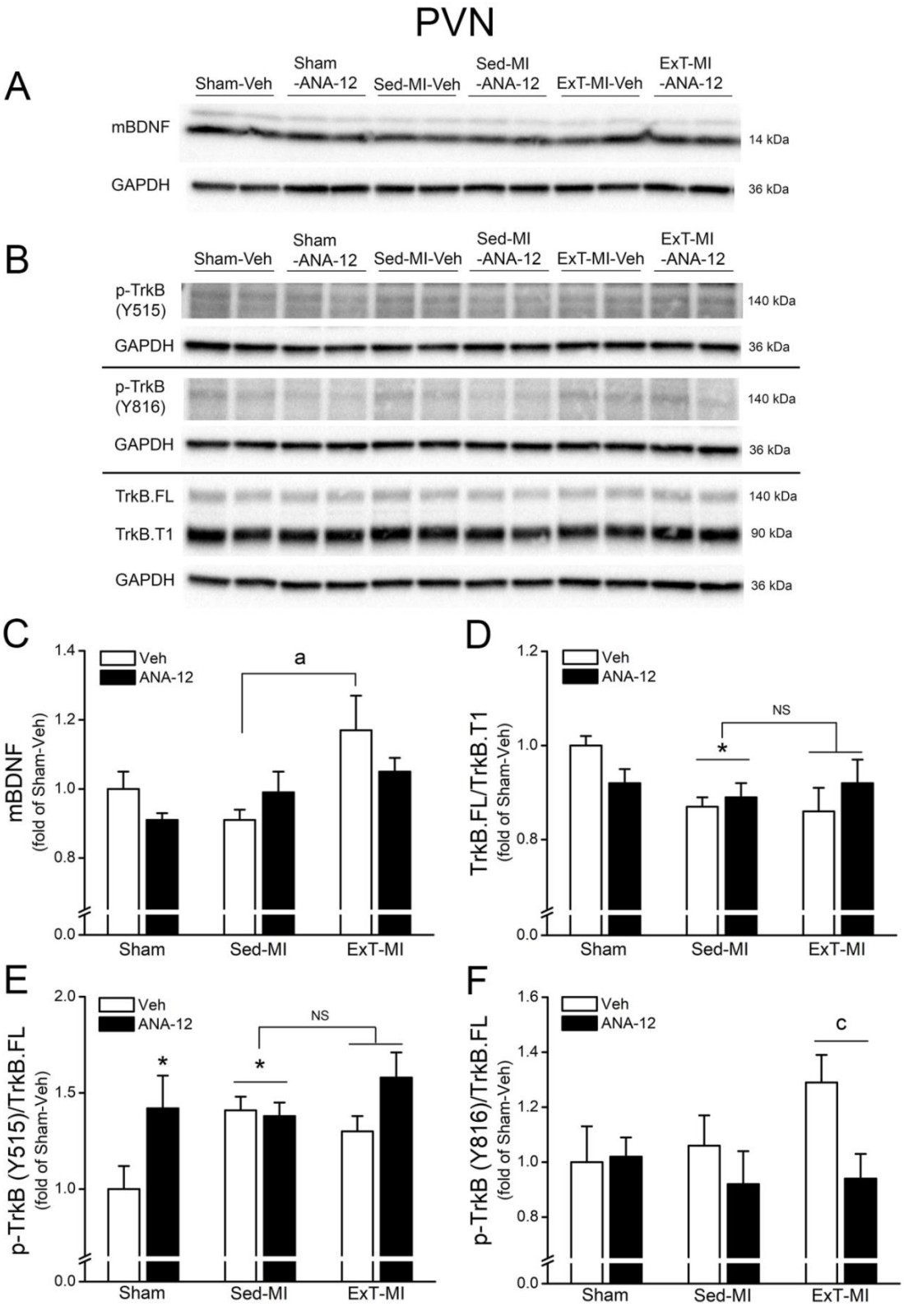
PVN
A
Sham-Veh
Sham -ANA-12
Sed-MI-Veh
Sed-MI -ANA-12
ExT-MI-Veh
ExT-MI -ANA-12
mBDNF
14 kDa
GAPDH
36 kDa
B
p-TrkB (Y515)
140 kDa
GAPDH
36 kDa
p-TrkB (Y816)
140 kDa
GAPDH
36 kDa
TrkB.FL
140 kDa
TrkB.T1
90 kDa
GAPDH
36 kDa
C
mBDNF (fold of Sham-Veh)
Veh
ANA-12
a
Sham
Sed-MI
ExT-MI
D
TrkB.FL/TrkB.T1 (fold of Sham-Veh)
NS
E
p-TrkB (Y515)/TrkB.FL (fold of Sham-Veh)
F
p-TrkB (Y816)/TrkB.FL (fold of Sham-Veh)
c

Figure 4-3. mBDNF protein, TrkB.FL/TrkB.T1 ratio, p-TrkB (Y515)/TrkB.FL and p-TrkB (Y816)/TrkB.FL in the PVN at 5 weeks post MI with or without regular dose ANA-12 or exercise training

Representative Western Blotting images for mature brain-derived neurotrophic factor (mBDNF) **(*A*)** and phosphorylated (p-) tropomyosin-related kinase B (TrkB) targeting tyrosine residue 515 (Y515) [p-TrkB (Y515)], p-TrkB targeting tyrosine residue 816 (Y816) [p-TrkB (Y816)], full-length form of TrkB (TrkB.FL) and truncated form of TrkB (TrkB.T1) with loading control (GAPDH) **(*B*)** in the paraventricular nucleus (PVN). mBDNF **(*C*)**, TrkB.FL/TrkB.T1 **(*D*)**, p-TrkB (Y515)/TrkB.FL ***(E)*** and p-TrkB (Y816)/TrkB.FL ***(F)*** of Sham and myocardial infarction (MI) rats with or without 0.5 mg/kg ANA-12 or exercise training. Veh, vehicle; Sed-MI, sedentary MI; ExT-MI, exercising MI. Values are means ± SE. Sham-Veh, n=9; Sham-ANA-12, n=6; Sed-MI-Veh, n=7, Sed-MI-ANA-12, n=9; ExT-MI-Veh, n=8; ExT-MI-ANA-12, n=7. All bands are normalized to GAPDH and represented as fold of Sham-Veh. Statistical analysis was done by two-way analysis of variance (ANOVA) followed by Bonferroni *post hoc* test within Sham and Sed-MI groups, and MI groups, respectively. *$P<0.05$ vs. Sham-Veh; $^{a}P<0.05$ vs. Sed-MI-Veh; $^{c}P\leq0.05$ vs. ExT-MI-Veh; NS, not significant

2. Intracellular factors Akt and CaMKII in the PVN

Representative blot images are presented in Fig 4-4A for p-Akt and t-Akt, and in Fig 4-4B for p-CaMKIIβ/α and t-CaMKIIβ/α. p-Akt (Ser473)/t-Akt was not different between Sham and Sed-MI rats, and ANA-12 did not affect p-Akt (Ser473)/t-Akt (Fig 4-4C). Exercise training significantly decreased p-Akt (Ser473)/t-Akt similarly in vehicle and ANA-12 treated MI groups (Fig 4-4C). In Sham rats, ANA-12 treatment decreased p-CaMKIIβ/α expression (for p-CaMKIIβ, 1.0 ± 0.07 vs. 0.59 ± 0.12, $P<0.01$; for p-CaMKIIα, 1.0 ± 0.07 vs. 0.71 ± 0.10, $P<0.05$, Sham-Veh vs. Sham-ANA-12), and their ratios to t-CaMKIIβ/α (Fig 4-4D and 4-4E). p-CaMKIIβ/α to t-CaMKIIβ/α were not changed post MI, but the ANA-12-induced decreases in p-CaMKIIβ/α expression and their ratios to t-CaMKIIβ/α noted in Sham rats were not observed in MI rats (Fig 4-4D and 4-4E). Exercise did not affect p-CaMKIIβ/α expression and their ratios to t-CaMKIIβ/α, and ANA-12 has no effect on these parameters (Fig 4-4D and 4-4E).

High dose ANA-12 did not show any further effects on proteins in the PVN (data not shown).

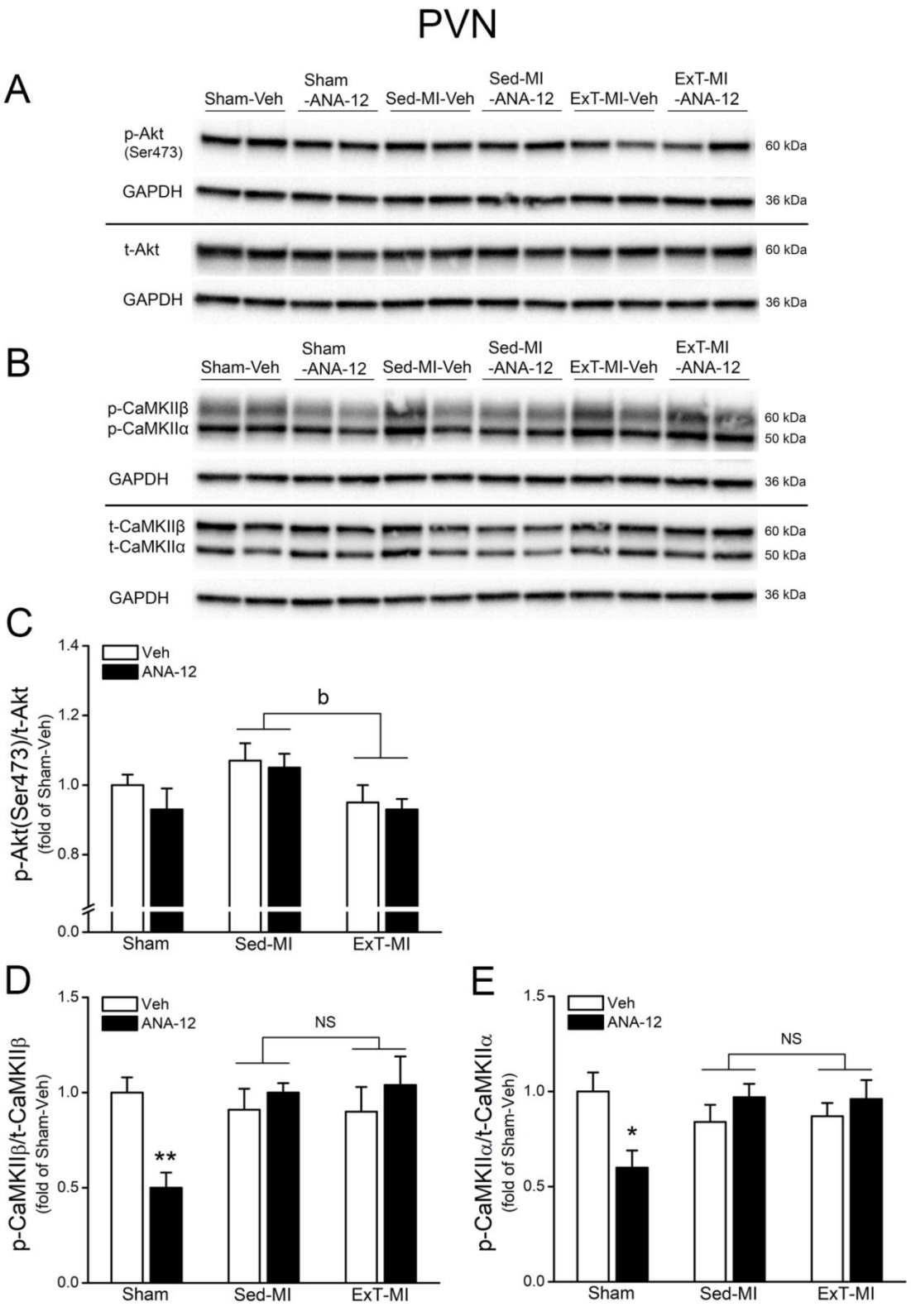
PVN
A
Sham-Veh
Sham -ANA-12
Sed-MI-Veh
Sed-MI -ANA-12
ExT-MI-Veh
ExT-MI -ANA-12
p-Akt (Ser473)
GAPDH
t-Akt
60 kDa
36 kDa
B
p-CaMKIIβ
p-CaMKIIα
t-CaMKIIβ
t-CaMKIIα
50 kDa
C
Veh
ANA-12
p-Akt(Ser473)/t-Akt (fold of Sham-Veh)
b
Sham
Sed-MI
ExT-MI
D
p-CaMKIIβ/t-CaMKIIβ (fold of Sham-Veh)
NS
**
E
p-CaMKIIα/t-CaMKIIα (fold of Sham-Veh)
*

Figure 4-4. p-Akt (Ser473)/t-Akt, p-CaMKIIβ/t-CaMKIIβ and p-CaMKIIα/t-CaMKIIα in the PVN at 5 weeks post MI with or without regular dose ANA-12 or exercise training

Representative Western Blotting images for phosphorylated (p-)Akt targeting serine residue 473 (Ser473) [p-Akt (Ser473)] and total Akt (t-Akt) **(A)**, and (p-)Ca^{2+}/Calmodulin-dependent protein kinase IIβ/α (p-CaMKIIβ/α) and total CaMKIIβ/α (t-CaMKIIβ/α) ***(B)*** with loading control (GAPDH) in the paraventricular nucleus (PVN). p-Akt (Ser473)/t-Akt ***(C)***, p-CaMKIIβ/t-CaMKIIβ ***(D)*** and p-CaMKIIα /t-CaMKIIα ***(E)*** of Sham and myocardial infarction (MI) rats with or without 0.5 mg/kg ANA-12 or exercise training. Veh, vehicle; Sed-MI, sedentary MI; ExT-MI, exercising MI. Values are means ± SE. Sham-Veh, n=9; Sham-ANA-12, n=6; Sed-MI-Veh, n=7, Sed-MI-ANA-12, n=9; ExT-MI-Veh, n=8; ExT-MI-ANA-12, n=7. All bands are normalized to GAPDH and represented as fold of Sham-Veh. Statistical analysis was done by two-way analysis of variance (ANOVA) followed by Bonferroni *post hoc* test within Sham and Sed-MI groups, and MI groups, respectively. **P*<0.05 and ***P*<0.01 vs. Sham-Veh; ^{b}P<0.05 vs. ExT-MI groups; NS, not significant

3. mBDNF and TrkB in the RVLM

Representative blot images are presented in Fig 4-5A for mBDNF and in Fig 4-5B for p-TrkB, TrkB.FL and TrkB.T1. mBDNF level (Fig 4-5C), and TrkB.FL and TrkB.T1 expression (Table 4-4) were not different among the groups. TrkB.FL/TrkB.T1 ratio was significantly lower in Sham rats treated with ANA-12 (Fig 4-5D). The TrkB.FL/TrkB.T1 ratio in the Sed-MI-Veh group was lower than Sham-Veh rats, but ANA-12 did not affect the ratio (Fig 4-5D). ExT-MI treated with either vehicle or ANA-12 did not affect the decrease in the TrkB.FL/TrkB.T1 post MI (Fig 4-5D). There were no group differences in p-TrkB (Y515)/TrkB.FL (Fig 4-5E). In Sham rats, p-TrkB (Y816)/TrkB.FL was not changed by ANA-12, and two-way ANOVA showed a significant MI effect for p-TrkB (Y816)/TrkB.FL ($F=5.74$, $P<0.05$; Fig 4-5F). The Sed-MI-ANA-12 group showed higher p-TrkB (Y816)/TrkB.FL compared to the Sham-ANA-12 group (Fig 4-5F). Exercise had no effect on p-TrkB (Y816)/TrkB.FL in both vehicle and ANA-12 treated MI rats (Fig 4-5F).

Table 4-4. TrkB.FL and TrkB.T1 expression in the RVLM at 5 weeks post MI with or without exercise training or regular dose ANA-12

	Sham		MI			
	Veh (n=9)	ANA-12 (n=6)	Sed-Veh (n=7)	Sed-ANA-12 (n=9)	ExT-Veh (n=8)	ExT-ANA-12 (n=7)
	TrkB expression (fold of Sham-Veh, normalized to GAPDH)					
TrkB.FL	1.0 ± 0.03	0.90 ± 0.03	0.91 ± 0.04	0.95 ± 0.03	0.89 ± 0.05	0.89 ± 0.06
TrkB.T1	1.0 ± 0.02	1.06 ± 0.05	1.04 ± 0.03	1.11 ± 0.02	1.06 ± 0.04	1.04 ± 0.04

Values are means ± SE.; Veh, vehicle; ANA-12, TrkB blocker; Sed-Veh, sedentary MI with Veh, Sed-ANA-12, sedentary MI with ANA-12; ExT-Veh, exercising MI with Veh; ExT-ANA-12, exercising MI with ANA-12; TrkB.FL, full-length form of tropomyosin-related kinase B; TrkB.T1, truncated form of TrkB; RVLM, rostral ventrolateral medulla.

Two-way ANOVA followed by Bonferroni
Effects of MI and drug (Sham groups vs. Sed-MI groups)
For TrkB.FL, MI, F=0.3, *P*=0.6; Drug, F=0.7, *P*=0.4; MI x Drug, F=4.2, *P*=0.05
For TrkB.T1, MI, F=2.0 *P*=0.2; Drug, F=3.5, *P*=0.07; MI x Drug, F=0.04, *P*=0.9

Effect of exercise and drug (within MI groups)
For TrkB.FL, ExT, F=0.7, *P*=0.4; Drug, F=0.2, *P*=0.7; ExT x Drug, F=0.03, *P*=0.6
For TrkB.T1, ExT, F=0.5, *P*=0.5; Drug, F=0.4, *P*=0.6; ExT x Drug, F=2.0, *P*=0.2

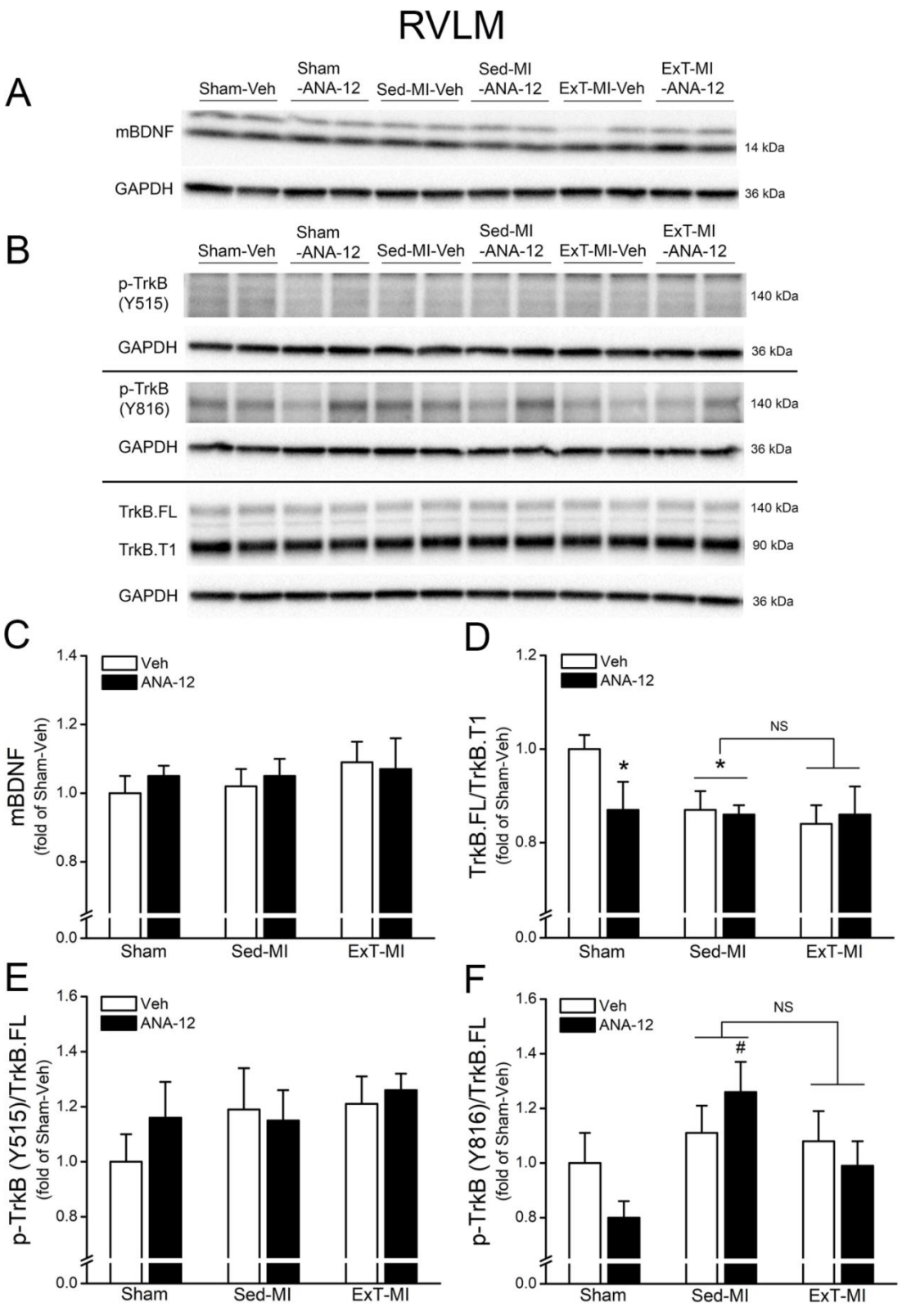
RVLM
A
Sham-Veh
Sham -ANA-12
Sed-MI-Veh
Sed-MI -ANA-12
ExT-MI-Veh
ExT-MI -ANA-12
mBDNF
14 kDa
GAPDH
36 kDa
B
p-TrkB (Y515)
140 kDa
p-TrkB (Y816)
TrkB.FL
TrkB.T1
90 kDa
C
Veh
ANA-12
mBDNF (fold of Sham-Veh)
Sham
Sed-MI
ExT-MI
D
TrkB.FL/TrkB.T1 (fold of Sham-Veh)
NS
E
p-TrkB (Y515)/TrkB.FL (fold of Sham-Veh)
F
p-TrkB (Y816)/TrkB.FL (fold of Sham-Veh)

Figure 4-5. mBDNF protein, TrkB.FL/TrkB.T1 ratio, p-TrkB (Y515)/TrkB.FL and p-TrkB (Y816)/TrkB.FL in the RVLM at 5 weeks post MI with or without regular dose ANA-12 or exercise training

Representative Western Blotting images for mature brain-derived neurotrophic factor (mBDNF) **(*A*)** and phosphorylated (p-) tropomyosin-related kinase B (TrkB) targeting tyrosine residue 515 (Y515) [p-TrkB (Y515)], p-TrkB targeting tyrosine residue 816 (Y816) [p-TrkB (Y816)], full-length form of TrkB (TrkB.FL) and truncated form of TrkB (TrkB.T1) with loading control (GAPDH) **(*B*)** in the rostral ventrolateral medulla (RVLM). mBDNF **(*C*)**, TrkB.FL/TrkB.T1 **(*D*)**, p-TrkB (Y515)/TrkB.FL ***(E)*** and p-TrkB (Y816)/TrkB.FL ***(F)*** of Sham and myocardial infarction (MI) rats with or without 0.5 mg/kg ANA-12 or exercise training. Veh, vehicle; Sed-MI, sedentary MI; ExT-MI, exercising MI. Values are means ± SE. Sham-Veh, n=9; Sham-ANA-12, n=6; Sed-MI-Veh, n=7, Sed-MI-ANA-12, n=9; ExT-MI-Veh, n=8; ExT-MI-ANA-12, n=7. All bands are normalized to GAPDH and represented as fold of Sham-Veh. Statistical analysis was done by two-way analysis of variance (ANOVA) followed by Bonferroni *post hoc* test within Sham and Sed-MI groups, and MI groups, respectively. *$P<0.05$ vs. Sham-Veh; $^{\#}P<0.05$ vs. Sham-ANA-12; NS, not significant

4. Intracellular factors Akt and CaMKII in the RVLM

Representative blot images are presented in Fig 4-6A for p-Akt and t-Akt, and in Fig 4-6B for p-CaMKIIβ and t-CaMKIIβ. In Sham rats, ANA-12 significantly lowered p-Akt (Ser473)/t-Akt (Fig 4-6C). Similarly, p-Akt (Ser473)/t-Akt decreased post MI without further effect of ANA-12 (Fig 4-6C). Exercise training did not affect the decrease in p-Akt (Ser473)/t-Akt post MI, and ANA-12 had no effect (Fig 4-6C). p-CaMKIIβ expression was not different in Sham and Sed-MI rats, and ANA-12 did not affect p-CaMKIIβ (Fig 4-6D). Exercise training post MI lowered p-CaMKIIβ and ANA-12 prevented the exercise-induced decrease in p-CaMKIIβ (Fig 4-6D). In Sham rats, ANA-12 did not change t-CaMKIIβ expression (Fig 4-6E). t-CaMKIIβ was not changed post MI, but ANA-12 treated MI rats showed higher t-CaMKIIβ than Sed-MI-Veh group (Fig 4-6E). Exercise tended to decrease t-CaMKIIβ (P=0.056) compared to the Sed-MI-Veh group, and ANA-12 prevented the exercise-induced decrease in t-CaMKIIβ (Fig 4-6E). p-CaMKIIβ/t-CaMKIIβ was similar among the groups (Fig 4-6F).

2.5 mg/kg ANA-12 did not show any further effects on proteins in the RVLM (data not shown).

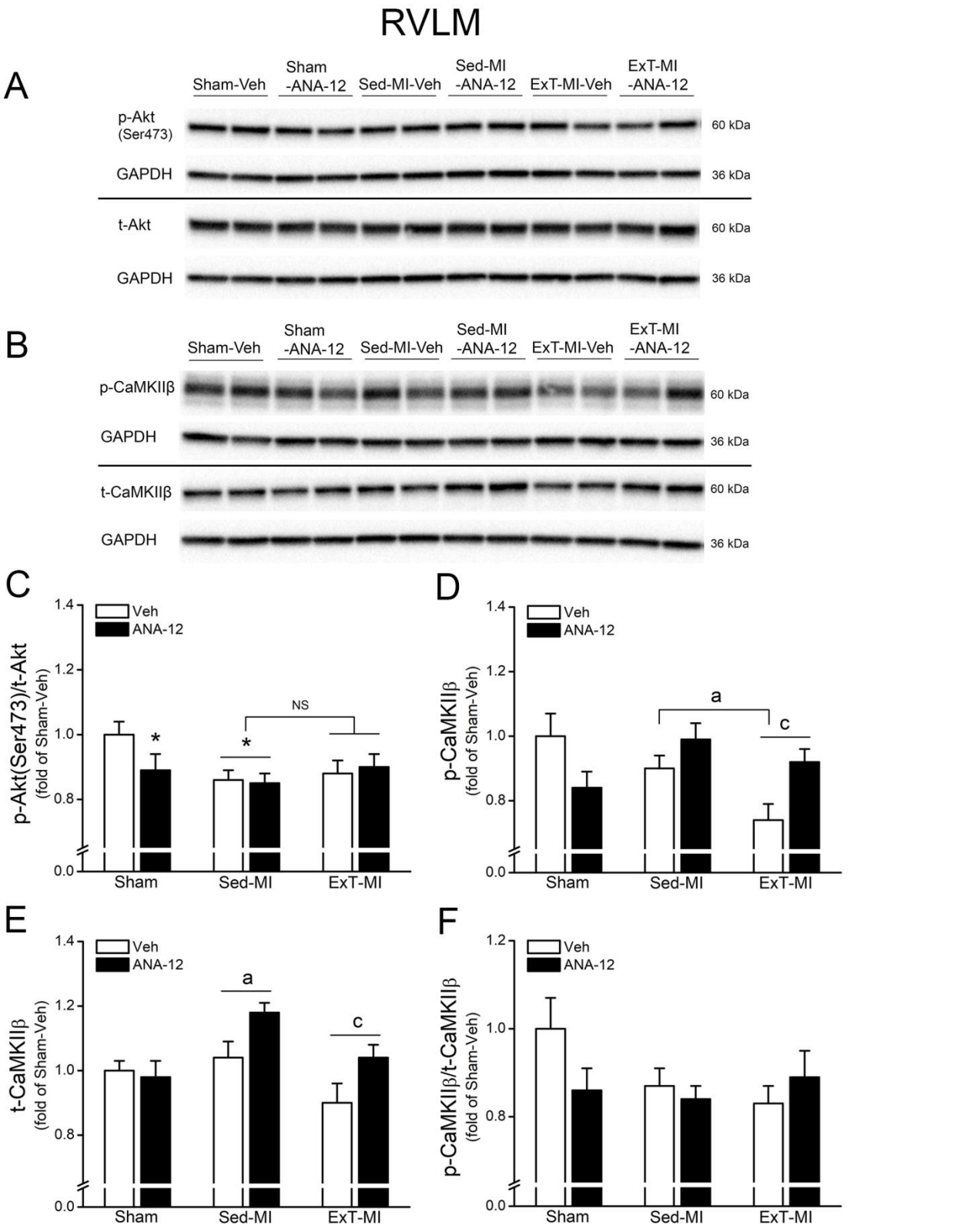
RVLM
A
Sham-Veh
Sham -ANA-12
Sed-MI-Veh
Sed-MI -ANA-12
ExT-MI-Veh
ExT-MI -ANA-12
p-Akt (Ser473)
GAPDH
t-Akt
GAPDH
60 kDa
36 kDa
B
p-CaMKIIβ
GAPDH
t-CaMKIIβ
GAPDH
C
p-Akt(Ser473)/t-Akt (fold of Sham-Veh)
Veh
ANA-12
NS
Sham
Sed-MI
ExT-MI
D
p-CaMKIIβ (fold of Sham-Veh)
a
c
E
t-CaMKIIβ (fold of Sham-Veh)
F
p-CaMKIIβ/t-CaMKIIβ (fold of Sham-Veh)

Figure 4-6. p-Akt (Ser473)/t-Akt, p-CaMKIIβ and t-CaMKIIβ expression, and p-CaMKIIβ/t-CaMKIIβ in the RVLM at 5 weeks post MI with or without regular dose ANA-12 or exercise training

Representative Western Blotting images for phosphorylated (p-)Akt targeting serine residue 473 (Ser473) [p-Akt (Ser473)] and total Akt (t-Akt) ***(A)***, and (p-)Ca^{2+}/Calmodulin-dependent protein kinase IIβ (p-CaMKIIβ) and total CaMKIIβ (t-CaMKIIβ) ***(B)*** with loading control (GAPDH) in the rostral ventrolateral medulla (RVLM). p-Akt (Ser473)/t-Akt ***(C)***, p-CaMKIIβ ***(D)***, t-CaMKIIβ ***(E)***, p-CaMKIIβ/t-CaMKIIβ ***(F)*** of Sham and myocardial infarction (MI) rats with or without 0.5 mg/kg ANA-12 or exercise training. Veh, vehicle; Sed-MI, sedentary MI; ExT-MI, exercising MI. Values are means ± SE. Sham-Veh, n=9; Sham-ANA-12, n=6; Sed-MI-Veh, n=7, Sed-MI-ANA-12, n=9; ExT-MI-Veh, n=8; ExT-MI-ANA-12, n=7. All bands are normalized to GAPDH and represented as fold of Sham-Veh. Statistical analysis was done by two-way analysis of variance (ANOVA) followed by Bonferroni *post hoc* test within Sham and Sed-MI groups, and MI groups, respectively. *$P<0.05$ vs. Sham-Veh; $^{a}P<0.05$ vs. Sed-MI-Veh; $^{c}P\leq0.05$ vs. ExT-MI-Veh; NS, not significant

Altogether, 0.5 mg/kg ANA-12 tends to decrease the TrkB.FL/TrkB.T1 ratio in the PVN and RVLM of Sham rats, and significantly decreases the activity of CaMKII in the PVN, but of Akt in the RVLM. These results indicate that in normal rats, ANA-12 affects different intracellular factors in the PVN and RVLM. The TrkB.FL/TrkB.T1 ratio is decreased in the PVN and RVLM of MI rats and this effect is similar to Sham rats treated with ANA-12, suggesting that responses of TrkB.FL to mBDNF may be reduced in the PVN and RVLM post MI. In the PVN, CaMKII activity is not decreased post MI and ANA-12-induced decrease in CaMKII activity noted in Sham rats is not observed in MI rats, suggesting that BDNF-TrkB signaling dependent regulation in CaMKII activity is different in Sham rats and MI rats. In the RVLM, Akt activity is decreased in MI rats similar to Sham rats treated with ANA-12, suggesting that BDNF-TrkB-Akt signaling is reduced post MI.

In the PVN of exercised MI rats, mBDNF is increased and this effect is attenuated by 0.5 mg/kg ANA-12. Exercise lowers Akt activity similarly in both vehicle and ANA-12 treated MI rats. In the RVLM of exercised MI rats, exercise decreases p-CaMKIIβ and tends to decrease t-CaMKIIβ expression and ANA-12 prevents these decreases. These results indicate that in the PVN, the exercise-induced decrease in Akt activity does not depend on BDNF-TrkB signaling, whereas in the RVLM, decreases in p-CaMKII and t-CaMKII by exercise are dependent on BDNF-TrkB signaling. None of the proteins assessed in the PVN and RVLM correlated with EF in the present study (data not shown).

Discussion

Major findings of the present study are outlined in Fig. 4-7 and 4-8, and are as follows. 1) In Sed-MI rats, TrkB.FL/TrkB.T1 ratio is decreased in the PVN and RVLM similar to Sham rats treated with ANA-12. In the PVN, p-TrkB (Y515)/TrkB.FL increases without affecting CaMKII and Akt activities, whereas in the RVLM, Akt activity decreases. Regular and high dose ANA-12 do not further affect BDNF-TrkB signaling in the Sed-MI group. 2) In the Sed-MI rats, regular dose ANA-12 does not affect echocardiographic and hemodynamic parameters, but high dose ANA-12 further deteriorates EF post MI. 3) In exercised MI rats, mBDNF increases and Akt activity decreases in the PVN, whereas in the RVLM, mBDNF is not changed but p-CaMKIIβ expression decreases. Regular dose ANA-12 prevents the exercise-induced increase in mBDNF in the PVN without affecting the decrease in Akt activity, and prevents the exercise-induced decrease in p-CaMKIIβ expression in the RVLM.

The decrease in the TrkB.FL/TrkB.T1 ratio in the PVN and RVLM post MI may reflect a decrease in responses of TrkB.FL to mBDNF, but changes in downstream pathways showed different patterns: in the PVN, p-TrkB (Y515)/TrkB.FL is increased post MI without changes in intracellular factors, whereas in the RVLM, TrkB activities are not affected but Akt activity is decreased. Exercise-induced decrease in p-CaMKIIβ expression in the RVLM is dependent on BDNF-TrkB signaling, but not of the exercise-induced decrease in Akt activity in the PVN.

Effects of MI on BDNF-TrkB signaling in the PVN and RVLM

A previous study reported that at 14 weeks post MI, BDNF protein was not changed, whereas TrkB mRNA and protein were decreased in the dmNTS (Becker et al., 2016). There are no studies on BDNF and TrkB expression post MI in the PVN and RVLM, key brain nuclei associated with cardiovascular regulation. Moreover, it has not yet been reported whether activities of Akt and CaMKII, which are known intracellular factors of BDNF-TrkB signaling in the hippocampus/cortex and heart, are similarly regulated by BDNF-TrkB signaling in the PVN and RVLM. In the present study, consistent with the changes noted in the dmNTS, mBDNF protein was not changed, but the TrkB.FL/TrkB.T1 ratio decreased at 5 weeks post MI both in the PVN and RVLM. Since mBDNF binding to TrkB.T1 in neurons inhibits mBDNF-induced phosphorylation of TrkB.FL by forming heterodimers with TrkB.FL (Eide et al., 1996; Haapasalo et al., 2001), a decrease in this ratio may indicate enhanced binding of mBDNF to TrkB.T1, and increase in inhibition of TrkB.FL mediated intracellular signaling responses to mBDNF. The MI-induced decrease in the TrkB.FL/TrkB.T1 ratio may therefore reflect a decrease in activation of TrkB.FL by endogenous mBDNF.

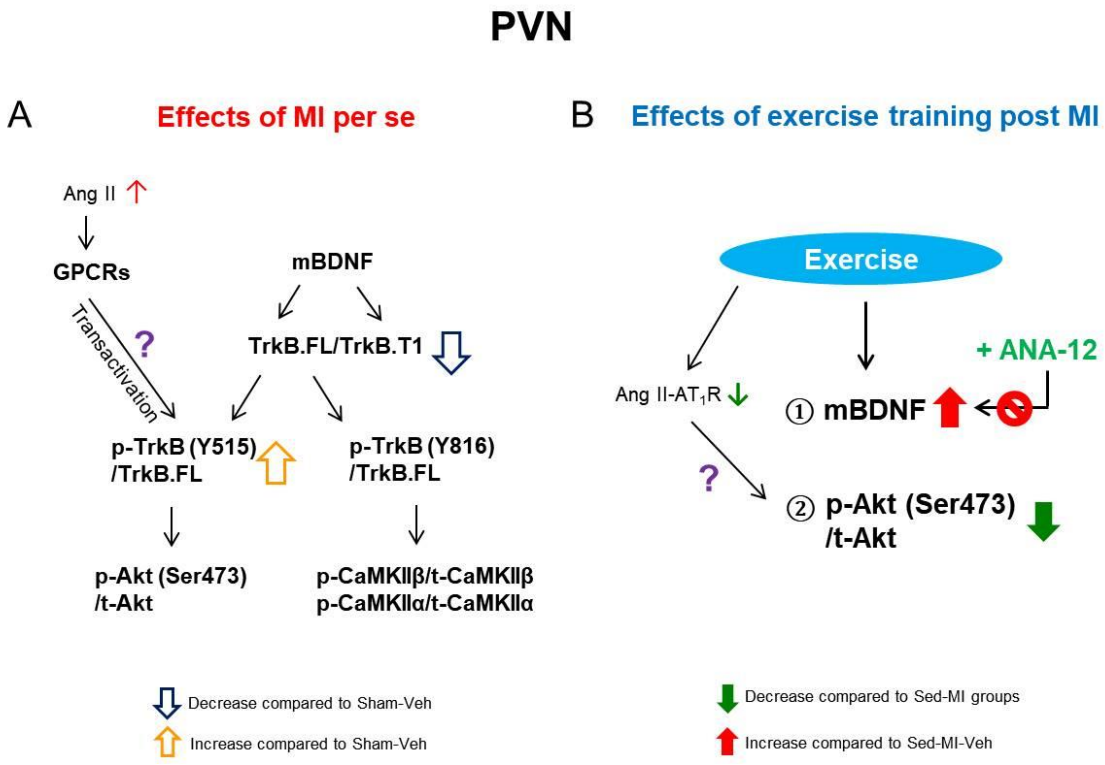

Figure 4-7. Changes in BDNF-TrkB signaling in the PVN post MI with or without exercise or ANA-12

(A) After myocardial infarction (MI), mature brain-derived neurotrophic factor (mBDNF) is not changed but ratio between full-length form of tropomyosin-related kinase B (TrkB.FL) and truncated form of TrkB (TrkB.T1) decreased. Ratio between phosphorylated (p-) TrkB targeting tyrosine residue 515 (Y515) and TrkB.FL [p-TrkB (Y515)/TrkB.FL] increased, which may stem from transactivation of TrkB via G-protein coupled receptors [GPCRs, (e.g. angiotensin II type 2 receptors)]. ANA-12 did not affect these changes post MI.

(B) ① Exercise increased mBDNF but did not affect the decrease in the TrkB.FL/TrkB.T1 ratio and the increase in the p-TrkB (Y515)/TrkB.FL post MI. ② Exercise also decreased Akt activity. ANA-12 prevented the exercise-induced increase in mBDNF, but did not prevent the exercise-induced decrease in Akt activity, indicating this effect is not dependent on BDNF-TrkB signaling. Other mechanisms such as exercise-induced down-regulation of angiotensin II (Ang II)-Ang II type I receptor (AT_1R) signaling may contribute to the decrease in Akt activity.

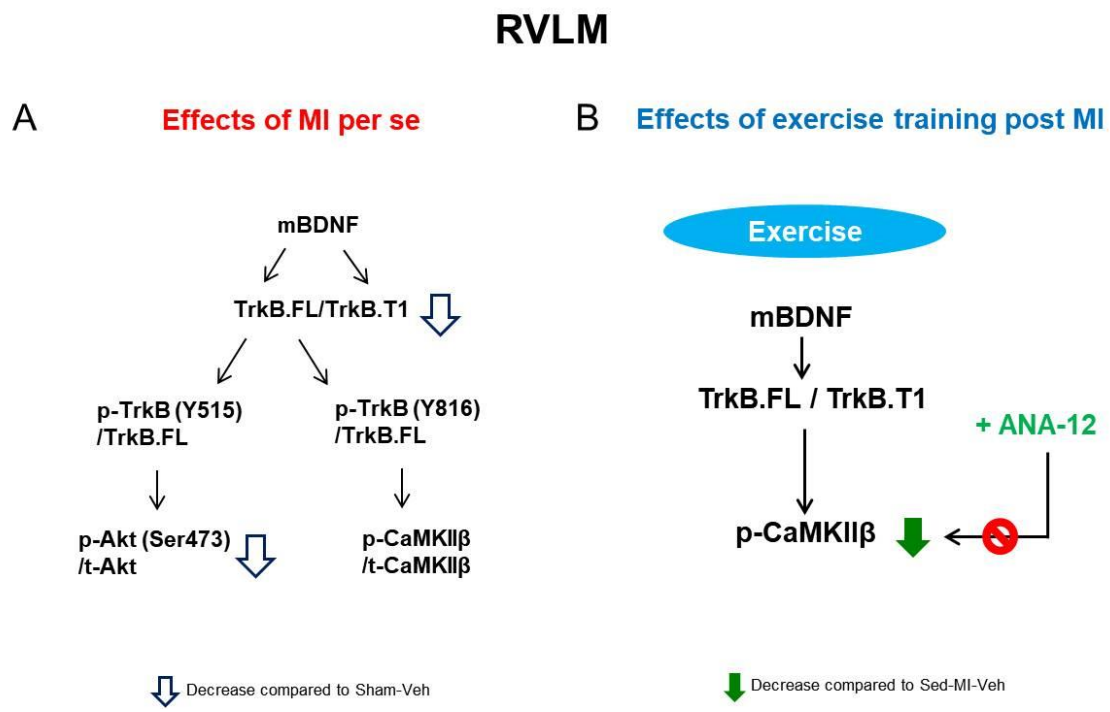

Figure 4-8. Changes in BDNF-TrkB signaling in the RVLM post MI with or without exercise or ANA-12

(A) After myocardial infarction (MI), mature brain-derived neurotrophic factor (mBDNF) is not changed but ratio between full-length form of tropomyosin-related kinase B (TrkB.FL) and truncated form of TrkB (TrkB.T1) decreased. No changes were observed in ratios between phosphorylated (p-) TrkB and TrkB.FL (p-TrkB/TrkB.FL), but Akt activity decreased. ANA-12 did not affect these changes post MI. ***(B)*** Exercise did not affect mBDNF or the decreases in the TrkB.FL/TrkB.T1 ratio post MI. Exercise decreased (p-) Ca^{2+}/Calmodulin-dependent protein kinase IIβ (p-CaMKIIβ), and this effect of exercise was prevented by ANA-12, indicating that the exercise-induced decrease in p-CaMKIIβ is dependent on BDNF-TrkB signaling.

It is well established that BDNF in hippocampal/cortical neuronal cultures induces phosphorylation of TrkB.FL targeting Y515, followed by activation of PI3K-Akt pathway, and phosphorylation of Y816 activating PLCγ-CaMKII pathway (Cunha et al., 2010; Park and Poo, 2012). However, in normal conditions, in vitro studies showed that BDNF-induced phosphorylation of TrkB occurs transiently (~15 min), then TrkB receptors are internalized by endocytosis to the cytoplasm (Aloyz et al., 1999; Nagappan and Lu, 2005). Duration of TrkB.FL phosphorylation can be affected by several factors including high K^+ (Guo et al., 2014) and vagal nerve stimulation (Furmaga et al., 2012). In addition, TrkB can be activated without binding of mBDNF (Boulle et al., 2012; Nagappan et al., 2008). Ligands such as adenosine and Ang II bind to their G protein-coupled receptors (GPCRs), adenosine 2a receptors and Ang II type 2 receptors, respectively, and thereby activate intracellular Src kinase, followed by transactivation of TrkB receptors (Diniz et al., 2018; Wiese et al., 2007).

On the other hand, in astrocytes and microglia, TrkB.T1 is expressed predominantly and ANA-12 decreases Akt activity in astrocytes, indicating that in astrocytes, Akt activity is dependent on TrkB.T1 (Saba et al., 2018). mBDNF can bind to and activate TrkB.T1 in microglia and astrocytes, followed by increases in intracellular Ca^{2+} concentration (Mizoguchi et al., 2009; Rose et al., 2003), suggesting that possibly CaMKII can be regulated by TrkB.T1 in microglia and astrocytes. In glial cells, both Akt and CaMKII therefore can be regulated independent of phosphorylation of TrkB.FL.

In the present study, in the PVN of MI rats, p-TrkB (Y515)/TrkB.FL was increased but without an increase in Akt activity. In contrast, in the RVLM, p-TrkB (Y515)/TrkB.FL was not changed post MI, but Akt activity was decreased. Both in the

PVN and RVLM, p-TrkB (Y816)/TrkB.FL and CaMKII activity were not changed. It is unclear which mechanisms contribute to the increase in p-TrkB (Y515)/TrkB.FL in the PVN. Since enhanced phosphorylation of TrkB (Y515) occurred without a significant increase in mBDNF, one may speculate that TrkB is transactivated by GPCRs (Boulle et al., 2012; Nagappan et al., 2008). Changes in p-TrkB and intracellular factors in whole PVN and RVLM are not in parallel and this may stem from opposite changes in neurons versus glia. For example, mBDNF binding to TrkB.T1 in glia increases CaMKII activity that may compensate for the decrease in CaMKII activity caused by reduced BDNF-TrkB.FL signaling in neurons, thus resulting in no overall change in CaMKII activity. Further studies are needed to determine which isoform of TrkB receptors and cell types in the PVN and RVLM regulate Akt and CaMKII activities post MI.

Effects of ANA-12 post MI on cardiac function and BDNF-TrkB signaling

Microinjection of ANA-12 into the dmNTS of normal rats decreased BP, HR and RSNA in a dose-dependent manner, but 50–60% less in MI rats (Becker et al., 2016), suggesting that BDNF-TrkB signaling decreases post MI in the dmNTS. Single intraperitoneal (i.p.) injection of 0.5 mg/kg ANA-12 in normal mice decreased p-TrkB/TrkB ratio by 20–25% in the hippocampus and cortex, and by 35% in the striatum (Cazorla et al., 2011). Chronic treatment with ANA-12 (0.2 mg/kg/day, i.p.) for 8 weeks in diabetic rats attenuated the beneficial effects of exercise on cognitive function (Allen et al., 2018). No studies so far reported effects of chronic systemic ANA-12 treatment on TrkB activity and BDNF-TrkB signaling in the PVN and RVLM of normal rats or rats post MI.

In the present study, in Sham rats, regular dose ANA-12 tended to decrease the TrkB.FL/TrkB.T1 ratio in the PVN and significantly decreased the ratio in the RVLM.

Both regular and high dose ANA-12 did not affect the decreases in TrkB.FL/TrkB.T1 ratio in the PVN and RVLM of MI rats. This may suggest that responses of mBDNF to TrkB.FL are already reduced post MI, and therefore ANA-12 does not further down-regulate this signaling. Also, different from Sham rats, ANA-12 did not decrease CaMKII activity in the PVN of the Sed-MI group. Since ANA-12 binds to the extracellular domain of the TrkB receptors (Cazorla et al., 2011), it is possible that the efficacy of ANA-12 depends on changes in the TrkB.FL/TrkB.T1 ratio, leading to different effects of ANA-12 in Sham and MI rats.

ANCOVA result showed that relative to MI size, only high dose ANA-12 significantly further deteriorated EF post MI. In our previous study (Lee et al., 2018), regular dose ANA-12 was sufficient to prevent exercise-induced increases in CaMKII and Akt activities in the non-infarct area of the LV, as well as improvement of EF. Altogether, these findings suggest that regular dose ANA-12 may not be enough to induce significant blockade of TrkB in the PVN and RVLM, but high dose ANA-12 was sufficient for blockade of TrkB in the brain in sedentary MI rats, thereby leading to further decrease in EF in sedentary MI rats. Overall changes in BDNF-TrkB signaling were not different in regular and high dose studies, but the brains were collected 6–7 hours after the last treatment when the effects of ANA-12 are already attenuated, whereas EF was measured 2–3 hours after dosing, at the peak time of TrkB inhibition (Allen et al., 2018; Cazorla et al., 2011).

Effects of ExT post MI on BDNF-TrkB signaling

In the hippocampus of normal rats, short-term (5–7 days) wheel running or treadmill exercise increased BDNF protein and p-TrkB, as well as p-Akt and p-CaMKII (Ding et al., 2011; Fang et al., 2013; Vaynman et al., 2007). In contrast, a 4-week treadmill exercise in normal rats increased BDNF protein in the hippocampus without change in p-CaMKII and t-CaMKII (Dao et al., 2015), whereas a 3-month treadmill exercise in mice increased BDNF protein and p-Akt in the cortex (Koo et al., 2013). In the PVN, 5 days wheel running exercise in aged rats (>1 year old) significantly increased BDNF immunoreactivity compared to sedentary rats, but not at 8 weeks wheel running exercise (Noble, 2014). 8 weeks treadmill exercise did not affect BDNF and TrkB immunoreactivity in the PVN (Noble, 2014). Altogether, exercise-induced increase in BDNF and activation of intracellular factors are obvious after short-term exercise, but effect of long-term exercise on BDNF-TrkB signaling appears to differ in different brain regions.

In the present study, mBDNF level was increased after a 4-week treadmill exercise post MI in the PVN, but not in the RVLM. This regional difference may stem from tissue-specific expression of BDNF transcripts in the PVN and RVLM. BDNF mRNA has 9 promoters which produce 24 different transcripts and expression of these BDNF transcripts are tissue-specific (Aid et al., 2007; Cunha et al., 2010). BDNF transcripts can be differently regulated by several stimuli, and changes in expression pattern may affect availability and/or translational efficiency of BDNF (Aid et al., 2007; Zheng et al., 2012a). Although the BDNF gene is transcribed from different promoters, each exon encodes an identical BDNF protein (Adachi et al., 2014; Cunha et al., 2010). Therefore, it

is possible that patterns of expression of specific BDNF transcripts are different in the PVN and RVLM, and exercise may increase or decrease different BDNF transcripts in these brain nuclei. The physiological significance of the increase in mBDNF in the PVN in response to exercise is not clear. mBDNF may bind to TrkB receptors in mitochondria, and thereby increase antioxidant mitochondrial uncoupling protein 2 (UCP2) and decrease oxidative stress, which is a major factor contributing to sympathetic hyperactivity post MI (Chan et al., 2010).

In spontaneously hypertensive rats, Akt activity was increased in the PVN and inhibition of Akt activity attenuated the increases in RSNA and plasma norepinephrine level, indicating that activation of Akt in the PVN contributes to sympathetic hyperactivity in hypertension (Sun et al., 2016). In the present study, Akt activity in the PVN is not changed post MI compared to Sham, suggesting that Akt acitvity may not directly contribute to sympathetic hyperactivity post MI, but the ExT-MI groups showed lower Akt activity than the Sed-MI rats. This suggests that decrease in Akt by exercise may be associated with a decrease in SNA. ANA-12 did not prevent the exercise-induced decrease in Akt activity, indicating that BDNF-TrkB signaling does not mediate this change. In the RVLM, exercise post MI decreased p-CaMKIIβ which was inhibited by ANA-12, suggesting that this response is mediated by TrkB. Activation of CaMKII in the RVLM mediates the Ang II-induced increase in SNA (Gao et al., 2007), and exercise-induced decrease in p-CaMKIIβ in the RVLM may therefore contribute to a decrease in SNA.

There are two limitations in the present study. First, subdivisions of the PVN and cell types were not differentiated. Further studies are needed to determine the actual

changes in BDNF-TrkB signaling in different cell types (e.g. neurons and astrocytes) and in subdivisions of the PVN. Second, the functional role of BDNF-TrkB signaling in the PVN and RVLM post MI with or without exercise was not assessed. Whether BDNF-TrkB signaling in the PVN and RVLM contribute to regulation of SNA post MI and by exercise should be studied.

In summary, post MI, the TrkB.FL/TrkB.T1 ratio is decreased in the PVN and RVLM which would suggest reduced intracellular responses to mBDNF-TrkB.FL axis. However, this was not associated with decrease in activities of intracellular factors, except for decrease in Akt activity in the RVLM. Exercise training post MI increases mBDNF in the PVN, but not in the RVLM. Exercise decreases Akt activity in the PVN and p-CaMKIIβ expression in the RVLM, but BDNF-TrkB signaling only mediates the effect of exercise on p-CaMKIIβ in the RVLM, but not of Akt in the PVN. Exercise-induced decreases in Akt activity in the PVN and p-CaMKIIβ expression in the RVLM may contribute to reduction in sympathetic hyperactivity post MI. Further studies are required to determine the exact role of BDNF-TrkB signaling in the PVN and RVLM, in particular, whether exercise effects on BDNF-TrkB signaling in the PVN or RVLM decrease Akt and CaMKII activities, and thereby contribute to attenuation of sympathetic hyperactivity post MI and of progressive cardiac dysfunction.

Author contributions

H.W.L. and F.H.H.L. conceived and designed study. H.W.L., M.A. and H.W.W. performed experiments; H.W.L., M.A. and H.W.W. analyzed data; H.W.L., H.W.W. and F.H.H.L. interpreted results of experiments; H.W.L. prepared the figures and drafted manuscript. H.W.L. and F.H.H.L. edited and revised manuscript; H.W.L., M.A., H.W.W. and F.H.H.L. approved final version of manuscript.

Grants

This work was supported by Canadian Institutes of Health Research Operating Grant [FRN: MOP-136923]. Frans H.H. Leenen holds the Pfizer Chair in Hypertension Research, an endowed chair supported by Pfizer Canada, University of Ottawa Heart Institute Foundation, and Canadian Institutes of Health Research. Heow Won Lee was the recipient of a University of Ottawa Endowed Graduate Award in Cardiac Research at the Heart Institute, supported by the University of Ottawa's Faculty of Medicine Endowed Funds in Cardiac Research and the University of Ottawa Heart Institute Foundation.

Declaration of interest

None.

Chapter 5

General Discussion

5.1. Summary of main findings

5.1.1. Alterations in BDNF-TrkB signaling in the LV, PVN and RVLM post MI

Plasma BDNF tended to decrease at 5 weeks post MI. mBDNF protein (but not mRNA) tended to be lower in the non-infarct area of the LV only at 5 weeks post MI, and significantly lower in the infarct area than in Sham and other areas at 5 and 8 weeks post MI (8 weeks data is shown in Appendix I; Appendix *7.1.2.*; Fig 7-1). In contrast, TrkB mRNA is increased in the infarct area at 2 and 5 weeks post MI, and TrkB.T1 protein at 5 and 8 weeks post MI without changes in other areas (Appendix *7.1.2.*; Fig 7-1). At 5 weeks post MI, in the non-infarct area of the LV, intracellular factors of BDNF-TrkB signaling such as p-CaMKII, p-Akt (Thr308) and p-Akt (Ser473) protein expression and activities of CaMKII and Akt are decreased.

At 5 weeks post MI, in the PVN and RVLM, mBDNF protein level is not altered, but the TrkB.FL/TrkB.T1 ratio is decreased in both brain nuclei. Changes in downstream factors were not observed in the PVN, but Akt activity is reduced in the RVLM.

5.1.2. Effects of exercise training on cardiac function and BDNF-TrkB signaling in the LV, PVN and RVLM post MI

Exercise training significantly improves EF, SV, cardiac index and LVEDP, but ANA-12 only prevents the exercise-induced improvement of EF. Exercise training post MI attenuates the decreases in plasma BDNF, and protein expression in the non-infarct area of the LV including mBDNF, p-CaMKII, p-Akt (Thr308) and p-Akt (Ser473) and Akt activities, which are all blocked by ANA-12 except for the exercise-induced increase in plasma BDNF. In the PVN, exercise increases mBDNF and decreases Akt activity, whereas in the RVLM, exercise does not affect mBDNF but decreases p-CaMKIIβ

protein expression. Exercise-induced increase in mBDNF in the PVN and exercise-induced decrease in p-CaMKIIβ expression in the RVLM are prevented by ANA-12.

5.2. BDNF-TrkB signaling in the LV post MI: Effects of exercise

5.2.1. Time course of changes in BDNF and TrkB expression in the LV post MI

Previous studies reported changes of BDNF and TrkB expression in the heart at different time points post MI (Halade et al., 2013; Hang et al., 2015; Hong et al., 2014; Okada et al., 2012; Wang et al., 2018). In rats post MI, BDNF protein increased at 6 h post MI but normalized at 24 h in the non-infarct area (Hang et al., 2015). A transient increase in BDNF protein was observed 1 day post MI in the peri- and infarct areas in cardiomyocytes, but remained increased in macrophages (Hong et al., 2014). In the infarct area of the LV of mice, mBDNF protein was increased at 1, 3 and 5 days post MI, but returned to baseline level at 7 days post MI (Halade et al., 2013), and was markedly decreased at 2 weeks post MI in the whole heart of mice (Okada et al., 2012). At 9 weeks post MI in rats, mBDNF protein was decreased in the ischemic heart zone (Wang et al., 2018). TrkB protein (isoform not specified) was increased in the whole heart of mice at 2 weeks (Okada et al., 2012) and the ischemic heart zone at 9 weeks post MI in rats (Wang et al., 2018).

Consistent with previous studies, we found that mBDNF protein was markedly decreased, whereas TrkB.T1 protein increased in the infarct area at 5 and 8 weeks post MI. BDNF mRNA was not altered, suggesting that the decrease in mBDNF protein in the infarct area may be related to post-transcriptional mechanisms, such as expression of micro RNAs targeting the BDNF gene in cardiomyocytes and repress translation to protein (Lin et al., 2010; Ma et al., 2015a). An acute increase in BDNF post MI, in

particular in the non-infarct area, may be a compensatory mechanism to preserve cardiomyocyte viability and prevent cardiomyocyte apoptosis (Hang et al., 2015). Thereafter, the decrease in BDNF in cardiomyocytes may contribute to cardiomyocyte death (Hong et al., 2014). In contrast, TrkB mRNA and TrkB.T1 protein are increased consistently in the infarct area without changes in other areas. The significance of the persistent increase in TrkB.T1 protein expression in the infarct area is unclear. An increase in TrkB post MI in the heart might be a cardioprotective response as deletion of cardiomyocyte specific TrkB gene before inducing MI further deteriorated cardiac dysfunction in mice at 2 weeks post MI (Okada et al., 2012).

5.2.2. Changes in CaMKII and Akt activities in the LV

In cardiomyocytes, BDNF increases phosphorylation of CaMKII, enhancing cardiomyocyte contractility and relaxation (Feng et al., 2015). BDNF also phosphorylates Akt, thus promoting cardiomyocyte viability (Okada et al., 2012). This indicates that CaMKII and Akt are intracellular factors for the cardiac BDNF-TrkB axis, and may contribute to normal myocardial contractility and cardiomyocyte survival.

At 5 weeks post MI, p-CaMKII protein and its activity [p-CaMKII/CaMKII (pan)]) were decreased in the non-infarct area of the LV without a change in CaMKII (pan) protein expression. Previous studies noted that at 2 weeks post MI, both p-CaMKII and t-CaMKII protein were decreased in the LV without a change in its activity (Zhao et al., 2014), and at 8 weeks post MI, p-CaMKII protein and CaMKII activity were both decreased in the non-infarct area of the LV (Netticadan et al., 2000). Collectively, the decreases in CaMKII activity may contribute to the decrease in myocardial contractility.

At 5 weeks post MI, both p-Akt (Thr308)/Akt (pan) and p-Akt (Ser473)/Akt (pan) were decreased in the non-infarct area of the LV, and this may lead to a decrease in cardiomyocyte viability in the non-infarct area. Previous studies reported that Akt activities were not significantly changed in the LV at 4–6 weeks post MI (Cai et al., 2016; Leosco et al., 2007; Manchini et al., 2017). These different findings may be attributed to different severity of cardiac dysfunction post MI and different areas (e.g. non-infarct vs. peri-infarct or whole LV) of the LV.

It should be noted that increases in p-CaMKII and t-CaMKII were observed in other models of HF such as pressure-overload cardiac hypertrophy induced by transverse aortic constriction (Respress et al., 2012; Zhang et al., 2003), which may promote pathological cardiac hypertrophy and cardiac apoptosis (Backs et al., 2009; Ling et al., 2009). The opposite changes in CaMKII activity in the rat MI model and transverse aortic constriction are due to different stimulus (e.g. volume vs. pressure) which show different phenotypes and molecular adaptations in cardiac hypertrophy (You et al., 2017).

5.2.3. Effects of exercise post MI on BDNF-TrkB signaling in the LV

A 4-week period of treadmill exercise training prevented the decreases in mBDNF, p-Akt (Thr308), p-Akt (Ser473) and p-CaMKII expression and Akt activity in the non-infarct area of the LV, and these effects were all inhibited by ANA-12. This indicates that exercise activates cardiac BDNF-TrkB signaling and the intracellular factors p-CaMKII and p-Akt, similarly as observed in the hippocampus and cortex of rats (Ding et al., 2011; Fang et al., 2013), and BDNF-TrkB signaling mediates the effects of exercise on p-CaMKII and p-Akt.

The mechanism(s) mediating these effects of exercise post MI are not clear. Wang et al. (2018) reported that treadmill exercise for 8 weeks in MI rats increased BDNF protein in the ischemic heart zone of the LV and this increase was inhibited by a nitric oxide synthase inhibitor, suggesting that an increase in nitric oxide contributes to increase in cardiac BDNF. Wrann et al. (2013) reported that a 4-week period of free-wheel running exercise in mice significantly increased BDNF mRNA in the hippocampus, which was mediated by an increase in FNDC5 in the hippocampus and skeletal muscle. However, we did not observe a significant increase in FNDC5 mRNA and protein in both skeletal muscle and the heart by exercise training post MI, and therefore FNDC5 is probably not a contributing factor to the increase in cardiac mBDNF post MI. This difference may be due to different species and disease status (healthy mice vs. MI rats), as well as different types of exercise (voluntary running vs. treadmill). Since mBDNF is an activity-dependent factor, increases in cardiac contraction and/or cardiac efferent nerve activity during exercise (Tsuchimochi et al., 2002) may contribute to increase in mBDNF similarly as observed in skeletal muscle (Hurtado et al., 2017; Matthews et al., 2009).

Exercise training post MI did not increase BDNF mRNA in the non-infarct area of the LV, and therefore it is also possible that circulating BDNF may be sequestered through cardiac TrkB.T1, similarly as observed in astrocytes (Alderson et al., 2000; Fenner, 2012). Jiménez-Maldonado et al. (2014) reported that a 8-week period of treadmill exercise increased plasma BDNF in healthy rats. We found that exercise training prevented the decrease in plasma BDNF post MI, and this response was not inhibited by ANA-12 treatment. However, ANA-12 prevented the exercise-induced increase in cardiac mBDNF, suggesting that ANA-12 binding to cardiac TrkB.T1

blocked the sequestration of circulating BDNF into the heart. The brain is the major source for the increase in circulating BDNF in response to exercise (Seifert et al., 2010; Rasmussen et al., 2009). No studies have found evidence that skeletal muscle releases BDNF to the circulation during/after exercise (Matthews et al., 2009; Walsh and Tschakovsky, 2018).

5.3. Effects of exercise training post MI on cardiac function: Role of BDNF-TrkB signaling

5.3.1. Effects of ANA-12 on cardiac function post MI

ANA-12 is a selective non-competitive antagonist of TrkB receptors which crosses the BBB and binds to the extracellular domain of TrkB (Cazorla et al., 2011). In the present study, we used 0.5 mg/kg as a regular dose of ANA-12 based on previous studies (Cazorla et al., 2011; Kishi et al., 2015). A single i.p. injection of 0.5 mg/kg ANA-12 decreased p-TrkB/TrkB by 25% in the whole brain of mice (Cazorla et al., 2011), and oral administration of 0.5 mg/kg/day of ANA-12 for 28 days attenuated beneficial effects of calorie restriction on cognitive function in rats (Kishi et al., 2015). No studies to date reported the effects of chronic systemic ANA-12 on cardiac function in normal and MI rats.

In the present study, oral treatment with 0.5 mg/kg ANA-12 in Sham rats did not affect echocardiographic and hemodynamic parameters, suggesting that overall role of endogenous BDNF-TrkB signaling in regulation of cardiac function is minimal in normal state. It is also possible that other mechanisms that regulate myocardial contractility, such as β-AR signaling, may compensate to maintain normal cardiac contraction (Feng et al., 2015). Cardiomyocyte specific TrkB knockout mice showed a decrease in baseline

dP/dt_{max}, but EF was not changed in these mice and the extent of increase in dP/dt_{max} by isoproterenol infusion was the same as in wildtype mice (Feng et al., 2015). In the present study, MI rats treated with 2.5 mg/kg of ANA-12 showed a tendency to lower mean EF than the MI rats treated with vehicle. Since MI size is a determinant of EF, wide range of MI size (15–35%) may obscure the real effect of ANA-12. Therefore, EF was plotted relative to MI size and ANCOVA was conducted to compare EF at equal MI size. Relative to MI size, 2.5 mg/kg ANA-12 significantly further deteriorated EF. The effect of high dose ANA-12 on EF might be associated with its action on brain TrkB, since regular dose ANA-12 may not be enough to induce significant blockade of TrkB in the brain, but was sufficient to prevent exercise-induced increases in CaMKII and Akt activities in the non-infarct area of the LV, as well as improvement of EF. Effects of exercise on cardiac function will be further discussed in the next section.

5.3.2. Effects of exercise training on cardiac function post MI

In animal studies, initiation of exercise at 1–2 weeks post MI with duration of 4–8 weeks improved EF and LVEDP (Cai et al., 2016; Wang et al., 2018; Xu et al., 2008a; Xu et al., 2008b), indicating that exercise training post MI improved both systolic and diastolic functions. Consistent with these studies, a 4-week period of treadmill exercise training improves EF and LVEDP post MI. Furthermore, exercise training post MI increased SV and cardiac index similarly as observed in healthy normal rats (Jin et al., 2000). The increase in SV and cardiac index was due to an increase in EDV, and not of HR. An exercise-induced increase in venous return to the heart by reduction in vascular resistances (Freitas et al., 2015; Hambrecht et al., 2000; Jin et al., 2000), as well as decrease in collagen contents (Xu et al., 2008b) may lead to increase in ventricular

compliance, and thereby increases EDV. The decrease in LVEDP by exercise training may reflect the larger LV volume and improved ventricular compliance (Radovits et al., 2013). However, different from EF, exercise training post MI did not affect dP/dt_{max}, a parameter which reflects LV contractile function (Monge Garcia et al., 2018). Since EF is influenced by loading conditions (Konstam and Abboud, 2017), the increase in EDV by exercise may contribute to a significant improvement of EF. Also, different levels of anesthesia may affect different responses to EF and dP/dt_{max}. EF was assessed by echocardiography under full anesthesia, while dP/dt_{max} was measured by a Miller catheter right before rats are awake.

In the present study, regular dose ANA-12 prevented the exercise-induced increase in EF, and attenuated the increases in SV and cardiac index. However, ANA-12 did not inhibit the exercise-induced increase in EDV and the decrease in LVEDP. These findings suggest that activation of BDNF-TrkB signaling by exercise may be more associated with an improvement of systolic function.

BDNF treatment on myotubes phosphorylates AMPK, and thereby enhances fatty acid oxidation (Matthews et al., 2009). Activation of cardiac AMPK enhances both glucose and fatty acid metabolism (Bairwa et al., 2016; Kim and Dyck, 2015), and attenuates cardiac fibrosis in isoproterenol-induced cardiac hypertrophy (Ma et al., 2015b). In the present study, exercise prevented the MI-induced decrease in p-AMPKα in the non-infarct area, but ANA-12 did not prevent this effect. The AMPK-mediated improvement of cardiac energy metabolism enhances substrate utilization that increases ATP production, as well as may increase mitochondrial biogenesis, and thereby improve cardiac function (Kim and Dyck, 2015). Exercise post MI may therefore may improve

cardiac energy metabolism and attenuate cardiac fibrosis by activation of AMPK, which is not dependent on BDNF-TrkB signaling in the LV.

5.4. BDNF-TrkB signaling in the PVN and RVLM post MI: Effects of exercise

5.4.1. Changes in BDNF-TrkB signaling post MI and effects of ANA-12

Okada et al. (2012) reported that BDNF protein was increased in the forebrain (thalamus/hypothalamus) at 2 weeks post MI in mice and brain specific BDNF knockout mice showed further deterioration in EF and increase in TUNEL-positive cardiomyocytes post MI. This suggests that the increase in brain BDNF post MI may play a cardioprotective role to attenuate progressive cardiac dysfunction post MI (Leenen, 2007; Okada et al., 2012). At 14 weeks post MI in rats, BDNF mRNA was increased without a change in BDNF protein, but both TrkB mRNA and protein were decreased in the dmNTS in the brainstem (Becker et al., 2016). In this study, RSNA, BP and HR responses to microinjection of BDNF and ANA-12 into the dmNTS were blunted in MI rats, suggesting that BDNF-TrkB signaling in the NTS was decreased post MI, and therefore contributes to sympathoexcitation and baroreflex desensitization.

In the present study, we assessed BDNF and TrkB protein expression in the PVN and RVLM, key brain nuclei that regulate cardiovascular homeostasis. At 5 weeks post MI, mBDNF protein was not changed, but the TrkB.FL/TrkB.T1 ratio was decreased both in the PVN and RVLM. In neurons, mBDNF binding to TrkB.T1 inhibits mBDNF-induced phosphorylation of TrkB.FL, and thereby inhibits TrkB.FL mediated intracellular signaling responses to mBDNF (Eide et al., 1996; Haapasalo et al., 2001). Therefore the decrease in the TrkB.FL/TrkB.T1 ratio post MI may reflect a reduction in the response to mBDNF to TrkB.FL. In the PVN, a significant increase in p-TrkB (Y515)/TrkB.FL was

observed without a change in mBDNF and this may be caused by transactivation from GPCRs (Boulle et al., 2012; Nagappan et al., 2008). On the other hand, changes in p-TrkB, and CaMKII and Akt activities in the PVN and RVLM were not in parallel. Causative factors are not clear, but a complex neuron-glia interaction (Clasadonte and Prevot, 2018; de Kloet et al., 2015), in particular a distinctive mBDNF-TrkB.T1 signaling in glia may affect CaMKII and Akt activities in the whole brain nucleus. TrkB.T1 is the predominant form expressed in astrocytes and microglia, and activation of mBDNF-TrkB.T1 signaling in glia can regulate Akt and CaMKII activity independent from phosphorylation of TrkB.FL in neurons (Mizoguchi et al., 2009; Rose et al., 2003; Saba et al., 2018). Further studies are needed to determine which cell types and isoforms of TrkB receptors regulate Akt and CaMKII activities in the PVN and RVLM post MI.

In the present study, oral treatment with regular dose of ANA-12 in Sham rats tended to decrease the TrkB.FL/TrkB ratio in the PVN and RVLM, and significantly decreased CaMKII activity in the PVN and Akt activity in the RVLM, suggesting that ANA-12 may inhibit BDNF-TrkB.FL signaling, but affect different intracellular factors in the PVN and RVLM. In contrast, both regular and high dose ANA-12 did not affect overall changes in BDNF-TrkB signaling in the PVN and RVLM of sedentary MI rats, which may because response to mBDNF is already reduced post MI, and therefore ANA-12 does not further down-regulate intracellular factors.

5.4.2. Effects of exercise training post MI with or without ANA-12 in the PVN and RVLM

Exercise training increases BDNF in the hippocampus of normal rats (Dao et al., 2015; Ding et al., 2011; Fang et al., 2013). In the PVN of normal rats, 8 week treadmill exercise

did not alter BDNF and TrkB immunoreactivity (Noble, 2014). There are no reports on changes in the RVLM. In the hippocampus, 5–7 days exercise increased p-CaMKII and p-Akt (Ding et al., 2011; Fang et al., 2013), but not after a 4-week exercise training (Dao et al., 2015). In the present study, effects of exercise training post MI showed different patterns in changes in BDNF-TrkB signaling in the PVN and RVLM. In the PVN, exercise training increased mBDNF and decreased Akt activity, whereas in the RVLM, exercise did not affect mBDNF level but decreased p-CaMKII expression. The significance of the exercise-induced increase in mBDNF in the PVN is unclear, but an increase in mBDNF by binding TrkB receptors in mitochondria may enhances antioxidant UCP2, and thereby reduces oxidative stress, which is a major contributing factor to increase sympathetic activity post MI (Chan et al., 2010).

In spontaneously hypertensive rats, Akt activity was higher in the PVN than control rats and a Akt inhibitor attenuated the increased RSNA, suggesting that activation of Akt in the PVN contributes to sympathetic hyperactivity (Sun et al., 2016). In the present study, Akt activity was not changed in sedentary MI rats compared to Sham rats, but the exercise MI groups showed a significant lower Akt activity than the sedentary MI rats. Microinjection of Ang II into the RVLM increased p-CaMKIIβ and SNA (Gao et al., 2007b). In the present study, exercise training post MI decreased p-CaMKIIβ in the RVLM. Collectively, the decreases in Akt activity in the PVN and p-CaMKIIβ in the RVLM by exercise training may contribute to attenuate sympathetic hyperactivity post MI. ANA-12 inhibited the effect of exercise on p-CaMKIIβ in the RVLM, but not of Akt activity in the PVN, indicating that BDNF-TrkB signaling only mediates the increase in

p-CaMKIIβ in the RVLM and other mechanisms contribute to decrease in Akt activity in the PVN in response to exercise.

It appears that activation of cardiac BDNF-TrkB signaling in response to exercise training post MI is the major contributing factor that leads to improvement of EF rather than BDNF-TrkB signaling in the PVN and RVLM. Regular dose ANA-12 was sufficient to inhibit the exercise-induced increases in intracellular factors CaMKII and Akt in the LV, but ANA-12 only prevented the exercise-induced decrease in p-CaMKIIβ expression in the RVLM. This may be because endogenous levels of BDNF protein in the heart is higher than the brain (Vieau et al., 2011), and TrkB.T1 is the predominant form of cardiac TrkB (Fulgenzi et al., 2015; Otani et al., 2017), which may enable cardiac sequestration of large amounts of circulating BDNF in response to exercise.

5.5. Conclusions

The present study assessed the role of BDNF-TrkB signaling as a possible molecular mechanism for the beneficial effects of exercise training post MI. Overall, reductions in BDNF-TrkB signaling post MI and normalization of the reduced BDNF-TrkB signaling in response to exercise are obvious in the heart and less in the PVN and RVLM. Down-regulation of BDNF-TrkB signaling and intracellular factors CaMKII and Akt may contribute to progressive cardiac dysfunction post MI. Exercise training increases BDNF in the brain and release to the circulation. The exercise-induced increase in circulating BDNF may sequester via cardiac TrkB.T1, and thereby activate cardiac BDNF-TrkB axis along with intracellular factors CaMKII and Akt, leading to improve EF. Exercise training post MI also improves LVEDP, SV and cardiac index, but other mechanisms are related to improvements of these parameters. In parallel, exercise training post MI

increases mBDNF in the PVN and this may play a role in reduction of oxidative stress in the PVN. Reductions in Akt activity in the PVN and p-CaMKII expression in the RVLM by exercise may contribute to attenuate sympathetic hyperactivity. Altogether exercise training post MI is able to balance BDNF-TrkB signaling in the LV (activation), and the PVN and RVLM (inhibition), which ultimately lead to attenuate cardiac dysfunction.

This study provides insights for better understanding into the cardiac and brain mechanisms activated by exercise training in patients with HF and attenuating progressive cardiac remodeling and dysfunction. Moreover, this concept provides novel perspectives on an important balancing mechanism in the heart and the CNS for the actions of BDNF to TrkB, followed by the intracellular factors CaMKII and Akt, which may beneficially affect cardiovascular homeostasis post MI. Actual mechanisms mediating the effects of MI and exercise post MI on BDNF-TrkB signaling in the LV, PVN and RVLM require further studies. Better understanding of these mechanisms and actions of BDNF-TrkB signaling may lead to new strategies to inhibit progressive HF post MI.

6. References

Abeyrathna P and Su Y (2015). The critical role of Akt in cardiovascular function. *Vascul Pharmacol* **74**, 38–48.

Adachi N, Numakawa T, Richards M, Nakajima S, Kunugi H (2014). New insight in expression, transport, and secretion of brain-derived neurotrophic factor: implications in brain-related diseases. *World J Biol Chem* **5**, 409–428.

Aid T, Kazantseva A, Piirsoo M, Palm K, Timmusk T (2007). Mouse and rat BDNF gene structure and expression revisited. *J Neurosci Res* **85**, 525–535.

Alderson RF, Curtis R, Alterman AL, Lindsay RM, DiStefano PS (2000) Truncated TrkB mediates the endocytosis and release of BDNF and neurotrophin-4/5 by rat astrocytes and schwann cells in vitro. *Brain Res* **871**, 210–222.

Allen RS, Hanif AM, Gogniat MA, Prall BC, Haider R, Aung MH, Prunty MC, Mees LM, Coulter MM, Motz CT, Boatright JH, Pardue MT (2018). TrkB signaling pathway mediates the protective effects of exercise in the diabetic rat retina. *Eur J Neurosci* **47**, 1254–1265.

Aloyz R, Fawcett JP, Kaplan DR, Murphy RA, Miller FD (1999)**.** Activity-dependent activation of TrkB neurotrophin receptors in the adult CNS. *Learn Mem* **6,** 216–231.

Amorim PA, Nguyen TD, Shingu Y, Schwarzer M, Mohr FW, Schrepper A, Doenst T (2010). Myocardial infarction in rats causes partial impairment in insulin response associated with reduced fatty acid oxidation and mitochondrial gene expression. *J Thorac Cardiovasc Surg* **140**, 1160–1167.

An JJ, Liao GY, Kinney CE, Sahibzada N, Xu B (2015). Discrete BDNF neurons in the paraventricular hypothalamus control feeding and energy expenditure. *Cell Metab* **22**, 175–188.

Arbat-Plana A, Cobianchi S, Herrando-Grabulosa M, Navarro X, Udina E (2017). Endogenous modulation of TrkB signaling by treadmill exercise after peripheral nerve injury. *Neuroscience* **340**, 188–200, 2017.

Aroeira RI, Sebastião AM, Valente CA (2015). BDNF, via truncated TrkB receptor, modulates GlyT1 and GlyT2 in astrocytes. *Glia* **63**, 2181–2197.

Azimi M. Gharakhanlou R, Naghdi N, Khodadadi D, Heysieattalab S (2018). Moderate treadmill exercise ameliorates amyloid-β-induced learning and memory impairment, possibly via increasing AMPK activity and up-regulation of the PGC-1α/FNDC5/BDNF pathway. *Peptides* **102**, 78–88.

Azogu I, Liang J, Plamondon H (2018). Sex-specific differences in corticosterone secretion, behavioral phenotypes and expression of TrkB. T1 and TrkB. FL receptor isoforms: Impact of systemic TrkB inhibition and combinatory stress exposure in adolescence. *Prog Neuropsychopharmacol Bio Psychiatry* **86**, 10–23.

Backs J, Backs T, Neef S, Kreusser MM, Lehmann LH, Patrick DM, Grueter CE, Qi X, Richardson JA, Hill JA, Katus HA, Bassel-Duby R, Maier LS, Olson EN (2009). The δ isoform of CaM kinase II is required for pathological cardiac hypertrophy and remodeling after pressure overload. *Proc Natl Acad Sci* U S A **106**, 2342–2347.

Bairwa SC, Parajuli N, Dyck JR (2016). The role of AMPK in cardiomyocyte health and survival. *Biochim Biophys Acta* **1862**, 2199–2210.

Baker AJ (2014). Adrenergic signaling in heart failure: a balance of toxic and protective effects. *Pflügers Arch* **466**, 1139–1150.

Baxter GT, Radeke MJ, Kuo RC, Makrides V, Hinkle B, Hoang R, Medina-Selby A, Coit D, Valenzuela P, Feinstein SC (1997). Signal transduction mediated by the truncated trkB receptor isoforms, trkB. T1 and trkB. T2. *J Neurosci* **17**, 2683–2690.

Becker BK, Tian C, Zucker IH, Wang HJ (2016). Influence of brain-derived neurotrophic factor-tyrosine receptor kinase B signalling in the nucleus tractus solitarius on baroreflex sensitivity in rats with chronic heart failure. *J Physiol* **594**, 5711–5725.

Becker BK, Wang H, Zucker IH (2017). Central TrkB blockade attenuates ICV angiotensin II-hypertension and sympathetic nerve activity in male Sprague-Dawley rats. *Auton Neurosci* **205**, 77–86.

Belardinelli R, Georgiou D, Cianci G, Purcaro A (2012). 10-year exercise training in chronic heart failure: a randomized controlled trial. *J Am Coll Cardiol* **60**, 1521–1528.

Bernstein D, Fajardo G, Zhao M (2011). The role of β-adrenergic receptors in heart failure: differential regulation of cardiotoxicity and cardioprotection. *Prog Pediatr Cardiol* **31**, 35–38.

Biancardi VC, Bomfim GF, Reis WL, Al-Gassimi S, Nunes KP (2017). The interplay between Angiotensin II, TLR4 and hypertension. *Pharmacol Res* **120**, 88–96.

Biancardi VC, Stranahan AM, Krause EG, de Kloet AD, Stern JE (2016). Cross talk between AT1 receptors and Toll-like receptor 4 in microglia contributes to angiotensin II-derived ROS production in the hypothalamic paraventricular nucleus. *Am J Physiol Heart Circ Physiol* **310**, H404–H415.

Black EAE, Smith PM, McIsaac W, Ferguson AV (2018). Brain-derived neurotrophic factor acts at neurons of the subfornical organ to influence cardiovascular function. *Physiol Rep* **6**, e13704.

Boström P, Wu J, Jedrychowski MP, Korde A, Ye L, Lo JC, Rasbach KA, Boström EA, Choi JH, Long JZ, Kajimura S, Zingaretti MC, Vind BF, Tu H, Cinti S, Højlund K, Gygi SP & Spiegelman BM (2012). A PGC1-α-dependent myokine that drives brown-fat-like development of white fat and thermogenesis. *Nature* **481**, 463–468.

Boulle F, Kenis G, Cazorla M, Hamon M, Steinbusch HW, Lanfumey L, van den Hove DL (2012). TrkB inhibition as a therapeutic target for CNS-related disorders. *Prog Neurobiol* **98**, 197–206.

Brown NJ (2013). Contribution of aldosterone to cardiovascular and renal inflammation and fibrosis. *Nat Rev Nephrol* **9**, 459–456.

Buller SA and Feng Y (2016). Neuronal expression of prorenin and the (pro) renin receptor in the paraventricular nucleus of the hypothalamus and brainstem in the central nervous system. *FASEB J* **30**, 1234.8 (Abstract)

Bunda S, Liu P, Wang Y, Liu K, Hinek A (2007). Aldosterone induces elastin production in cardiac fibroblasts through activation of insulin-like growth factor-I receptors in a mineralocorticoid receptor-independent manner. *Am J Pathol* **171**, 809–819.

Burgos JI, Yeves AM, Barrena JP, Portiansky EL, Vila-Petroff MG, Ennis IL (2017). Nitric oxide and CaMKII: Critical steps in the cardiac contractile response To IGF-1 and swim training. *J Mol Cell Cardiol* **112**, 16–26.

Buttler L, Ribeiro IM, Ferreira-Neto HC, Antunes VR (2016). Angiotensin II acting on PVN induces sympathoexcitation and pressor responses via the PI3K-dependent pathway. *Auton Neurosci* **198**, 54–58.

Cao L, Zhang L, Chen S, Yuan Z, Liu S, Shen X, Zheng X, Qi X, Lee KK, Chan JY, Cai D (2012). BDNF-mediated migration of cardiac microvascular endothelial cells is impaired during ageing. *J Cell Mol Med* **16**, 3105–3115.

Cai D, Holm JM, Duignan IJ, Zheng J, Xaymardan M, Chin A, Ballard VL, Bella JN, Edelberg JM (2006). BDNF-mediated enhancement of inflammation and injury in the aging heart. *Physiol Genomics* **24**, 191–197.

Cai MX, Shi XC, Chen T, Tan ZN, Lin QQ, Du SJ, Tian ZJ (2016) Exercise training activates neuregulin 1/ErbB signaling and promotes cardiac repair in a rat myocardial infarction model. *Life Sci* **149**, 1–9.

Calabrese F, Rossetti AC, Racagni G, Gass P, Riva MA, Molteni R (2014). Brain-derived neurotrophic factor: a bridge between inflammation and neuroplasticity. *Front Cell Neurosci* **8**, 430.

Cannavo A, Bencivenga L, Liccardo D, Elia A, Marzano F, Gambino G, D'Amico ML, Perna C, Ferrara N, Rengo G, Paolocci N (2018). Aldosterone and Mineralocorticoid Receptor System in Cardiovascular Physiology and Pathophysiology. *Oxid Med Cell Longev* **2018**, 1204598.

Cannavo A, Liccardo D, Eguchi A, Elliott KJ, Traynham CJ, Ibetti J, Eguchi S, Leosco D, Ferrara, N, Rengo G, Koch WJ (2016). Myocardial pathology induced by aldosterone is dependent on non-canonical activities of G protein-coupled receptor kinases. *Nat Commun* **7**, 10877.

Carim-Todd L, Bath KG, Fulgenzi G, Yanpallewar S, Jing D, Barrick CA, Becker J, Buckley H, Dorsey SG, Lee FS, Tessarollo L (2009). Endogenous truncated TrkB. T1 receptor regulates neuronal complexity and TrkB kinase receptor function in vivo. *J Neurosci* **29**, 678–685.

Castrén E and Kojima M (2017). Brain-derived neurotrophic factor in mood disorders and antidepressant treatments. *Neurobiol Dis* **97**, 119–126.

Castren E. Thoenen H, Lindholm D (1995). Brain-derived neurotrophic factor messenger RNA is expressed in the septum, hypothalamus and in adrenergic brain stem nuclei of adult rat brain and is increased by osmotic stimulation in the paraventricular nucleus. *Neuroscience* **64**, 71–80.

Cato MJ and Toney GM (2005). Angiotensin II excites paraventricular nucleus neurons that innervate the rostral ventrolateral medulla: an in vitro patch-clamp study in brain slices. *J Neurophysiol* **93**, 403–413.

Cazorla M, Prémont J, Mann A, Girard N, Kellendonk C, Rognan D (2011). Identification of a low–molecular weight TrkB antagonist with anxiolytic and antidepressant activity in mice. *J Clin Invest* **121**, 1846–1857.

Chaanine AH and Hajjar RJ (2011). AKT signalling in the failing heart. *Eur J Heart Fail* **13**, 825–829.

Chan SH, Wu CW, Chang AY, Hsu KS, Chan JY (2010). Transcriptional upregulation of brain-derived neurotrophic factor in rostral ventrolateral medulla by angiotensin II: significance in superoxide homeostasis and neural regulation of arterial pressure. *Circ Res* **107**, 1127–1139.

Charan J and Kantharia N (2013). How to calculate sample size in animal studies? *J Pharmacol Pharmacother* **4**, 303–306.

Chen A, Huang BS, Wang HW, Ahmad M, Leenen FH (2014). Knockdown of mineralocorticoid or angiotensin II type 1 receptor gene expression in the paraventricular nucleus prevents angiotensin II hypertension in rats. *J Physiol* **592**, 3523–3536.

Chen K, Yan M, Li Y, Dong Z, Huang D, Li J, Wei M (2017). Intermedin1-53 enhances angiogenesis and attenuates adverse remodeling following myocardial infarction by activating AMP-activated protein kinase. *Mol Med Rep* **15**, 1497–1506.

Chen WW, Xiong XQ, Chen Q, Li YH, Kang YM, Zhu GQ (2015). Cardiac sympathetic afferent reflex and its implications for sympathetic activation in chronic heart failure and hypertension. *Acta Physiol* **213**, 778–794.

Choi SH, Bylykbashi E, Chatila ZK, Lee SW, Pulli B, Clemenson GD, Kim E, Rompala A, Oram, MK, Asselin C, Aronson J, Zhang C, Miller SJ, Lesinski A, Chen JW, Kim DY, van Praag H, Spiegelman BM, Gage FH, Tanzi RE (2018). Combined adult neurogenesis and BDNF mimic exercise effects on cognition in an Alzheimer's mouse model. *Science* **361**, eaan8821.

Clasadonte J and Prevot V (2018). The special relationship: glia–neuron interactions in the neuroendocrine hypothalamus. *Nat Rev Endocrinol* **14**, 25–44.

Condorelli G, Drusco A, Stassi G, Bellacosa A, Roncarati R, Iaccarino G, Russo MA, Gu Y, Dalton N, Chung C, Latronico MV, Napoli C, sadoshima J, Croce CM, Ross J Jr. (2002). Akt induces enhanced myocardial contractility and cell size in vivo in transgenic mice. *Proc Natl Acad Sci* U S A **99**, 12333–12338.

Cunha C, Brambilla R, Thomas KL (2010). A simple role for BDNF in learning and memory? *Front Mol Neurosci* **3**, 1.

Cuppini R, Sartini S, Agostini D, Guescini M, Ambrogini P, Betti M, Bertini L, Vallasciani M, Stocchi V (2007). BDNF expression in rat skeletal muscle after acute or repeated exercise. *Arch Ita Biol* **145**, 99–110.

Dao AT, Zagaar MA, Alkadhi KA (2015). Moderate treadmill exercise protects synaptic plasticity of the dentate gyrus and related signaling cascade in a rat model of Alzheimer's disease. *Mol Neurobiol* **52**, 1067–1076. Erratum: Mol. Neurobiol. 55, 901.

Davies EJ, Moxham T, Rees K, Singh S, Coats AJ, Ebrahim S, Lough F, Taylor RS (2010). Exercise training for systolic heart failure: Cochrane systematic review and meta-analysis. *Eur J Heart Fail* **12**,706–715.

de Haan JJ, Smeets MB, Pasterkamp G, Arslan F (2013). Danger signals in the initiation of the inflammatory response after myocardial infarction. *Mediators Inflamm* **2013**, 206039.

de Kloet AD, Liu M, Rodríguez V, Krause EG, Sumners C (2015). Role of neurons and glia in the CNS actions of the renin-angiotensin system in cardiovascular control. *Am J Physiol Regul Integr Comp Physiol* **309**, R444–R458.

de Lores Arnaiz, GR (2007). Na+, K+-ATPase in the brain: structure and function, *Handbook of Neurochemistry and Molecular Neurobiology*. Springer, 209–224.

de Lucia C, Eguchi A, Koch WJ (2018). New insights in cardiac β-adrenergic signaling during heart failure and aging. *Front Pharmacol* **9**, 904.

Diep QN, El Mabrouk M, Yue P, Schiffrin EL (2002). Effect of AT(1) receptor blockade on cardiac apoptosis in angiotensin II-induced hypertension. *Am J Physiol Heart Circ Physiol* **282**, H1635–H1641.

Ding Q, Ying Z, Gómez-Pinilla F (2011). Exercise influences hippocampal plasticity by modulating brain-derived neurotrophic factor processing. *Neuroscience* **192**, 773–780.

Diniz CRAF, Casarotto PC, Fred SM, Biojone C, Castrén E, Joca SRL (2018). Antidepressant-l ike effect of losartan involves TRKB transactivation from angiotensin receptor type 2 (AGTR2) and recruitment of FYN. *Neuropharmacology* **135**, 163–171.

Dinoff A, Herrmann N, Swardfager W, Lanctôt KL (2017). The effect of acute exercise on blood concentrations of brain-derived neurotrophic factor in healthy adults: a meta-analysis. *Eur J Neurosci* **46**, 1635–1646.

Dinoff A, Herrmann N, Swardfager W, Liu CS, Sherman C, Chan S, Lanctôt KL (2016). The effect of exercise training on resting concentrations of peripheral brain-derived neurotrophic factor (BDNF): a meta-analysis. *PLoS One* **11**, e0163037.

Du D, Chen J, Liu M, Zhu M, Jing H, Fang J, Shen L, Zhu D, Yu J, Wang J (2013). The effects of angiotensin II and angiotensin-(1–7) in the rostral ventrolateral medulla of rats on stress-induced hypertension. *PLoS One* **8**, e70976.

Dutta P and Nahrendorf M (2015). Monocytes in myocardial infarction. *Arterioscler Thromb Vasc Biol* **35**, 1066–1670.

Dworak M, Stebbing M, Kompa AR, Rana I, Krum H, Badoer E (2014). Attenuation of microglial and neuronal activation in the brain by ICV minocycline following myocardial infarction. *Auton Neurosci* **185**, 43–50.

Egan B and Zierath JR (2013). Exercise metabolism and the molecular regulation of skeletal muscle adaptation. *Cell Metab* **17**, 162–184.

Eide FF, Vining ER, Eide BL, Zang K, Wang XY, Reichardt LF (1996). Naturally occurring truncated trkB receptors have dominant inhibitory effects on brain-derived neurotrophic factor signaling. *J Neurosci* **16**, 3123–3129.

El Hayek L, Khalifeh M, Zibara V, Abi Assaad R, Emmanuel N, Karnib N, El-Ghandour R, Nasrallah P, Bilen M, Ibrahim P, Younes J, Abou Haidar E, Barmo N, Jabre V, Stephan JS, Sleiman SF (2019). Lactate mediates the effects of exercise on learning and memory through SIRT1-dependent activation of hippocampal brain-derived neurotrophic factor (BDNF). *J Neurosci* **39**, 2369–2382.

Epstein SE, Luger D, Lipinski MJ (2017). Paracrine-Mediated Systemic Anti-Inflammatory Activity of Intravenously Administered Mesenchymal Stem Cells: A Transformative Strategy for Cardiac Stem Cell Therapeutics. *Circ Rse* **121**, 1044–1046.

Erdos B, Backes I, McCowan ML, Hayward LF, Scheuer DA (2016). Brain-derived neurotrophic

factor modulates angiotensin signaling in the hypothalamus to increase blood pressure in rats. *Am J Physiol Heart Circ Physiol* **308**, H612–H622.

Erickson HP (2013). Irisin and FNDC5 in retrospect: An exercise hormone or a transmembrane receptor? *Adipocyte* **2**, 289–293.

Ethell IM and Ethell DW (2007). Matrix metalloproteinases in brain development and remodeling: synaptic functions and targets. *J Neurosci Res* **85**, 2813–2823.

Evans M, Cogan KE, Egan B (2017). Metabolism of ketone bodies during exercise and training: physiological basis for exogenous supplementation. *J Physiol* **595**, 2857–2871.

Fahimi A, Baktir MA, Moghadam S, Mojabi FS, Sumanth K, McNerney MW, Ponnusamy R, Salehi A (2017). Physical exercise induces structural alterations in the hippocampal astrocytes: exploring the role of BDNF-TrkB signaling. *Brain Struct Funct* **222**, 1797–1808.

Fang ZH, Lee CH, Seo MK, Cho H, Lee JG, Lee BJ, Park SW, Kim YH (2013). Effect of treadmill exercise on the BDNF-mediated pathway in the hippocampus of stressed rats. *Neurosci Research* **76**, 187–194.

Faul F, Erdfelder E, Lang AG, Buchner A (2007). G* Power 3: A flexible statistical power analysis program for the social, behavioral, and biomedical sciences. *Behav Res Methods* **39**, 175–191.

Feng N, Huke S, Zhu G, Tocchetti CG, Shi S, Aiba T, Kaludercic N, Hoover DB, Beck SE, Mankowski JL, Tomaselli GF, Bers DM, Kass DA, Paolocci N (2015). Constitutive BDNF/TrkB signaling is required for normal cardiac contraction and relaxation. *Proc Natl Acad Sci* U S A **112**, 1880–1885.

Fenner BM (2012). Truncated TrkB: beyond a dominant negative receptor. *Cytokine Growth Factor Rev* **23**, 15–24.

Ferguson AV (2009). Angiotensinergic regulation of autonomic and neuroendocrine outputs: critical roles for the subfornical organ and paraventricular nucleus. Neuroendocrinology **89**, 370–376.

Ferguson RE, Carroll HP, Harris A, Maher ER, Selby PJ, Banks RE (2005). Housekeeping proteins: a preliminary study illustrating some limitations as useful references in protein expression studies. *Proteomics* **5**, 566–571.

Ferrario CM (2016). Cardiac remodelling and RAS inhibition. *Ther Adv Cardiovasc Dis* **10**, 162–171.

Ferrini F and De Koninck Y (2013). Microglia control neuronal network excitability via BDNF signalling. *Neural Plast* **2013**, 429815.

Frangogiannis NG (2012). Regulation of the inflammatory response in cardiac repair. *Circ Res*

110, 159–173.

Frangogiannis NG (2014). The inflammatory response in myocardial injury, repair, and remodelling. *Nat Rev Cardiol* **11**, 255–265.

Frangogiannis NG (2015). Interleukin-1 in cardiac injury, repair, and remodeling: pathophysiologic and translational concepts. *Discoveries(Craiova)* **3**, e41.

Frank L, Ventimiglia R, Anderson K, Lindsay RM, Rudge JS (1996). BDNF down-regulates neurotrophin responsiveness, TrkB protein and TrkB mRNA levels in cultured rat hippocampal neurons. *Eur J Neurosci* **8**, 1220–1230.

Freitas SC, Harthmann Âd, Rodrigues B, Irigoyen MC, De Angelis K (2015). Effect of aerobic exercise training on regional blood flow and vascular resistance in diabetic rats. *Diabetol Metab Syndr* **7**, 115.

Fu YC, Chi CS, Yin SC, Hwang B, Chiu YT, Hsu SL (2004). Norepinephrine induces apoptosis in neonatal rat cardiomyocytes through a reactive oxygen species–TNFα–caspase signaling pathway. *Cardiovasc Res* **62**, 558–567.

Fukushima A, Kinugawa S, Homma T, Masaki Y, Furihata T, Yokota T, Matsushima S, Takada S, Kadoguchi T, Oba K, Okita K, Tsutsui H (2015). Serum brain-derived neurotropic factor level predicts adverse clinical outcomes in patients with heart failure. *J Card Fail* **21**, 300–306.

Fulgenzi G, Tomassoni-Ardori F, Babini L, Becker J, Barrick C, Puverel S, Tessarollo L (2015). BDNF modulates heart contraction force and long-term homeostasis through truncated TrkB. T1 receptor activation. *J Cell Biol* **210**,1003–1012.

Furmaga H, Carreno FR, Frazer A (2012). Vagal nerve stimulation rapidly activates brain-derived neurotrophic factor receptor TrkB in rat brain. *PloS One* **7**, e34844.

Gabor A and Leenen FH (2012). Central neuromodulatory pathways regulating sympathetic activity in hypertension. *J Appl Physiol* **113**, 1294–1303.

Gao L, Schultz HD, Patel KP, Zucker IH, Wang W (2005a). Augmented input from cardiac sympathetic afferents inhibits baroreflex in rats with heart failure. *Hypertension* **45**, 1173–1181.

Gao L, Wang W, Li YL, Schultz HD, Liu D, Cornish KG, Zucker IH (2004). Superoxide mediates sympathoexcitation in heart failure: roles of angiotensin II and NAD (P) H oxidase. *Circ Res* **95**, 937–944.

Gao L, Wang W, Li YL, Schultz HD, Liu D, Cornish KG, Zucker IH (2005b). Sympathoexcitation by central ANG II: roles for AT1 receptor upregulation and NAD (P) H oxidase in RVLM. *Am J Physiol Heart Circ Physiol* **288**, H2271–H2279.

Gao L, Wang W, Li YL, Zucker IH (2007a). Exercise training normalizes sympathetic outflow by central antioxidant mechanisms in rabbits with pacing-induced chronic heart failure. *Circulation* **115**, 3095–3102.

Gao L, Wang W, Wang W, Zucker IH (2007b). Abstract 1381: Ang II Induced Sympathetic Overactivity in the RVLM of Normal Rats Involves the PKC Pathway *Circulation* **116**, Issue suppl_16.

Monge Garcia MI, Jian Z, Settels JJ, Hunley C, Cecconi M, Hatib F, Pinsky MR (2018). Performance comparison of ventricular and arterial dP/dt_{max} for assessing left ventricular systolic function during different experimental loading and contractile conditions. *Crit Care* **22,** 325.

Garnier A, Fortin D, Delomenie C, Momken I, Veksler V & Ventura-Clapier R (2003). Depressed mitochondrial transcription factors and oxidative capacity in rat failing cardiac and skeletal muscles. *J Physiol* **551**, 491–501.

Gielen S, Laughlin MH, O'Conner C, Duncker DJ (2015). Exercise training in patients with heart disease: review of beneficial effects and clinical recommendations. *Prog Cardiovasc Dis* **57**, 347–355.

Gleeson M, Bishop NC, Stensel DJ, Lindley MR, Mastana SS, Nimmo MA (2011). The anti-inflammatory effects of exercise: mechanisms and implications for the prevention and treatment of disease. *Nat RevImmunol* **11**, 607–615.

Goldenberg I, Grossman E, Jacobson KA, Shneyvays V, Shainberg A (2001). Angiotensin II-induced apoptosis in rat cardiomyocyte culture: a possible role of AT1 and AT2 receptors. *J Hypertens* **19**, 1681–1689.

Gomes JR, Costa JT, Melo CV, Felizzi F, Monteiro P, Pinto MJ, Inácio AR, Wieloch T, Almeida, RD, Grãos M, Duarte CB (2012). Excitotoxicity downregulates TrkB. FL signaling and upregulates the neuroprotective truncated TrkB receptors in cultured hippocampal and striatal neurons. *J Neurosci* **32**, 4610–4622.

Gomes-Santos IL, Fernandes T, Couto GK, Ferreira-Filho JC, Salemi VM, Fernandes FB, Casarini DE, Brum PC, Rossoni LV, de Oliveira EM, Negrao CE (2014). Effects of exercise training on circulating and skeletal muscle renin-angiotensin system in chronic heart failure rats. *PLoS One* **9**, e98012.

Gordan R, Gwathmey JK, Xie LH (2015). Autonomic and endocrine control of cardiovascular function. *World J Cardiol* **7**, 204–214.

Greenberg ME, Xu B, Lu B, Hempstead BL (2009). New insights in the biology of BDNF synthesis and release: implications in CNS function. *J Neurosci* **29**, 12764–12767.

Greengard P (2001). The neurobiology of slow synaptic transmission. *Science* **294**, 1024–1030.

Griffin EW, Bechara RG, Birch AM, Kelly ÁM (2009). Exercise enhances hippocampal-dependent learning in the rat: Evidence for a BDNF-related mechanism. *Hippocampus* **19**, 973–980.

Grune T, Jung T, Merker K, Davies KJ (2004). Decreased proteolysis caused by protein aggregates, inclusion bodies, plaques, lipofuscin, ceroid, and 'aggresomes' during oxidative stress, aging, and disease. *Int J Biochem Cell Biol* **36**, 2519–2530.

Guan Z and Fang J (2006). Peripheral immune activation by lipopolysaccharide decreases neurotrophins in the cortex and hippocampus in rats. *Brain Behav Immun* **20**, 64–71.

Guggilam A, Cardinale JP, Mariappan N, Sriramula S, Haque M, Francis J (2011). Central TNF inhibition results in attenuated neurohumoral excitation in heart failure: a role for superoxide and nitric oxide. *Basic Res Cardiol* **106**, 273–286.

Guggilam A, Patel KP, Haque M, Ebenezer PJ, Kapusta DR, Francis J (2008). Cytokine blockade attenuates sympathoexcitation in heart failure: cross-talk between nNOS, AT-1R and cytokines in the hypothalamic paraventricular nucleus. *Eur J Heart Fail* **10**, 625–634.

Gullestad L, Ueland T, Vinge LE, Finsen A, Yndestad A, Aukrust P (2012). Inflammatory cytokines in heart failure: mediators and markers. *Cardiology* **122**, 23–35.

Guo W, Ji Y, Wang S, Sun Y, Lu B (2014). Neuronal activity alters BDNF–TrkB signaling kinetics and downstream functions. *J Cell Sci* **127**, 2249–2260.

Guyenet PG (2006). The sympathetic control of blood pressure. *Nat Rev Neurosci* **7**, 335–346.

Haack KK, Engler CW, Papoutsi E, Pipinos II, Patel KP, Zucker IH (2012). Parallel changes in neuronal AT1R and GRK5 expression following exercise training in heart failure. *Hypertension* **60**, 354–361.

Haapasalo A, Koponen E, Hoppe E, Wong G, Castrén E (2011). Truncated trkB. T1 is dominant negative inhibitor of trkB. TK+-mediated cell survival. *Biochem Biophys Res commun* **280**, 1352–1358.

Halade GV, Ma Y, Ramirez TA, Zhang J, Dai Q, Hensler JG, Lopez EF, Ghsaemi O, Jin YF, Lindsey ML (2013). Reduced BDNF attenuates inflammation and angiogenesis to improve survival and cardiac function following myocardial infarction in mice. *Am J Physiol Heart Circ Physiol* **305**, H1830–H1842.

Halade GV, Norris PC, Kain V, Serhan CN, Ingle KA (2018). Splenic leukocytes define the resolution of inflammation in heart failure. *Sci Signal* **11**, eaao1818.

Hambrecht R, Gielen S, Linke A, Fiehn E, Yu J, Walther C, Schoene N, Schuler G (2000). Effects of exercise training on left ventricular function and peripheral resistance in patients with chronic heart failure: a randomized trial. *JAMA* **283**, 3095–3101.

Hamid T, Gu Y, Ortines RV, Bhattacharya C, Wang G, Xuan YT, Prabhu SD (2009). Divergent tumor necrosis factor receptor–related remodeling responses in heart failure: role of nuclear factor-κB and inflammatory activation. *Circulation* **119**, 1386–1397.

Hamid T, Guo SZ, Kingery, JR, Xiang X, Dawn B, Prabhu SD (2011). Cardiomyocyte NF-κB p65 promotes adverse remodelling, apoptosis, and endoplasmic reticulum stress in heart failure. *Cardiovas Res* **89**, 129–138.

Hang P, Zhao J, Cai B, Tian S, Huang W, Guo J, Sun C, Li Y, Du Z (2015). Brain-derived neurotrophic factor regulates TRPC3/6 channels and protects against myocardial infarction in rodents. *Int J Biol Sci* **11**,536–545.

Hang P, Zhao J, Sun L, Li M, Han Y, Du Z, Li Y (2017). Brain-derived neurotrophic factor attenuates doxorubicin-induced cardiac dysfunction through activating Akt signalling in rats. *J Cell Mol Med* **21**, 685–696.

Hartupee J and Mann DL (2017). Neurohormonal activation in heart failure with reduced ejection fraction. *Nat Rev Cardiol* **14**, 30–38.

Hashimoto K (2013). Sigma-1 receptor chaperone and brain-derived neurotrophic factor: Emerging links between cardiovascular disease and depression. *Prog Neurobiol* **100**, 15–29.

Hedayat M, Mahmoudi MJ, Rose NR, Rezaei N (2010). Proinflammatory cytokines in heart failure: double-edged swords. *Heart Fail Rev* **15**, 543–562.

Higuchi Y, Otsu K, Nishida K, Hirotani S, Nakayama H, Yamaguchi O, Matsumura Y, Ueno H, Tada M, Hori M (2002). Involvement of reactive oxygen species-mediated NF-κB activation in TNF-α-induced cardiomyocyte hypertrophy. *J Mol Cell Cardiol* **34**, 233–240.

Hong JH, Park HM, Byun KH, Lee BH, Kang WC, Jeong GB (2014). BDNF expression of macrophages and angiogenesis after myocardial infarction. *Int J Cardiol* **176**, 1405–1408.

Huang BS, Ahmadi S, Ahmad M, White RA, Leenen FH (2010). Central neuronal activation and pressor responses induced by circulating ANG II: role of the brain aldosterone-"ouabain" pathway. *Am J Physiol Heart Circ Physiol* **299**, H422–H430.

Huang BS, Chen A, Ahmad M, Wang HW, Leenen FH (2014a). Mineralocorticoid and AT1 receptors in the paraventricular nucleus contribute to sympathetic hyperactivity and cardiac dysfunction in rats post myocardial infarct. *J Physiol* **592**, 3273–3286.

Huang BS and Leenen FH (2005). Blockade of brain mineralocorticoid receptors or Na+ channels prevents sympathetic hyperactivity and improves cardiac function in rats post-MI. *Am J Physiol Heart Circ Physiol* **288**, H2491–H2497.

Huang BS and Leenen FH (2009). The brain renin-angiotensin-aldosterone system: a major mechanism for sympathetic hyperactivity and left ventricular remodeling and dysfunction after myocardial infarction. *Curr Heart Fail Rep* **6**, 81–88.

Huang BS, Zheng H, Tan J, Patel KP, Leenen FH (2011). Regulation of hypothalamic renin–angiotensin system and oxidative stress by aldosterone. *Exp Physiol* **96**, 1028–1038.

Huang T, Larsen KT, Ried-Larsen M, Møller NC, Andersen LB (2014b). The effects of physical activity and exercise on brain-derived neurotrophic factor in healthy humans: A review. *Scand J Med Sci Sports* **24**, 1–10.

Hurtado E, Cilleros V, Nadal L, Simó A, Obis T, Garcia N, Santafé MM, Tomàs M, Halievski K, Jordan CL, Lanuza MA, Tomàs J (2017). Muscle Contraction Regulates BDNF/TrkB Signaling to Modulate Synaptic Function through Presynaptic cPKCα and cPKCβI. *Front Mol Neurosci* **10**, 147.

Ichige MH, Santos CR, Jordão CP, Ceroni A, Negrão CE, Michelini LC (2016). Exercise training preserves vagal preganglionic neurones and restores parasympathetic tonus in heart failure. *J Physiol* **594**, 6241–6254.

Isegawa K, Hirooka Y, Katsuki M, Kishi T, Sunagawa K (2014). Angiotensin II type 1 receptor expression in astrocytes is upregulated leading to increased mortality in mice with myocardial infarction-induced heart failure. *Am J Physiol Heart Circ Physiol* **307**, H1448–H1455.

Jiménez-Maldonado A, de Álvarez-Buylla ER, Montero S, Melnikov V, Castro-Rodríguez E, Gamboa-Domínguez A, Rodríguez-Hernández A, Lemus M, Murguía JM (2014). Chronic exercise increases plasma brain-derived neurotrophic factor levels, pancreatic islet size, and insulin tolerance in a TrkB-dependent manner. *PLoS one* 9: e115177.

Jiménez-Maldonado A, Cerna-Cortés J, Castro-Rodríguez EM, Montero SA, Muñiz J, Rodríguez-Hernández A, Lemus M, De Álvarez-Buylla ER (2015). Effects of moderate- and high-intensity chronic exercise on brain-derived neurotrophic factor expression in fast and slow muscles. *Muscle Nerve* **53**, 446–451.

Jin H, Yang R, Li W, Lu H, Ryan AM, Ogasawara AK, Van Peborgh J, Paoni NF (2000). Effects of exercise training on cardiac function, gene expression, and apoptosis in rats. *Am J Physiol Heart Circ Physiol* **279**, H2994–H3002.

Johar S, Cave AC, Narayanapanicker A, Grieve DJ, Shah AM (2006). Aldosterone mediates angiotensin II-induced interstitial cardiac fibrosis via a Nox2-containing NADPH oxidase. *FASEB J* **20**, 1546–1548.

Johnson-Farley NN, Travkina T, Cowen DS (2006). Cumulative activation of akt and consequent inhibition of glycogen synthase kinase-3 by brain-derived neurotrophic factor and insulin-like growth factor-1 in cultured hippocampal neurons. *J Pharmacol Exp Ther* **316**, 1062–1069.

Kang YM, Zhang ZH, Johnson RF, Yu Y, Beltz T, Johnson AK, Weiss RM, Felder RB (2006). Novel effect of mineralocorticoid receptor antagonism to reduce proinflammatory cytokines and hypothalamic activation in rats with ischemia-induced heart failure. *Circ Res* **99**, 758–766.

Kang YM, Zhang ZH, Xue B, Weiss RM, Felder RB (2008). Inhibition of brain proinflammatory cytokine synthesis reduces hypothalamic excitation in rats with ischemia-induced heart failure. *Am J Physiol Heart Circ Physiol* **295**, H227–H236.

Kar S, Gao L, Zucker IH (2010). Exercise training normalizes ACE and ACE2 in the brain of rabbits with pacing-induced heart failure. *J Appl Physiol* **108**, 923–932.

Katare RG, Kakinuma Y, Arikawa M, Yamasaki F, Sato T (2009). Chronic intermittent fasting improves the survival following large myocardial ischemia by activation of BDNF/VEGF/PI3K signaling pathway. *J Mol Cell Cardiol* **46**, 405–412.

Kemi OJ, Ellingsen Ø, Ceci M, Grimaldi S, Smith GL, Condorelli G, Wisløff U (2007). Aerobic interval training enhances cardiomyocyte contractility and Ca 2+ cycling by phosphorylation of CaMKII and Thr-17 of phospholamban. *J Mol Cell Cardiol* **43**, 354–361.

Kent MA, Huang BS, Van Huysse JW, Leenen FH (2004). Brain Na+, K+-ATPase isozyme activity and protein expression in ouabain-induced hypertension. *Brain Res* **1018**, 171–180.

Kesherwani V, Chavali V, Hackfort BT, Tyagi SC, Mishra PK (2015). Exercise ameliorates high fat diet induced cardiac dysfunction by increasing interleukin 10. *Front Physiol* **6**, 124.

Kim TT and Dyck JR (2015). Is AMPK the savior of the failing heart? *Trends Endocrinol Metab* **26**, 40–48.

Kingsbury TJ, Murray PD, Bambrick LL, Krueger BK (2003). Ca^{2+}-dependent regulation of TrkB expression in neurons. *J Biol Chem* **278**, 40744–40748.

Kishi T, Hirooka Y, Nagayama T, Isegawa K, Katsuki M, Takesue K, Sunagawa K (2015). Calorie restriction improves cognitive decline via up-regulation of brain-derived neurotrophic factor. *Int Heart J* **56**, 110–115.

Kleiber AC, Zheng H, Schultz HD, Peuler JD, Patel KP (2008). Exercise training normalizes enhanced glutamate-mediated sympathetic activation from the PVN in heart failure. *Am J Physiol Regul Integr Comp Physiol* **294**, R1863–R1872.

Klein R, Nanduri V, Jing SA, Lamballe F, Tapley P, Bryant S, Cordon-Cardo C, Jones KR, Reichardt LF, Barbacid M (1991). The trkB tyrosine protein kinase is a receptor for brain-derived neurotrophic factor and neurotrophin-3. *Cell* **66**, 395–403.

Knudsen JG, Murholm M, Carey AL, Biensø RS, Basse AL, Allen TL, Hidalgo J, Kingwell BA, Febbraio MA, Hansen JB, Pilegaard H (2014). Role of IL-6 in exercise training-and cold-induced UCP1 expression in subcutaneous white adipose tissue. *PLoS One* **9**, e84910.

Knaepen K, Goekint M, Heyman EM, Meeusen R (2010). Neuroplasticity—exercise-induced response of peripheral brain-derived neurotrophic factor. *Sports Med* **40**, 765–801.

Koba S (2018). Angiotensin II, Oxidative Stress, and Sympathetic Nervous System Hyperactivity in Heart Failure. *Yonago Acta Med* **61**, 103–109.

Kolettis TM (2018). Autonomic function and ventricular tachyarrhythmias during acute myocardial infarction. *World J Exp Med* **8**, 8–11.

Kolwicz SC Jr, Olson DP, Marney LC, Garcia-Menendez L, Synovec RE, Tian R (2012). Cardiac-specific deletion of acetyl CoA carboxylase 2 prevents metabolic remodeling during pressure-overload hypertrophy. *Circ Res* **111**, 728–738, 2012.

Konstam MA and Abboud FM (2017). Ejection fraction: misunderstood and overrated (changing the paradigm in categorizing heart failure). *Circulation* **135**, 717–719.

Koo JH, Kwon IS, Kang EB, Lee CK, Lee NH, Kwon MG, Cho IH, Cho JY (2013). Neuroprotective effects of treadmill exercise on BDNF and PI3-K/Akt signaling pathway in the cortex of transgenic mice model of Alzheimer's disease. *J Exerc Nutr Biochem* **17**, 151–160.

Koshimizu H, Hazama S, Hara T, Ogura A, Kojima M (2010). Distinct signaling pathways of precursor BDNF and mature BDNF in cultured cerebellar granule neurons. *Neurosci Lett* **473**, 229–232.

Kougias P, Weakley SM, Yao Q, Lin PH, Chen C (2010). Arterial baroreceptors in the management of systemic hypertension. Medical science monitor: *Med Sci Monit* **16**, RA1–RA8.

Kowiański P, Lietzau G, Czuba E, Waśkow M, Steliga A, Moryś J (2018). BDNF: A key factor with multipotent impact on brain signaling and synaptic plasticity. *Cell Mol Neurobiol* **38**,579–593.

Kreusser MM, Lehmann LH, Haass M, Buss SJ, Katus HA, Lossnitzer D (2017). Depletion of cardiac catecholamine stores impairs cardiac norepinephrine re-uptake by downregulation of the norepinephrine transporter. *PloS One* **12**, e0172070.

Krishnamurthy P, Rajasingh J, Lambers E, Qin G, Losordo DW, Kishore R (2009). IL-10 inhibits inflammation and attenuates left ventricular remodeling after myocardial infarction via activation of STAT3 and suppression of HuR. *Circ Res* **104**, e9–e18.

Kumagai H, Oshima N, Matsuura T, Iigaya K, Imai M, Onimaru H, Sakata K, Osaka M, Onami T, Takimoto C, Kamayachi T, Itoh H, Saruta T (2012). Importance of rostral ventrolateral

medulla neurons in determining efferent sympathetic nerve activity and blood pressure. *Hyperten Res* **35**, 132–141.

Labandeira-Garcia JL, Rodríguez-Perez AI, Garrido-Gil P, Rodriguez-Pallares J, Lanciego JL, Guerra MJ (2017). Brain renin-angiotensin system and microglial polarization: implications for aging and neurodegeneration. *Front Aging Neurosci* **9**, 129.

Lapchak PA, Araujo DM, Hefti F (1993). Systemic interleukin-1β decreases brain-derived neurotrophic factor messenger RNA expression in the rat hippocampal formation. *Neuroscience* **53**, 297–301.

Lecker SH, Zavin A, Cao P, Arena R, Allsup K, Daniels KM, Joseph J, Schulze PC, Forman DE (2012). Expression of the irisin precursor FNDC5 in skeletal muscle correlates with aerobic exercise performance in patients with heart failure. *Circ Heart Fail* **5**, 812–818.

Lee HW, Ahmad M, Wang HW, Leenen FH (2017). Effects of exercise training on brain-derived neurotrophic factor in skeletal muscle and heart of rats post myocardial infarction. *Exp Physiol* **102**, 314–328.

Lee HW, Ahmad M, Weldrick JJ, Wang HW, Burgon PG, Leenen FHH (2018). Effects of exercise training and TrkB blockade on cardiac function and BDNF-TrkB signaling postmyocardial infarction in rats. *Am J Physiol Heart Circ Physiol* **315**, H1821–H1834.

Lee R, Kermani P, Teng KK, Hempstead BL (2001). Regulation of cell survival by secreted proneurotrophins. *Science* **294**, 1945–1948.

Leenen FH (1999). Cardiovascular consequences of sympathetic hyperactivity. *Can J Cardiol* **15**, 2A–7A.

Leenen FH (2007). Brain mechanisms contributing to sympathetic hyperactivity and heart failure. *Circ Res* **101**, 221–223.

Leenen FH (2010). The central role of the brain aldosterone–"ouabain" pathway in salt-sensitive hypertension. *Biochim Biophys Acta* **1802**, 1132–1139.

Leenen FH (2014). Actions of circulating angiotensin II and aldosterone in the brain contributing to hypertension. *Am J Hypertens* **27**, 1024–1032.

Leenen FHH, Blaustein MP, Hamlyn JM (2017). Update on angiotensin II: new endocrine connections between the brain, adrenal glands and the cardiovascular system. *Endocr Connect* **6**, R131–R145.

Leenen FH and Tuana BS (2012). Cardioprotective Brain Mechanisms. *Arterioscler Thromb Vasc Biol* **32**, 1749–1750.

Leenen FH, Skarda V, Yuan B, White R (1999). Changes in cardiac ANG II postmyocardial infarction in rats: effects of nephrectomy and ACE inhibitors. *Am J Physiol* **276**, H317–H325.

Lehnen A, Leguisamo N, Pinto G, Markoski M, De Angelis K, Machado U, Schaan B (2011). Exercise-stimulated GLUT4 expression is similar in normotensive and hypertensive rats. *Horm Metab Res* **43**, 231–235.

Leosco D, Rengo G, Iaccarino G, Golino L, Marchese M, Fortunato F, Zincarelli C, Sanzari E, Ciccarelli M, Galasso G, Altobelli GG, Conti V, Matrone G, Cimini V, Ferrara N, Filippelli A, Koch WJ, Rengo F (2008). Exercise promotes angiogenesis and improves β-adrenergic receptor signalling in the post-ischaemic failing rat heart. *Cardiovasc Res* **78**, 385–394.

Leuschner F, Panizzi P, Chico-Calero I, Lee WW, Ueno T, Cortez-Retamozo V, Waterman P, Gorbatov R, Marinelli B, Iwamoto Y, Chudnovskiy A, figueiredo JL, Sosnovik DE, Pittet MJ, Swirski FK, Weissleder R, Nahrendorf M (2010). Angiotensin-converting enzyme inhibition prevents the release of monocytes from their splenic reservoir in mice with myocardial infarction. *Circ Res* **107**, 1364–1373.

Li B, Tian J, Sun Y, Xu TR, Chi RF, Zhang XL, Hu XL, Zhang YA. Qin FZ, Zhang WF (2015). Activation of NADPH oxidase mediates increased endoplasmic reticulum stress and left ventricular remodeling after myocardial infarction in rabbits. *Biochim Biophys Acta* **1852**, 805–815.

Li DP, Chen SR, Pan HL (2003). Angiotensin II stimulates spinally projecting paraventricular neurons through presynaptic disinhibition. *J Neurosci* **23**, 5041–5049.

Li DP, Zhou JJ, Zhang J, Pan HL (2017). CaMKII regulates synaptic NMDA receptor activity of hypothalamic presympathetic neurons and sympathetic outflow in hypertension. *J Neurosci* **37**, 10690–10699.

Li JM, Fan LM, Christie MR, Shah AM (2005). Acute tumor necrosis factor alpha signaling via NADPH oxidase in microvascular endothelial cells: role of p47phox phosphorylation and binding to TRAF4. *Mol Cell Biol* **25**, 2320–2330.

Li P, Sun HJ, Cui BP, Zhou YB, Han Y (2013). Angiotensin-(1–7) in the rostral ventrolateral medulla modulates enhanced cardiac sympathetic afferent reflex and sympathetic activation in renovascular hypertensive rats. *Hypertension* **61**, 820–827.

Li Q, Dong QT, Yang YJ, Tian XQ, Jin C, Huang PS, Jiang LP, Chen GH (2016). AMPK-mediated cardioprotection of atorvastatin relates to the reduction of apoptosis and activation of autophagy in infarcted rat hearts. *Am J Transl Res* **8**, 4160–4171.

Li W, Peng H, Cao T, Sato R, McDaniels SJ, Kobori H, Navar LG, Feng Y (2012). Brain-targeted (pro)renin receptor knockdown attenuates angiotensin II–dependent hypertension. *Hypertension* **59**, 1188–1194.

Li W, Peng H, Mehaffey EP, Kimball CD, Grobe JL, van Gool JM, Sullivan MN, Earley S, Danser AH, Ichihara A, Feng Y (2014). Neuron-specific (pro)renin receptor knockout prevents the development of salt-sensitive hypertension. *Hypertension* **63**, 316–323.

Li Y, Luikart BW, Birnbaum S, Chen J, Kwon CH, Kernie SG, Bassel-Duby R, Parada LF (2008). TrkB regulates hippocampal neurogenesis and governs sensitivity to antidepressive treatment. *Neuron* **59**, 399–412.

Lin RC, Weeks KL, Gao XM, Williams RB, Bernardo BC, Kiriazis H, Matthews VB, Woodcock EA, Bouwman RD, Mollica JP, Speirs HJ, Dawes IW, Daly RJ, Shioi T, Izumo S, Febbraio MA, DuXJ, McMullen JR (2010). PI3K(p110α) protects against myocardial infarction-induced heart failure: identification of PI3K-regulated miRNA and mRNA. *Arterioscler Thromb Vasc Biol* **30**, 724–732.

Lind RW, Swanson LW, Ganten D (1985). Organization of angiotensin II immunoreactive cells and fibers in the rat central nervous system. An immunohistochemical study *Neuroendocrinology* **40**, 2–24.

Ling H, Zhang T, Pereira L, Means CK, Cheng H, Gu Y, Dalton ND, Peterson KL, Chen J, Bers D, Brwon JH (2009). Requirement for Ca 2+/calmodulin–dependent kinase II in the transition from pressure overload–induced cardiac hypertrophy to heart failure in mice. *J Clin Invest* **119**, 1230–1240.

Llewellyn TL, Sharma NM, Zheng H, Patel KP (2014). Effects of exercise training on SFO-mediated sympathoexcitation during chronic heart failure. *Am J Physiol Heart Circ Physiol* **306**, H121–H131.

Loennechen JP, Støylen A, Beisvag V, Wisløff U, Ellingsen Ø (2001). Regional expression of endothelin-1, ANP, IGF-1, and LV wall stress in the infarcted rat heart. *Am J Physiol Heart Circ Physiol* **280**, H2902–H2910.

Lu B, Pang PT, Woo NH (2005). The yin and yang of neurotrophin action. *Nat Rev Neurosci* **6**, 603–614.

Lu K, Wang L, Wang C, Yang Y, Hu D & Ding R (2015). Effects of high-intensity interval versus continuous moderate-intensity aerobic exercise on apoptosis, oxidative stress and metabolism of the infarcted myocardium in a rat model. *Mol Med Rep* **12**, 2374–2382.

Lymperopoulos A, Rengo G, Koch WJ (2013). Adrenergic nervous system in heart failure: pathophysiology and therapy. *Circ Res* **113**, 739–753.

Ma JC, Duan MJ, Sun LL, Yan ML, Liu T, Wang Q, Liu CD, Wang X, Kang XH, Pei SC, Zong DK, Chen X, Wang N, Ai J (2015a). Cardiac over-expression of microRNA-1 induces impairment of cognition in mice. *Neuroscience* **299**, 66–78.

Ma X, Fu Y, Xiao H, Song Y, Chen R, Shen J, An X, Shen Q, Li Z, Zhang Y (2015b). Cardiac fibrosis alleviated by exercise training is AMPK-dependent. *PLoS One* **10**, e0129971.

Madamanchi A (2007). β-Adrenergic receptor signaling in cardiac function and heart failure. *McGill J M* **10**, 99–104.

Mahata SK, Zheng H, Mahata S, Liu X, Patel KP (2016). Effect of heart failure on catecholamine granule morphology and storage in chromaffin cells. *J Endocrinol* **230**, 309–323.

Manchini MT, Antônio EL, Silva Junior JA, de Carvalho PT, Albertini R, Pereira FC, Feliciano R, Montemor J, Vieira SS, Grandinetti V, Yoshizaki A, Chaves M, da Silva MP, de Lima RD, Bocalini DS, de Melo BL, Tucci PJ, Serra AJ (2017). Low-level laser application in the early myocardial infarction stage has no beneficial role in heart failure. *Front Physiol* **8**, 309–323.

Mann DL (2002). Inflammatory mediators and the failing heart: past, present, and the foreseeable future. *Circ Res* **91**, 988–998.

Manning BD and Toker A (2017). AKT/PKB signaling: navigating the network. *Cell* **169**, 381–405.

Marmigère F, Rage F, Tapia-Arancibia L (2003). GABA–glutamate interaction in the control of BDNF expression in hypothalamic neurons. *Neurochem Int* **42**, 353–358.

Marmigère F, Rage F, Tapia-Arancibia L (2001). Regulation of brain-derived neurotrophic factor transcripts by neuronal activation in rat hypothalamic neurons. *J Neurosci Res* **66**, 377–389.

Matsuo Y, Gleitsmann K, Mangner N, Werner S, Fischer T, Bowen TS, Kricke A, Matsumoto Y, Kurabayashi M, Schuler G, Linke A & Adams V (2015). Fibronectin type III domain containing 5 expression in skeletal muscle in chronic heart failure-relevance of inflammatory cytokines. *J Cachexia Sarcopenia Muscle* **6**, 62–72.

Matthews V, Åström MB, Chan MH, Bruce CR, Krabbe KS, Prelovsek O, Åkerström T, Yfanti C, Broholm C, Mortensen OH, Penkowa M, Hojman P, Zankari A, Watt MJ, Bruunsgaard H, Pedersen BK, Febbraio MA (2009). Brain-derived neurotrophic factor is produced by skeletal muscle cells in response to contraction and enhances fat oxidation via activation of AMP-activated protein kinase. *Diabetologia* **52**, 1409–1418.

McIsaac W and Ferguson AV (2017). Glucose concentrations modulate brain-derived neurotrophic factor responsiveness of neurones in the paraventricular nucleus of the hypothalamus. *J Neuroendocrinol* **29**, 1–10.

McMurray JJ, Adamopoulos S, Anker SD, Auricchio A, Böhm M, Dickstein K, Falk V, Filippatos G, Fonseca C, Gomez-Sanchez MA, Jaarsma T, Køber L, Lip GY, Maggioni AP, Parkhomenko A, Pieske BM, Popescu BA, Rønnevik PK, Rutten FH, Schwitter J, Seferovic P, Stepinska J, Trindada PT, Voors AA, Zannad F, Seiher A; ESC Committee for Practice Guidelines (2012). ESC Guidelines for the diagnosis and treatment of acute and chronic heart failure 2012: the task force for the diagnosis and treatment of acute and chronic heart failure 2012 of the European Society of Cardiology. Developed in collaboration with the Heart Failure Association (HFA) of the ESC. *Eur Heart J* **33**, 1787–1847.

Michelini LC and Stern JE (2009). Exercise-induced neuronal plasticity in central autonomic networks: role in cardiovascular control. *Exp Physiol* **94**, 947–960.

Middlemas DS, Lindberg RA, Hunter T (1991). trkB, a neural receptor protein-tyrosine kinase: evidence for a full-length and two truncated receptors. *Mol Cell Biol* **11**, 143–153.

Minisi AJ and Thames MD (1991). Activation of cardiac sympathetic afferents during coronary occlusion. Evidence for reflex activation of sympathetic nervous system during transmural myocardial ischemia in the dog. *Circulation* **84**, 357–367.

Mizoguchi Y, Monji A, Kato T, Seki Y, Gotoh L, Horikawa H, Suzuki SO, Iwaki T, Yonaha M, Hashioka S, Kanba S (2009). Brain-derived neurotrophic factor induces sustained elevation of intracellular Ca2+ in rodent microglia. *J Immunol* **183**, 7778–7786.

Moreira JB, Bechara LR, Bozi LH, Jannig PR, Monteiro AW, Dourado PM, Wisløff U, Brum PC (2013). High-versus moderate-intensity aerobic exercise training effects on skeletal muscle of infarcted rats. *J Appl Physiol* **114**, 1029–1041.

Mousavi K and Jasmin BJ (2006). BDNF is expressed in skeletal muscle satellite cells and inhibits myogenic differentiation. *J Neurosci* **26**, 5739–5749.

Mowla SJ, Pareek S, Farhadi HF, Petrecca K, Fawcett JP, Seidah NG, Morris SJ, Sossin WS, Murphy RA (1999). Differential sorting of nerve growth factor and brain-derived neurotrophic factor in hippocampal neurons. *J Neurosci* **19**, 2069–2080.

Murray PJ (2005). The primary mechanism of the IL-10-regulated antiinflammatory response is to selectively inhibit transcription. *Proc Natl Acad Sci* U S A **102**, 8686–8691.

Nagappan G and Lu B (2005). Activity-dependent modulation of the BDNF receptor TrkB: mechanisms and implications. *Trends Neurosci* **28**, 464–471.

Nagappan G, Woo NH, Lu B (2008). Ama “zinc” link between TrkB transactivation and synaptic plasticity. *Neuron* **57**, 477–479.

Nakagawa P and Sigmund CD (2017). How Is the Brain Renin–Angiotensin System Regulated? Hypertension **70**, 10–18.

Neeper SA, Gómez-Pinilla F, Choi J, Cotman CW (1996). Physical activity increases mRNA for brain-derived neurotrophic factor and nerve growth factor in rat brain. *Brain Res* **726**, 49–56.

Netticadan T, Temsah RM, Kawabata K, Dhalla NS (2000). Sarcoplasmic reticulum Ca2+/calmodulin-dependent protein kinase is altered in heart failure. *Circ Res* **86**, 596–605.

Nguyen G, Delarue F, Burcklé C, Bouzhir L, Giller T, Sraer JD (2002). Pivotal role of the renin/prorenin receptor in angiotensin II production and cellular responses to renin. *J Clin Invest* **109**, 1417–1427.

Nio Y, Matsubara H, Murasawa S, Kanasaki M, Inada M (1995). Regulation of gene transcription of angiotensin II receptor subtypes in myocardial infarction. *J Clin Invest* **95**, 46–54.

Noble EE. Exercise, neuropeptides and the hypothalamic regulation of appetite and energy balance (2014). Retrieved from the University of Minnesota Digital Conservancy, http://hdl.handle.net/11299/163876.

Norheim F, Langleite TM, Hjorth M, Holen T, Kielland A, Stadheim HK, Gulseth HL, Birkeland KI, Jensen J, Drevon CA (2014). The effects of acute and chronic exercise on PGC-1α, irisin and browning of subcutaneous adipose tissue in humans. *FEBS J* **281**, 739–749.

Nunes RB, Alves JP, Kessler LP, Dal Lago P (2013). Aerobic exercise improves the inflammatory profile correlated with cardiac remodeling and function in chronic heart failure rats. *Clinics* **68**, 876–882.

Ogborn DI and Gardiner PF (2010). Effects of exercise and muscle type on BDNF, NT-4/5, and TrKB expression in skeletal muscle. *Muscle Nerve* **41**, 385–391.

Ohbuchi T, Haam J, Tasker JG (2015). Regulation of Neuronal Activity in Hypothalamic Vasopressin Neurons. *Interdiscip Inf Sci* **21**, 225–234.

Okada S, Yokoyama M, Toko H, Tateno K, Moriya J, Shimizu I, Nojima A, Ito T, Yoshida Y, Kobayashi Y, Katagiri H, Minamino T, Komuro I (2012). Brain-derived neurotrophic factor protects against cardiac dysfunction after myocardial infarction via a central nervous system–mediated pathway. *Arterioscler Thromb Vasc Biol* **32**, 1902–1909.

Ong SB, Hernández-Reséndiz S, Crespo-Avilan GE, Mukhametshina RT, Kwek XY, Cabrera-Fuentes HA, Hausenloy DJ (2018). Inflammation following acute myocardial infarction: Multiple players, dynamic roles, and novel therapeutic opportunities. *Pharmacol Ther* **186**, 73–87.

Ono K, Matsumori A, Shioi T, Furukawa Y, Sasayama S (1998). Cytokine gene expression after myocardial infarction in rat hearts: possible implication in left ventricular remodeling. *Circulation* **98**, 149–156.

Oshima N, Onimaru H, Takechi H, Yamamoto K, Watanabe A, Uchida T, Nishida Y, Oda T, Kumagai H (2013). Aldosterone is synthesized in and activates bulbospinal neurons through mineralocorticoid receptors and ENaCs in the RVLM. *Hypertens Res* **36**, 504–512.

Otani K, Okada M, Yamawaki H (2017). Diverse distribution of tyrosine receptor kinase B isoforms in rat multiple tissues. *J Vet Med Sci* **79**, 1516–1523.

Palojoki E, Saraste A, Eriksson A, Pulkki K, Kallajoki M, Voipio-Pulkki LM & Tikkanen I (2001). Cardiomyocyte apoptosis and ventricular remodeling after myocardial infarction in rats. *Am J Physiol Heart Circ Physiol* **280**, H2726–H2731.

Pang PT, Teng HK, Zaitsev E, Woo NT, Sakata K, Zhen S, Teng KK, Yung WH, Hempstead BL, Lu B (2004). Cleavage of proBDNF by tPA/plasmin is essential for long-term hippocampal plasticity. *Science* **306**, 487–491.

Park H and Poo MM (2012). Neurotrophin regulation of neural circuit development and function. *Nat Rev Neurosci* **14**, 7–23.

Passino C, Severino S, Poletti R, Piepoli MF, Mammini C, Clerico A, Gabutti A, Nassi G, Emdin M (2006). Aerobic training decreases B-type natriuretic peptide expression and adrenergic activation in patients with heart failure. *J Am Coll Cardiol* **47**, 1835–1839.

Patel KP, Salgado HC, Liu X, Zheng H (2013). Exercise training normalizes the blunted central component of the baroreflex in rats with heart failure: role of the PVN. *Am J Physiol Heart Circ Physiol* **305**, H173–H181.

Paxinos, G., Watson, C., 1998. The Rat Brain in Stereotaxic Coordinates, fourth ed., Academic Press, New York.

Pedersen BK and Fischer CP (2007). Beneficial health effects of exercise–the role of IL-6 as a myokine. *Trends Pharmacol Sci* **28**, 152–156.

Pekkala S, Wiklund PK, Hulmi JJ, Ahtiainen JP, Horttanainen M, Pöllänen E, Mäkelä KA, Kainulainen H, Häkkinen K, Nyman K, Alén M, Herzig KH & Cheng S (2013). Are skeletal muscle FNDC5 gene expression and irisin release regulated by exercise and related to health? *J Physiol* **591**, 5393–5400.

Prigent-Tessier A, Quirié A, Maguin-Gaté K, Szostak J, Mossiat C, Nappey M, Devaux S, Marie, C, Demougeot C (2013). Physical training and hypertension have opposite effects on endothelial brain-derived neurotrophic factor expression. *Cardiovas Res* **100**, 374-382.

Puhl SL, Müller A, Wagner M, Devaux Y, Bohm M, Wagner DR, Maack C (2015). Exerciselimits scar thinning after myocardial infarction in mice. *Am J Physiol Heart Circ Physiol* **309**, H345–H359.

Pyner S and Coote J (2000). Identification of branching paraventricular neurons of the hypothalamus that project to the rostroventrolateral medulla and spinal cord. *Neuroscience* **100**, 549–556.

Radovits T, Oláh A, Lux Á, Németh BT, Hidi L, Birtalan E, Kellermayer D, Mátyás C, Szabó G, Merkely B (2013). Rat model of exercise-induced cardiac hypertrophy: hemodynamic characterization using left ventricular pressure-volume analysis. *Am J Physiol Heart Circ Physiol* **305**, H124–H134.

Rafatian N, Westcott KV, White RA, Leenen FH (2014). Cardiac macrophages and apoptosis after myocardial infarction: effects of central MR blockade. *Am J Physiol Regul Integr Comp Physiol* **307**, R879–R887.

Ramchandra R and Barrett CJ (2015). Regulation of the renal sympathetic nerves in heart failure. *Front Physiol* **6**, 238.

Ramchandra R, Hood SG, Xing D, Lambert GW, May CN (2018). Mechanisms underlying the increased cardiac norepinephrine spillover in heart failure. *Am J Physiol Heart Circ Physiol* **305**, H340–H347.

Rasmussen P, Brassard P, Adser H, Pedersen MV, Leick L, Hart E, Secher NH, Pedersen BK, Pilegaard H (2009). Evidence for a release of brain-derived neurotrophic factor from the brain during exercise. *Exp. Physiol.* **94**, 1062–1069.

Ren X, Zhang F, Zhao M, Zhao Z, Sun S, Fraidenburg DR, Tang H, Han Y (2017). Angiotensin-(1-7) in paraventricular nucleus contributes to the enhanced cardiac sympathetic afferent reflex and sympathetic activity in chronic heart failure rats. *Cell Physiol Biochem* **42**, 2523–2539.

Respress JL, van Oort RJ, Li N, Rolim N, Dixit SS, Voigt N, Lawrence WS, Skapura DG, Skårdal K, Wisløff U, Wieland T, Ai T, Powizd SM, Dobrev D, Wehrens XH (2012). Role of RyR2 phosphorylation at S2814 during heart failure progression. *Circ Res* **110**, 1474–1483.

Roberge S, Roussel J Andersson DC, Meli AC, Vidal B, Blandel F, Lanner JT, Le Guennec JY, Katz A, Westerblad H, Lacampagne A, Fauconnier J (2014). TNF-α-mediated caspase-8 activation induces ROS production and TRPM2 activation in adult ventricular myocytes. *Cardiovasc Res* **103**, 90–99.

Rogatzki MJ, Ferguson BS, Goodwin ML, Gladden LB (2015). Lactate is always the end product of glycolysis. *Front Neurosci* **9**, 22.

Roger VL (2013). Epidemiology of heart failure. *Circ Res* **113**, 646–659.

Rose CR, Blum R, Pichler B, Lepier A, Kafitz KW, Konnerth A (2003). Truncated TrkB-T1 mediates neurotrophin-evoked calcium signalling in glia cells. *Nature* **426**, 74–78.

Rosenblatt-Velin N, Montessuit C, Papageorgiou I, Terrand J, Lerch R (2001). Postinfarction heart failure in rats is associated with upregulation of GLUT-1 and downregulation of genes of fatty acid metabolism. *Cardiovasc Res* **52**, 407–416.

Roveda F, Middlekauff HR, Rondon MU, Reis SF, Souza M, Nastari L, Barretto AC, Krieger EM, Negrão CE (2003). The effects of exercise training on sympathetic neural activation in advanced heart failure: a randomized controlled trial. *J Am Coll cardiol* **42**, 854–860.

Saba J, Turati J, Ramírez D, Carniglia L, Durand D, Lasaga M, Caruso C (2018). Astrocyte truncated-TrkB mediates BDNF antiapoptotic effect leading to neuroprotection. *J Neurochem* **146**, 686–702.

Sager HB, Kessler T, Schunkert H (2017). Monocytes and macrophages in cardiac injury and repair. *J Thorac Dis* **9**, S30–S35.

Sakuma K and Yamaguchi A (2011). The recent understanding of the neurotrophin's role in skeletal muscle adaptation. *J Biomed Biotechnol* **2011**, 201696.

Sam F, Sawyer DB, Chang DL, Eberli FR, Ngoy S, Jain M, Amin J, Apstein CS, Colucci WS (2000). Progressive left ventricular remodeling and apoptosis late after myocardial infarction in mouse heart. *Am J Physiol Heart Circ Physiol* **279**, H422–H428.

Schaich CL, Wellman TL, Einwag Z, Dutko RA, Erdos B (2018). Inhibition of BDNF signaling in the paraventricular nucleus of the hypothalamus lowers acute stress-induced pressor responses. *J Neurophysiol* **120**, 633–643.

Schaich CL, Wellman TL, Koi B, Erdos B (2016). BDNF acting in the hypothalamus induces acute pressor responses under permissive control of angiotensin II. *Auton Neurosci* **197**, 1–8.

Schmittgen TD and Livak KJ (2008). Analyzing real-time PCR data by the comparative C(T) method. *Nat Protoc* **3**, 1101–1108.

Seifert, T, Brassard P, Wissengerg M, Rasmussen P, Nordby P, Stalknecht B, Adser H, Jakobsen AH, Pilegaard H, Nielsen HB & Secher NH (2010). Endurance training enhances BDNF release from the human brain. *Am J Physiol Regul Integr Comp Physiol* **298**, R372–R377.

Shan Z, Cuadra AE, Sumners C, Raizada MK (2008). Characterization of a functional (pro)renin receptor in rat brain neurons. *Exp Physiol* **93**, 701–708.

Sharma A, Masri J, Jo OD, Bernath A, Martin J, Funk A, Gera J (2007). Protein kinase C regulates internal initiation of translation of the GATA-4 mRNA following vasopressin-induced hypertrophy of cardiac myocytes. *J Biol Chem* **282**, 9505–9516.

Shen Y, Park JB, Lee SY, Han SK, Ryu PD (2018). Exercise training normalizes elevated firing rate of hypothalamic presympathetic neurons in heart failure rats. *Am J Physiol Regul Integr Comp Physiol* **316**, R110–R120.

Shenton F and Pyner S (2016). Vagal afferents, sympathetic efferents and the role of the PVN in heart failure. *Auton Neurosci* **199**, 38–47.

Sheriff MJ, Fontes MA, Killinger S, Horiuchi J, Dampney RA (2006). Blockade of AT1 receptors in the rostral ventrolateral medulla increases sympathetic activity under hypoxic conditions. *Am J Physiol Regul Integr Comp Physiol* **290**, R733–R740.

Shinde AV and Frangogiannis NG (2014). Fibroblasts in myocardial infarction: a role in inflammation and repair. *J Mol Cell Cardiol* **70**, 74–82.

Shiojima I, Schiekofer S, Schneider JG, Belisle K, Sato K, Andrassy M, Galasso G, Walsh K (2012). Short-term akt activation in cardiac muscle cells improves contractile function in failing hearts. *Am J Pathol* **181**, 1969–1976.

Sigmund CD, Diz DI, Chappell MC (2017). No brain renin–angiotensin system: déjà vu all over again? *Hypertension* **69**, 1007–1010.

Simpson NJ and Ferguson AV (2017). The proinflammatory cytokine tumor necrosis factor-α excites subfornical organ neurons. *J Neurophysiol* **118**, 1532–1541.

Simpson NJ and Ferguson AV (2018). Tumor necrosis factor alpha potentiates the effects of angiotensin II on subfornical organ neurons. *Am J Physiol Regul Integr Comp Physiol* **315**, R425–R433.

Sleiman SF, Henry J, Al-Haddad R, El Hayek L, Haidar EA, Stringer T, Ulja D, Karuppagounder SS, Holson EB, Ratan RR, Ninan I, Chao MV (2016). Exercise promotes the expression of brain derived neurotrophic factor (BDNF) through the action of the ketone body β-hydroxybutyrate. *Elife* **5**, e15092.

Sommerfeld MT, Schweigreiter R, Barde YA, Hoppe E (2000). Down-regulation of the neurotrophin receptor TrkB following ligand binding. Evidence for an involvement of the proteasome and differential regulation of TrkA and TrkB. *J Biol Chem* **275**, 8982–8990.

Sorescu D and Griendling KK (2002). Reactive oxygen species, mitochondria, and NAD (P) H oxidases in the development and progression of heart failure. *Congest Heart Fail* **8**, 132–140.

Sousa-Pinto B, Ferreira-Pinto MJ, Santos M, Leite-Moreira AF (2014). Central nervous system circuits modified in heart failure: pathophysiology and therapeutic implications. *Heart Fail Rev* **19**, 759–779.

Spencer-Segal JL, Waters EM, Bath KG, Chao MV, McEwen BS, Milner TA (2011). Distribution of phosphorylated TrkB receptor in the mouse hippocampal formation depends on sex and estrous cycle stage. *J Neurosci* **31**, 6780–6790.

Stas S, Whaley-Connell A, Habibi J, Appesh L, Hayden MR, Karuparthi PR, Qazi M, Morris EM, Cooper SA, Link CD, Stump C, Hay M, Ferrario C, Sowers JR (2007). Mineralocorticoid receptor blockade attenuates chronic overexpression of the renin-angiotensin-aldosterone system stimulation of reduced nicotinamide adenine dinucleotide phosphate oxidase and cardiac remodeling. *Endocrinology* **148**, 3773–3780.

Stern JE, Son S, Biancardi VC, Zheng H, Sharma N, Patel KP (2016). Astrocytes contribute to angiotensin II stimulation of hypothalamic neuronal activity and sympathetic outflow. *Hypertension*, **68** 1483–1493.

Straub RE, Lipska BK, Egan MF, Goldberg TE, Callicott JH, Mayhew MB, Vakkalanka RK, Kolachana BS, Kleinman JE, Weinberger DR (2007). Allelic variation in GAD1 (GAD 67) is associated with schizophrenia and influences cortical function and gene expression. *Mol Psychiatry* **12**, 854–869.

Su Q, Huo CJ, Li HB, Liu KL, Li X, Yang Q, Song XA, Chen WS, Cui W, Zhu GQ, Shi XL, Liu JJ, Kang YM (2017). Renin-angiotensin system acting on reactive oxygen species in paraventricular nucleus induces sympathetic activation via AT1R/PKCγ/Rac1 pathway in salt-induced hypertension. *Sci Rep* **7**, 43107.

Sun C, Sellers KW, Sumners C, Raizada MK (2005). NAD (P) H oxidase inhibition attenuates neuronal chronotropic actions of angiotensin II. *Circ Res* **96**, 659–666.

Sun HJ, Chen D, Han Y, Zhou YB, Wang JJ, Chen Q, Li YH, Gao XY, Kang YM, Zhu GQ (2016). Relaxin in paraventricular nucleus contributes to sympathetic overdrive and hypertension via PI3K-Akt pathway. *Neuropharmacology* **103**, 247–256.

Sung MM, Zordoky BN, Bujak AL, Lally JS, Fung D, Young ME, Horman S, Miller EJ, Light PE, Kemp BE, Steinberg GR, Dyck JR (2015). AMPK deficiency in cardiac muscle results in dilated cardiomyopathy in the absence of changes in energy metabolism. *Cardiovasc Res* **107**, 235–245.

Sutton MG and Sharpe N (2000). Left ventricular remodeling after myocardial infarction: pathophysiology and therapy. *Circulation* **101**, 2981–2988.

Swirski FK, Nahrendorf M, Etzrodt M, Wildgruber M, Cortez-Retamozo V, Panizzi P, Figueiredo JL, Kohler RH, Chudnovskiy A, Waterman P, Akiawa E, Mempel TR, Libby P, Weissleder R, Pittet MJ (2009). Identification of splenic reservoir monocytes and their deployment to inflammatory sites. *Science* **325**, 612–616.

Szczepanska-Sadowska E, Czarzasta K, Cudnoch-Jedrzejewska A (2018). Dysregulation of the renin-angiotensin system and the vasopressinergic system interactions in cardiovascular disorders. *Curr Hypertens Rep* **20**, 19.

Szuhany KL, Bugatti M, Otto MW (2015). A meta-analytic review of the effects of exercise on brain-derived neurotrophic factor. *J Psychiatric Res* **60**, 56–64.

Takashio S, Sugiyama S, Yamamuro M, Takahama H, Hayashi T, Sugano Y, Izumiya Y, Hokimoto S, Minamino N, Yasuda S, Anzai T, Ogawa H (2015). Significance of low plasma levels of brain-derived neurotrophic factor in patients with heart failure. *Am J Cardiol* **116**, 243–249.

Tan J, Wang H, Leenen FH (2004). Increases in brain and cardiac AT1 receptor and ACE densities after myocardial infarct in rats. *Am J Physiol Heart Circ Physiol* **286**, H1665–H1671.

Tao L, Bei Y, Lin S, Zhang H, Zhou Y, Jiang J, Chen P, Shen S, Xiao J, Li X (2015). Exercise training protects against acute myocardial infarction via improving myocardial energy metabolism and mitochondrial biogenesis. *Cell Physiol Biochem* **37**, 162–175.

Tao X, Finkbeiner S, Arnold DB, Shaywitz AJ, Greenberg ME (1998). Ca 2+ influx regulates BDNF transcription by a CREB family transcription factor-dependent mechanism. *Neuron* **20**. 709–726.

Tapia-Arancibia L, Rage F, Givalois L, Arancibia S (2004). Physiology of BDNF: focus on hypothalamic function. *Front Neuroendocrinol* **25**,77–107.

Teng HK, Teng KK, Lee R, Wright S, Tevar S, Almeida RD, Kermani P, Torkin R, Chen Z-Y, Lee FS (2005). ProBDNF induces neuronal apoptosis via activation of a receptor complex of p75NTR and sortilin. *J Neuroscience* **25**, 5455–5463.

Toriya M, Maekawa F, Maejima Y, Onaka T, Fujiwara K, Nakagawa T, Nakata M, Yada T (2010). Long-term infusion of brain-derived neurotrophic factor reduces food intake and body weight via a corticotrophin-releasing hormone pathway in the paraventricular nucleus of the hypothalamus. *J Neuroendocrinol* **22**, 987–995.

Triposkiadis F, Karayannis G, Giamouzis G, Skoularigis J, Louridas G, Butler J (2009). The sympathetic nervous system in heart failure: Physiology, pathophysiology, and clinical implications. *J Am Coll Cardiol* **54**, 1747–1762.

Tsuchimochi H, Matsukawa K, Komine H, Murata J (2002). Direct measurement of cardiac sympathetic efferent nerve activity during dynamic exercise. *Am J Physiol Heart Circ Physiol* **283,** H1896–H1906.

Tu H, Zhang D, Li YL (2018). Cellular and molecular mechanisms underlying arterial baroreceptor remodeling in cardiovascular diseases and diabetes. *Neurosci Bull* **35,** 98–112.

Uysal N, Kiray M, Sisman A, Camsari U, Gencoglu C, Baykara B, Cetinkaya C, Aksu I (2015). Effects of voluntary and involuntary exercise on cognitive functions, and VEGF and BDNF levels in adolescent rats. *Biotech Histochem* **90,** 55–68.

Vaynman S, Ying Z, Gomez-Pinilla F (2007). The select action of hippocampal calcium calmodulin protein kinase II in mediating exercise-enhanced cognitive function. *Neuroscience* **144**, 825–833.

Vaynman S, Ying Z, Gomez-Pinilla F (2004). Hippocampal BDNF mediates the efficacy of exercise on synaptic plasticity and cognition. *Eur J Neurosci* **20**, 2580–2590.

Vecile E, Dobrina A, Salloum FN, Van Tassell BW, Falcione A, Gustini E, Secchiero S, Crovella S, Sinagra G, Finato N (2013). Intracellular function of interleukin-1 receptor antagonist in ischemic cardiomyocytes. *PloS One* **8**, e53265.

Vidal-Martínez G, Vargas-Medrano J, Gil-Tommee C, Medina D, Garza NT, Yang B, Segura-Ulate I, Dominguez SJ, Perez RG (2016). FTY720/Fingolimod reduces synucleinopathy

and improves gut motility in A53T Mice: Potential Contributions of Pro-and Mature-Brain Derived Neurotrophic Factor. *J Biol Chem* **291**, 20811–20821.

Vidaurre ÓG, Gascón S, Deogracias R, Sobrado M, Cuadrado E, Montaner J, Rodríguez-Peña A, Díaz-Guerra M (2013). Imbalance of neurotrophin receptor isoforms TrkB-FL/TrkB-T1 induces neuronal death in excitotoxicity. *Cell Death Dis* **3**, e256.

Vieau D, Mayeur S, Lukaszewski M-A, Delahave F, Dutriez-Casteloot I, Laborie C, Deloof S, Lesage J, Breton C (2011). Perinatal undernutrition and brain-derived neurotrophic factor. In: *Handbook of behavior, food and nutrition*. Springer, 2055–2068.

Vinod P, Krishnappa V, Chauvin AM, Khare A, Raina R (2017). Cardiorenal syndrome: Role of arginine vasopressin and vaptans in heart failure. *Cardiol Res* **8**, 87–95.

Waldman BM, Augustyniak RA, Chen H, Rossi NF (2017). Effects of voluntary exercise on blood pressure, angiotensin II, aldosterone, and renal function in two-kidney, one-clip hypertensive rats. *Integr Blood Press Control* **10**, 41–51.

Walsh JJ and Tschakovsky ME (2018). Exercise and circulating BDNF: mechanisms of release and implications for the design of exercise interventions. *Appl Physiol Nutr Metab* **43**, 1095–1104.

Wan W, Powers AS, Li J, Zhang JQ, Ji L, Erikson JM (2007). Effect of Post–Myocardial Infarction Exercise Training on the Renin-Angiotensin-Aldosterone System and Cardiac Function. *Am J Med Sci* **334**, 265–273.

Wang BL, Jin H, Han XQ, Xia Y, Liu NF (2018). Involvement of brain-derived neurotrophic factor in exercise-induced cardioprotection of post-myocardial infarction rats. *Int J Mol Med* **42**, 2867–2880.

Wang C, Godar RJ, Billington CJ, Kotz CM (2010). Chronic administration of brain-derived neurotrophic factor in the hypothalamic paraventricular nucleus reverses obesity induced by high-fat diet. *Am J Physiol Regul Integr Comp Physiol* **298**, R1320–R1332.

Wang G, Anrather J, Glass MJ, Tarsitano MJ, Zhou P, Frys KA, Pickel VM, Iadecola C (2006a). Nox2, Ca2+, and protein kinase C play a role in angiotensin II-induced free radical production in nucleus tractus solitarius. *Hypertension* **48**, 482–489.

Wang HJ, Wang W, Cornish KG, Rozanski GJ, Zucker IH (2014). Cardiac sympathetic afferent denervation attenuates cardiac remodeling and improves cardiovascular dysfunction in rats with heart failure. *Hypertension* **64**, 745–755.

Wang HJ, Zhang F, Zhang Y, Gao XY, Wang W, Zhu GQ (2005). AT1 receptor in paraventricular nucleus mediates the enhanced cardiac sympathetic afferent reflex in rats with chronic heart failure. *Auto Neurosci* **121**, 56–63.

Wang HW, Lu J, Ahmad M, Leenen FH (2015). Abstract P142: Regulation of brain derived neurotrophic Factor (BDNF) expression by angiotensin II in the adrenals and the brain. *Hypertension* **66**, AP142.

Wang HW, Huang BS, Ganten D, Leenen FH (2004). Prevention of sympathetic and cardiac dysfunction after myocardial infarction in transgenic rats deficient in brain angiotensinogen. *Circ Res* **94**, 843–849.

Wang H and Zhou XF (2002). Injection of brain-derived neurotrophic factor in the rostral ventrolateral medulla increases arterial blood pressure in anaesthetized rats. *Neuroscience* **112**, 967–975.

Wang HJ, Rozanski GJ, Zucker IH (2017). Cardiac sympathetic afferent reflex control of cardiac function in normal and chronic heart failure states. *J Physiol* **595**, 2519–2534.

Wang WZ, Gao L, Pan YX, Zucker IH, Wang W (2006b). Differential effects of cardiac sympathetic afferent stimulation on neurons in the nucleus tractus solitarius. *Neurosci Lett* **409**, 146–150.

Wang WZ, Gao L, Wang HJ, Zucker IH, Wang W (2008). Interaction between cardiac sympathetic afferent reflex and chemoreflex is mediated by the NTS AT1 receptors in heart failure. *Am J Physiol Heart Circ Physiol* **295**, H1216–H1226.

Wang X, Dai Y, Ding Z, Khaidakov M, Mercanti F, Mehta JL (2013). Regulation of autophagy and apoptosis in response to angiotensin II in HL-1 cardiomyocytes. *Biochem Bophys Res Commun* **440**, 696–700.

Wasilewski MA, Myers VD, Recchia FA, Feldman AM, Tilley DG (2016). Arginine vasopressin receptor signaling and functional outcomes in heart failure. *Cell Signal* **28**, 224–233.

Wei SG, Yu Y, Felder RB (2017). Blood-borne Interleukin-1β Acts upon the Subfornical Organ to Upregulate the Sympathoexcitatory Milieu of the Hypothalamic Paraventricular Nucleus. *Am J Physiol Regul Integr Comp Physiol* **314**, R447–R458.

Wei SG, Yu Y, Zhang ZH, Felder RB (2015). Proinflammatory cytokines upregulate sympathoexcitatory mechanisms in the subfornical organ of the rat. *Hypertension* **65**, 1126–1133.

Wei SG, Zhang ZH, Beltz TG, Yu Y, Johnson AK, Felder RB (2013). Subfornical Organ Mediates Sympathetic and Hemodynamic Responses to Blood-Borne Proinflammatory Cytokines. *Hypertension* **62**, 118–125.

Wiese S, Jablonka S, Holtmann B, Orel N, Rajagopal R, Chao MV, Sendtner M (2007). Adenosine receptor A2A-R contributes to motoneuron survival by transactivating the tyrosine kinase receptor TrkB. *Proc Natl Acad Sci* U S A **104**, 17210–17215.

Wong J, Rothmond DA, Webster MJ, Shannon Weickert C (2013). Increases in two truncated TrkB isoforms in the prefrontal cortex of people with schizophrenia. *Schizophr Bull* **39**, 130–140.

Wrann CD, White JP, Salogiannnis J, Laznik-Bogoslavski D, Wu J, Ma D, Lin JD, Greenberg ME, Spiegelman BM (2013). Exercise induces hippocampal BDNF through a PGC-1α/FNDC5 pathway. *Cell Metab* **18**, 649–659.

Wu KL, Chan SH, Chan JY (2012). Neuroinflammation and oxidative stress in rostral ventrolateral medulla contribute to neurogenic hypertension induced by systemic inflammation. *J Neuroinflammation* **9**, 212.

Wu X, He L, Chen F, He X, Cai Y, Zhang G, Yi Q, He M, Luo J (2014). Impaired autophagy contributes to adverse cardiac remodeling in acute myocardial infarction. *PLoS One* **9**, e112891.

Xing Y, Musi N, Fujii N, Zou L, Luptak I, Hirshman MF, Goodyear LJ, Tian R (2003). Glucose metabolism and energy homeostasis in mouse hearts overexpressing dominant negative α2 subunit of AMP-activated protein kinase. *J Biol Chem* **278**, 28372–28377.

Xu B and Li H. Brain mechanisms of sympathetic activation in heart failure: Roles of the renin-angiotensin system, nitric oxide and pro-inflammatory cytokines (2015). *Mol Med Rep* **12**, 7823–7829.

Xu B, Zheng H, Patel KP (2012). Enhanced Activation of RVLM Projecting PVN Neurons in Rats with Chronic Heart Failure. *Am J Physiol Heart Circ Physiol* **302**, H1700–H1711.

Xu Q, Jensen DD, Peng H, Feng Y (2016). The critical role of the central nervous system (pro) renin receptor in regulating systemic blood pressure. *Pharmacol Ther* **164**, 126–134.

Xu X, Wan W, Ji L, Lao S, Powers AS, Zhao W, Erikson JM, Zhang JQ (2008a). Exercise training combined with angiotensin II receptor blockade limits post-infarct ventricular remodelling in rats. *Cardiovasc Res* **78**, 523–532.

Xu X, Wan W, Powers AS, Li J, Ji LL, Lao S, Wilson B, Erikson JM, Zhang JQ (2008b). Effects of exercise training on cardiac function and myocardial remodeling in post myocardial infarction rats. *J Mol Cell Cardiol* **44**, 114–122.

Xue B, Zhang Z, Roncari CF, Guo F, Johnson AK (2012). Aldosterone acting through the central nervous system sensitizes angiotensin II-induced hypertension. *Hypertension* **60**, 1023–1030.

Yang C, Liu Z, Liu K, Yang P (2014a). Mechanisms of Ghrelin anti-heart failure: inhibition of Ang II-induced cardiomyocyte apoptosis by down-regulating AT1R expression. *PloS One* **9**, e85785.

Yang J, Harte-Hargrove LC, Siao CJ, Marinic T, Clarke R, Ma Q, Jing D, LaFrancois JJ, Bath KG, Mark W, Ballon D, Lee FS, Scharfman HE, Hempstead BL (2014b). proBDNF negatively regulates neuronal remodeling, synaptic transmission, and synaptic plasticity in hippocampus. *Cell Rep* **7**, 796–806.

Yeung DF, Boom NK, Guo H, Lee DS, Schultz SE, Tu JV (2012). Trends in the incidence and outcomes of heart failure in Ontario, Canada: 1997 to 2007. *CMAJ* **184**, E765–E773.

You J, Wu J, Zhang Q, Ye Y, Wang S, Huang J, Liu H, Wang X, Zhang W, Bu L, Li J, Lin L, Ge J, Zou Y (2017). Differential cardiac hypertrophy and signaling pathways in pressure versus volume overload. *Am J Physiol Heart Circ Physiol* **314**, H552–H562.

Yu T, Chang Y, Gao XL, Li H, Zhao P (2017). Dynamic expression and the role of BDNF in exercise-induced skeletal muscle regeneration. *Int J Sports Med* **38**, 959–966.

Yu Y, Wei S-G, Weiss RM, Felder RB (2018). Angiotensin II type 1a Receptors in the Subfornical Organ Modulate Neuroinflammation in the Hypothalamic Paraventricular Nucleus in Heart Failure Rats. *Neuroscience* **381**, 46–58.

Zhan G, Huang N, Li S, Hua D, Zhang J, Fang X, Yang N, Luo A, Yang C (2018). PGC-1α–FNDC5–BDNF signaling pathway in skeletal muscle confers resilience to stress in mice subjected to chronic social defeat. *Psychopharmacology* **235**, 3351–3358.

Zhang D, Muelleman RL, Li Y (2015). Angiotensin II-superoxide-NFκB signaling and aortic baroreceptor dysfunction in chronic heart failure. *Front Neurosci* **9**, 382.

Zhang P (2017). CaMKII: The molecular villain that aggravates cardiovascular disease. *Exp Thr Med* **13**, 815–820.

Zhang T and Brown JH (2004). Role of Ca2+/calmodulin-dependent protein kinase II in cardiac hypertrophy and heart failure. *Cardiovac Res* **63**, 476–486.

Zhang T, Maier LS, Dalton ND, Miyamoto S, Ross J Jr, Bers DM, Brown JH (2003). The δC isoform of CaMKII is activated in cardiac hypertrophy and induces dilated cardiomyopathy and heart failure. *Circ Res* **92**, 912–919.

Zhang Y, Fang X, Fan W, Tang W, Cai J, Song L, Zhang C (2018). Interaction between BDNF and TNF-α genes in schizophrenia. *Psychoneuroendocrinology* **89**, 1–6.

Zhao Y, Hu HY, Sun D-R, Feng R, Sun XF, Guo F, Hao LY (2014). Dynamic alterations in the CaV1. 2/CaM/CaMKII signaling pathway in the left ventricular myocardium of ischemic rat hearts. *DNA Cell Biol* **33**, 282–290.

Zheng F, Soellner D, Nunez J, Wang H (2008). The basal level of intracellular calcium gates the activation of phosphoinositide 3-kinase-Akt signaling by brain-derived neurotrophic factor in cortical neurons. *J Neurochem* **106**, 1259–1274.

Zheng F, Zhou X, Moon C, Wang H (2012a). Regulation of brain-derived neurotrophic factor expression in neurons. *Int J Physiol Pathophysiol Pharmacol* **4**, 188–200.

Zheng H, Li YF, Cornish KG, Zucker IH, Patel KP (2005). Exercise training improves endogenous nitric oxide mechanisms within the paraventricular nucleus in rats with heart failure. *Am J Physiol Heart Circ Physiol* **288**, H2332–H2341.

Zheng H, Sharma NM, Liu X, Patel KP (2012b). Exercise training normalizes enhanced sympathetic activation from the paraventricular nucleus in chronic heart failure: role of angiotensin II. *Am J Physiol Regul Integr Comp Physiol* **303**, R387–R394.

Zhong MK, Duan YC, Chen AD, Xu B, Gao XY, De W, Zhu GQ (2008). Paraventricular nucleus is involved in the central pathway of cardiac sympathetic afferent reflex in rats. *Exp Physiol* **93**, 746–753.

Zhou L-M, Shi Z, Gao J, Han Y, Yuan N, Gao XY, Zhu GQ (2010). Angiotensin-(1–7) and angiotension II in the rostral ventrolateral medulla modulate the cardiac sympathetic afferent reflex and sympathetic activity in rats. *Pflügers Arch* **459**, 681–688.

Zhu GQ, Gao L, Li Y, Patel KP, Zucker IH, Wang W (2004). AT1 receptor mRNA antisense normalizes enhanced cardiac sympathetic afferent reflex in rats with chronic heart failure. *Am J Physiol Heart Circ Physiol* **287**, H1828–H1835.

Zhu GQ, Zucker IH, Wang W (2002). Central AT1 receptors are involved in the enhanced cardiac sympathetic afferent reflex in rats with chronic heart failure. *Basic Res Cardiol* **97**, 320–326.

Zimmerman MC, Lazartigues E, Lang JA, Sinnayah P, Ahmad IM, Spitz DR, Davisson RL (2002). Superoxide mediates the actions of angiotensin II in the central nervous system. *Circ Rese* **91**, 1038–1045.

Zimmerman MC, Sharma RV, Davisson RL (2005). Superoxide mediates angiotensin II–induced influx of extracellular calcium in neural cells. *Hypertension* **45**, 717–723.

Zordoky BN, Nagendran J, Pulinilkunnil T, Kienesberger PC, Masson G, Waller TJ, Kemp BE, Steinberg GR, Dyck JR (2014). AMPK-dependent inhibitory phosphorylation of ACC is not essential for maintaining myocardial fatty acid oxidation. *Circ Res* **115**, 518–524.

Zubcevic J, Santisteban MM, Perez PD, Arocha R, Hiller H, Malphurs WL, Colon-Perez LM, Sharma RK, de Kloet A, Krause EG (2017). A single angiotensin II hypertensive stimulus is associated with prolonged neuronal and immune system activation in Wistar-Kyoto rats. *Front Physiol* **8**, 592.

Zucker IH, Xiao L, Haack KK (2014). The central renin–angiotensin system and sympathetic nerve activity in chronic heart failure. *Clin Sci* **126**, 695–706.

.

7. Appendix I

7.1. Cardiac mBDNF and TrkB.T1 protein at 8 weeks post MI

7.1.1. General information of rats

Table 7-1. General characteristics, echocardiographic and hemodynamic measurements at 8 weeks post MI

	Sham (n=6)	MI (n=7)
General characteristics		
Body weight (g)	605 ± 33	531 ± 17
MI size (%)	N/A	28 ± 1
LV weight (mg/100g BW)	168 ± 4	206 ± 6**
RV weight (mg/100g BW)	41 ± 1	62 ± 8
Echocardiographic parameters		
SD (mm)	4.0 ± 0.1	7.4 ± 0.2**
DD (mm)	7.9 ± 0.3	10.2 ± 0.1**
EF (%)	79 ± 1	51 ± 2**
Hemodynamic parameters		
LVPSP (mmHg)	123 ± 2	109 ± 4*
LVEDP (mmHg)	2.8 ± 0.3	17 ± 2**
dP/dt_{max} (mmHg/sec)	7915 ± 193	5611 ± 179**

Values are means ± SE. LV, left ventricle; RV, right ventricle; MI, myocardial infarction, SD, systolic diameter; DD, diastolic diameter; EF, ejection fraction; LVPSP, left ventricular peak systolic pressure; LVEDP, left ventricular end diastolic pressure; dP/dt_{max}, maximal first derivative of change in pressure over time; N/A, not applicable.
Student *t*-test, *P< 0.05 and **P< 0.01 vs. Sham.

7.1.2. Changes in mBDNF and TrkB.T1 protein expression in the LV

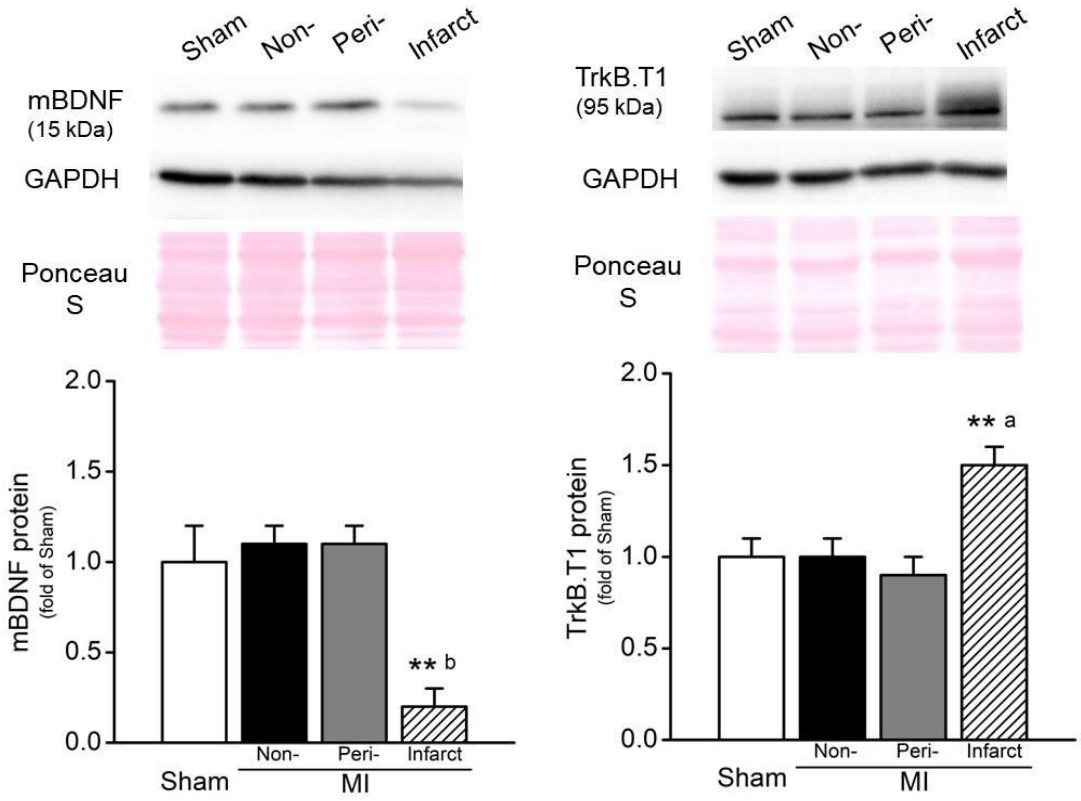

Figure 7-1. mBDNF and TrkB.T1 protein expression in the LV at 8 weeks post MI
Values are means ± SE. Sham, n=6; MI, n=7. mBDNF, mature brain derived-neurotrophic factor; TrkB.T1, truncated form of tropomyosin-related kinase B receptor.
One-way ANOVA followed by Bonferroni.
For mBDNF protein, F=12.0, P <0.001; for TrkB.T1 protein, F=5.5, P<0.01
**P<0.01 vs. Sham; [a]P <0.05 and [b]P <0.01 vs. other areas.

7.2. Sample size calculations

Post hoc sample size for each study was determined using a software G*Power 3.1. (Faul et al., 2007) using values of the factors below (Charan and Kantharia, 2013).

1) α (probability of a false positive finding) = 0.05

2) Power (probability of detecting an effect; 1–β) = 0.8

- β (probability of a false negative finding) = 0.2

3) Effect size (the minimum difference in means among groups) = 0.3

4) Anticipated mean and standard deviation (SD)

- Control = 1.0 ± 0.2

- MI = 0.7 ± 0.2

3) and 4) were estimated based on published studies which reported changes in cardiac BDNF protein levels post MI (Okada et al., 2012; Halade et al., 2013). Based on the information above, proper sample size per group was 9–10 for each of the study. At the end, final sample size for MI groups was adjusted according to number of rats' death after MI and having small MI (MI size < 15%).

- 40% death after inducing MI (60% survival rate)

- 20% of survival MI rats have small MI (80% of survival MI rats have medium to large MI)

→ Percentage for attrition of MI rats = [1-(0.6 x 0.8)] x100% = 52%

Adjusted sample size = Sample size/[1-(% attrition/100)]

= 10 rats/(1-0.52) = 20.83

To get enough number of medium to large MI per MI group, at least 21 rats were required for MI surgery.

8. Appendix II

JOHN WILEY AND SONS LICENSE TERMS AND CONDITIONS

Mar 28, 2019

This Agreement between Ms. Heow Won Lee ("You") and John Wiley and Sons ("John Wiley and Sons") consists of your license details and the terms and conditions provided by John Wiley and Sons and Copyright Clearance Center.

License Number	4557681202355
License date	Mar 28, 2019
Licensed Content Publisher	John Wiley and Sons
Licensed Content Publication	Experimental Physiology
Licensed Content Title	Effects of exercise training on brain-derived neurotrophic factor in skeletal muscle and heart of rats post myocardial infarction
Licensed Content Author	Heow Won Lee, Monir Ahmad, Hong-Wei Wang, et al
Licensed Content Date	Feb 28, 2017
Licensed Content Volume	102
Licensed Content Issue	3
Licensed Content Pages	15
Type of use	Dissertation/Thesis
Requestor type	Author of this Wiley article
Format	Print and electronic
Portion	Full article
Will you be translating?	No
Order reference number	
Title of your thesis / dissertation	Role of BDNF in cardiac remodeling and dysfunction in rats after myocardial infarction
Expected completion date	Oct 2019
Expected size (number of pages)	200
Requestor Location	

Publisher Tax ID	EU826007151
Total	0.00 CAD
Terms and Conditions	

TERMS AND CONDITIONS

This copyrighted material is owned by or exclusively licensed to John Wiley & Sons, Inc. or one of its group companies (each a"Wiley Company") or handled on behalf of a society with which a Wiley Company has exclusive publishing rights in relation to a particular work (collectively "WILEY"). By clicking "accept" in connection with completing this licensing

transaction, you agree that the following terms and conditions apply to this transaction (along with the billing and payment terms and conditions established by the Copyright Clearance Center Inc., ("CCC's Billing and Payment terms and conditions"), at the time that you opened your RightsLink account (these are available at any time at http://myaccount.copyright.com).

Terms and Conditions

- The materials you have requested permission to reproduce or reuse (the "Wiley Materials") are protected by copyright.

- You are hereby granted a personal, non-exclusive, non-sub licensable (on a stand-alone basis), non-transferable, worldwide, limited license to reproduce the Wiley Materials for the purpose specified in the licensing process. This license, **and any CONTENT (PDF or image file) purchased as part of your order,** is for a one-time use only and limited to any maximum distribution number specified in the license. The first instance of republication or reuse granted by this license must be completed within two years of the date of the grant of this license (although copies prepared before the end date may be distributed thereafter). The Wiley Materials shall not be used in any other manner or for any other purpose, beyond what is granted in the license. Permission is granted subject to an appropriate acknowledgement given to the author, title of the material/book/journal and the publisher. You shall also duplicate the copyright notice that appears in the Wiley publication in your use of the Wiley Material. Permission is also granted on the understanding that nowhere in the text is a previously published source acknowledged for all or part of this Wiley Material. Any third party content is expressly excluded from this permission.

- With respect to the Wiley Materials, all rights are reserved. Except as expressly granted by the terms of the license, no part of the Wiley Materials may be copied, modified, adapted (except for minor reformatting required by the new Publication), translated, reproduced, transferred or distributed, in any form or by any means, and no derivative works may be made based on the Wiley Materials without the prior permission of the respective copyright owner.**For STM Signatory Publishers clearing permission under the terms of the STM Permissions Guidelines only, the terms of the license are extended to include subsequent editions and for editions in other languages, provided such editions are for the work as a whole in situ and does not involve the separate exploitation of the permitted figures or extracts,** You may not alter, remove or suppress in any manner any copyright, trademark or other notices displayed by the Wiley Materials. You may not license, rent, sell, loan, lease, pledge, offer as security, transfer or assign the Wiley Materials on a stand-alone basis, or any of the rights granted to you hereunder to any other person.

- The Wiley Materials and all of the intellectual property rights therein shall at all times remain the exclusive property of John Wiley & Sons Inc, the Wiley Companies, or their respective licensors, and your interest therein is only that of having possession of and the right to reproduce the Wiley Materials pursuant to Section 2 herein during the continuance of this Agreement. You agree that you own no right, title or interest in or to the Wiley Materials or any of the intellectual property rights therein. You shall have no rights hereunder other than the license as provided for above in Section 2. No right, license or interest to any trademark, trade name, service mark or other branding ("Marks") of WILEY or its licensors is granted hereunder, and you agree that you

shall not assert any such right, license or interest with respect thereto

- NEITHER WILEY NOR ITS LICENSORS MAKES ANY WARRANTY OR REPRESENTATION OF ANY KIND TO YOU OR ANY THIRD PARTY, EXPRESS, IMPLIED OR STATUTORY, WITH RESPECT TO THE MATERIALS OR THE ACCURACY OF ANY INFORMATION CONTAINED IN THE MATERIALS, INCLUDING, WITHOUT LIMITATION, ANY IMPLIED WARRANTY OF MERCHANTABILITY, ACCURACY, SATISFACTORY QUALITY, FITNESS FOR A PARTICULAR PURPOSE, USABILITY, INTEGRATION OR NON-INFRINGEMENT AND ALL SUCH WARRANTIES ARE HEREBY EXCLUDED BY WILEY AND ITS LICENSORS AND WAIVED BY YOU.

- WILEY shall have the right to terminate this Agreement immediately upon breach of this Agreement by you.

- You shall indemnify, defend and hold harmless WILEY, its Licensors and their respective directors, officers, agents and employees, from and against any actual or threatened claims, demands, causes of action or proceedings arising from any breach of this Agreement by you.

- IN NO EVENT SHALL WILEY OR ITS LICENSORS BE LIABLE TO YOU OR ANY OTHER PARTY OR ANY OTHER PERSON OR ENTITY FOR ANY SPECIAL, CONSEQUENTIAL, INCIDENTAL, INDIRECT, EXEMPLARY OR PUNITIVE DAMAGES, HOWEVER CAUSED, ARISING OUT OF OR IN CONNECTION WITH THE DOWNLOADING, PROVISIONING, VIEWING OR USE OF THE MATERIALS REGARDLESS OF THE FORM OF ACTION, WHETHER FOR BREACH OF CONTRACT, BREACH OF WARRANTY, TORT, NEGLIGENCE, INFRINGEMENT OR OTHERWISE (INCLUDING, WITHOUT LIMITATION, DAMAGES BASED ON LOSS OF PROFITS, DATA, FILES, USE, BUSINESS OPPORTUNITY OR CLAIMS OF THIRD PARTIES), AND WHETHER OR NOT THE PARTY HAS BEEN ADVISED OF THE POSSIBILITY OF SUCH DAMAGES. THIS LIMITATION SHALL APPLY NOTWITHSTANDING ANY FAILURE OF ESSENTIAL PURPOSE OF ANY LIMITED REMEDY PROVIDED HEREIN.

- Should any provision of this Agreement be held by a court of competent jurisdiction to be illegal, invalid, or unenforceable, that provision shall be deemed amended to achieve as nearly as possible the same economic effect as the original provision, and the legality, validity and enforceability of the remaining provisions of this Agreement shall not be affected or impaired thereby.

- The failure of either party to enforce any term or condition of this Agreement shall not constitute a waiver of either party's right to enforce each and every term and condition of this Agreement. No breach under this agreement shall be deemed waived or excused by either party unless such waiver or consent is in writing signed by the party granting such waiver or consent. The waiver by or consent of a party to a breach of any provision of this Agreement shall not operate or be construed as a waiver of or consent to any other or subsequent breach by such other party.

- This Agreement may not be assigned (including by operation of law or otherwise) by you without WILEY's prior written consent.
- Any fee required for this permission shall be non-refundable after thirty (30) days from receipt by the CCC.
- These terms and conditions together with CCC's Billing and Payment terms and conditions (which are incorporated herein) form the entire agreement between you and WILEY concerning this licensing transaction and (in the absence of fraud) supersedes all prior agreements and representations of the parties, oral or written. This Agreement may not be amended except in writing signed by both parties. This Agreement shall be binding upon and inure to the benefit of the parties' successors, legal representatives, and authorized assigns.
- In the event of any conflict between your obligations established by these terms and conditions and those established by CCC's Billing and Payment terms and conditions, these terms and conditions shall prevail.
- WILEY expressly reserves all rights not specifically granted in the combination of (i) the license details provided by you and accepted in the course of this licensing transaction, (ii) these terms and conditions and (iii) CCC's Billing and Payment terms and conditions.
- This Agreement will be void if the Type of Use, Format, Circulation, or Requestor Type was misrepresented during the licensing process.
- This Agreement shall be governed by and construed in accordance with the laws of the State of New York, USA, without regards to such state's conflict of law rules. Any legal action, suit or proceeding arising out of or relating to these Terms and Conditions or the breach thereof shall be instituted in a court of competent jurisdiction in New York County in the State of New York in the United States of America and each party hereby consents and submits to the personal jurisdiction of such court, waives any objection to venue in such court and consents to service of process by registered or certified mail, return receipt requested, at the last known address of such party.

WILEY OPEN ACCESS TERMS AND CONDITIONS

Wiley Publishes Open Access Articles in fully Open Access Journals and in Subscription journals offering Online Open. Although most of the fully Open Access journals publish open access articles under the terms of the Creative Commons Attribution (CC BY) License only, the subscription journals and a few of the Open Access Journals offer a choice of Creative Commons Licenses. The license type is clearly identified on the article.

The Creative Commons Attribution License

The Creative Commons Attribution License (CC-BY) allows users to copy, distribute and transmit an article, adapt the article and make commercial use of the article. The CC-BY license permits commercial and non-

Creative Commons Attribution Non-Commercial License

The Creative Commons Attribution Non-Commercial (CC-BY-NC)License permits use, distribution and reproduction in any medium, provided the original work is properly cited and is not used for commercial purposes.(see below)

Creative Commons Attribution-Non-Commercial-NoDerivs License

The Creative Commons Attribution Non-Commercial-NoDerivs License (CC-BY-NC-ND) permits use, distribution and reproduction in any medium, provided the original work is properly cited, is not used for commercial purposes and no modifications or adaptations are made. (see below)

Use by commercial "for-profit" organizations

Use of Wiley Open Access articles for commercial, promotional, or marketing purposes requires further explicit permission from Wiley and will be subject to a fee.

Further details can be found on Wiley Online Library http://olabout.wiley.com/WileyCDA/Section/id-410895.html

Other Terms and Conditions:

v1.10 Last updated September 2015

Questions? customercare@copyright.com or +1-855-239-3415 (toll free in the US) or +1-978-646-2777.